GDANSK UNIVERSITY OF TECHNOLOGY
FACULTY OF OCEAN ENGINEERING AND SHIP TECHNOLOGY
SECTION OF TRANSPORT TECHNICAL MEANS
OF TRANSPORT COMMITEE OF POLISH ACADEMY OF SCIENCES
UTILITY FOUNDATIONS SECTION
OF MECHANICAL ENGINEERING COMMITTEE OF POLISH ACADEMY OF SCIENCE

ISSN 1231 – 3998
ISBN 83 – 900666 – 2 – 9

Journal of

POLISH CIMAC

DIAGNOSIS, RELIABILITY AND SAFETY

Vol. 7 **No. 2**

Gdansk, 2012

Science publication of Editorial Advisory Board of POLISH CIMAC

Editorial Office:

GDANSK UNIVERSITY OF TECHNOLOGY
Faculty of Ocean Engineering and Ship Technology
Department of Ship Power Plants
G. Narutowicza 11/12 80-233 GDANSK POLAND
tel. +48 58 347 29 73, e – mail: sek4oce@pg.gda.pl

www.polishcimac.pl

This journal is devoted to designing of diesel engines, gas turbines and ships' power transmission systems containing these engines and also machines and other appliances necessary to keep these engines in movement with special regard to their energetic and pro-ecological properties and also their durability, reliability, diagnostics and safety of their work and operation of diesel engines, gas turbines and also machines and other appliances necessary to keep these engines in movement with special regard to their energetic and pro-ecological properties, their durability, reliability, diagnostics and safety of their work, and, above all, rational (and optimal) control of the processes of their operation and specially rational service works (including control and diagnosing systems), analysing of properties and treatment of liquid fuels and lubricating oils, etc.

All papers have been reviewed

ISSN 1231 – 3998
ISBN 83 – 900666 – 2 – 9

Printed in Poland

CONTENTS

Caban J., Gardyński L.: DETERMINATION OF THE INFLUENCE OF THE STIFFNESS OF THE DIESEL ENGINE SUSPENSION CUSHIONS IN THE TERRAIN CAR 7

Charchalis A.: DIAGNOSTICS OF VESSEL POWER PLANTS 17

Dyl T.: FINISHING OF THE METAL MATRIX COMPOSITE COATINGS APPLIED TO REGENERATED PARTS OF SHIP MACHINERY 23

Gębura A., Tokarski T.: DIAGNOSING OF ELECTRO - MECHANICAL CONVERTERS BY USING A METHOD OF FREQUENCY MODULATION ANALYSIS 31

Girtler J.: NECESSITY FOR AND POSSIBILITY OF APPLICATION OF THE THEORY OF SEMI-MARKOV PROCESSES TO DETERMINE RELIABILITY OF DIAGNISING SYSTEMS 45

Grządziela A., Kluczyk M.: APPLICATION OF COHERENCE FUNCTIONS OF VIBROACOUSTIC SIGNALS FROM PISTON ENGINES, RECORDED IN SET STATES, FOR THEIR TECHNICAL EVALUATION 55

Kałaczyński T., Łukasiewicz M.: MULTIDIMENSIONAL ANALYSIS AND ASSESSMENT OF COMBUSTION ENGINE TECHNICAL STATE BASIS ON SVD METHOD WITH MODERN ENGINEERS SOFTWARE APPLICATION 65

Kluj S.: TURBO DIESEL 5 – THE NEW SIMULATOR FOR MARITIME ENGINEERING TRAINING ... 79

Knopik L.: MODEL OF PROFIT IMPROVEMENT IN MAINTENANCE SYSTEM 87

Knopik L.: STATISTICAL ANALYSIS OF FAILURES 91

Kyzioł L.: STRESS IN A SALVAGE FAYING FACE OF A SUBMARINE WHILE MOORING A RECOVERY VESSEL 97

Landowski B., Perczyński D., Kolber P.: APPLICATION OF MARKOV PROCESS FOR MODELING CHANGES OF TRANSPORT MEANS OPERATION STATES 107

Liberacki R.: RISK CRITERIA FOR SEA-GOING SHIPS ARISING FROM THE OPERATION OF THE MAIN ENGINES' CRANKSHAFT – CONECTING ROD – PISTON SYSTEMS 115

Merkisz J., Markowski J., Pielecha J., Pielecha I.: EXHAUST EMISSIONS FROM THE PZL SW-4 PUSZCZYK HELICOPTER BASED ON THE MEASUREMENTS OF THE CONCENTRATIONS OF EXHAUST COMPONENTS IN THE EXHAUST GASES DURING A PRE-FLIGHT TEST 123

Migawa K.: APPLICATION OF SEMI-MARKOV'S PROCESS FOR CONTROL OF AVAILABILITY OF EXECUTIVE SUBSYSTEM WITH A THRESHOLD STRUCTURE 131

Pawletko R., Polanowski S.: INFLUENCE OF GAS CHANNELS OF MEDIUM SPEED MARINE ENGINES ON THE ACCURACY OF DETERMINATION OF DIAGNOSTIC PARAMETERS BASED ON THE INDICATOR DIAGRAMS 139

Piaseczny L., Walkowski M.: THE SELECTED CHARACTERISTICS OF FUEL INJECTION IN THE SYSTEMS OF MARINE COMBUSION ENGINE COMMON RAIL TYPE 147
Polanowski S., Pawletko R.: LOW SPEED MARINE DIESEL ENGINE DIAGNOSIS BASED ON PASSIVE EXPERIMENT 161
Rudnicki J.: THE EVALUATION OF THE VIBRATION MEASUREMENT USABILITY OF ELECTRONIC INDICATOR LEMAG „PREMET C" 167
Rychlik A., Szczyglak P.: METHOD OF DIAGNOSING THE POWER TRANSMISSION SYSTEM IN A TARPAN HONKER MILITARY VEHICLE 175

Rychter M.: FORMING RECOMMENDATIONS OF DIGITAL RECORDING DEVICES 183
Stelmaszewski A., Król K.: CHANGES OF OPTICAL PROPERTIES OF LUBRICATING OIL DURING ITS USE 197
Tarelko W.: DEVELOPMENT OF SHIP TECHNICAL REQUIREMENTS BY INTERNATIONAL MARITIME ORGANIZATION 205

Tylicki H.: THE PROGNOSIS OF MACHINES CONDITION STATE 217
Valishin A., Adamkiewicz A.: DETERMINATION OF CYLINDER LINER FREE VIBRATION FREQUENCIES IN DIESEL MARINE ENGINES 227

Wierzbicki S.: ANALYSIS OF PISTON-CRANK SYSTEM BALANCING IN V-VR ENGINES 235

Wilczarska J.: STRATEGIES IN DEDICATED DIAGNOSTIC SYSTEMS 243
Witkowski K.: THE IMPORTANCE OF MEASURING MASS INTENSITY OF FLOW AIR THROUGH THE COMPRESSOR IN DIAGNOSTICS THE TURBOCHARGER SYSTEM MARINE ENGINE 249
Zacharewicz M.: AN ANALYSIS OF THE ASSESSMENT OF THE TECHNICAL CONDITION OF A MARINE DIESEL-ELECTRIC SET BASED ON THE EXHAUST GAS PRESSURE AND OTHER ENERGY PARAMETERS MEASUREMENTS 255
Żółtowski B., Tylicki H.: NEW ELEMENTS IN THE TESTS PROGRAMMES OF MACHINE VIBRATIONS 265

Journal of Polish CIMAC
Gdansk University of Technology
The Faculty of Ocean Engineering and Ship Technology

DETERMINATION OF THE INFLUENCE OF THE STIFFNESS OF THE DIESEL ENGINE SUSPENSION CUSHIONS IN THE TERRAIN CAR

Jacek Caban, Leszek Gardyński

Lublin University of Technology, Mechanical Engineering Faculty
ul. Nadbystrzycka 36, 20-618 Lublin, Poland
tel.: +48 81 5384258; +48 81 5384215 fax: +48 81 5384258
e-mail: j.caban@pollub.pl l.gardynski@pollub.pl

Abstract

The article presents the results of experimental investigations carried out for different types of diesel engine suspension cushions in the terrain car. The study was performed using two types of suspension cushions in a variety of combustion engine operating conditions. The effect of engine displacement as a result of vibrations between the engine and vehicle body was tested. The endurance testing of the suspension cushions was done using the endurance testing machine Zwick Z-100. Next, we analyzed the results obtained in experimental studies of the differences between the vibration of the suspension cushions.

The results of the tests of different types of plate connectors for the engine suspension can be useful when designing propulsion systems for military vehicles and military utility terrain cars, or as shown by the author [1, 4] to modernize of the existing military vehicles stock.

Key words: *machine diagnostics, engine vibration, rubber vibroisolator, military vehicle*

1. Introduction

The purpose of experimental researches described in the article was to determine the stiffness of the diesel engine front suspension cushions. The object of research is the terrain car UAZ-31 512 (formerly 469B), with a diesel engine mounted – Andoria 4C90 by WSW Andoria, liquid-cooled, indirect fuel injection into the swirl chamber. The issue of changes in the vehicle engine is described in detail in [1-4]. The tests were performed using hard suspension cushions – "old", at which there were significant vibrations in the body of the engine at the operating idle speed and soft – "new" ones. It should be noted that the test suspension cushions are not original cushions used in this car, because gasoline engines were fitted as standard. It was necessary to adjust the suspension so that you could mount the 4C90 diesel engine, using cushions applied to this engine types, which are also in Lublin vehicle.

The researches was conducted using a specially designed device to study the movement as a result of vibrations between the engine and body, and using the endurance testing machine Zwick Z-100.

Machines, in connection with the work performed, are a subject to various external loads, derived from the reaction of the impact of the machine, as well as from its surroundings. These phenomena have diverse and evolving nature. It manifests itself as mechanical and acoustics vibrations. It has a huge and significant impact on humans, its safety and ergonomics in the use of machinery. In-vehicle vibration is the main source of propulsion system, which like the internal

combustion engine performs significantly periodic cycle with variable characteristics. The kinematic excitation of vibrations caused by driving on an uneven road surface or track are additional issues in vehicle dynamics [6]. Frequency range in which the phenomena are caused by these sources, lie in different frequency bands, and so the pathway will be accordingly others [4]. Uneven road surfaces cause the force lying in a very wide band, ranging from 0.5 to 250 Hz, including a range of vibrations coming from the propulsion system [4]. Analysis of the impact of these vibrations and vehicle design modifications are one of the most important tasks thoroughly studied experimentally and theoretically.

The vibrations generated by the source are transmitted via the machine by [4]:

- special elastic-damping elements eg. tires, suspension components, etc.;
- machine kinematics system, such as steering in a car, etc.;
- structure of the machine.

Different ranges of natural frequencies determine the vibration properties of the transition path. This can be recognized in a very simplified way, that in the frequency range of 0.5÷15 Hz the main route of transmission is a special elastic-damping system, used to mitigate the effects of vibration [4]. In the engine vehicle suspension there is used the plate connector which consists mostly of two metal plates and vulcanised rubber layer. The plate connectors are made mostly of rubber: natural rubber, chloroprene, and in exceptional cases, nitrile rubber [10]. To prevent the spread of strain on the engine frame and the vehicle hull vibration, the heavy rubber cushions are mounted under the engine mounting brackets [12]. Improper distribution of stiffness and bags arrangement can cause significant engine vibration, which will be brought back to the car especially when idle.

In conditions of dynamic loading the rubber stiffness is increased, the natural frequency of the dynamic stiffness c_{dvn} is substituted to the formula, while [7]:

$$c_{dyn} = X \bullet C, \tag{1}$$

where:

c_{dyn} – dynamic stiffness,
X – the coefficient of rigidity,
C – number of degrees of freedom.

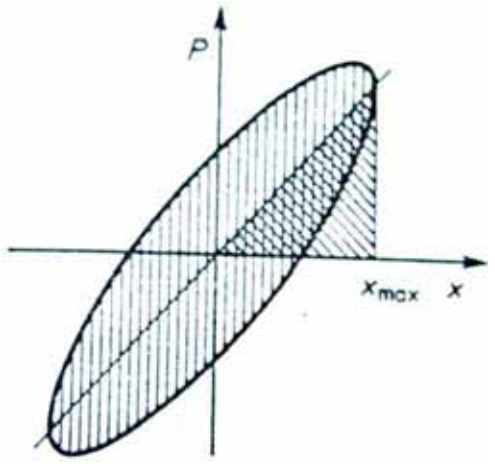

Fig. 1. The hysteresis loop with a dynamic load of rubber [7, 9]

The coefficient of rigidity X for rubber with a hardness 35...95 °ShA (IRHD) shall be within 1.1...1.4 [7]. In a system with C degrees of freedom, as for example in the automotive powertrain suspension, the frequency of natural vibration for each direction is taken into account. The behaviour of rubber under the influence of dynamic loads illustrates in the general case the graph in Fig. 1. Ascending and descending curves of strain do not coincide but form the shape of the hysteresis loop similar to the ellipse. It is also called dynamic suppression loop [7]. Area under the curve of the graph is a measure of the increasing strain energy absorbed and the surface energy of an ellipse as changed into heat [7].

2. Characteristics of the tested cushions

One of the main features of elastic rubber elements is the ability to transfer and absorb the complex loads [9]. Fig. 2 shows the used plate connectors. Cushions, despite the difference of hardness, yet different in thread ("hard" cushion has a normal thread – M8x1.25, and according to the seller information is called a substitute, produced by a private manufacturer, and "soft" – the "original" with a fine thread – M8x1). No other significant differences were found.

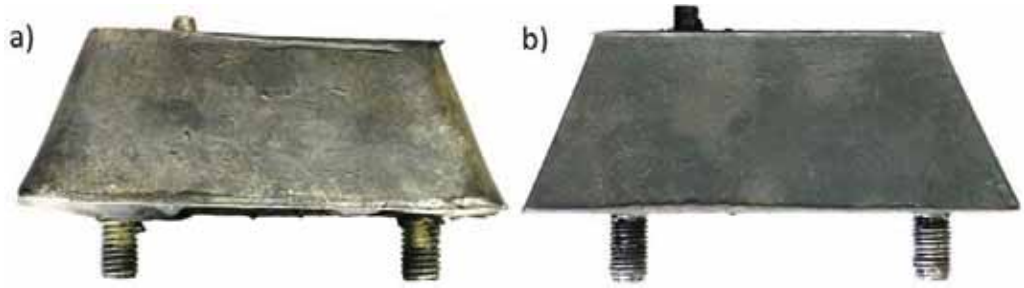

Fig. 2. The tested engine cushions in the terrain car Uaz, a) – "hard" cushion, b) – "soft" cushion

"Hard" cushions were operated in the vehicle for about 15.000 km, most in the field. During the dismounting it was found out that one of them was torn apart during use, .while "soft" cushions were new and unused.

Rubber hardness testing was carried out using Shor's method, a portable hardness tester, with the scale of 0 to 100 °Sh-A, and an accuracy of 2 °Sh-A. Average hardness for hard cushions is: cushion 1. – 79 °Sh-A, cushion 2. – 83 °Sh-A, soft cushions, respectively, cushion 3. – 61 °Sh-A and cushion 4. – 62 °Sh-A.

The flexibility study was carried out on the endurance testing machine Zwick Z-100, the selected data are summarized in Table 1.

Tab. 1. Specifications of the testing machine Zwick Z-100

Model	100SN3A WN:136119
traverse path sensor	WN:136119
force measurement head	ID:0 WN:136120
force measuring range [kN]	2,5÷100
temperature range of thermal chambers [^{o}C]	-75÷250
extensometer	electronic

When examining the cushions in the endurance testing machine, additional plates were fastened to the head in order to allow the compression tests. The test cushions have been squeezed by increasing cyclic deflection value of 2 mm. The head squeezed cushions for each cycle of 2 mm

and returned to the state of 1 mm, up to 10 mm of the cushions deflection. Piston rod with which the cushions deflection was exerted, moved at a speed of V = 20 mm/min. The power that was needed to squeeze the cushions for a given value of the deflection was controlled in the studies. In this way, two hard and two soft cushions have been investigated, which after the study were fitted to the car. The resulting graphs show the hysteresis field, resulting from the energy absorbed by the cushions.

Based on the obtained results, the following formula can be used to calculate the stiffness:

$$k = \frac{F}{l}, \tag{2}$$

While the elasticity (sensitivity), we shall calculate with the formula [8]:

$$p = \frac{l}{F}, \tag{3}$$

where:

k – stiffness,
F – the force exerted by the piston rod,
l – displacement,,
p – elasticity (sensitivity).

Fig.3 shows that the force exerted by the piston on the cushion – 1 is relatively large in the last phase of the deflection, at 10mm it equals to 8467.08 N. It may be noted that the characteristics has rather large hysteresis of deflection and is progressive, what might be expected on the basis of cushion shape (trapezium). The maximum stiffness was calculated from the results: k = 846.708 N/mm, and flexibility: p = 1,181$^{(-3)}$ mm/N.

The force exerted on the cushion – 2, amounted to 10802.1 N at deflection of 10 mm. Clearly visible large field of hysteresis at piston load and slow growth of force in the initial part of the characteristics to approximately 500 N. The maximum stiffness was calculated from the results: k = 1080.21 N/mm, and flexibility: p = 0.9257$^{(-3)}$ mm/N.

The measurements of the "hard" cushions show a large difference in power between the first and second cushion at up 2335.02 N. This could be due to the difference between hardness of rubber, measured by Shor, which was 4 °Sh. We can only guess why there is such a difference in hardness between the two cushions. Presumably, cushions can be from different production batches, in which a blend of gum differed from each other or the heterogeneity of rubber used was so big. The difference of compared cushion stiffness amounted to: k = 233.502 N/mm, while the difference in flexibility was: p = 0.2553$^{(-3)}$ mm/N.

It is possible that such an impact on the difference in stiffness structure was exerted due to the fact that one of them was broken, or that the cushion worked on the more side more loaded by the torque. The oil pouring from the leak engine on the cushion, which changed its structure and influence the stiffness and hardness could contribute to this as well. It can not be excluded that all of these factors could have an influence on it. The calculated mean stiffness of the cushions was as follows: k = 963.459 N/mm, while the average elasticity was: p = 1.0533$^{(-3)}$ mm/N.

In the case of soft cushions (Fig. 3) we see that the maximum force exerted by the piston on the cushion – 3 was 5727.11 N at deflection of 10 mm. You can also see a fairly small field hysteresis fields. Calculated from the results of maximum stiffness k = 572.711 N/mm, while flexibility: p = 1.746$^{(-3)}$ mm/N.

The maximum force at 10 mm deflection for a cushion – 4, is 6105.1 N and has a fairly small hysteresis deflection field. The maximum stiffness was calculated from the results: k = 610.51 mm/N and flexibility p = $1{,}638^{(-3)}$ mm/N.

In two "soft" cushions we can see a difference in the force exerted by the piston rod, and it is 377.99 N. This could be due to the rubber hardness difference measured by the method of Shor, which was around 1 °Sh. The difference of compared cushion stiffness amounted to: k = 37.799 N/mm, while the difference in flexibility was: p = $0.108^{(-3)}$ mm/N.

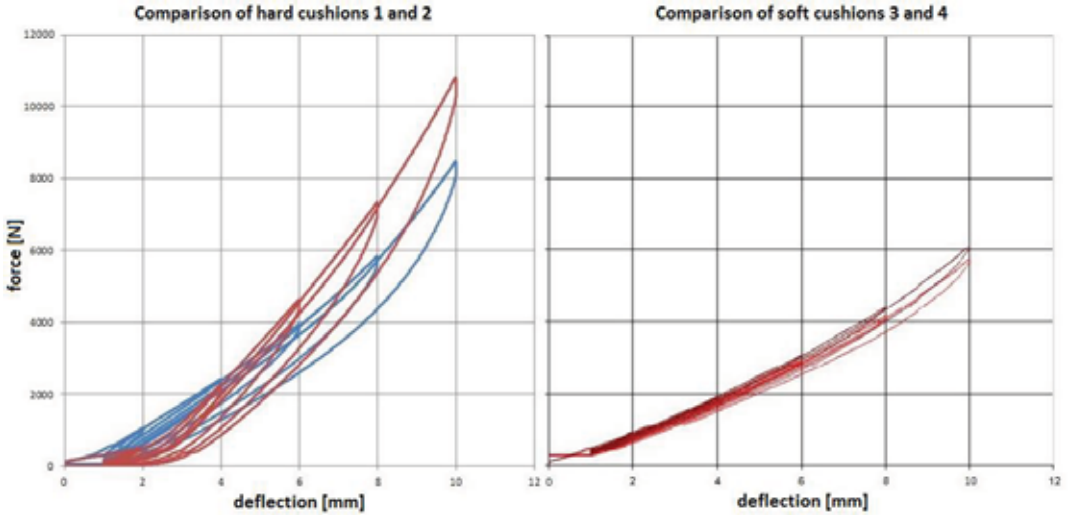

Fig. 3. Comparison of hard cushions tested 1 – blue, and 2 – red, and soft cushions 3 – red, and 4 – black

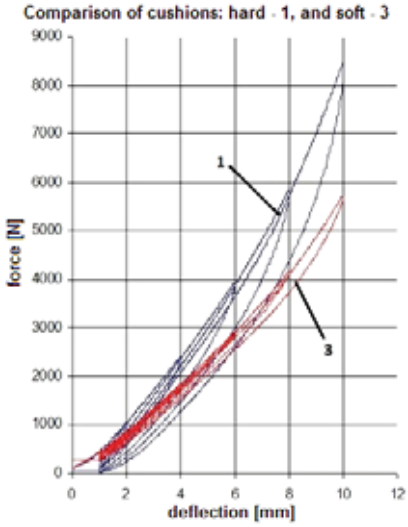

Fig. 4. Graph comparing the results of selected tested cushions, hard – 1, and soft – 3

The graph (Fig. 4) comparing the cushion 1 and 3 shows a rather large difference in strength for the same deflection. This difference is due to the large difference in hardness of used cushions. You might also notice that the hard cushion has a larger deflection hysteresis, which means that slowly returns to its initial state.

This difference is probably due to manufacturing reasons, it is possible that during the production of cushions there was a discrepancy in hardness of rubber. Probably due to the heterogeneity of the rubber used for the production of cushions. What was also evident when measuring the hardness of a cushion in many locations. Comparison of selected average values of stiffness and flexibility of hard and soft cushions are summarized in Table 2. From the comparison of average values can be seen that both the stiffness and flexibility differ by about 38% between hard and soft cushions.

Tab. 2. Comparison of selected average values of the parameters tested cushions

Type of cushion:	The mean value of Stiffness k:	The average value of Flexibility p:
Hard	963.459 N/mm	$1.0533^{(-3)}$ mm/N
Soft	591.610 N/mm	$1.6920^{(-3)}$ mm/N
Difference	371.849 N/mm 38.6%	$0.6387^{(-3)}$ mm/N 37.8%

3. Dynamic cushions researches

Dynamic cushions researches were conducted on running engine at different speeds of the crankshaft. The engine vibrations caused the internal forces of the combustion mixture were measured. Vibrations of a running engine were moved by the arm of a potentiometer (Fig. 5), which processed them and passed voltage to the oscilloscope DSO-2902 256K. The oscilloscope then saved the data after processing them, and the result can be watched on a monitor in graphical form.

Fig. 5. Fixing the measuring system in the engine compartment, 1 – arm mounting location, 2 – the potentiometer arm connecting, 3 – potentiometer

The graphs of the dynamic cushions tests show two colored charts. The graph in green shows the vibration of the engine along with the interference. The graph in black represents the average engine vibration recording parameters, which eliminated the visible peaks of interference. 1 mm deflection in the graph corresponds to 84.75 mA output.

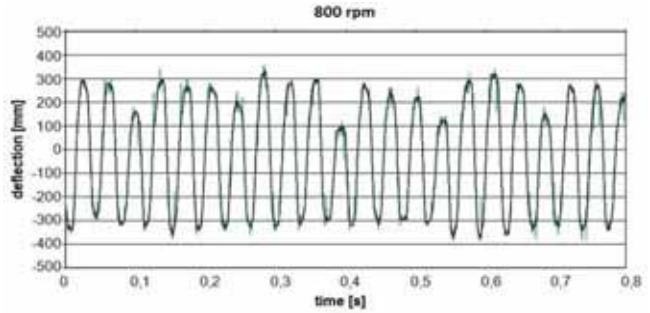

Fig. 6. Sample graph engine vibrations at that speed 800 rpm for hard cushions [11]

Fig. 6 shows a graph of engine vibration on the hard cushions at the speed of 800 rpm. At this engine speed the average deflection was 569.04 mA, which corresponds to 6.71 mm.

Fig. 7 shows a graph of engine vibrations on hard cushions at a speed of 1000 rpm. At this engine speed the average deflection was 479.3 mA, which corresponds to 5.655 mm.

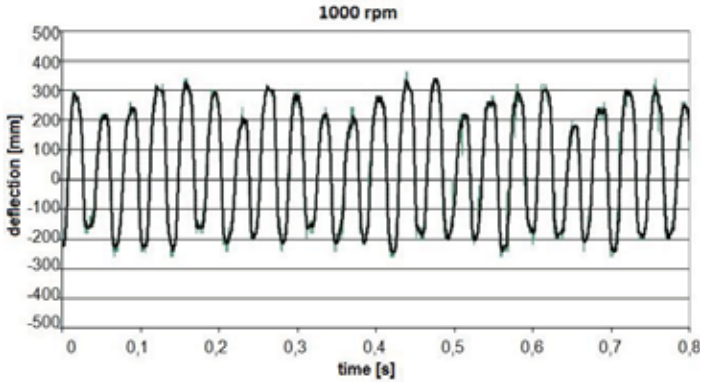

Fig. 7. Sample graph engine vibrations at that speed 1000 rpm for hard cushions [11]

Fig. 8 shows a graph of engine vibration on hard cushions at a speed of 1500 rpm. At this engine speed the average deflection was 59 mA, which corresponds to 0.696 mm.

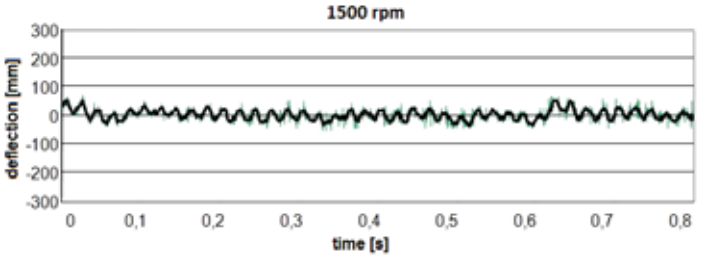

Fig. 8. Sample graph engine vibrations at that speed 1500 rpm for hard cushions

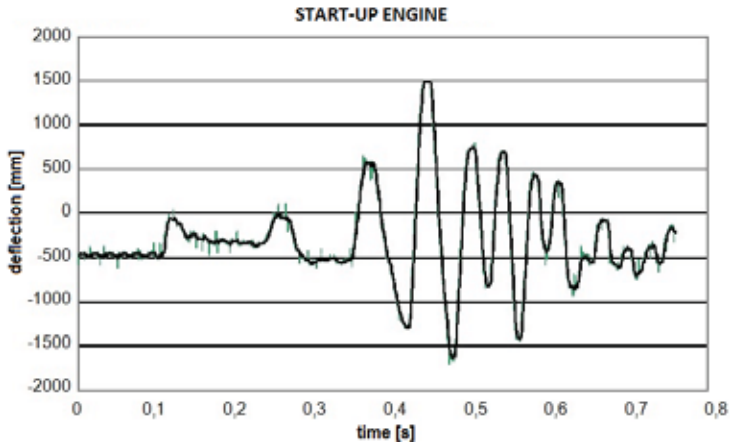

Fig. 9. Sample graph engine vibrations at the start-up process for hard cushions [11]

While in Fig. 9 there is a graph of engine vibrations on hard cushions at the start. At this point, the maximum deflection was 3163 mA, it is 37.3234 mm.

The graph shown in Fig. 10 is an engine vibrations sample chart at speed of 800 rpm, for the soft cushions. At this engine speed the average deflection was 537.91 mA, which corresponds to 6.35 mm.

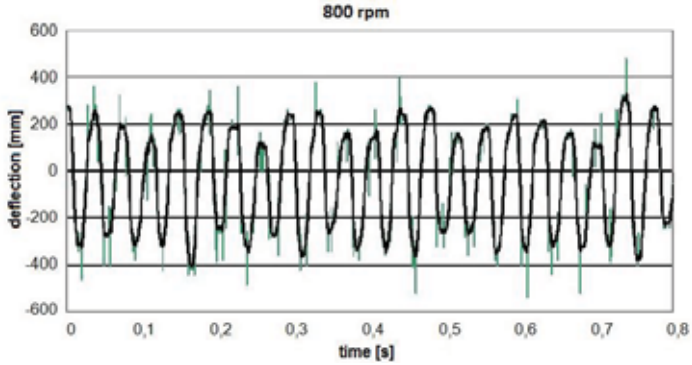

Fig. 10. Sample graph engine vibrations at that speed 800 rpm for soft cushions [11]

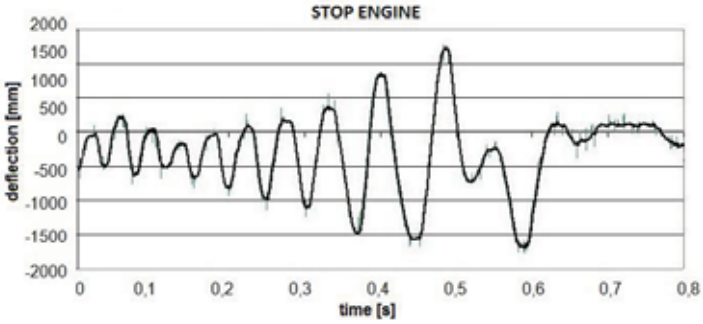

Fig. 11. Sample graph engine vibrations at the stop engine process for soft cushions [11]

Fig. 11 shows a graph of vibration when the engine is stopped for a soft cushion. At this point, the maximum deflection of the engine was 2930 mA, which is appropriate for the value of 34.57 mm. Resonant frequency is below the idle speed as shown on the chart of the course of engine start and stop. The value of the resonant frequency of operation in these states is 12.5 Hz.

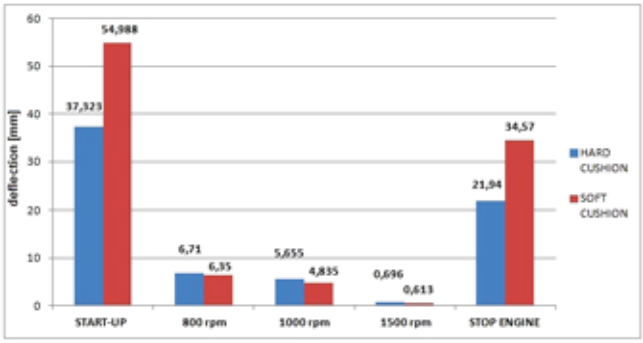

Fig. 12. Sample comparison chart of the amplitude of vibration engine in various states of his work

Figure 12 summarizes the mean amplitude values for the studied operating conditions of diesel engines. The amplitude values of vibration for each status and the type of cushions were indicated. Clearly, two work states stand out from the rest and there are: engine starting and stopping. It was also noted that smaller vibrations occur when the engine works on hard cushions. When stopping the engine for maximum deflection of the hard cushion was 21.94 mm (1859 mA), and 34.57 mm for soft cushion (2930 mA). The difference between the type of cushions are up to about 38%. At the time of commissioning the difference amounted to about 32%. The amplitude of the engine vibration for soft cushions was 4660 mA (54.988 mm), and for the hard cushions – 3163 mA (37.323 mm).

In the other operating conditions, ie when the crankshaft rotational speed: 800, 1000 and 1500 rpm, the difference between the amount of amplitude are smaller. Under these operating conditions the vibration differences are smaller and do not exceed 17%.

4. Conclusions

The researches showed large differences in the application of investigated types of cushions in 4C90 diesel engine in a terrain car UAZ. The assumption of differences in Shor hardness test method for cushions were confirmed: the "hard" (83 and 79) °Sh and "soft" (61 and 62) °Sh. Researches have shown flexibility in large variations of forces at the maximum deflection of 10 mm for a "hard" cushion (10802.10, 8467.08) N and for "soft" (5727.11, 6105.20) N. Average stiffness of "hard" cushions was 963.459 N/mm, while of the "soft" ones was 591.61 N/mm, a difference of 371.849 N/mm (approx. 38%). This discrepancy is probably due to different composition of the mixture of rubber used in the production of those connectors.

It was observed that at the "soft" cushions the engine vibration were smaller relative to the body, which was also felt in the car while driving and at the idling engine speed. While "hard" cushions caused great vibration and generated more noise inside the vehicle. Analyzing graphs of the engine vibration height differences of amplitudes can be observed. This is probably due to differences in the way of combustion of the mixture in each cylinder of the engine. It is clear that every fourth peak on the graph is smaller than the other three. It follows that one of the cylinders produces less power and can testify about its disability.

Such researches can also be used to determine the efficiency in each cylinder. The authors are preparing for further research on this vehicle with a new diesel engine fitted with direct injection into the combustion chamber. The results of the tests of different types of plate connectors for the

engine suspension can be useful when designing propulsion systems for military vehicles and military terrain cars, or as shown by the author [1, 4] to modernize of the existing military vehicles stock.

References

[1] Gardyński, L., *Spostrzeżenia z eksploatacji samochodu terenowego Uaz 31512 z zamontowanym silnikiem wysokoprężnym Andoria 4C90*, Problemy eksploatacji uzbrojenia i sprzętu wojskowego EKSPLOLOG 2004, pod red. K. Kowalskiego, s. 51-60, Wrocław 2004.

[2] Gardyński, L., Kiernicki, Z., *Diesel do uaza cz. I. czy warto?,* Off-road pl magazyn 4x4, nr 6/2001, s. 22-29, Kraków 2001.

[3] Gardyński, L., Kiernicki, Z., *Diesel do uaza cz. II. no to montujemy*, Off-road pl magazyn 4x4, nr 7/2001, s. 17-19, Kraków 2001.

[4] Gardyński, L., Kiernick,i Z., *Wpływ zastosowania silnika wysokoprężnego na właściwości trakcyjne samochodu terenowego uaz-469b*, Teka Komisji Motoryzacji i Energetyki Rolnictwa PAN tom 1., s. 122-129, Lublin 2001.

[5] Grajnert, J., *Izolacja drgań w maszynach i pojazdach*, Oficyna Wydawnicza Politechniki Wrocławskiej, Wrocław 1997.

[6] Gryboś, R*., Drgania maszyn*, Wydawnictwo Politechniki Śląskiej, Gliwice 2009.

[7] Jaworski, J., *Guma w pojazdach mechanicznych*, WKiŁ, Warszawa 1976.

[8] Parszewski, Z., *Drgania i dynamika maszyn,* WNT, Warszawa 1982.

[9] Pękalak, M., Radkowski, S., *Gumowe elementy sprężyste,* PWN, Warszawa 1989.

[10] Praca zbiorowa: *Guma, Podręcznik inżyniera i technika*, WNT, Warszawa 1981.

[11] Praca dyplomowa, Drzewny, J., *Układy zawieszenia zespołu napędowego w pojeździe,* Politechnika Lubelska, Lublin 2011.

[12] Wajand, J. A., Wajand, J. T., *Tłokowe silniki spalinowe średnio- i szybkoobrotowe*, WNT, Warszawa 2005.

Journal of Polish CIMAC
Gdansk University of Technology
The Faculty of Ocean Engineering and Ship Technology

DIAGNOSTICS OF VESSEL POWER PLANTS

Adam Charchalis

Gdynia Maritime University
Morska str. 81-87, 81-225 Gdynia, Poland
Tel.: +48 58 69 01 347
e-mail:achar@am.gdynia.pl

Abstract

In this paper, the problems of diagnostics of main propulsion marine engines are presented. Marine engine is a complex technical object. For the purpose of diagnostics is convenient to divide the engine into several units – subsystems such as: piston –crank assembly; working medium exchange system, fuel supply system, lubricating system, cooling system, starting up – reversing system; combustion chamber. The organization of the marine engine diagnostic process can usually come down to two stages, general diagnostics and damage location. The diagnostic system of marine engine is able to assess the current engine condition and give forecast concerning its future operation in a complex way with the use of computer technology. Working out operating decision was based on proper preparation of operational parameters which were processed in a computer according to defined algorithms. Diesel engine diagnostic systems of merchant vessel engines are discussed. Marine engines operate under specific conditions which have a considerable influence on their characteristics change and can cause their increased wear and even failure.

Marine engines run in constant rolling conditions. Although rolling does not directly affect the characteristic change, it can cause systematic wear of engine components i.e. bearings.

Keywords: *technical diagnostics, piston engines, gas turbine engines, vessel power plants*

1. Introduction

Type and number of technical parameters which require assessment without disassembling, can affect diagnostic method and have indirectly influence at the costs of a diagnostic system. The most numerous are the engine construction parameters which are as follows:

- components dimensions in their wear areas
- clearances
- condition of working surfaces and their wear geometry
- assembly and adjustment settings
- cleanness of heat exchange surfaces and flow of working medium ducts
- parameters characterizing static connections condition (bolts tension etc.)

The parameters which characterize the quality of lubricating oils, fuel, cooling water should be included in the set of engine technical condition parameters. Engine technical condition parameters with their graphic values and the frequency of overhauls and checks are given in operating manuals by the manufacturers. It appears that the number of engine technical condition parameters is about 50 only for one section of medium speed engine. If this number is multiplied by the number of cylinders and they are added to parameters characteristic for the whole engine, its

machinery and systems – the total number will be enormous and as a result the task of technical condition evaluation without disassembly will practically be impossible. In marine engine, diagnostic evaluation without disassembly, most of these parameters is rejected and attention is paid to the most relevant parameters from the point of view of engine reliability, economical work and cost effective operation. Therefore each engine is divides into particular functional, tribological units [3].

2. Description of test equipment

Contemporary exploitation of machines requires certain level of supervision, due to their high level of complication of the structure. That kind of supervising relay on detection of pre-failure states and evaluation of condition of elements or modules. In the frame of development of research capacity in Mechanical Faculty of Gdynia Maritime University, has been developed the exploitation decision assistance system for industrial machinery, including marine mechanisms, in the way of building from scratch the laboratories of:

- Technical Diagnostics
- Tribology
- Surface Engineering

Those three laboratories, which equipment was funded by Ministry of Science and High Education in the frame …….are expected to enable realization of advanced research programs and contracted research in diapason of technical diagnostic, technical security engineering, analysis of mechanisms reliability, tribology and surface engineering.
The Technical Diagnostic Laboratory consist of equipment listed below:

- ✓Vibration Analyzer PULSE by Brüel & Kjaer,
- ✓ Acoustic Emission Set by Vallen System,
- ✓Analyzer/Recorder of working process by Sefram Instrumens & Systems,
- ✓Mobile Gas Analyzer by Testo,
- ✓Industrial Video endoscope XLG3 by Everest,
- ✓ Thermo vision Camera by NEC Avio Co.,Ltd,
- ✓Electronic Indicator of cylinder pressure of the piston engine

2.1. Vibroacoustics

Vibration signals are carrying much information about technical condition of a machine and are a base for utilization in signals' monitoring systems as a condition trends factor of a machine. Spectral analysis of signals enables an identification of a failure type. Vibration signals monitoring is useful also for evaluation of bearing nodes, condition of shafts, and frictional couplings, including gears meshing and blades arrangements into rotary machines.

The vibration analyzer is the 6. channel recorder type 3050-A-60, the module LAN-XI 51,2 kHz (CCLD, V) Brüel & Kjaer. The set includes also the acoustic calibrator 4231 and the calibration's exciter 4294. The set consist also the tachometer probe MM360, set of microphones 4189-A-021 and the accelerometer 4515-B. Measurements and analysis are carried out using computer program PULSE time (FFT analysis program, harmonic analysis, signals' recorder). All is governed by the central station. The range of output voltage for typical accelerometer/microphone with build-in amplifier CCLD is 120 dB for broad band 10 Hz – 51 kHz, and 160 dB for narrow band 6 kHz. Maximum peak voltage is 10 V, and linearity ± 0,03 dB in the range of 120 dB. Data processing in the analyzer is 24 bit mode. Registered frequencies band is DC – 51 kHz. Measurement's windows are presented in the fig. l.

2.2. Oil spectral analysis

The spectrometer is analyzing traces of radicals coming from: oil additives, wear processes and outer contamination. Comparison of results with previous ones and permitted limits enables observation of the normal mechanical wear process or early detection of potential damage, at its early stage. Moreover, enables evaluation of oil condition in reference to content of additives. It concerns mostly synthetic oils.

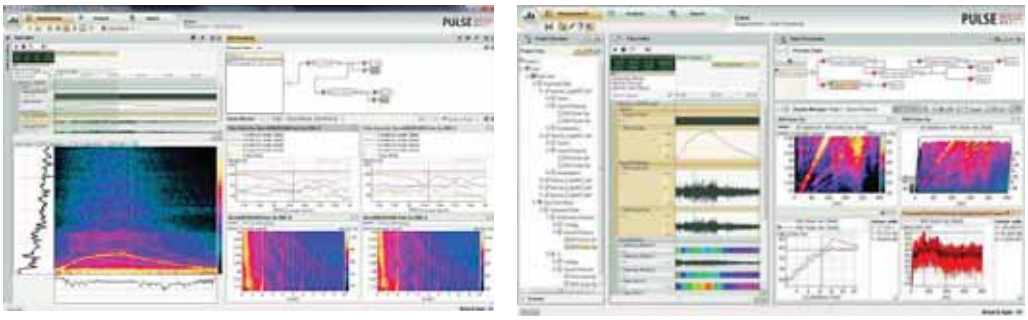

Fig. 1. Samples of display windows

The spectrometer measures contents of radicals dissolved or floating particles in mineral or synthetic products, using the method of a rotational disc electrode (RDE). Basic configuration of the spectrometer enables detection of 22 radicals, ie. : Al, Ba, B, Cd, Ca, Cr, Cu, Fe, Pb, Mg, Mn, Mo, Ni, P, K, Si, Ag, Na, Sn, Ti, V, Zn.

The spectrometer range can be extended, what let detection additional radicals:
Sb, Bi, As, In, Co, Zr, W, Sr, Li, Ce and detection of radicals In cooling liquids and water. In the fig.3. is presented the picture of Spectrometer Spectroil Q100.

Fig.2. Picture of spectrometer Spectroil Q100

2.3. Video endoscope research

Video endoscope Everest XL G3 enables evaluation of technical condition of internal spaces, for example marine engines and machines, permanent and mobile pressure tanks, pipelines and masts, with possibility of dimensional evaluation of defects, visualization at LCD display and

video recording. 3D phase measurement enables inspection and measurement of defects by only one lens, what eliminate necessity of its replacing by measurement lens. It lets scanning and measurement in 3 dimensions every detected discontinuity. Phase measurement analyzes available in observation zone (105^0) surface, and creates 3 dimensional movable model. Working probe in the system XL G3 is exchangeable. The sample of quantity evaluation of a damage is presented in fig.3.

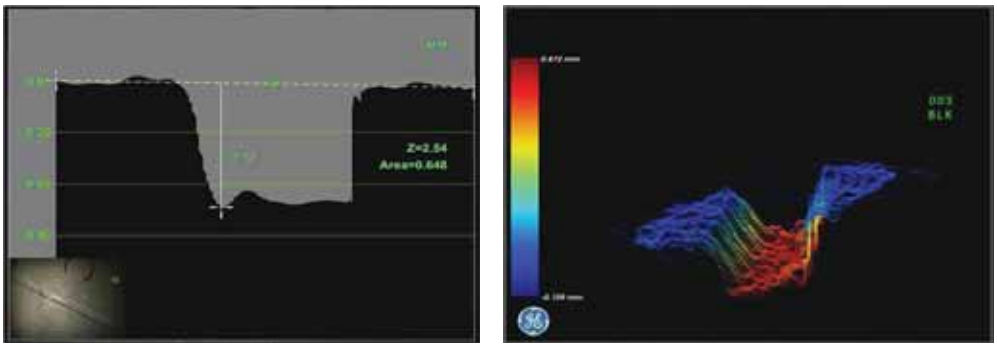

Fig.3. Sample of evaluation of damage parameters

2.3. Thermo vision research

Thermo vision camera Thermo Gear G100 from Japanese manufacturer NEC-AVIO Co., Ltd. enables tracking processes related to changes of temperature or emission in time or related to differentiation of thermal pictures of selected individual objects. The camera gives to operator many possibilities if measurement. It has a temperature preview function for 5 random points of the picture, with possibility of setting up individual coefficients of emission for every point. The camera enables also maximum/minimum temperature at whole display or in selected area, the value of difference of temperatures between two selected points, or linear profile of temperature.
As the camera is equipped with the optical focus with resolution 2 000 000 pixels, also registration of optical picture is possible. Pictures can be presented separately, parallel (one next to one at the display) or in penetrating mode.

During analysis of the picture one has to put attention at changes of mutual position of pictures in relation to the distance from observed object. In fig 4. the sample of modified optic-thermal picture is presented.

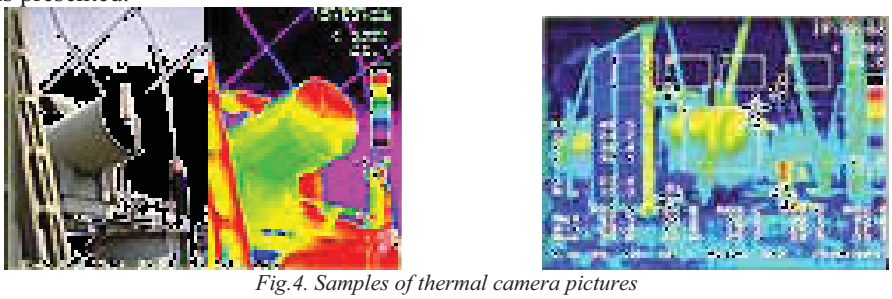

Fig.4. Samples of thermal camera pictures

The camera enables broad implementation for diagnostic research of machines and mechanisms as well research of technologic or energetic process.
The camera is equipped with the detector with dimension 320x249 elements. Works in real time, with refreshing frequency 60Hz. It has thermal sensitivity at least 0,08 ^{0}C at ambient temperature

30^0C. The camera can register temperatures in diapason from -400^0C to 500^0C, divided to two sub-ranges: -400^0C to 120^0C and 0^0C to 500^0C with accuracy ±20^0C or ±2%.

2.4. Acoustic emission measurement method

The AE method relay on detection and analysis of acoustic signal, emitted by a material being under mechanical stress. Emitted elastic waves are a result of interval elastic energy release. Thus energy is a phenomenon related to physical process taking place in materials or at their surface. Processes accompanying by acoustic emission are plastic displacement, cracking, structural and phase changes, corrosion, leaking and fibers cracking in composite materials. Accurate analysis enables definition of sources and kind of acoustic emission. Fig.5. presents the sample of AE signal run.

The set for non-invasive (without disassembling or destroying) measurement of a wear level of machines elements being under stress, deformations or load e.g. the wear of injectors, pumps, hydraulic elements, stress state of a fuselage or a hull sheets, pipelines e.t.c.

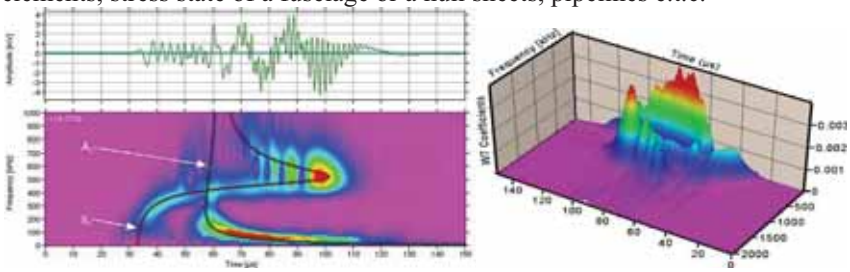

Fig.5. The run of AE signal in domain of time

The AE measurement set consist of 4 channels signal recorder AMSY 6 and the measurement module ASIP-2/S by Vallen System (Fig.6). The system is equipped with pre amplifier with a frequency range 20kHz to 1MHz and amplification 34dB, and AE signal sensor with range 100 – 450 kHz. The set has the recording module, putting down 8 MB's data bunches for every channel and data registration and analysis program.

Fig. 6. The AE method measurement set by enterprise Vallen

2.5. Marine engines exhaust gas analysis

The mobile set dedicated for marine engines exhaust gas analysis enables measurement of emission of exhaust gases' toxic substances of different kinds of internal combustion engines, stationary or locomotive.

The set consist of high quality exhaust gas analyzer 350 XL by TESTO, including a industrial probe with particles filter, a infrared sensor calibration system and a rigid case. The analyzer has

the Germanischer Lloyd Certificate, giving legacy for tests on board ships, in accordance to MARPOL Convention Attachment VI. Moreover, the set is equipped with the integrated temperature and humidity sensor, and atmospheric pressure gauge. Sensors are connected by 16 channels digital - analog transducer with industrial computer with dedicated programs, as a recorder. The recorder lets simultaneously connect all gas sensors, ambient parameters gauges and additional 13 random physical values sensors having standard 0-10 V outputs. The recorder has built-in parallel port RS-232, for connection with the recorder of TESTO analyzer. In fig.7. is presented the set of Exhaust gas analyzer Testo 350XL, and in tab.1.,exhaust gas measurement range.

Fig.7. Exhaust gas analyzer Testo 350XL

Tab. 1. Gas analyzer measurement range

Parameter	Range	Unit
oxygen - O_2	**0 – 21**	**% Vol.**
carbon monoxide - CO	**0 – 5000**	**ppm**
carbon dioxide - CO_2	**0 – 20**	**% Vol.**
nitric oxide - NO	**0 – 2500**	**ppm**
nitro dioxide - NO_2	**0 – 500**	**ppm**
sulphur dioxide - SO_2	**0 – 3000**	**ppm**
gas temperature at measurement point	**0 – 1000**	**ºC**
dynamic pressure	**do 20**	**kPa**

References

[1] Charchalis A., *Conditions of Drive and Diagnostic Measurements During Sea Tests* Journal of Kones vol. 14/4, Warszawa 2007.

[2] Charchalis A., *Nadzór eksploatacyjny siłowni z turbinowymi silnikami spalinowymi* PROBLEMY EKSPLOATACJI nr 4/2001.

[3] Pawletko R. Polanowski S., *Influence of TDC determination methods on mean indicated pressure errors in marine diesel engines*. Journal of KONES, Vol. 18, No. 2, Warsaw 2011.

[4] Pawletko R. Polanowski S., *Acquisition of diagnostic information from the indicator diagrams of marine engines using the electronic indicators.* Journal of KONES, Vol. 18, No.3, Warsaw. 2011

[5] Pawletko R. Polanowski S., *Research of the influence of Marine diesel engine Sulzer AL 25/30 load on the TDC position on the indication graph.* Journal of Kones Powertrain and Transport, Vol. 17, No. 3, Warsaw 2010.

Journal of Polish CIMAC
Gdansk University of Technology
The Faculty of Ocean Engineering and Ship Technology

FINISHING OF THE METAL MATRIX COMPOSITE COATINGS APPLIED TO REGENERATED PARTS OF SHIP MACHINERY

Tomasz Dyl

Gdynia Maritime University
Faculty of Marine Engineering
Department of Marine Maintenance
Morska Street 81-87, 81-225 Gdynia, Paland
tel.: +48 58 69 01 249, fax: +48 58 69 01 399
e-mail: dylu@am.gdynia.pl

Abstract

Most elements of ship machinery parts are regenerated during the cruise ship. Engineer often regenerates cylindrical outer surfaces (for example torque pump shaft neck). The welding technology of applying alloy and composite coatings is very common. The technology of infrasound thermal spraying of metal matrix composite coatings was presented. It is a simple technology and a very useful one in ship machinery regeneration during the cruise craft (e.g. internal combustion engines, torque pumps, separators). The metal matrix composite coatings must undergo finishing due to high surface roughness after application. The most popular is machining (e.g. turning or grinding). The authors also propose the application of finishing through turning. The paper should influence of the type of inserts on the geometric structure of the alloy Ni-5%Al and composite Ni-5%Al-15%Al_2O_3 coatings. Nickel - aluminium matrix composite coatings on were sprayed with a torch Casto-Dyn 8000 a steel substrate, and then turned lengthwise. In order to determine the optimum geometry of indexing, it is now synonymous with the selection of the optimum shape and dimensions of the insert and an appropriate holder. The insert was used in different shapes and geometries: square, triangular, trigon, made tungsten carbide and cubic boron nitride (CBN).

Keywords*: finishing coatings, metal matrix composite coatings, flame spraying, regenerated parts of ship machinery*

1. Introduction

The processes of production and regeneration of the applied metal matrix composite coating products are recognized among engineers, technologists, because of the possibility of increasing the performance characteristics of the surface layer (strength, tribological, corrosion and decorative). Metal matrix composite and metal alloy and coatings of metal matrix dispersion inclusions of non-metallic phase is characterized by high resistance to tribological wear and corrosion [1÷10]. Metal matrix composite are used in such fields of technology, such as: aerospace, electronics, energy, industry, defense, automotive, aviation, shipbuilding, and more. Based on a literature review, the study assumed composite coatings based on nickel with aluminum and with a variable content of alumina [11÷15]. Coatings obtained by flame spraying have a large surface roughness. Therefore, these coatings must be subjected to finishing (eg, turning finishing, grinding). Flame sprayed coatings are applied taking into account the allowance for finishing. Finishing should ensure not only the thickness of coatings related to the nominal dimension of the object, but also to obtain the required surface roughness and waviness. Choosing

parameters (feed rate, depth, cutting speed) machining coatings must be remembered that the tool does not always cut sprayed particles, but may cause them breaking the surface. This occurs primarily in coatings of high porosity. Cutting knives, cutting elements should be made of cubic boron nitride or diamond, also allows the insert tool made of tungsten carbide is recommended by "Castolin-Eutectic" [16].

On ships, outboard water systems (eg, a central cooling system), often used in centrifugal pumps. In the case of pump shafts are the most common disability shaft neck wear (corrosion and friction) at the installation location of seals (stuffing-box). Currently, the primary method of regeneration is the shaft bushing. As an alternative to the method used to repair worn of centrifugal pumps shafts neck proposed flame spraying. The flame sprayed technology is inexpensive and easy to implement. Therefore it can be successfully used for regeneration of machine parts by the crew of ship engine room. Flame sprayed coatings are characterized by porosities, oxide inclusions and the presence of a strongly developed surface float. In order to obtain a suitable surface texture coatings finishing must be used. For this purpose, the turning and grinding. The paper proposes turning the finishing flame sprayed coatings. Alloy coatings were investigated Ni-5%Al and composite Ni-5%Al-15%Al_2O_3 powders obtained by flame spraying. Using a torch "Casto-Dyn 8000" Messer Eutectic Castolin company. In practice, the thermally sprayed coatings are machined using the same tool as machined surface. For example, a company Messer Eutectic Castolin proposed multi tool with a square or cylindrical inserts. Machining alloy coatings were carried out for the cutting speed V_c=214m/min in the case of treatment with inserts of CBN, V_c=107m/min cutting plates for tungsten carbide, used feed f_n=0.06mm/rev and depth of cut a_p=0.3mm. Metal cutting the surface of steel samples coated with a composite coating containing, conducted for the cutting speed V_c=157m/min when machining with CBN inserts and for V_c=83m/min inserts with tungsten carbide for feed f_n=0.06 mm/rev and depth of cut a_p=0.3mm. On ships during the voyage is made of many elements of the repair of ship engines. Often the cylindrical surfaces are regenerated (eg pump shaft). Technologies are widely applied welding coating alloy and composite. This paper proposes the use of technology subsonic flame thermal spraying and surface treatment by turning alloy and composite coatings. These are simple technologies, useful for repair of ship engines (such as engines, pumps, separators) during the voyage.

2. Research methodology

Alloy and composite coatings were applied for degreased samples stainless steel. Coatings on nickel-based alloy was flame sprayed powder material 21021 ProXon company "Castolin", where the percentage share of the mass was: Ni - 93.45%, Al - 5%, B - 0.8%, Fe - 0.34% , Cr - 0.18%, Si - 0.15%, C - 0.08%. Coatings for metal matrix composite MMC, were sprayed with a mixture of powdered ProXon 21021 and MetaCeram 28020 (Al_2O_3 - 97.7%, TiO_2 - 2.2%, SiO_2 - 0.1%). These powders were manufactured by Castolin. Composite coating material consisted of a matrix of Ni-5%Al and 15% of the disperse phase volume fraction of alumina (Al_2O_3). Spray torch was used, "Casto-Dyn 8000", the company Castolin. Flame spraying alloy coatings and composites were carried out assuming the following process parameters: pressure flammable gas - acetylene: 0.07MPa oxygen pressure: 0.4MPa, air pressure: 0.1MPa, the speed of the torch 25m/min, feed rate: 3mm/rev, the distance from the torch surface to be sprayed: 150mm, the number of superimposed layers: 6. Steel substrate pre-heated in the temperature range 60÷100°C. Flame spraying was carried out at temperatures exceeding 250°C. Then the coating have been subjected to very thorough turning straight. To determine the parameters of machining alloy coatings and composites based on nickel flame sprayed onto the substrate steel, preexperimental study was conducted longitudinal turning high precision. Fought with different cutting speed (V_c = 45 ÷ 214 m/min), feed rate (f_n = 0.06 ÷ 0.2 mm/rev) and depth of cut (a_p = 0.05 ÷ 0.3 mm). Based on analysis of test results determined that the best surface quality obtain samples of coated steel,

nickel based alloys for the cutting speed V_c = 214 m/min in the case of treatment with inserts of borazon, V_c = 107m/min platelets treated with cemented carbide cutting. Then determined that the best gain of the sample surface quality of coated steel composite for cutting speed V_c = 157 m/min, in the case of treatment with CBN inserts, Vc = 83 m/min after treatment cemented carbide inserts.

For machining alloy coatings and composites used feed f_n=0.06mm/rev and depth of cut a_p=0.3mm.

Longitudinal turning, were subjected to a thorough external cylindrical surfaces of steel samples of alloy and composite coatings ϕ41mm in diameter with a thickness of 2 mm. To determine the optimal geometry of the cutting tool, now it is synonymous with the selection of the optimum shape and dimensions of the insert and the appropriate holder, edged square tiles were chosen, round, triangular, trigon, made of tungsten carbide (with grades: GC2015, GC3205, GC3210, GC3215, GC4015, H10F) and cubic boron nitride (CBN, grade CB7015). The research program is presented in Table 1. Surface texture of the alloy and composite coatings was measured with a Hommel Tester T1000 profilometer. During the turning of alloy and composite coatings is usually short durability of the insert. It is therefore important to determine the spiral cutting length. This is the length cutting, which are chosen for recommended cutting, thus allowing for a reliable process. Spiral cutting length is applied to the insert, geometry, and grade, depth of cut and material that shall be subject machined. Spiral cutting length (SCL, m) can be calculated from the formula [17]:

$$SCL = \frac{\pi \ D_m}{1000} \frac{l_m}{f_n} \tag{1}$$

where: D_m - the diameter of the workpiece in the machined surface, mm (ϕ41mm),
l_m - length of the machined surface, mm,
f_n - feed rate, mm/rev.

Table 1. The shape and grade inserts

Sample Number Alloy Coating	Sample Number Composite Coating	Insert Shape	Insert Type	Holder Type	Insert Grade
1	1.123	Square	SNGA 120408 S01030A	DSDNN 2525M 12	CB7015
2	2.123	Round	N123J1-0600-RE	RF 123J13-2525BM	CB7015
3	3.100	Triangular	TNMX 160408 - WM	DTGNR 2020K 16	GC4015
4	4.100	Triangular	TNMG 160408 - 23	DTGNR 2020K 16	H10F
5	4.020	Trigon	WNMG 080408 - WF	DWLNRL 2525M 08	GC2015
6	5.123	Trigon	WNMG 080408 S01030A	DWLNRL 2525M 08	CB7015
7	6.100	Trigon	WNMA 080408 - KR	DWLNRL 2525M 08	GC3205
8	6.020	Trigon	WNMG 080408 - KM	DWLNRL 2525M 08	GC3205
9	6.003	Trigon	WNMG 080408 - KM	DWLNRL 2525M 08	GC3210
11	4.003	Trigon	WNMG 080408 - KF	DWLNRL 2525M 08	GC3215

3. Results of research

Samples with applied alloy and composite coatings was turned by turning tools the different types of inserts by Sandvik-Coromant. The study allowed for determination, that there are

relationships between the surface texture of alloy and composite coatings and the type of grade used and the shape of the inserts. Trigon insert WNMG 080 408 S01030A and round insert N123J1-0600-RE 7015 of CBN was characterized by a smaller flank wear as compared to a square insert with SNGA 120 408 S01030A 7015 of CBN.

Table 2. Surface texture parameters turned alloy coatings Ni-5%Al

Sample Number	R_a, µm	R_z, µm	R_k, µm	R_{pk}, µm	R_{vk}, µm	$R_{mr(50.0\%)}$, µm	M_{r1}, %	M_{r2}, %	R_{sk}, µm	W_t, µm
1	1,07	5,79	3,29	1,60	0,91	4,78	13,1	91,1	0,481	3,99
2	0,39	3,29	1,26	0,62	0,99	2,16	13	86,2	-0,336	2,05
3	0,49	2,87	1,29	0,57	0,61	1,95	6,7	88,8	-0,156	2,35
4	0,82	4,21	2,96	1,41	0,38	3,97	15,3	97,4	0,882	12,24
5	0,51	3,52	1,71	0,96	0,69	2,57	10,6	92,1	0,555	2,39
6	0,47	2,79	1,51	0,81	0,55	2,58	9,6	88,3	0,546	1,63
7	0,79	5,22	2,41	0,71	1,25	3,27	7,1	84,2	-0,456	2,65
8	0,85	5,86	2,54	0,54	1,58	2,61	7,1	85,1	-0,685	1,38
9	0,65	4,20	2,09	0,61	0,95	1,89	8,6	87,9	-0,317	2,53
11	0,54	3,79	1,52	0,45	1,26	1,54	6,7	83,2	-0,904	3,07

Surface roughness (refer with: Table 2) of the surface texture alloy coatings of Ni-5%Al turned insert trigon (R_a=0,47µm) and round (R_a=0,39µm) is nearly three times smaller than the roughness of the coatings faced a square insert (R_a=1,07µm). Using the trigon insert made of tungsten carbide determined that the minimum surface roughness of alloy coatings are obtained for grade GC3215 (R_a=0,54µm). After turning composite Ni-5%Al-15%Al_2O_3 using square insert SNGA120408S01030A 7015, specifies that the arithmetical mean deviation of the assessed profile reached a lower value of R_a=1.08µm (refer with: Table 3) in comparison to the roughness of the surface texture with the trigon insert made of the same grades (CB7015) and also with the trigon of tungsten carbide (about the grades: GC2015, GC3205, GC3210, GC3215) and tungsten carbide (for grades: GC4015, H10F) for triangular inserts. The lowest surface roughness R_a=0.65µm (refer with: Table 3) is achieved, composite coating turned insert round N123J1-0600-RE 7015. Round insert after turning composite coatings are characterized by the lowest flank wear compared to the square, trigon and triangular.

Table 3. Surface texture parameters turned composite coatings Ni-5%Al-15%Al_2O_3

Sample Number	R_a, µm	R_z, µm	R_k, µm	R_{pk}, µm	R_{vk}, µm	$R_{mr01(50.0\%)}$, µm	M_{r1}, %	M_{r2}, %	R_{sk}, µm	W_t, µm
1.123	1,08	6,72	3,34	1,49	1,28	4,89	11,9	88,1	0,224	4,69
2.123	0,65	6,33	2,68	0,81	2,23	2,82	7,1	89,9	-1,775	5,89
3.100	2,98	17,45	6,96	2,59	8,73	9,56	9,1	79,9	-1,148	19,87
4.100	3,04	18,98	7,24	1,93	7,65	7,85	6,7	79,1	-0,926	10,26
4.020	2,74	15,70	3,57	1,82	9,94	5,73	8,6	72,2	-1,721	6,58
5.123	1,51	13,6	3,89	2,93	6,42	6,58	8,3	84,9	-1,864	11,99
6.100	3,00	20,63	6,40	2,33	9,12	7,87	6,5	76,2	-1,619	13,03
6.020	3,55	23,82	8,24	1,97	9,27	9,05	6	75,9	-1,181	17,32
6.003	3,71	21,19	9,24	4,09	9,42	13,58	4,8	79,7	-1,062	14,85
4.003	3,75	22,73	9,08	2,21	10,13	8,84	7,0	79,3	-0,948	11,63

Figure 1 and Figure 2 shows the arithmetical mean deviation of the assessed profile for turned alloy Ni-5%Al and composite Ni-5%Al-Al_2O_3 coatings.

a)

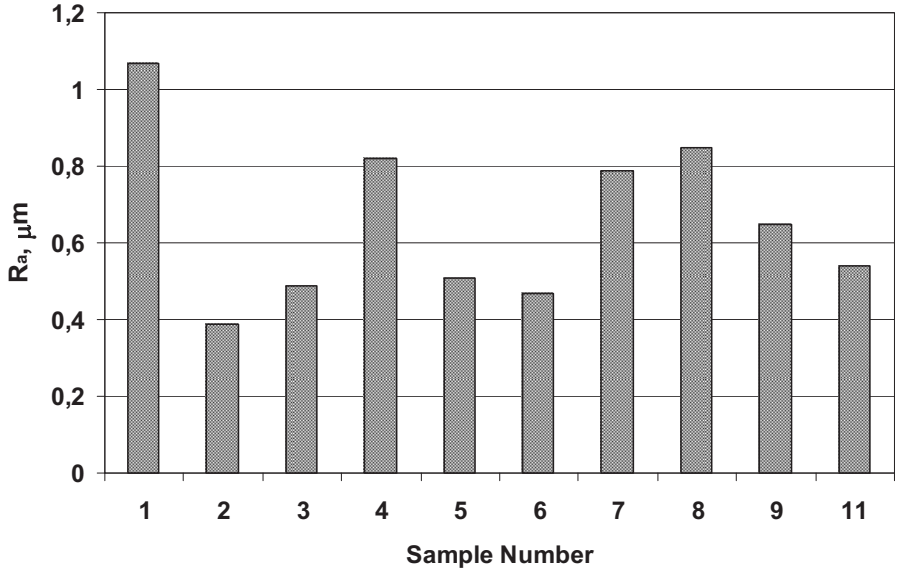

b)

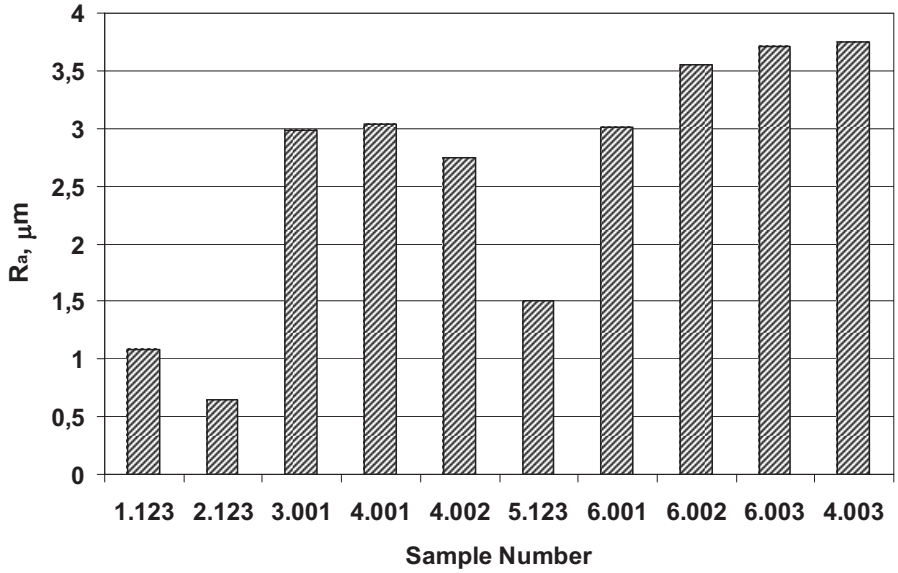

Fig. 1. The arithmetical mean deviation for coatings: a) alloy Ni-5%Al and b) composite Ni-5%Al-15%Al_2O_3 for turned samples inserts according to the research program

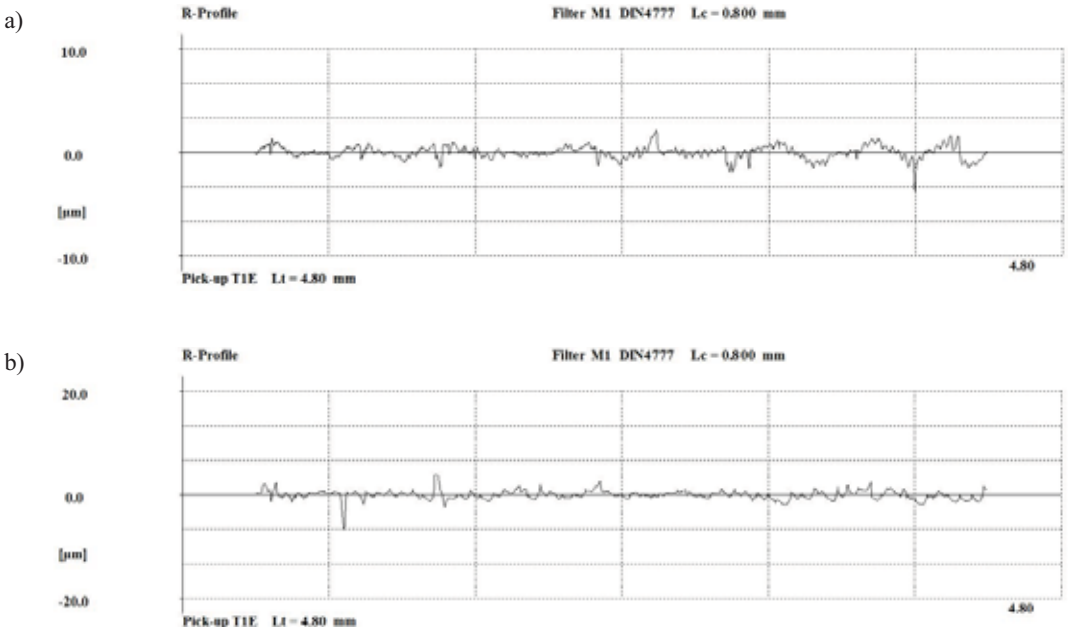

Fig. 2. The arithmetical mean deviation for coatings a) alloy Ni-5%Al (R_a=0,39µm) and b) composite Ni-5%Al-15%Al_2O_3 (R_a=0,65µm) for round insert N123J1-0600-RE 7015

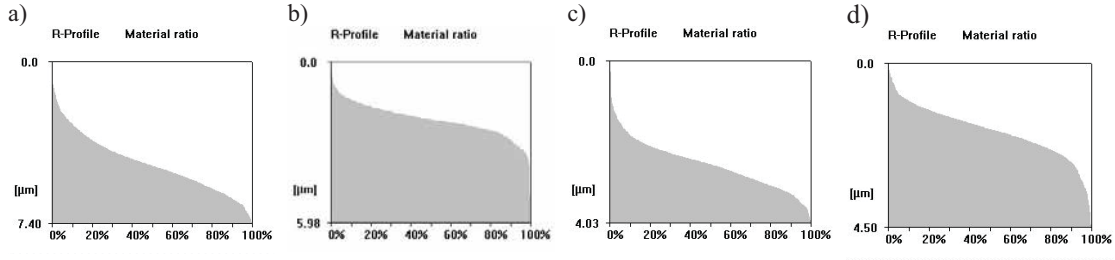

Fig. 3. The Abbott-Firestone curve surface roughness alloy coatings Ni-5%Al for inserts with CB7015: a) square SNGA120408S01030A (No. 1) and b) round N123J1-0600-RE (No. 2) and c) trigon WNMG 080408 S01030A (No. 6) and d) trigon WNMG 080408 - KF with GC3215 (No. 11)

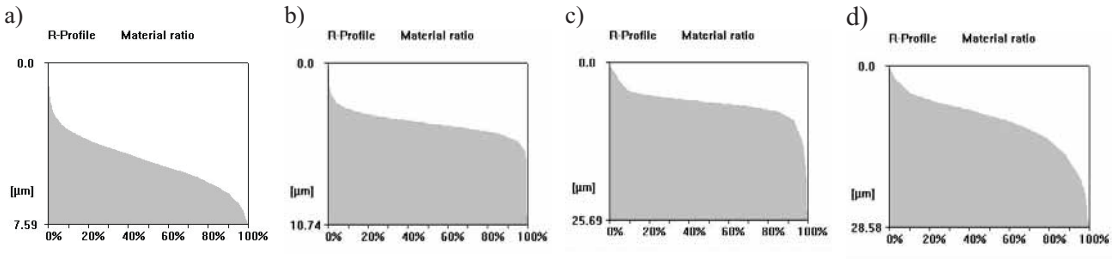

Fig. 4. The Abbott-Firestone curve surface roughness composite coatings Ni-5%Al-15%Al_2O_3 for inserts with CB7015: a) square SNGA120408S01030A (No. 1.123) and b) round N123J1-0600-RE (No. 2.123) and c) trigon WNMG 080408 S01030A (No. 5.123) and d) trigon WNMG 080408 - KF with GC3215 (No. 4.003)

Turning surfaces of have been subjected to the external cylindrical stainless steel samples of coated alloys and composites. After experimental studies determined that there are relationships between surface texture and the type of material used and the shape of the tool inserts. Based on analysis of test results determined that due to obtaining the smallest surface roughness alloy coatings, it was expedient to use trigon inserts made of tungsten carbide with grade GC3215 and cubic boron nitride grade CB7015 and round inserts (CB7015). For samples No. 2 coated Ni-5%Al subjected to turning determined that the arithmetical mean deviation of the assessed profile and the Abbott-Firestone curve surface roughness parameters take the smallest value (refer with: Fig.3).
Based on analysis of test results determined that due to obtaining the smallest surface roughness turned alloy coatings of Ni-5% Al, with the least wear on the insert flank face and tool face, for a constant spiral cutting length (SCL = 1073m), targeted to was the use of trigon inserts made of cubic boron nitride on the grade CB7015 and a insert grade GC3215 and the round profile of the CB7015. Roughness of the surface texture of Ni-5%Al subjected to turning by trigon insert with CBN is three times smaller than the roughness of the alloy coatings a square insert. Thus, it is advisable not use square inserts for machining alloy coatings. Based on analysis of experimental results after turning composite coatings can be determined that the roughness profile parameters and parameter values of the bearing area curve reached the lowest values for samples No. 2.123 (refer with: Fig. 4).

Conclusions

Surface texture is very important where it has a direct influence on the quality of the elements machine parts. Therefore, it has to be defined as precisely as possible with the help of standardized surface texture parameters. The best tool contour and angles, selected the required shape and grade the inserts, you need to obtain a minimum surface roughness. After you finish turning of studies of alloy and composite coatings determined that due to obtaining the smallest surface roughness, with the least wear on the insert flank face and tool face, for a constant spiral cutting length, targeted to be the use of inserts round with CBN.
Alloy and composite coatings used in the production and regeneration, it appears possible to achieve the technological quality of the elements machine parts (eg shafts of centrifugal pumps).
It can be argued that due to the surface quality coatings and durability of the turning inserts:

- for turning shafts of centrifugal pumps with a coating alloy would need to be round and trigon inserts with grade CB7015 and trigon with grade GC3215,
- for turning shafts of centrifugal pumps with composite coatings should be applied round inserts with grade CB7015.

References

[1] Chang, J.T., Yeh, C.H., He, J.L., Chen, K.C., *Cavitation erosion and corrosion behavior of Ni–Al intermetallic coatings*, Wear, 255, pp.162-169, 2003.

[2] Duraiselvam, M., Galun, R., Wesling, V., Mordike, B.L., Reiter, R., Oligmüller, J., *Cavitation erosion resistance of AISI8 420 martensitic stainless steel laser-clad with nickel aluminide intermetallic composites and matrix composites with TiC reinforcement*, Surface&Coatings Technology, 201, pp. 1289-1295, 2006.

[3] Dyl, T., Skoblik, R., Starosta, R., *The Effect of the Ceramic Dispersion on the Nickel Matrix Composite Coating Properties after Plastic Working*, Solid State Phenomena, 147-149, pp.813-818, 2009.

[4] Grądzka-Dahlke, M., Bukrym, A., Choińska, E., *Effect of TiN Coating on Functional Properties of Implant Titanium Alloy*, Solid State Phenomena, 147-149, pp.782-787, 2009.

[5] Dudzik, K., Czechowski, M., *Analysis of possible shipbuilding application of friction stir welding (FSW) method to joining elements made of AlZn5Mg1 alloy*, Polish Maritime Research, 16, pp. 37-40, 2009.

[6] Dudzik, K., Czechowski, M., *Stress Corrosion Cracking of 5083 and 7020 Aluminium Alloys Jointed by Friction Stir Welding*, Solid State Phenomena, 165, pp.37-42, 2010.

[7] Dyl, T., Starosta, R., *Effect of the Ceramic Dispersion in the Nickel Matrix Composite Coatings on Corrosion Properties after Plastic Working*, Solid State Phenomena, 183, pp.43-48, 2012.

[8] Starosta, R., *Corrosion of Ni-Al and Ni-Al-Al_2O_3 Flame Sprayed Coatings of "CastoDyn8000" System in 0.01MH_2SO_4 and 3.5%NaCl Solutions*, Solid State Phenomena, 183, pp.185-192, 2012.

[9] Pochrząst, M., Marciniak, J., Wróbel, K., Bączkowski, B., *Electrochemical Properties of Ni-Cr and Co-Cr Alloys Used in Prosthodontics*, Solid State Phenomena, 183, pp. 143-148, 2012.

[10] Serbiński, W., Wierzchoń, T., *Wear and Corrosion Characteristics of the Layers Type (Mn-P) Formed on Aluminium Alloys*, Solid State Phenomena 183, pp.149-154, 2012.

[11] Molins, R., Normand, B., Rannou, G., Hannoyer, B., Liao, H., *Interlamellar boundary characterization in Ni-based alloy thermally sprayed coating*, Materials Science and Engineering, A351, pp. 325-333, 2003.

[12] Sampath, S., Jiang, X.Y., Matejicek, J., Prchlik, L., Kulkarni, A., Vaidya, A., *Role of thermal spray processing method on the microstructure, residual stress and properties of coatings: an integrated study for Ni–5 wt.%Al bond coats*, Materials Science and Engineering, 364, pp. 216-231, 2004.

[13] Sierra, C., Vazquez, A.J., *NiAl coating on carbon steel with an intermediate Ni gradient layer*, Surface&Coatings Technology, 200, pp. 4383-4388, 2006.

[14] St-Georges, L., *Development and characterization of composite Ni-Cr+WC laser cladding*, Wear, 263, pp. 562-566, 2007.

[15] Dyl, T., Starosta, R., *The influence of treatment parameters on the quality of MMC coatings surfaces applied to recondition parts of ship machinery*, Journal of POLISH CIMAC, Vol.3, No. 2, s. 39-46, 2008.

[16] *Machining powder of sprayed layers 19000, 21000, 12000*, Materials of the company "Castolin Eutectic" 2001.

[17] *Manual machining*, AB Sandvik Coromant, Sandviken, Sweden 2010.

Journal of Polish CIMAC
Gdansk University of Technology
The Faculty of Ocean Engineering and Ship Technology

DIAGNOSING OF ELECTRO - MECHANICAL CONVERTERS BY USING A METHOD OF FREQUENCY MODULATION ANALYSIS

Andrzej Gębura, Tomasz Tokarski

Air Force Institute of Technology
ul. Księcia Bolesława 6, 01-494 Warszawa, skr. poczt. 96
tel. 0-22 - 6856510
e-mail: andrzej.gebura@itwl.pl

Abstract

This paper describes methods for the diagnosing of aircraft electro-mechanical converters, used by the Aircraft Equipment Laboratory , Avionics Division , Polish Air Force Technical Institute (PAFTI). Each of them has been discussed on the basis of systematized, available theoretical knowledge verified by using results of the authors' laboratory research.

Especially is exposed the diagnostic method , elaborated by these authors and implemented under their supervision, based on measuring and analyzing the parameters of one of the components of the direct current pulsations. The method is called FAM-C (where FM stands for frequency modulation , A – alternating current, C – the method's development level). Also, a related method based on measuring and analyzing one of the components of DC pulsations , is presented. It is called FDM-A (where FM stands for frequency modulation, D – direct current, A – the method's development level) . Results of laboratory tests are also attached.

Possible using the converter groove pulsations during rotor's rundown phase after external feeding the excitation winding, has been also discussed – in this case DC motor turns into DC generator. This makes it possible to apply the FDM-A method. As DC generator usually shows a few times greater resolving power, it is possible to monitor mechanical elements which generate higher frequencies. To highlight the problem, have been discussed effects of physical phenomena which influence the forming of output voltage pulsation component of DC generators .

Keywords *: technical diagnostics , electro-mechanical converter , frequency modulation , FAM-C and FDM-A diagnostic methods , machine rundown phase.*

1. Introduction

Converter constitutes an electro-mechanical device which converts one kind of electric energy into another one. Onboard aircraft electric power converters serve to supply local electric power networks with alternating current [1]. The electro-mechanical converter is a set of two electric machines seated onto common shaft :

a) compound , separately excited DC motor,
b) synchronous generator [2].

The electro-mechanical converter converts 28 V direct current into the one-phase alternating current of 115 V and 400 Hz, the three-phase current of the line-to line voltage of 3×36 V and 400 Hz frequency, or a current of a special voltage and frequency.

[1] In special installations , e. g. weapon systems , can be also met an output voltage of 10 kHz frequency of direct current with keying, and other ones as well. However they are not onboard electric power installations and this paper does not cover them.
[2] In certain designs two generators fixed onto common shaft are used, such as in PTO-1000/1500W converter.

The device is a secondary voltage source of great stability of parameters (as compared with that of the primary electric power source , i.e. onboard alternating current generator). To ensure stabilization of output voltage and frequency the so called control box is applied.

In modern aviation the application of electro-mechanical converters has been definitely left out because of their low energy efficiency, large weight and high level of noise. However on older types of aircrafts such converters are still in use. Simultaneously this is a simple assemblage of two electric machines. Rotors of the two machines have a common shaft whose ends are seated in two bearings. The mechanical simplicity of the converter's design makes it possible easily to identify failures of mechanical elements during its monitoring by means of the FAM-C method. The electro-mechanical converters constitute a small-size driving set which faces a.o. wear kinds typical for large machinery sets, such as assembling and wear defects.

The converters used in Polish Air Force aircrafts had not and have not any diagnostic devices [3] which could make it possible to monitor their wear progress - and in the opinion of these authors the portable measuring stands (i.e. a ground-based control board of electric power unit) fitted with indicating instruments : voltmeter, ammeter and frequency meter , cannot fulfil such function.

Theoretically , the most accurate information (in this case – diagnostic information) is gained directly from its source , but not from indirect agents as then the information may be very distorted. Hence it should be strongly stressed that a diagnostic system should be applied to make it possible to check current technical state of converters. It will be short- term forecasts.

Another problem constitutes long-term forecasts. They are more and more important in view of necessity to make savings in military aviation. Hence in practice , overhaul lives of a.o. converters are as a rule extended. Failures defined by servicemen as defects , e.g. of a radio receiver , really result from incorrect work of a converter, and inversely. In such situation it is urgent task to elaborate a precise diagnostic tool for making it possible to earlier assess technical state of converters and elaborate a long-term forcast (for 100÷200 h long flight). Such diagnostic systems should ensure the monitoring and comprehensive assessment of technical state of converters. Then the operation according to a current technical state will be possible – now it is run according to duration of operation time (acc. „ flying time hours" as well as acc. „calendar period").

In this paper the authors describe the investigations realized during their professional activity [4] on aircrafts , which make it possible to locate defects on the basis of parametric models at disposal, determined either in special standards or resulting from multi-year practical experience. The FAM-C method elaborated in the PAFTI plays here an important role.

Also, are described laboratory tests where determined defects were introduced and resulting changes in diagnostic parameters were measured. The tests have been aimed at determination of a comprehensive set of diagnostic levels for electro-mechanical converters of different types. Consequently, it can make it possible to elaborate field diagnostic testers being small, light and friendly in use. As assumed , both the FAM-C and FDM-A method have been comprehensively used [1, 2, 5, 6, 9-11, 13, 18], as well as the „classical" parameters of electric power quality [15] measured. Both the mechanical defects (state of bearings, assembling errors) and electrical defects (failures of filtering system, rotational speed stabilization system and generator's winding, worsening of comutation state of brushes of motor) have been located.

2. Frequency methods for testing aircraft converters - FAM-C and FDM-A method

The FAM-C method [1, 2] was elaborated in the 1990s in the PAFTI and has been still under systematic development. Shortly, it can be said that it is based on observations of dynamics of natural vibrations of particular units of a driving set . The synchronous generator converts mechanical natural vibrations into electrical vibrations. By analyzing changes in output voltage frequency

[3] In the conclusions of this paper a preliminary design concept of such diagnostic device is proposed.

[4] Projects on extension of operating lives of aircrafts and those connected with investigations of aircraft accidents.

modulation it is possible to diagnose a driving set, as the run of changes of instantaneous frequency (of output voltage of synchronous generator) :

$$f_i = f(t) = \sum_{j=1}^{j=m} 2\pi f_{ej}(t) \tag{1}$$

is a discrete representation of the run of angular speeds of particular units of the driving set :

$$\omega(t) = \sum_{j=1}^{j=m} \omega_{mj}(t) = \sum_{j=1}^{j=m} 2\pi f_{mj}(t) \tag{2}$$

where :

j – number of an observed subassembly or kinematic pair,

f_{mj} – frequency of mechanical vibrations , characteristic for a given subassembly or kinematic pair,

f_{ej} – frequency of electrical vibrations, which discretely maps frequency of mechanical vibrations , characteristic for a given subassembly or kinematic pair.

In the Laboratory of Aircraft Electric Power Equipment and Electric Drives , Polish Air Force Technical Institute , it is possible to carry out observation , by using the FAM-C method, of instantaneous values of output voltage on the plane (t, f_i) as well as to represent characteristic sets on the plane (f_p, ΔF). In view of that both the machines (generator and driving motor) are seated onto common shaft it is hard to expect many characteristic sets in the converter to occur. Due to a common nominal speed a defect , e.g. an eccentricity of generator rotor and an eccentricity of driving motor rotor, will be placed in the same characteristic set. Characteristic points of a skewness defect of both the machines [13] will be placed as a rule in another set than characteristic points of an eccentricity defect. The eccentricity defect will be characterized by a set of base frequency equal to the first harmonic of rotational speed of converter's rotor (Tab. 1 and 2) , and the skewness defect – that equal to its second harmonic. And, superposition of the both defects – that equal to to the first subharmonic of rotational speed.

3. Laboratory tests of converters with controlled defects, by means of FAM-C method

Tests of electrical parameters of converters having different controlled (introduced by researchers) wear levels of their electrical and mechanical elements , were performed. The tests were carried out both by using classical methods (fast Fourier transform) and novel ones (e.g. the FAM-C method). Real wear level was assessed by using mechanical measurements . The tests concerned the PAG-1F, PT-500 and PO-750 converters. The converters were adjusted to introducing controlled assembling errors (Fig. 1) : eccentricity, skewness of rotor rotation axis against stator symmetryaxis . One- and three –phase measurement systems (Fig. 2 and 3) made it possible to monitor the above specified assembling errors . The both measurement systems were described in detail in [3].

a) b)

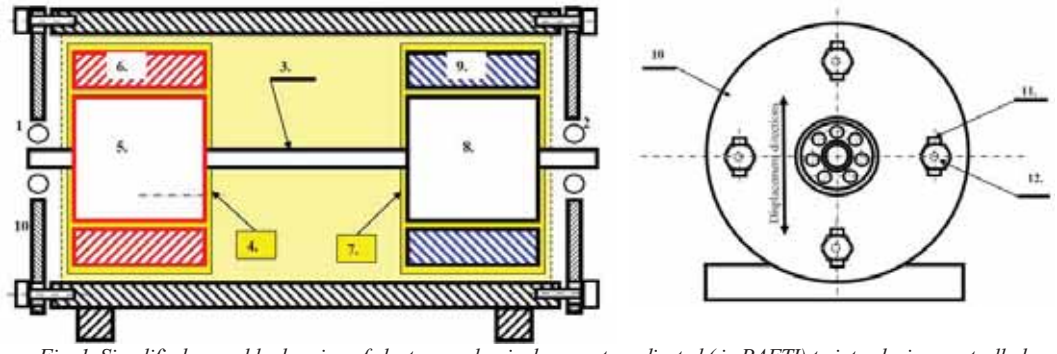

Fig. 1. Simplified assembly drawing of electro-mechanical converter adjusted (in PAFTI) to introducing controlled assembling errors : a) longitudinal section, b) view from the side of side cover bearing disc. 1, 2 – rolling bearing, 3 – shaft, 4 – DC motor, 5 – rotor of DC motor, 6 – stator of DC motor, 7 – AC generator, 8 – rotor of AC generator, 9 – stator of AC generator, 10 – bearing disc (side cover), 11 – vertically milled grooves, 12 – fasting bolt.

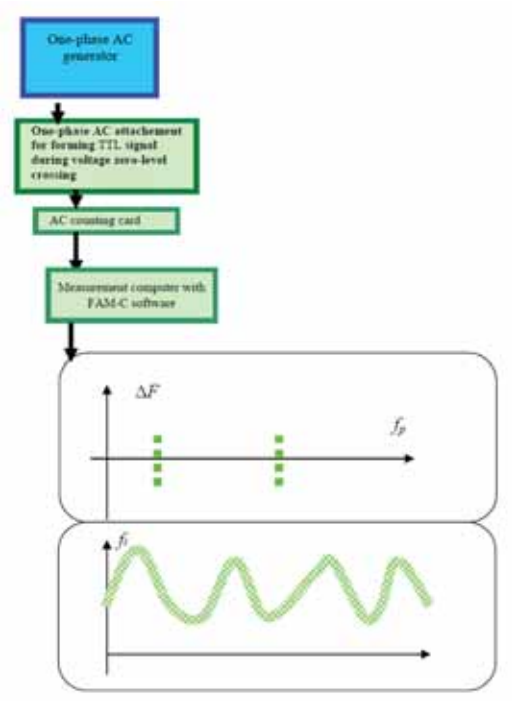

Fig. 2. Way of obtaining diagnostic signal from a tested one-phase converter (or generator) by using FAM-C method

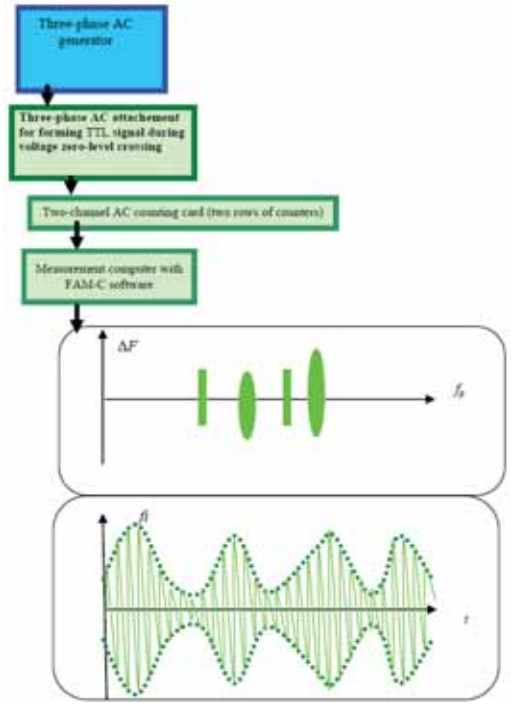

Fig. 3. Way of obtaining diagnostic signal from a tested three-phase converter (or generator) by using FAM-C method

Next, the tests of electrical parameters of converters having different controlled wear levels of elements, were performed. The tests concerned the following „defects" :

a) electrical ones – changes in brush pressure of electric motor,
b) mechanical ones – changes in geometry of position of rotor rotation axis against stator symmetry axis : change of skew angle, change of eccentricity value.

The tests were performed by using both classical methods (Fourier fast transform) and novel ones (e.g. the FAM-C method). Real wear level was assessed by using mechanical measurements. Detailed discussion is given in the successive chapter.

3.1. Lowered comutating brush pressure

The PAG-1F converter serves for electro-mechanical conversion of 28 V DC voltage into three-phase voltage of the 3×36 V effective line voltage at the frequency f_{uN} = 400 Hz. The converter is composed of two electric machines :

- DC motor,
- three-phase AC generator.

Observations made with the use of FAM-C method showed , in the initial state (i.e. before changing brush pressure) the fluctuations in running the instantaneous frequency $f_i = f(t)$, of the amplitude $A = 2\Delta F$ = 7,5 Hz. The fluctuations were stable as regards both their amplitude and frequency (Fig. 5 and 6). The mean frequency level was equal to 431,25 Hz. The fluctuation frequency of the run $f_i = f(t)$ was equal to f_p = 50 Hz (Fig. 4). The images of $\Delta F = f(f_p)$ revealed also some characteristic sets of different f_p - values (Fig. 6).

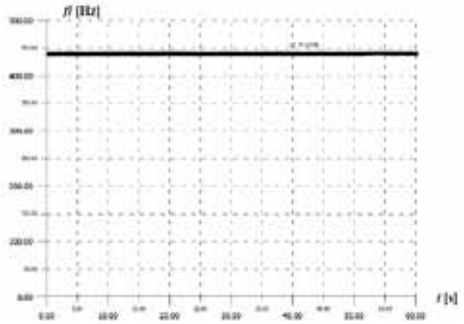

Fig. 4. Run of changes in instantaneous frequency of PAG-1F converter before changing comutating brush pressure of electric motor

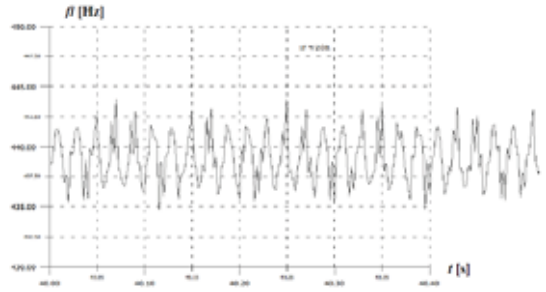

Fig. 5. Run of changes in instantaneous frequency of PAG-1F converter before changing comutating brush pressure of electric motor (initial state) – enlargement

In the **PAG-1F** converter, pressure of one brush was lowered - then increased sparking occurred under its operation. Mean frequency of initial voltage after failure decreases by abt. 50 Hz (it reaches the level of abt. 350 Hz). In the runs $f_i = f(t)$ the fast-changing component measured by means of the one-phase attachement FAM-C, shows the frequency of abt. 50Hz (Fig. 7 and 8). The slow-changing component is characterized by the deflection duration time t_{od} ~5÷10 s and the amplitude increase ΔF~3÷25Hz. Sudden „jumps" of frequency level of the amplitude ΔF = abt. 7 Hz , occur stochastically. In the run shown in Fig. 8 can be observed some „undercuts" which probably result from the edge catching of a brush of regular pressure on certain edges of comutator bars. The images $\Delta F = f(f_p)$ show decrease of f_p -values of particular sets and increase of height of characteristic sets (Fig. 9).

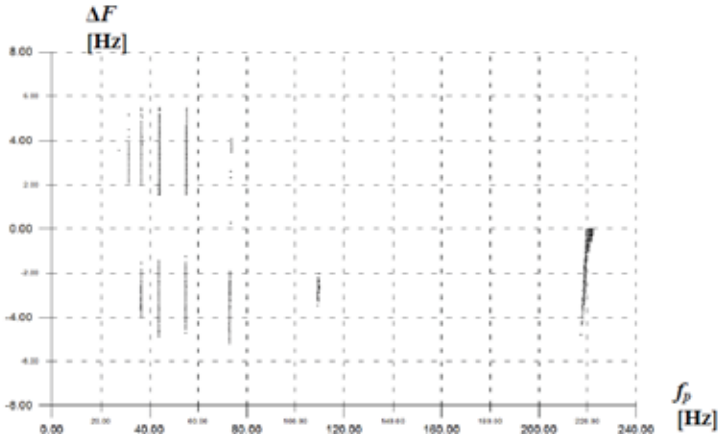

Fig. 6. Characteristic sets of PAG-1F converter before changing comutating brush pressure of electric motor (initial state)

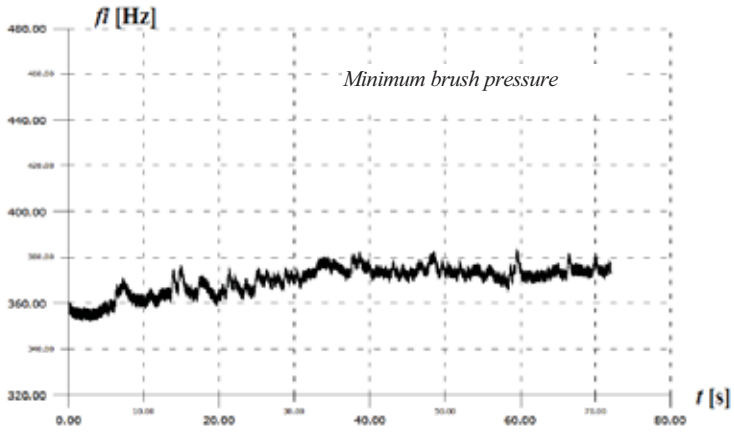

Fig. 7. Run of changes in PAG-1F converter's frequency at comutating brush pressure lowered below its permissible value

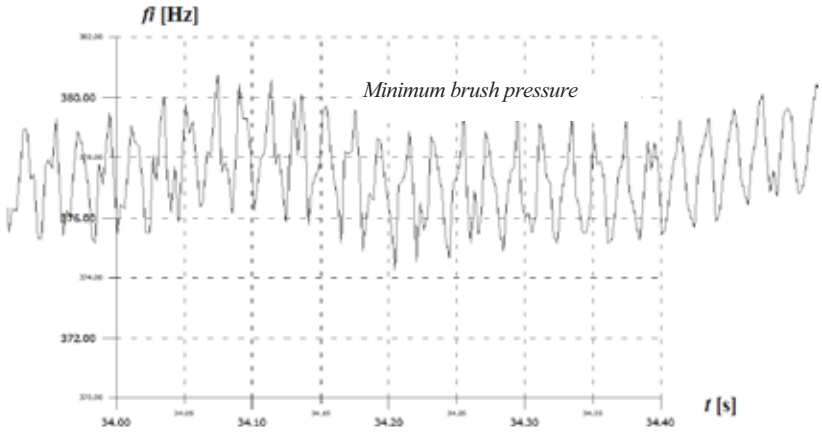

Fig. 8. Run of changes in PAG-1F converter's frequency at comutating brush pressure lowered below its permissible value - enlargment

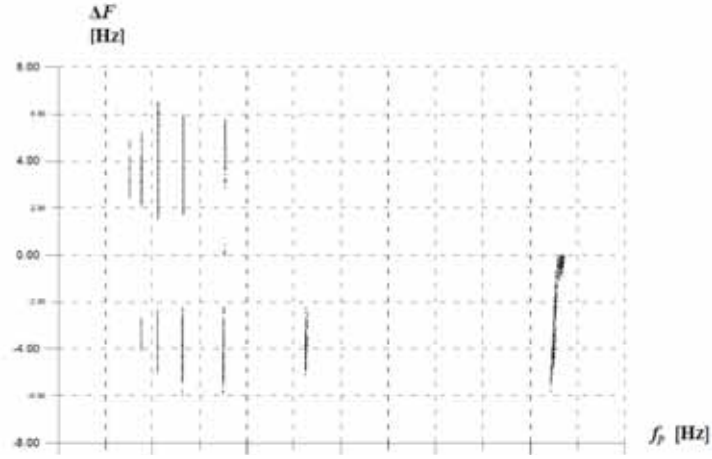

Fig. 9. Characteristic sets of PAG-1F converter at comutating brush pressure lowered below its permissible value

3.2. Skewness of rotor rotation axis against stator symmetry axis

The skewness was obtained by milling longitudinal, vertically orientated enlargement of assembly holes for blots fixing side cover (bearing seating plate) to cylindrical part of the machine. By displacing one bearing disc (side cover) upwards and the other downwards a measurable skew angle could be set.

For the PAG-1F converter before displacing its side cover **,** was obtained a run in which modulations of abt. 75 Hz frequency can be observed. They were located close to the first subharmonic of rated rotational speed , that shows that some small eccentricity and skewness in seating the rotor against stator took place (according to calculations the value of the skew angle in question amounted to about 0,0079 ^{o}) . In the case of skewing the rotor by the angle of abt. 0,04^{o} (Tab. 1, p. 6) the frequency of the second harmonic of rated rotational speed begins to dominate. The value of the fluctuation amplitude of the „run" of instantaneous frequency, increases from the level of ΔF = 4,11 Hz (0,95% in relation to the mean frequency value) to ΔF = 13,94 Hz (1,09%).

For the PT-500C converter before displacing its side cover **,** was obtained a run in which modulations of abt. 200 Hz frequency can be observed. They were located close to the first harmonic of rated rotational speed of converter's rotor , that shows that some small eccentricity and skewness in seating the rotor against stator took place . In the case of skewing the rotor by the angle of abt. 0,2^{o} (Tab. 1, p. 8) the frequency of the second harmonic of rated rotational speed starts to dominate. (Fig. 11). The value of the fluctuation amplitude of the „run" of instantaneous frequency increases from the level of ΔF = 0,17 Hz (0,04% in relation to the mean frequency value) to ΔF = 12,29 Hz (1,02%).

For the PO-750 converter before displacing its side cover **,** was obtained a run in which modulations of abt. 175 Hz frequency can be observed. This is close to the first harmonic of rated rotational speed, that shows that some small eccentricity and skewness in seating the rotor against stator took place . In the case of skewing the rotor by the angle of abt. 0,2^{o} (Tab. 1, p. 10) the frequency of the second harmonic of rated rotational speed starts to dominate. The value of the fluctuation amplitude of the „run" of instantaneous frequency increases from the level of ΔF = 0,24 Hz (0,067% in relation to the mean frequency value) to ΔF = 1,87 Hz (0,52%).

Because of not satisfying the Kotelnikov-Shannon condition, the above presented data should be taken only as a rough information - the assessment of relations between skewness and frequency modulation should be made with the use of the FDM-A method during machine rundown phase.

At increasing values of the skew angle between rotor rotation axis and stator symmetry axis it can be observed that the amplitude of modulation of the instantaneous frequency equal to the second harmonic of rotational speed, also increases. The amplitude of the modulations increases along with increasing values of the skew angle (Tab. 1).

In Tab. 2 are presented the values for classifying mechanical defects with respect to their size (A – very low wear, B – mean level of wear, C – high level of wear, D – very high level of wear, i.e. taking-out of service).

3.3. Eccentricity of rotor rotation axis against stator symmetry axis

Parallel displacement of rotor rotation axis against stator symmetry axis was made by using the vertically orientated, longitudinally enlarged by milling , assembly holes for bolts fastening side cover (bearing seating plate) to cylindrical part of the machine, prepared for realization of the preceding tests. By displacing both the bearing seating plates downwards a measurable eccentricity value could be set.

For the PAG-1F conveter before displacing its side cover**,** was obtained a run in which modulations of abt. 75 Hz frequency can be observed. This is close to the first subharmonic of rated rotational speed, that shows that some small eccentricity and skewness in seating the rotor against stator took place. In the case of setting the eccentricity value a = 0,2 mm (Tab.1, p. 11) the value of the fluctuation amplitude of the „run" of instantaneous frequency increases from the level of ΔF = 4,11 Hz (0,95%)

to that of 13,94 Hz (1,09%). For the PT-500C conveter before displacing its side cover**,** was obtained a run in which modulations of abt. 200 Hz frequency can be observed. This is close to the first harmonic of rated rotational speed, that shows that some small eccentricity in seating the rotor against stator took place and 200 Hz frequency occurred. In the case of setting the eccentricity a = 0,35 mm (Tab. l, p. 15) the value of the fluctuation amplitude of the „run" of instantaneous frequency increases from the level of ΔF = 0,17 Hz (0,04%) to that of 12,29 Hz (1,022%).

For the PO-750 conveter before displacing its side cover**,** was obtained a run in which modulations of abt. 175 Hz frequency can be observed. This is close to the first harmonic of rated rotational speed, that shows that some small eccentricity and skewness in seating the rotor against stator took place. In the case of setting the eccentricity a = 0,4 mm (Tab. l, p. 13) the value of the fluctuation amplitude of the „run" of instantaneous frequency increases from the level of ΔF = 0,24 Hz (0,067%) to that of 0,52 Hz (0,52%).

At increasing values of the eccentricity between rotor rotation axis and stator symmetry axis it can be observed that the amplitude of modulation of the instantaneous frequency equal to the second harmonic of rotational speed, also increases. The amplitude of the modulations increases along with increasing values of the eccentricity. (Tab. 2).

The values for classifying mechanical defects with respect to their size to particular diagnostic classes, are presented in Tab. 2.

4. Tests of the converters during their rundown phase

The rundown phase is an energy state of a driving set, in which the machine brought up to its rated speed, is deprived of external power supply . In this case two complexes of physical phenomena appear, namely :

a) **decreasing level of the rotational speed *n*** (usually quasi-fluent), along with time counted from the instant of stopping external power supply, of particular , mutually coupled kinematic pairs, through successive lower and lower rated speeds (Fig. 10) ; for each of the speeds different dynamic phenomena can be observed , a.o. occurrence of different local mechanical resonances (Fig. 11);

b) **decomposition of dynamics of driving set's motion** into kinematic links individually vibrating within constraints and limits resulting from their design.

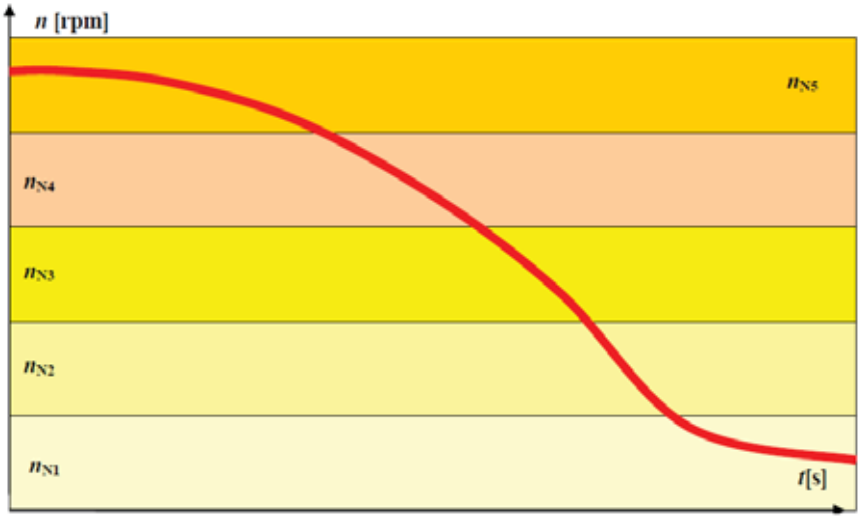

Fig. 10. Run of changes in mean rotational speed after switching-off power source, with marked bands of the rated speeds {nN1, nN2, nN3, nN4, nN5} – slow-variable component

Tab. 1. Statement of parameters of selected assembling defects of converters as well as parameters of their representation in electrical phenomena

No.	Type of converter	Value of linear displacement mechanically measured		Distance between supports	D_N	β	a	f_{max}	f_{min}	$f_{śr}$	ΔF	Parameters of defects according to electrical calculations	
		A_1	A_2	L								a	β
-	-	mm	mm	mm	mm	°	mm	Hz	Hz	Hz	Hz	mm	°
1	PAG-1F	0,3	0,2	145	55,5	0,19757	0,1	1290,32	1281,23	1285,5	9,09	0,0981	0,15506
2	PT-500C	0,35	0,35	203,3	69,3	0,19728	0	1224,36	1183,78	1203,2	40,58	0	0,65866
3	PT-500	0,35	0,35	203,3	69,3	0,19728	0	1212	1200	1203,2	12	0,1727	0,19478
4	PO-750	0,5	0,0	258	70	0,11104	0	356,57	354,7	355,84	1,87	0	0,08169
5	PAG-1F	0,01	0,01	145	55,5	0,0079	0,01	434,59	430,48	432,51	4,11	0,13185	0,2084
6	PAG-1F	0,3	-0,2	145	55,5	0,03951	0,5	1287,83	1273,89	1277,8	13,94	0,1513	0
7	PT-500	0,01	0,01	203,3	69,3	0,00564	0,01	402,58	402,41	402,49	0,17	0,00732	0,00825
8	PT-500	0,35	0,35	203,3	69,3	0,19728	0,35	1208,46	1196,17	1202,32	12,29	0,17709	0,19964
9	PO-750	0,03	0,03	258	70	0,01332	0,03	357,77	357,53	357,7	0,24	0,01174	0,01043
10	PO-750	0,5	0	258	70	0,11104	0	356,57	354,7	355,84	1,87	0	0,08169
11	PAG-1F	0,3	-0,2	145	55,5	0,03951	0,2	1287,83	1273,89	1277,8	13,94	0,15137	0,23925
12	PT-500	0,35	-0,35	203,3	69,3	0	0,35	1208,46	1196,17	1202,32	12,29	0,17709	0,19964
13	PO-750	0,5	-0,4	258	70	0,02221	0,4	338,7	338,18	338,58	0,52	0,02688	0,02387

Tab. 2. Statement of limit states obtained from the frequency analysis method

l. p.	Kind of defect	Class	PAG-1F			PT-500C			PO-750		
			ΔF	f_{sr}	f_p	ΔF	f_{sr}	f_p	ΔF	f_{sr}	f_p
			Hz	Hz	Hz	Hz	Hz	Hz	Hz	Hz	Hz
1	Lowered brush pressure	**A**	<10	>380	0,2 ÷ 0,02	<10	>380	0,1 ÷ 0,025	< 8	>390	0,1 ÷ 0,025
		B	10÷25	350 ÷ 380		10÷25	360 ÷ 380		8 ÷ 15	370 ÷ 390	
		C	>25	<350		>25	≤360		> 15	≤370	
2	Skewness	**A**	$< 0{,}3\%f_s$	-	400	$< 0{,}3\%f_s$	-	400	-	-	-
		B	$0{,}3 \div 0{,}8\%f_s$	-	400	$0{,}3 \div 0{,}8\%f_s$	-	400	-	-	-
		C	$0{,}8 \div 1{,}1\%f_s$	-	400	$0{,}8 \div 1{,}1\%f_s$	-	400	-	-	-
		D	$>1{,}1\%f_s$	-	400	$>1{,}1\%f_s$	-	400	-	-	-
3	Eccentricity	**A**	$< 0{,}3\%f_s$	-	200	$< 0{,}3\%f_s$	-	200	$< 0{,}2\%f_s$	-	200
		B	$0{,}3 \div 0{,}8\%f_s$	-	200	$0{,}3 \div 0{,}8\%f_s$	-	200	$0{,}2 \div 0{,}4\%f_s$	-	200
		C	$0{,}8 \div 1{,}1\%f_s$	-	200	$0{,}8 \div 1{,}1\%f_s$	-	200	$0{,}4 \div 0{,}5\%f_s$	-	200
		D	$>1{,}1\%f_s$	-	200	$>1{,}1\%f_s$	-	200	$>0{,}5\%f_s$	-	200

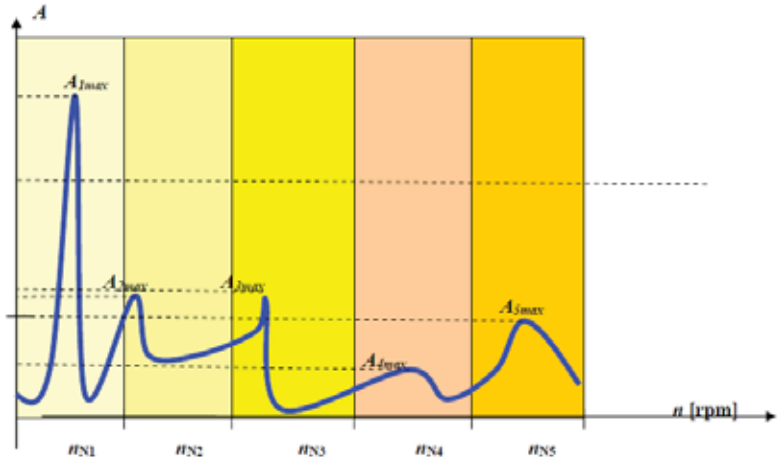

Fig. 11. Local resonance phenomena observed for rotational speed after switching-off power source, with marked bands of the rated speeds {n_{N1}, n_{N2}, n_{N3}, n_{N4}, n_{N5}} – exemplified by results of the Fourier analysis $A = f(n)$

In manuals of aircraft equipment producers and also aircraft operational instructions are contained many limitations for rundown time of rotary machines (in engine instructions it is called in a different way). According to practice and literature premises the shorter rundown time the greater total resistance moments of a given mechnical set. Therefore in many instructions to control rotor bearing units is recommended. Moreover, during rundown time natural decomposition of all driving set subsystems into independent kinematic pairs, occurs. The pairs , to a large extent independent from neigbouring kinematic pairs , perform angular oscillations called free vibrations . Fading time of the oscillations depends on dry friction component as well

as that of viscous friction, i.e. wet one, as well as on possible air damping (at higher levels of rotational speed). Frequency of the oscillations depends on many factors , e.g. :

- inertia moment– the greater inertia moments the greater period of natural vibrations, i.e. the lower frequency;
- flexibility – the greater flexibility coefficient (the greater moment of force accumulated in an element during its deformation by unit twisting angle), the shorter period of natural vibrations, i.e. the greater frequency.

During converter's rundown phase , frequency of exitation acting onto its particular mechanical units , smoothly decreases. Therefore it is possible to generate and locate resonance excitations of particular mechanical units of a converter , e.g. bearing supports . Their locating and observing is very important from the point of view of determination of their survivability and issuance of a credible service forcast. For bearing supports a measure of hazard state is mechanical Q-factor of a resonance system – if $Q > 10$ it is recommended to withdaw a given system from operation. If excitation frequency is close to natural (free) vibration frequency of a given system then danger of occurrence of a resonance will appear. Machinery shafts , due to their abruptly varying cross-section , weight , mass unbalance and bearing gaps , constitute complex vibrating sytems. Resonance vibrations of one element affect other elements of the system. In such system can happen several critical speeds (Fig. 12) which are usually calculated by approximation methods. If , for instance , certain number of rotating masses, e.g. m_1, m_2, m_4, … , m_n, are fixed onto a shaft then critical speed of the whole system can be calculated from Dunkerlev formula in the following form :

$$1/\omega_{kr}^2 = 1/\omega_{kr1}^2 + 1/\omega_{kr2}^2 + 1/\omega_{kr3}^2 + \ldots + 1/\omega_{krm}^2$$

Stresses resulting from resonance vibrations can lead to fatigue failures. Angular speed at which a resonance occurs , is called the critical speed (ω_{kr2}^2) and expressed as follows :

$$\omega_{kr2} = (g/l)^{1/2}$$

which , for engineering practice , can be expressed in the following form :

$$n_{kr} \approx 300 \cdot (1/f) \text{ [rpm]}$$

where : f – statical deflection [cm], g – gravity acceleration.

It should be strongly stressed that shafts should not operate with such rotational speed. They should work with the so called rated speed lower at least by 15 % from ω_{kr2}. The permissible values of shaft deflection are roughly as follows :

$$(0{,}0002 \div 0{,}0003) \cdot l \text{ – for machine shafts,}$$

$$(0{,}005 \div 0{,}01) \cdot m_u \text{ – for toothed reduction gears,}$$

where :

l – distance between neighbouring supports, m_u – module pitch of a gear.

4. Final comments

In this paper was presented a way of diagnosing the selected defects of electro-mechanical converters : lowered comutating brush pressure , skewness of rotor rotation axis against stator symmetry axis , eccentricity of rotor rotation axis against stator symmetry axis. The tests were carried out in PAFTI laboratory by using the novel diagnostic methods called FAM-C and FDM-

A, based on analysis of dynamics of changes in output AC voltage of converter. The FAM-C method makes it possible a.o. to determine values of eccentricity of rotor rotation axis against stator symmetry axis , value of skew angle between the axis , value and dynamics of changes in radial clearances of bearings. The FDM-A method (based on the use of observations of changes in frequency modulation of component pulsation of DC generator) makes it possible to observe rolling uniformity of elements of rolling bearings , detect their resonance states , monitor resistance moments of particular bearing supports.

Also, were described theoretically the tests of converters during their rundown phase , carried out in the PAFTI practice. To this end , AC motor , after running –up its rotor , was converted into DC generator . DC generator is of a much greater resolution than AC one, thus it is possible to monitor fast-varying diagnostic processes such as vibrations of rolling bearings. Tests of converters during their rundown phase make it possible not only to increase the resolution - it is simultaneously another type of diagnosing a mechanical object (not only electro-mechanical converters). This way a versatile image of dynamic structures of a much greater number of mechanical units than that during monitoring a converter at only one rotational speed. can be fast obtained.

Generally, these authors demonstrated that the representations obtained experimentally at increasing controlled parameters of mechanical defects and electrical faults can be monitored by means of the FAM-C and FDM-A methods . In the methods two types of representation are used : form of characteristic sets, form of runs of instantaneous frequency in function of time. The methods in question are characterized by a high sensitivity in determining size of a defect – for increasing value of a defect parameter distinct increase in height of its characteristic set was observed.

REFERENCES

1. Biarda D., Falkowski P., Gębura A., Kowalczyk A.: Opis patentowy PL 175674B1, *Sposób diagnozowania technicznego elementów sprzęgających silnik, a zwłaszcza lotniczy silnik spalinowy, z prądnicą prądu stałego*, zgłoszenie 08.07.1996, udzielenie patentu 29.01.1999.
2. Biarda D., Falkowski P., Gębura A., Kowalczyk A.: Opis patentowy PL 175645B1, *Sposób diagnozowania technicznego elementów sprzęgających silnik, a zwłaszcza lotniczy silnik spalinowy, z prądnicą prądu stałego*, zgłoszenie 08.07.1996, udzielenie patentu 29.01.1999.
3. Gębura A.: *Metoda modulacji częstotliwości napięcia prądnic pokładowych w diagnozowaniu zespołów napędowych*. Wydawnictwo Instytutu Technicznego Wojsk Lotniczych, Warszawa 2010.
4. Gębura A.: *Cechy diagnostyczne składowej pulsacji prądnic prądu stałego*. „Prace Naukowe ITWL" 2003, zeszyt 16.
5. Gębura A.: *Diagnostic of aircraft power transmission track based on the analysis of generator's frequency.* "Journal of Technical Physics" 2002, No. 1.
6. Gębura A.: *Modulacja częstotliwości napięcia wyjściowego prądnicy a stan techniczny układu napędowego*. „Prace Naukowe ITWL" 1998, zeszyt 4.
7. Gębura A.: *Przekoszenia połączeń wielowypustowych a modulacja częstotliwości prądnic.* „Zagadnienia Eksploatacji Maszyn" 1999, zeszyt 4(120*)*.
8. Gębura A.: *Związki modulacji częstotliwości napięcia wyjściowego prądnicy z wybranymi wadami układu napędowego*. W: „Turbinowe silniki lotnicze w ujęciu problemowym"; red. prof. M. Orkisz, Polskie Naukowo-Techniczne Towarzystwo Eksploatacyjne, Lublin 2000, s. 75-94.
9. Gębura A., Falkowski P., Kowalczyk A., Lindstedt P.: *Diagnozowanie skrzyń napędowych.* „Zagadnienia Eksploatacji Maszyn" 1997, zeszyt 4.
10. Gębura A., Prażmowski W., Kowalczyk A., Falkowski P., Głowacki T., Budzyński P., Pisarska K.: *Sprawozdanie z pracy – określenie związków pomiędzy parametrami jakości*

energii prądnic pokładowych a stanem zużycia skrzyń napędowych, Warszawa 1997, niepublikowane, nr BT ITWL 11818/I.
11. Gębura A., Prażmowski W., Kowalczyk A., Falkowski P., Głowacki T., Budzyński P., Gajewski T., Pisarska K.: *Sprawozdanie z pracy – określenie związków pomiędzy parametrami jakości energii prądnic pokładowych a stanem zużycia skrzyń napędowych – część I*, Warszawa 1997, niepublikowane, nr BT ITWL 12023/I.
12. Gębura A., Tokarski T.: *Sprawozdanie z pracy – Badanie trwałości lotniczych urządzeń elektroenergetycznych – badanie przetwornic lotniczych*, Warszawa 2000, niepublikowane, nr BT ITWL 19/50.
13. Lindstedt P., Gębura A.: *Diagnozowanie napędów lotniczych w oparciu o analizę parametrów prądnicy* (in Polish). *Diagnostic of air-drives basing on analysis of parameters of generator*. 5-th International Conference „Aircraft and helicopters diagnostic AIRDIAG'97", Warsaw 1997.
14. Liwschitz-Garik M.: *Direct-current machines*. D. Van Nostand Company, New York 1962.
15. NO-15-A200:2007 Wojskowe statki powietrzne – Pokładowe układy zasilania elektrycznego – Podstawowe parametry, wymagania i badania.
16. Plamitzer M.: *Maszyny elektryczne*. Wydawnictwo Naukowo-Techniczne, Warszawa 1962.
17. Wróbel T.: *Studium teoretyczne i eksperymentalne zagadnienia pulsacji napięcia prądnic tachometrycznych prądu stałego.* Dodatek do „Biuletynu WAT" nr 3(259), Warszawa 1974.
18. Wróbel T.: *Studium zagadnienia pulsacji napięcia prądnic tachometrycznych o wyjściu stałoprądowym*. Dodatek do „Biuletynu WAT" nr 6(298), Warszawa 1977.

Journal of Polish CIMAC
Gdansk University of Technology
The Faculty of Ocean Engineering and Ship Technology

NECESSITY FOR AND POSSIBILITY OF APPLICATION OF THE THEORY OF SEMI-MARKOV PROCESSES TO DETERMINE RELIABILITY OF DIAGNISING SYSTEMS

Jerzy Girtler

Gdansk University of Technology
Faculty of Ocean Engineering and Ship Technology
Department of Marine and Land Power Plants
tel. (+48 58) 347-24-30; fax (+48 58) 347-19-81
e-mail: jgirtl@pg.gda.pl

Abstract

The paper provides justification for the necessity to define reliability of diagnosing systems (SDG) in order to develop a diagnosis on state of any technical mechanism being a diagnosed system (SDN). It has been shown that the knowledge of SDG reliability enables defining diagnosis reliability. It has been assumed that the diagnosis reliability can be defined as a diagnosis property which specifies the degree of recognizing by a diagnosing system (SDG) the actual state of the diagnosed system (SDN) which may be any mechanism, and the conditional probability $p(S^*/\boldsymbol{K}^*)$ of occurrence (existence) of state S^* of the mechanism (SDN) as a diagnosis measure provided that at a specified reliability of SDG, the vector $\boldsymbol{K}^*$ of values of diagnostic parameters implied by the state, is observed. The probability that SDG is in the state of ability during diagnostic tests and the following diagnostic inferences leading to development of a diagnosis about the SDN state, has been accepted as a measure of SDG reliability. The attention has been paid that in order to make an operating decision not only the knowledge of a diagnosis reliability is required, but also the knowledge of consequences (c) of making a given decision that belongs to a set of decisions possible to be made in a given operating situation. The Bayesian statistical decision theory has been proposed to apply for making operating decisions. Herein, it has been used the simplest decision model which assumes that there can only be made one from among two possible operating decisions: 1) perform, first of all, a suitable preventive service for the mechanism (SDN) under operation, in order to renew its functional properties and then start executing the task, 2) start executing the ordered task without prior performance of a preventive maintenance of the mechanism. The theory of semi-Markov processes has been used for defining the SDG reliability, that enabled to develop a SDG reliability model in the form of a seven-state (continuous-time discrete-state) semi-Markov process of changes of SDG states.

Keywords: *decision, diagnostics, probability, reliability, diagnosing system*

1. Introduction

A reasonable operation of mechanisms requires making the right decisions that are appropriate for the current operating situation. An opportunity to make right decisions exists when the reliability of the diagnosis on the technical state of the operated mechanisms is known and it is possible to identify the consequences (*c*) of making the given decision [1, 2, 3, 4]. An assessment of the reliability of the diagnosis on the technical condition of each mechanism (as *SDN* - diagnosed system) is possible only if the reliability of the appropriate diagnosing system (*SDG*) is known, which is necessary to develop a diagnosis on the technical state of *SDN*. The probability of the system's correct work during tests and

diagnostic inference that results in a diagnosis, can be taken as a measure of *SDG* reliability. This probability can be determined by applying the theory of semi-Markov processes. The requirement to determine the mentioned probability can be justified wider by describing the importance of the *SDG* reliability for making operating decisions.

2. An importance of reliability of diagnosing systems for making operating decisions during operation of the mechanisms

Knowledge of the reliability of a diagnosing system (*SDG*) is indispensable to define the reliability of the diagnosis on technical state of a diagnosed system (mechanism) (*SDN*), which can be understood differently [2, 4, 5]. However, diagnosis reliability can be regarded:

- in descriptive sense, as a diagnosis property that defines the degree of recognizing by a diagnosing system (*SDG*) an actual technical state of the diagnosed system (*SDN*), which may be any mechanism, and
- in evaluative sense, as a diagnosis property determined by a conditional probability $p(S^*/\mathbf{K}^*)$ of occurrence (existence) of state S^* of the mechanism (*SDN*), provided that the vector $\mathbf{K}^*$ of values of diagnostic parameters being implied by the state, is observed.

Knowing reliability of the diagnosis on technical state of the mechanism (*SDN*), during the phase of its operation, one of the following decisions can be made:

- decision d_1 – perform, first of all, suitable preventive service for the *SDN*, in order to renew its functional properties which are indispensable to execute the task Z_D, and then start executing the task at the time defined by the orderer,
- decision d_2 – start executing the ordered task Z_D without prior performance of the preventive maintenance of the mechanism, which in a formal term can be defined as follows:

$$Z_D = \langle \Phi, W \rangle, t\rangle \tag{1}$$

where: Φ – correct operation (work) of *SDN*, W – conditions under which *SDN* should properly operate (work), t – time of performing the task Z_D.

However, making a rational operating decision in the phase of operation of the mechanism, requires the knowledge of not only the diagnosis reliability but also the consequences (c) of making the decision. In this situation, for making decisions it is convenient to apply the Bayesian statistical decision theory [1, 3, 4].

Execution of Z_D is possible when *SDN* (mechanism) is in state of ability (s_1^*). The task cannot be performed if *SDN* is in state of disability (s_2^*). However, the mentioned states (s_1^* and s_2^*) that belong to the set of states $S^* = \{s_1^*, s_2^*\}$should be such defined that their occurrences are the mutually exclusive events, so such events whose the probabilities of occurrence satisfy the equations: $P(s_1^* \cup s_2^*) = P(s_1^*) + P(s_2^*)$ and $P(s_1^* \cap s_2^*) = 0$.

Selection of the best decision from among these two (d_1 or d_2) when during performance of the task Z_D a possibility of occurring the states s_i^* (i = 1, 2) exists, requires to take into account the following decision criteria:

- expected value of consequences $E(c|d_1)$ corresponding to decision d_1;
- expected value of consequences $E(c|d_2)$ corresponding to decision d_2.

After estimation of the expected values $E(c|d_k)$, where k = 1, 2; the following logic (rule) of making decisions should be applied [1]: *from among decisions* $d_k(k = 1, 2)$ *this one should be selected which the highest value of* $E(c|d_k)$ *is assigned to*.

Estimation of these expected values is possible when reliability or rightness of the diagnosis is identified [4, 5]. In order to avoid misunderstanding it should be assumed that the diagnosis reliability is determined only when the probability that *SDG* is in state of ability is less than unity. Whereas, rightness of diagnosis is identified only when the probability that *SDG* is in state of ability is equal to unity [4, 5].

Usefulness of the diagnosis reliability $p(S^*/\mathbf{K}^*)$ can be presented on the example of the decision situation of which the dendrite is demonstrated in Fig. 1.

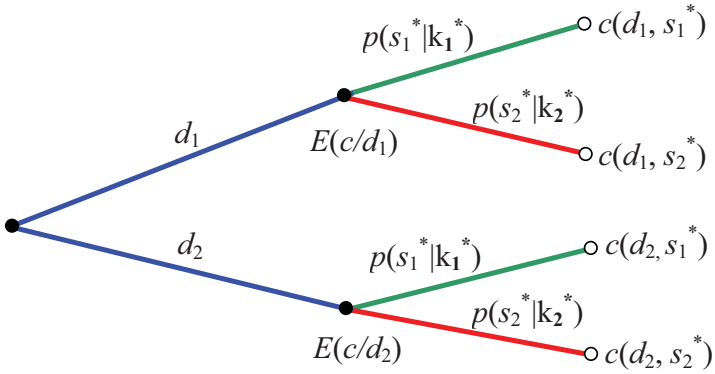

Fig. 1. Exemplary dendrite of the operating decisions for any mechanism: $p(s_1^*/\mathbf{k}_1^*)$ – probability of existence of state s_1 under the condition that the vector $\mathbf{k}_1^*$ of diagnostic parameters is observed, $p(s_2^*/\mathbf{k}_2^*)$ – probability of existence of state s_2 under the condition that the vector $\mathbf{k}_2^*$ of diagnostic parameters is observed, s_1^* – state of ability of the mechanism, s_2^* – state of disability of the mechanism, $c(d_1, s_1^*)$ – consequence resulting from decision d_1 for state s_1^* of the mechanism, $c(d_1, s_2^*)$ – consequence resulting from decision d_1 for state s_2^* of the mechanism, $c(d_2, s_1^*)$ – consequence resulting from decision d_2 for state s_1^* of the mechanism, $c(d_2, s_2^*)$ – consequence resulting from decision d_2 for state s_2^* of the mechanism.

The decision dendrite in Fig. 1 shows that the expected values $E(c|d_1)$ and $E(c|d_2)$ can be derived from the relationships:

$$\left.\begin{aligned} E(c|d_1) &= p(s_1^*|\mathbf{k_1}^*)c(d_1, s_1^*) + p(s_2^*|\mathbf{k_2}^*)c(d_1, s_2^*) \\ E(c|d_2) &= p(s_1^*|\mathbf{k_1}^*)c(d_2, s_1^*) + p(s_2^*|\mathbf{k_2}^*)c(d_2, s_2^*) \end{aligned}\right\} \quad (2)$$

Therefore, in compliance with the presented rule for making decisions, if $E(c|d_1) > E(c|d_2)$ the decision which should be made is d_1 and inversely – if $E(c|d_1) < E(c|d_2)$ the decision which should be made is d_2.

From the considerations it follows that for making operating decisions we need among others the knowledge of diagnosis reliability $p(S^*/\mathbf{K}^*)$ about the technical state of the mechanism whose the measure can be the probability of occurrence of the state s_1^* or s_2^*.

In extreme cases:

- ⇒ reliable (fully reliable) diagnosis can be assigned with a digit 1, which should be considered that the diagnosis is entirely reliable, i.e. right;
- ⇒ unreliable diagnosis can be assigned with a digit 0, which should be considered that the diagnosis is entirely unreliable, i.e. wrong.

In the operating practice, such an alternative assessment of diagnosis reliability, consisting in assigning it with a digit 1 or 0, is insufficient. Therefore, the papers [4, 5] present a proposal to determine diagnosis reliability in the form of the probability $P(S^*/\mathbf{K}^*)$,

where S^* – state of mechanism, $\mathbf{K}^*$ – vector of values of diagnostic parameters characteristic for state S^*. The papers provide an assumption that in the evaluative sense the diagnosis reliability as a diagnosis property, can be determined by the values of important in certain cases indexes characterizing the degree of recognizing by SDG the state of SDN (mechanism), so this may be understood as the conditional probability $P(S^*/\mathbf{K}^*)$, logical probability $P_L(S^*)$ or statistical probability $P_S(S^*)$ [9].

The paper [4, 5] submits a proposal of formulas as the measures of the diagnosis reliability and accuracy. For deriving the formulas there were applied: a conditional probability formula for the events A_1, S^*, $\mathbf{K}^*$ and a continuous-time discrete-state semi-Markov model of the process of using *SDG* $\{W(t): t \geq 0\}$ [4, 5], where:

- A_1 – event representing a proper operation of *SDG* during development of the diagnosis,
- S^* – event representing an occurrence of state S^* of the mechanism (*SDN* – diagnosed system),
- $\mathbf{K}^*$ – event indicating an occurrence of a particular vector $\mathbf{K}^*$ of values of diagnostic parameters as a result of occurring the state S^* of *SDN*.

In consequence, the formula defining probability $P(S^*/\mathbf{K}^*)$ as a measure of diagnosis reliability, is obtained in the form [4, 5] as follows:

$$P(S^* / \mathbf{K}^*) = \frac{P(A_1)P(S^*)P(\mathbf{K}^* / S^*)}{P(\mathbf{K}^*)P(A_1 / \mathbf{K}^* \cap S^*)} \tag{3}$$

For a reliable *SDG* (so such *SDG* for which $P(A_1) = 1$ exists) the formula (3) takes the form as follows:

$$P(S^* / \mathbf{K}^*) = \frac{P(S^*)P(\mathbf{K}^* / S^*)}{P(\mathbf{K}^*)}, \tag{4}$$

which is the measure of the diagnosis accuracy [4, 5].

From the formula (4) it follows that even when *SDG* works reliably during diagnostic tests and then during diagnostic inference until the diagnosis on *SDN* technical state is developed, the diagnosis cannot be certain. This results from the fact that while developing a diagnosis (inference) about the state S^* of *SDN*, the statement $\mathbf{K}^*$, so the statement that just this and not any other vector ($\mathbf{K}^*$, in this case) of values of diagnostic parameters was recorded by *SDG*, is regarded to be completely certain premise. While the sentence S^*, saying that just this and not any other state (S^*, in this case) of *SDN*, is an inference developed on the basis of the statement $\mathbf{K}^*$, which is the result of completed non-deductive inference. Therefore, identification of the technical state of *SDN* consists in developing the hypothesis: *SDN is in state* S^* *because vector* $\mathbf{K}^*$ *of the values of diagnostic parameters is observed.* In this case this inference is a reductive inference, so proceeds according to the following scheme [9]:

$$\mathbf{K}^*, S^* \Rightarrow \mathbf{K}^* \vdash S^* \tag{5}$$

where:

- $\mathbf{K}^*$ – completely certain premise,
- S^* – inference developed on basis of the sentence $\mathbf{K}^*$.

In the case, when the sentence S^* is an inference being developed on the basis of the sentence $\mathbf{K}^*$ (regarded as a completely certain premise) in the process of inferring, it can be assumed that the sentence S^* is made probable by the sentence $\mathbf{K}^*$. The measure for this can

be a conditional probability defined by the formula (3) if there is no certainty that *SDG* works reliably or by the formula (4) if *SDG* works reliably during diagnostic tests and inference.

In general, there is no certainty that SDG works reliably during tests and diagnostic inference [8, 10] and therefore, it is important to determine the probability of its correct operation. For this reason, it is necessary to identify the reliability of *SDG*. This requires consideration of at least a two-state reliability model for *SDG*, thus an assumption that this can find in only two mutually exclusive states, i.e. state of ability (s_0) and state of disability ($\bar{s}_0$). However, due to the fact that in diagnostics of mechanisms (*SDN*) there are applied different methods of testing their states (and hence different diagnosing devices), it becomes necessary to distinguish instead of one state $\bar{s}_0$, a number of states of disability s_j (j = 1, 2, …., n) of *SDG*, which occur in consequence of failures in diagnosing devices that belong to *SDG* used along with the taken methods for testing the *SDN* state. The further considerations on the reliability of *SDG* include the states of disability s_j, j = 1, 2, …, 6 ($s_j \in \bar{s}_0$), where j – type of *SDG* disability resulting from a failure of its subsystem SDG_j, where the indexes $j = \overline{1,6}$ denote e.g.: 1 – subsystem for testing the acoustic emission, 2 – subsystem for visual (endoscopic) testing, 3 – subsystem for thermal (temperature, pressure) testing, 4 – subsystem for vibration testing (for NVH tests), 5 – subsystem for wear testing by employing the method of radionuclide X-ray fluorescence (*XRF*), 6 – subsystem for thermographic testing (for infrared thermal image analysis).

To determine the *SDG* reliability, at such approach to testing the reliability of *SDG*, we can apply the theory of semi-Markov processes (of continuous-time discrete-state type) and develop a seven-state semi-Markov model of the process of changes of *SDG* states (state of ability s_0 and states of disability s_j, $j = \overline{1,6}$), which is necessary to derive the formula for the probability of staying the *SDG* in state of ability (s_0), so in a state which is indispensable to develop a reliable diagnosis.

3. A semi-Markov model of the process of changes of states for diagnosing systems

Application of the semi-Markov model of the process of changes of states for a diagnosing system (*SDG*) enables consideration of its preventive maintenance service [2, 8, 10] and, therefore, consideration of *SDG* reliability state s_0, i.e. state of ability and states of disability s_j ($j = \overline{1,6}$) of its particular subsystems SDG_j, j = 1, 2, …, 6.

The semi-Markov model of the process of changes of reliability states for a the diagnosing system (*SDG*) can therefore, be considered as a semi-Markov process $\{W(t): t \geq 0\}$ with the set of states $S = s_i$; i = 0, 1, ... ,6. The interpretation of the states $s_i \in S(i = 0, 1, ... ,6)$ is as follows: s_0 – state of ability of *SDG* and simultaneously of all its subsystems SDG_j, ($j = \overline{1,6}$), s_1 – state of disability of the subsystem SDG_1 for acoustic emission testing, s_2 – state of disability of the subsystem SDG_2 for visual (endoscopic) testing, s_3 – state of disability of the subsystem SDG_3 for thermal (temperature, pressure) testing, s_4 – state of disability of the subsystem SDG_4 for vibration (NVH) testing, s_5 – state of disability of the subsystem SDG_5 for wear testing by using X-ray radionuclide fluorescence method (*XRF*), s_6 – state of disability of the subsystem SDG_6 for thermographic testing (infrared thermal image analysis). Changes of the listed states s_i (i = 0, 1, ..., 6) proceed at subsequent times t_n ($n \in N$), where at time t_0 = 0 a diagnosing system (*SDG*) is in state s_0. The state s_0 lasts until any of the distinguished subsystems SDG_j ($j = \overline{1,6}$) fails. The states s_j(i = 1, ..., 6) last as long as the failed subsystem SDG_j is renovated or replaced by another one in case the renovation is found unprofitable. It can be assumed that the state of *SDG* at time t_{n+1} and the time interval of

duration of the state achieved at time t_n do not depend on the states occurred at times t_0, t_1, ..., t_{n-1} or the time intervals of their duration. Thus, the process $\{W(t): t \geq 0\}$ of changes of states s_i; $i = 0, 1, \ldots, 6$ is a semi-Markov process [4, 6]. The graph of changes of the reliability states s_j of SDG ($i = \overline{0,6}$) is shown in Fig. 2.

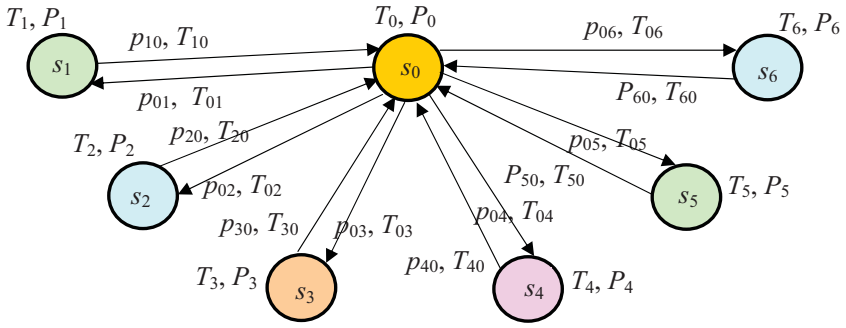

Fig.2. Graph of changes of reliability states s_i; $i = 0, 1, \ldots, 6$ for a diagnosing system SDG for a crank-piston mechanism of crosshead main engine:
s_0 – state of full ability of SDG, s_1 – state of disability of the subsystem SDG for acoustic emission testing, s_2 – state of disability of the subsystem SDG for visual (endoscopic) testing, s_3 – state of disability of the subsystem SDG for thermal (temperature, pressure) testing, s_4 – state of disability of the subsystem SDG for vibration (NVH) testing; s_5 – state of disability of the subsystem SDG for wear testing by using X-ray radionuclide fluorescence method (XRF); s_6 – state of disability of the subsystem SDG for thermographic testing (infrared thermal image analysis); T_0 – time of duration of the state of ability s_0; T_1 – time of duration of the state of disability s_1, T_2 – time of duration of the state of disability s_2; T_3 – time of duration of the state of disability s_3; T_4 – time of duration of the state of disability s_4; T_5 – time of duration of the state of disability s_5; T_6 – time of duration of the state of disability s_6;
P_0 – probability of staying SDG in state s_0, P_1 – probability of staying SDG in state s_1, P_2 – probability of staying SDG in state s_2, P_3 – probability of staying SDG in state s_3, P_4 – probability of staying SDG in state s_4, P_5 – probability of staying SDG in state s_5,
P_6 – probability of staying SDG in state s_6, p_{ij} – probability of transition from state s_i to state s_j; T_{ij} – time of duration of state s_i providing that the subsequent state is s_j; $i,j = 0,1,2,\ldots, 6$; $i \neq j$.

The initial distribution of the process $\{W(t): t \geq 0\}$ is as follows:

$$P\{W(0) = s_i\} = \begin{cases} 1 & dla \quad i = 0 \\ 0 & dla \quad i = 1,\ 2,\ \ldots,\ 6 \end{cases} \tag{6}$$

whereas its matrix function (in accordance with the graph shown in Fig. 2) is of the following form:

$$\mathbf{Q(t)} = \begin{bmatrix} 0 & Q_{01}(t) & Q_{02}(t) & Q_{03}(t) & Q_{04}(t) & Q_{05}(t) & Q_{06}(t) \\ Q_{10}(t) & 0 & 0 & 0 & 0 & 0 & 0 \\ Q_{20}(t) & 0 & 0 & 0 & 0 & 0 & 0 \\ Q_{30}(t) & 0 & 0 & 0 & 0 & 0 & 0 \\ Q_{40}(t) & 0 & 0 & 0 & 0 & 0 & 0 \\ Q_{50}(t) & 0 & 0 & 0 & 0 & 0 & 0 \\ Q_{60}(t) & 0 & 0 & 0 & 0 & 0 & 0 \end{bmatrix} \tag{7}$$

The matrix function **Q(t)** is a model of changes of the reliability states of *SDG*.

Non-zero elements $Q_{ij}(t)$ of the matrix **Q(t)** depend on the distributions of random variables which are the time intervals of staying the process $\{W(t): t \geq 0\}$ in states $s_i \in S(i = 0, 1,..., 6)$. The elements are the probabilities of transition of the mentioned process from state s_i to state s_j ($s_i, s_j \in S$) at time not longer than t, defined as follows:

$$Q_{ij}(t) = P\{W(\tau_{n+1}) = s_j,\ \tau_{n+1} - \tau_n < t | W(\tau_n) = s_i\} = p_{ij}F_{ij}(t) \tag{8}$$

where:

p_{ij} – probability of transition at one step in homogeneous Markov chain;

$p_{ij} = P\{Y(\tau_{n+1}) = s_j | Y(\tau_n) = s_i = \lim_{t\to\infty} Q_{ij}(t)$;

$F_{ij}(t)$- distribution function for the random variable T_{ij}, denoting the time of duration of state s_i of the process $\{W(t): t \geq 0\}$, providing that the subsequent state of the process is s_j.

Due to the matrix (7) of the process $\{W(t): t \geq 0\}$ is a stochastic matrix, the matrix of the probability of transition of the Markov chain embedded in this process is as follows [6]:

$$\mathbf{P} = \begin{bmatrix} 0 & p_{01} & p_{02} & p_{03} & p_{04} & p_{05} & p_{06} \\ 1 & 0 & 0 & 0 & 0 & 0 & 0 \\ 1 & 0 & 0 & 0 & 0 & 0 & 0 \\ 1 & 0 & 0 & 0 & 0 & 0 & 0 \\ 1 & 0 & 0 & 0 & 0 & 0 & 0 \\ 1 & 0 & 0 & 0 & 0 & 0 & 0 \\ 1 & 0 & 0 & 0 & 0 & 0 & 0 \end{bmatrix} \tag{9}$$

The process $\{W(t): t \geq 0\}$ is irreducible [6, 7] and random variables T_{ij} have finite positive expected values. Therefore, its limiting distribution

$$P_j = \lim_{t\to\infty} P_{ij}(t) = \lim_{t\to\infty} P\{W(t) = s_j\},\ s_j \in S(j = 0, 1, ..., 6) \tag{10}$$

is of the following form [6]:

$$P_j = \frac{\pi_j E(T_j)}{\sum_{k=0}^{6} \pi_k E(T_k)} \tag{11}$$

Probabilities $\pi_j (j = 0, 1,..., 6)$ in the formula (11) are the limiting probabilities of the embedded Markov chain.

Determination of the limiting distribution (11) requires solution of the following system of equations:

$$\left.\begin{aligned} &[\pi_0, \pi_1, \pi_2, \pi_3, \pi_4, \pi_5, \pi_6] = [\pi_0, \pi_1, \pi_2, \pi_3 \pi_4, \pi_5, \pi_6]\cdot\mathbf{P} \\ &\sum_{k=0}^{6} \pi_k = 1 \end{aligned}\right\} \qquad (12)$$

As a result of solving the system of equations (12) by using the formula (11) the following relationships can be obtained:

$$\left.\begin{aligned} &P_0 = \frac{E(T_0)}{E(T_0) + \sum_{k=0}^{6} p_{0k} E(T_k)},\ P_1 = \frac{p_{01} E(T_1)}{E(T_0) + \sum_{k=0}^{6} p_{0k} E(T_k)},\ P_2 = \frac{p_{02} E(T_2)}{E(T_0) + \sum_{k=0}^{6} p_{0k} E(T_k)}, \\ &P_3 = \frac{p_{03} E(T_3)}{E(T_0) + \sum_{k=0}^{6} p_{0k} E(T_k)}, P_4 = \frac{p_{04} E(T_4)}{E(T_0) + \sum_{k=0}^{6} p_{0k} E(T_k)},\ P_5 = \frac{p_{05} E(T_5)}{E(T_0) + \sum_{k=0}^{6} p_{0k} E(T_k)}, \\ &P_6 = \frac{p_{06} E(T_6)}{E(T_0) + \sum_{k=0}^{6} p_{0k} E(T_k)}. \end{aligned}\right\} \qquad (13)$$

The probability P_0 is a limiting probability that in longer period of operation (in theory at $t \to \infty$) *SDG* is in state s_0. This probability is therefore a coefficient of the system's technical readiness for diagnosing. However, the probabilities $P_j (j = 1, 2,..., 6)$ are limiting probabilities of existing states $s_j \in$ S of the system at $t \to \infty$, i.e. the probabilities of being its subsystems SDG_j ($j = 1, 2, \ldots, 6$) in states of disability, so also the whole *SDG*, due to its serial reliability structure.

An exemplary realization of the process $\{W(t): t \geq 0\}$, showing an occurrence of the reliability states of *SDG* during operation, is presented in Fig. 3.

For the operating practice of *SDG* adopted to identify the states of the diagnosed systems (*SDN*), important is also one-dimensional distribution of the process $\{W(t): t \geq 0\}$, whose elements are the functions $P_k(t)$ denoting the probability that at (any) time t the process is in state $s_k \in S (k = 0, 1, ..., 6)$. This momentary distribution can be calculated by using the initial distribution (6) of the process $\{W(t): t \geq 0\}$ and the functions $P_{ij}(t)$ being the probabilities of transition of the process from state s_i to state s_j ($s_i \in$ S, $s_j \in S$, $i \neq j$; $i, j = 0, 1, ..., 6$). Calculation of the transition probabilities requires the knowledge of the functions $F_{ij}(t)$, i.e. distribution functions of random variables $T_{ij} (i = j; i, j = 0, 1, ..., 6)$, which are also needed to determine the functions Q_{ij}(t) (with interpretation (8)), which are the elements of the matrix **Q(t)** defined by the relationship (7). Therefore, there are needed the proper reliability tests of *SDG*.

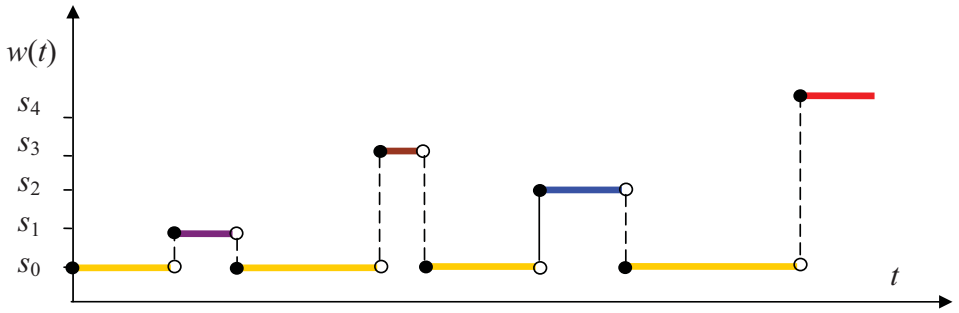

Fig. 3. Exemplary realization of the process {W(t): t ≥ 0} for a diagnosing system (SDG): s_0 – state of full ability of SDG, s_1 – state of disability of the subsystem SDG for acoustic emission testing, s_2 – state of disability of the subsystem SDG for visual (endoscopic) testing, s_3 – state of disability of the subsystem SDG for thermal (temperature, pressure) testing, s_4 – state of disability of the subsystem SDG for vibration testing (NVH testing)

The presented reliability description of diagnosing systems (*SDG*) can, of course, be developed by specifying as many reliability states as they are essential for the operating practice of the systems, i.e. needed by a user of a given type of systems to ensure their rational operation.

4. Remarks and conclusions

Application of the theory of semi-Markov processes for testing the reliability of diagnosing systems (*SDG*) enables to define not only the probability of staying the systems of this type in state of ability (s_0) and in particular states of disability $s_j(\ j = \overline{1,6}\ )$, but also the reliability of the diagnosis on the technical state of the diagnosed systems (*SDN*), which can be any mechanisms.

Semi-Markov processes are more and more often used for solving various problems in the field of reliability, mass service and diagnostics of mechanisms.

Application of the processes in the practice requires to satisfy the two conditions:

– collection of the relevant mathematical statistics;

– development of a semi-Markov model of changes of reliability states of a system with a small number of states and a simple (in the mathematical sense) matrix function **Q(t)**.

The second condition is particularly important for calculation of the momentary distribution $P_{ij}(t)$, $(i \neq j;\ i, j = 0, 1, ..., 6)$ for the process of changes of reliability states $\{W(t)$: $t \geq 0\}$ for a diagnosing system (*SDG*). As known, this distribution can be calculated when we know the initial distribution of the process $\{W(t)$: $t \geq 0\}$ and the functions $Q_{ij}(t)$ of the matrix **Q(t)**, which are the conditional probabilities of transition of the process from one reliability state to another. Calculation of the transition probabilities $P_{ij}(t)$ consists in solving a system of Volterra integral equations of the second kind (system of equations of convolution type) [6], in which the known quantities are the elements $Q_{ij}(t)$ of the matrix function **Q(t)** for the studied process $\{W(t)$: $t \geq 0\}$. When the number of states of the process is small and/or its matrix function is simple, the system can be solved by applying a Laplace–Stieltjes transform. However, if the number of states of this process is high or when at small number of states its matrix function is very complex, it is possible to obtain only an approximate solution for the system of equations. The solution (numeric) does not provide possibility to determine the probabilities of occurring the particular states of the process, when time of its duration has a

large value (in theory, when $t \to \infty$). From the theory of semi-Markov processes it results that in case of ergodic semi-Markov processes, the probabilities tend over time to strictly defined (constant) numbers. The numbers are called limiting probabilities of the states, and the sequence of the numbers makes a limiting distribution (13).

The limiting distribution enables to define a coefficient of a diagnosing system readiness for proper operation and developing a reliable diagnosis at any time [2, 6].

5. References

[1] Benjamin J.R., Cornell C.A.: *Probability*, *Statistics*, *and Decision for Civil Engineers*. Wyd. polskie *Rachunek prawdopodobieństwa, statystyka matematyczna i teoria decyzji dla inżynierów*. WNT, Warszawa 1977.

[2] Girtler J.: *Diagnostyka jako warunek sterowania eksploatacją okrętowych silników spalinowych*. Studia Nr 28. WSM, Szczecin 1997.

[3] Girtler J.: *Zastosowanie bayesowskiej statystycznej teorii decyzji do sterowania procesem eksploatacji urządzeń*. Materiały XXII Zimowej Szkoły Niezawodności nt. *Wartościowanie niezawodnościowe w procesach realizacji zadań technologicznych w ujęciu logistycznym*. SPE KBM PAN, Szczyrk 1994, s.55–62.

[4] Girtler J.: *Wiarygodność diagnozy a podejmowanie decyzji eksploatacyjnych*. Materiały Kongresu Diagnostyki Technicznej KDT'96 TII. Zespół Diagnostyki SPE KBM PAN, PTDT, IMP PAN w Gdańsku, Politechnika Śląska w Gliwicach, Politechnika Poznańska, Gdańsk 1996, s.271–276.

[5] Girtler J.: *Probabilistic measures of a diagnosis' likelihood about the technical state of transport means*. Archives of Transport, vol. 11, iss. 3-4. Polish Academy of Sciences. Committee of Transport, pp.33–42.

[6] Grabski F.: *Teoria semi-markowskich procesów eksploatacji obiektów technicznych*. Zeszyty Naukowe AMW, nr 75 A, Gdynia 1982.

[7] Grabski F.: *Semi-markowskie modele niezawodności i eksploatacji*. PAN. IBS, Warszawa 2002.

[8] Niziński S., Michalski R.: Diagnostyka obiektów technicznych. Wyd. ITE, Radom 2002.

[9] Pabis S.: *Metodologia i metody nauk empirycznych*. PWN, Warszawa 1985.

[10] Żółtowski B.: Podstawy diagnostyki maszyn. Wyd. ATR w Bydgoszczy, Bydgoszcz 1996

Journal of Polish CIMAC
Gdansk University of Technology
The Faculty of Ocean Engineering and Ship Technology

APPLICATION OF COHERENCE FUNCTIONS OF VIBROACOUSTIC SIGNALS FROM PISTON ENGINES, RECORDED IN SET STATES, FOR THEIR TECHNICAL EVALUATION

Andrzej GRZĄDZIELA, Marcin KLUCZYK

Polish Naval Academy
Ul. Śmidowicza 69, 81-103 Gdynia, Poland
Tel.:+48 58 626 23 82
tel. (58) 626 27 24, tel. (58) 626 26 67
e-mail a.grzadziela@amw.gdynia.pl, m.kluczyk@amw.gdynia.pl

Abstract

This paper presents the results of the test carried out on the Sulzer 6 AL 20/24 engine. The study was carried out during the testing following a restoration of two turbochargers of the type Napier C 045 / C. The article attempts to evaluate the suitability of the coherence function between the signals coming from diagnostically sensitive selected points of turbocharged piston engine. The study primarily focused only on the turbocharged piston engines, as it is this type of engine, which is currently the most widely used in the shipbuilding industry, both for main propulsion boats and marine plants. The paper contains results of first step of researches, focused on possibilities of using new methods in nondestructive technical state monitoring.

Keywords: *vibration, reciprocating engines, coherence*

Introduction

The aim of the study was to record vibration signals at selected points of the engine, and using the coherence function, to determine the degree of usefulness of this method of analyzing noise and vibration signals for technical inspection of piston turbocharged marine engines. Authors consider application of results coherence function as a symptom of qualitative diagnostic of combustion engines. Researches results were verified with results of the active experiments made in test bed of the engine.

The study was conducted in three stages. In the first stage, spatial selection of vibration signals of a marine piston engine was carried out. The remaining phases focused on the measurement of vibration signals and their analysis. The study used two types of refurbished turbochargers of the type Napier C 045C. It should be noted that the turbocharger has been renovated by an external company and their condition was evaluated just before a substantial part of the study. As a result of evaluation, it was concluded that one of the turbochargers was fully efficient while the latter was characterized by a significant unbalance of the rotor (acceleration value was above $a_{RMS} = 20$ m/s^2 - implemented to measure the bearing of the motor when the maximum power was reached).

The analysis of vibration signals can determine the suitability of the coherence function determined for the signals coming from the cylinder heads and the signal from the turbo, to evaluate the technical condition of marine turbocharged piston engine.

Description of the research

The study was carried out on six-cylinder, linear, four-stroke, turbocharged engine SULZER 6 AL 20/24 with the following specifications: diameter of the cylinder D - 0.2 m; stroke S - 0.24 m; the compression ratio π - 12.7; rated speed n - 750 rev / min; rated power N_e - 420 kW; fuel injection pressure p_w - 24.5 Mpa; firing order 1-4-2-6-3-5; number of valves: 2 inlet and 2 outlet. The engine is equipped with a turbocharger Napier C 045 / C at maximum speed n_s = 41000 rev / min; the number of turbine blades equal to 13 and the number of compressor blades to 15. The receiver of the power and torque from the engine is a water brake of type DPY6D securing the motor throughout the full rev range.

Prior to the testing of engine, the condition was verified by carrying out the process of indicating pressure of all cylinders and by making vibration measurements of the base frame. The study confirmed the good condition of the engine according to the quality assessment classification of indicated pressure and vibration standards PN-90/N01358. The test engine is shown in Figure No. 1, Figure 2 is a diagram of the position, on which the study was conducted.

Fig. 1 The position of the piston marine engine type SULZER 6AL20/24

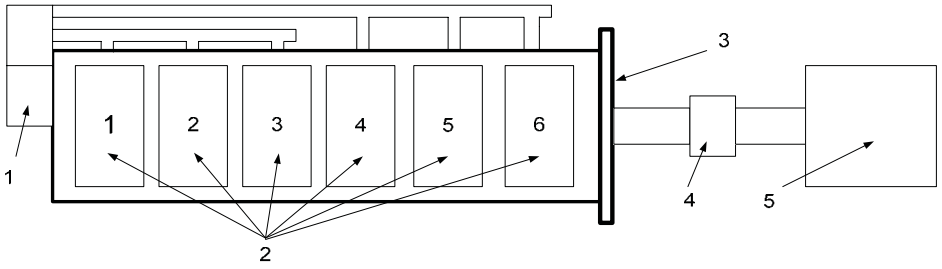

Fig. 2 Test set up. 1 – Napier C - 045 / C turbocharger, 2 - cylinder heads, 3 - flywheel, 4 - bearing bracket, 5 - DPY6D water brake

Spatial selection of vibration signals for the determination of the values, locations and ways of the measurement

The analysis of vibration signals of the piston engine is complicated due to the complex nature of the signal that is caused by the simultaneous operation of multiple sources [6].

Marine piston combustion engine is an object subject to the action of direct and secondary excitation and external influences. Vibration signal recorded in a random part of the body is the

sum of responses to all elementary events occurring at the functioning time, such as: reciprocating movements of the piston systems, valves, needle injectors, crankshaft rotational movements, timing, turbocharger, gear drives of suspended mechanisms, and pressure pulses associated with the combustion and fuel delivery to the cylinders.

Vibration signals generated by each kinematic pair and accessories of the piston engine can be considered as non-stationary due to the prevalence of different types of backlashes, and non-linear characteristics of elastic elements. Frequency characteristics of the signals depend significantly on transmission path of the propagation of component signals from the source to the measurement point [6]. For this reason, it is advisable to measure as close to the selected source of vibration as possible.

After a theoretical analysis of extortion occurring in the engine and structural analysis of potential data points as the accelerometer mounting locations, the motor heads from I to VI were selected (Figure 1 and 2) – as the most sensitive to changes in pressure in the cylinder, and the body of the plain bearing turbocharger.

During the measurements using two accelerometers type B & K 4514B were used. One of them was permanently fixed on the hull of the turbocharger, and the other mounted successively on all of the cylinder heads. Measurements were carried out in the vertical direction, in line with the gas-dynamic forces occurring during operation. Simultaneously with the measurement of vibration signals, measurements of the rotational speed of synchronous signal were carried out on the motor shaft using optical probe MM024.

After measuring the still warm accelerometers recalibration was done in order to find out the influence of temperature on the work of calibration of the transducer.

Methodology

Measurements were carried out at an engine speed of n = 600 rev/min. For each of the turbochargers two series of measurements were performed. In the first series, the aim was to analyze the relationship between vibration signals coming from the measuring points for a fully efficient fuel system of the engine. The second option predicted simulation of the injector failure of one of the cylinders. For this purpose, the dose of fuel was reduced using the overflow valve located on the injection pump (motor has an independent one-section injection pump for each cylinder). The degree of simulated damage was examined by driving continuous indicating of pressure waveforms in the engine cylinder [4]. By reducing the dose of fuel, a reduction of its combustion in the pressure cylinder was obtained. The results of this procedure are shown in the graph - Figure 3, where the upper gray line shows the course of the pressure in the cylinder during normal operation of the fuel system whereas the red curve underneath represents the pressure after reduction of the dose of fuel. As you can see the value of the maximum pressure in the cylinder of a simulated inoperative injector decreased from p = 6.92 MPa to p_1=5.13 MPa which confirms that the damage was simulated correctly. All measurements were carried out after stabilization of the operating parameters of the engine. At the time of registration of vibration signals sampling frequency of f_p = 8192 Hz was used, while the analysis bandwidth was limited to f = 0.5 Hz - 3.2 kHz.

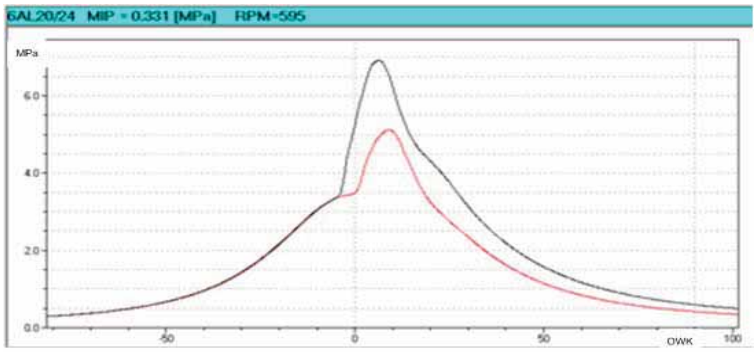

Fig. 3 Graph of cylinder number 6 - upper curve shows the course of the pressure in the efficient fuel system, lower curve shows it at partially inefficient system

Results of the study and their analysis

Aim of this study was to analyze the vibration parameters and assess the usefulness of the coherence function in the diagnosis of supercharged marine reciprocating engines. In order to achieve the task PULSE software was used, in which spectral analysis was performed using a linear velocity scale. An example of such analysis is shown in Figure number 4. It shows the velocity spectrum of vibrations during the measurements using the efficient turbocharger. The continuous red line represents the spectrum recorded in the sixth cylinder head during its normal operation. The green dotted line refers to the spectrum recorded at the same point in time as simulating a damaged fuel system of that cylinder. Table 1 shows the velocity values read for 10 consecutive harmonics

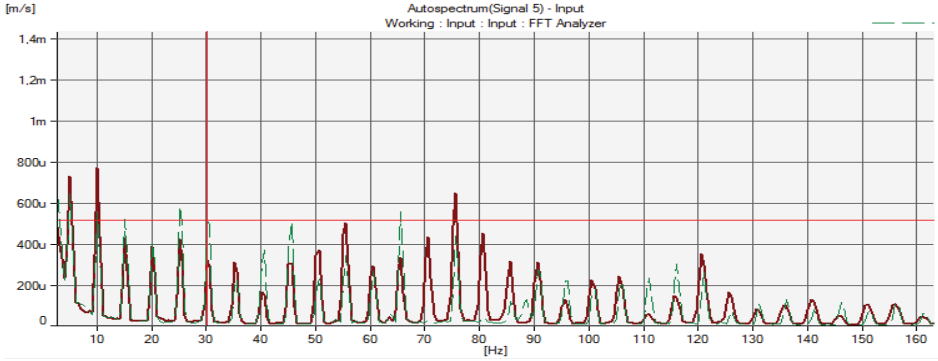

Fig. 4 Amplitude-frequency spectrum of velocity recorded at six cylinder during normal operation - solid line, and the damaged fuel apparatus - the dotted line

Table 1 Velocity amplitude measured at the head of 6-efficient and faulty injector

Number of the harmonics	I	II	III	IV	V	VI	VII	VIII	IX	X
value of v [mm/s] – injector "efficient"	0,77	0,38	0,32	0,16	0,37	0,24	0,23	0,45	0,31	0,22
value of v [mm/s] – injector "inefficient"	0,54	0,41	0,51	0,22	0,37	0,23	0,26	0,03	0,04	0,16

It should be noted that in spite of such a large change in simulating the fuel injection pressure it is not possible to diagnose a malfunction of the unit on the basis of the measurements, since the values of the amplitudes do not exceed the limits set out for example in the standard

PN-ISO 10816 [9]. Therefore, in the search for more sensitive symptoms, the authors reached for the coherence function and the cross - spectrum as potentially sensitive, dimensionless, intermediate parameters.

Coherence function which is a measure of the consistency of vibroacoustic two processes is defined as follows [1,4,6,10]:

$$\gamma_{xy}^2(f) = \frac{\left|G_{xy}(f)\right|}{G_{xx}(f)G_{yy}(f)}, \tag{1}$$

where:

x - the signal recorded on the hull of the turbocharger,

y - the signal recorded on the next cylinder heads,

G_{xy} (f) - the function of the cross-spectrum of signals x and y,

G_{xx} (f) - the function of the auto spectrum of the signal x,

G_{yy} (f) - the function of the autospectrum signal.

In a not so sophisticated, fully operational devices coherence function between the vibration signals from different points of the device will take a value of 1 or close to 1. However, any damage will be a new source of vibration signals and will affect the consistency of the existing functions i.e. decrease the value of the coherence function [2,3]. It is slightly different in the situation of such complex device i.e. supercharged piston engine. Sample coherence function between the signal recorded on the turbocharger (reference signal) and the signal recorded on the sixth cylinder head, Figures 5 and 6. Figure 5 shows the situation in which the engine is fully operational, whereas Figure 6 shows the results of a series, in which a failure of the injector of sixth cylinder is simulated.

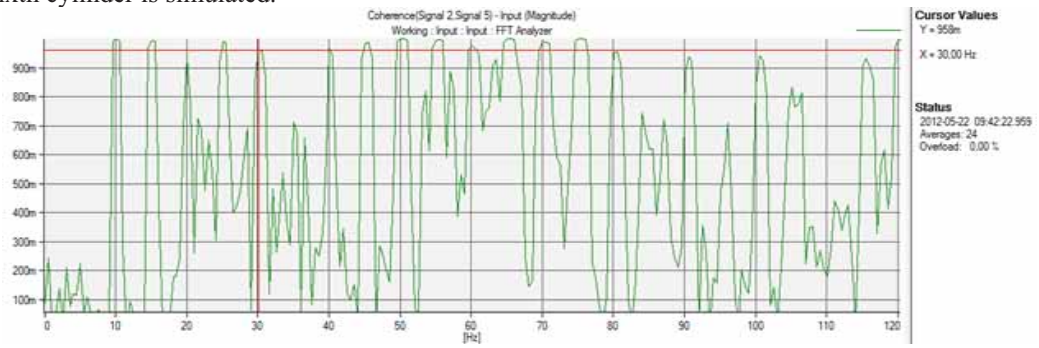

Fig. 5 Running of the coherence function calculated for the signal from the turbocharger (reference signal) and signal from the 6th cylinder head during totally smooth engine operation

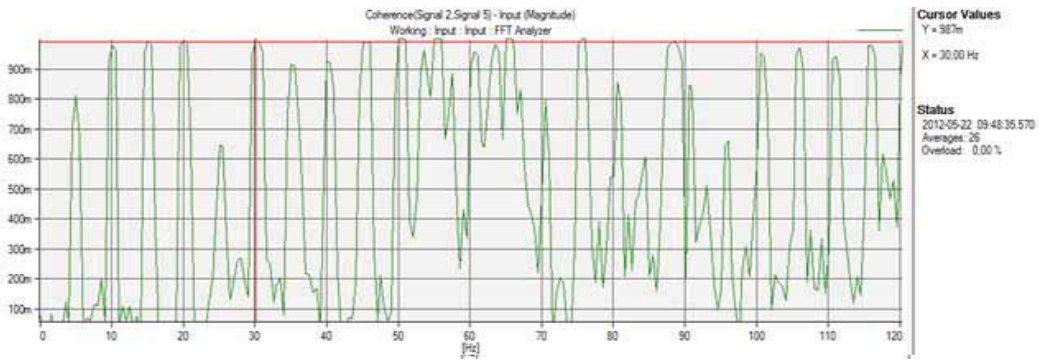

Fig. 6 Running of the coherence function calculated for the signal from the turbocharger (reference signal) and the signal from the 6th cylinder head registered during a simulated fuel apparatus damage of the 6th cylinder

The analysis of all recorded signals was made in a similar matter and the values of the coherence function between the signals recorded on the hull of the turbocharger and the signals from the consecutive engine heads for all previously presented series of measurements. It should be noted that the vibration signal coming from the hull of the turbocharger was always treated as a reference signal. The values of the cross-spectrum function and the autospectrum of the two signals were also recorded. Readings were performed at the frequency corresponding to the harmonic of the speed of the engine (I to X harmonic).

The analysis of the vibration signals recorded during a smooth engine operation

Measurement 1,2…,6 (meas. 1,2…,6) responds to measurements made during recordings on head 1,2…,6, one of the accelerometers was permanently mounted on turbocharger the second one was mounted successively on all engine heads.

Figures 7 - 10 show the results of analysis of the smooth engine vibration. On Figure 7 we can see fairly high velocity amplitudes of harmonic VII of engine speed resulting from additivity of velocity amplitudes of the basic harmonic of the rotational speed of the turbocharger.

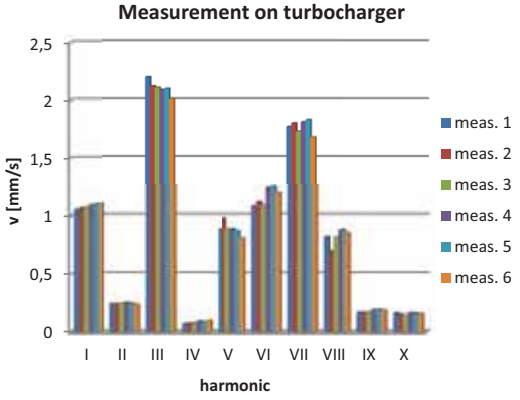

Fig. 7. Velocity amplitudes of turbocharger vibrations – efficient engine

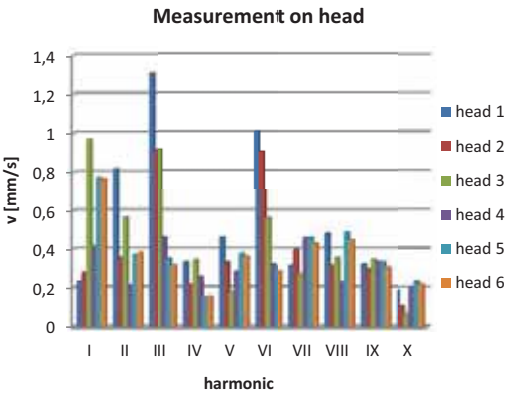

Fig. 8. Velocity amplitudes of engine heads – efficient engine

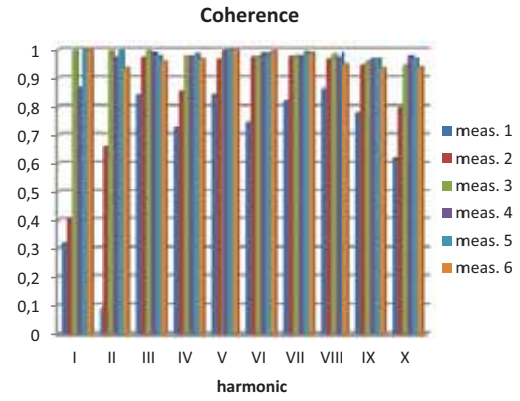

Fig. 9. Values of coherent functions – efficient engine

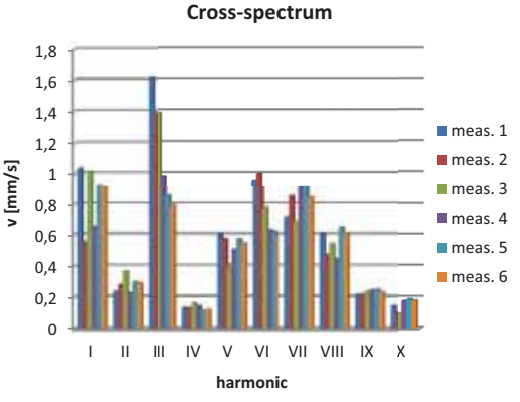

Fig. 10. Values of the cross – spectrum function – efficient engine

In addition, the dominant values are the values of harmonic III and VI of rotational speed of the engine, which is associated with the combustion process (three times to force the turn - six-

cylinder four-stroke), and the forces of inertia (six excitations per revolution). You'll also see a low value of the coherence function for the signals coming from cylinder 1 and 2 and the turbocharger.

The analysis of the vibration signals recorded at the time of the experiments - damage to the fuel system of the 6th cylinder, efficient turbocharger

In the case of a decrease in the fuel injection pressure in one of the cylinders, values of the individual harmonics measured on both the heads and the turbocharger do not vary much, however clearly visible is the increase of the coherence function between the signals of 1st and 2nd cylinder (simulated damage on the cylinder No. 6) - figure 13

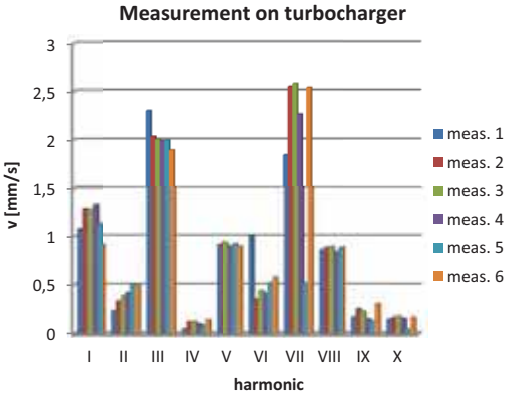

Fig. 11. Velocity amplitudes of turbocharger vibrations – damaged cylinder no. 6

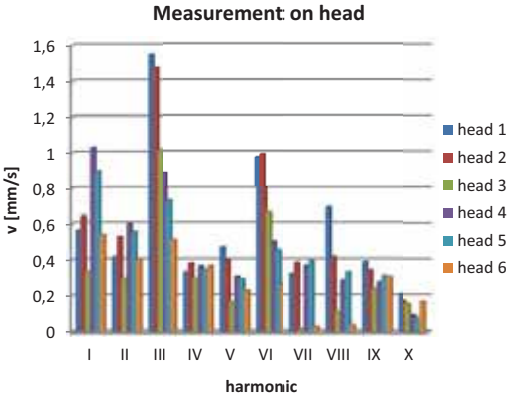

Fig. 12. Velocity amplitudes of engine heads vibrations – damaged cylinder no. 6

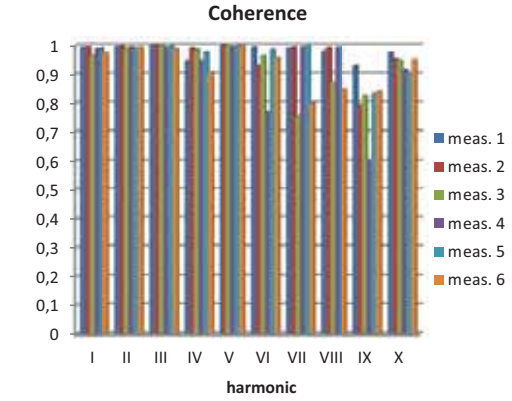

Fig. 13. Values of the coherent function – damaged cylinder no. 6

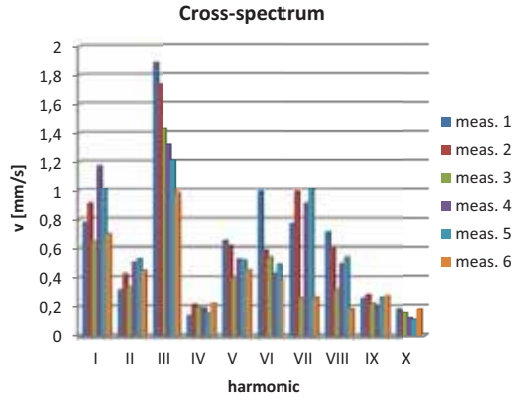

Fig. 14. Values of the cross- spectrum function – damaged cylinder no. 6

Efficient fuel system, turbocharger failure due to unbalance

In case of a turbocharger rotor unbalance, while maintaining proper operation of the fuel system of all cylinders, still the dominant harmonic are the III and VI harmonic of engine speed. Looking at the values of the coherence function, a decrease in its value for the signals coming from the turbocharger and the 2nd, 3rd and 4th cylinder is seen - Figure 17.

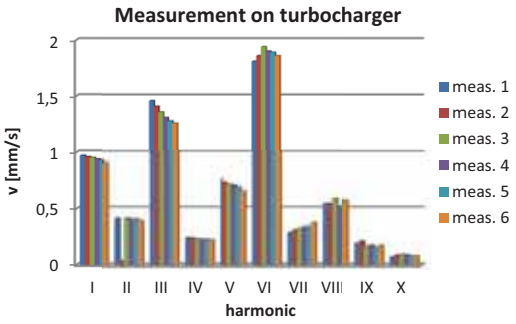

Fig. 15. Velocity amplitudes of the turbocharger vibrations – damaged turbocharger

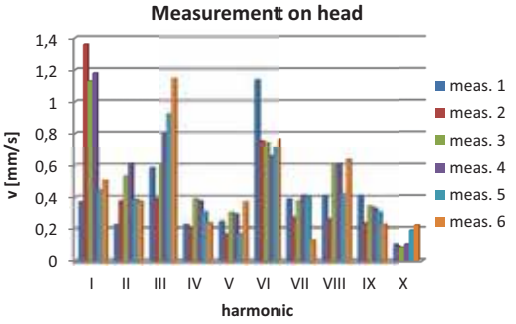

Fig. 16. Velocity amplitudes of the engine heads – damaged turbocharger

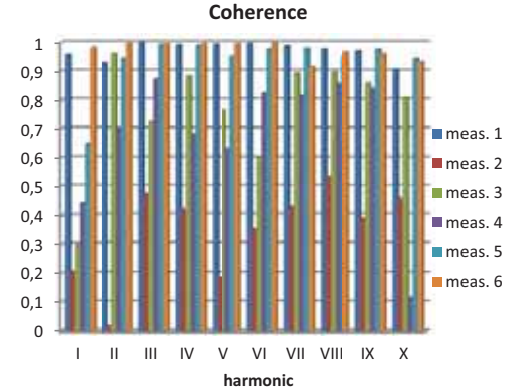

Fig. 17. Values of the coherent function – damaged turbocharger

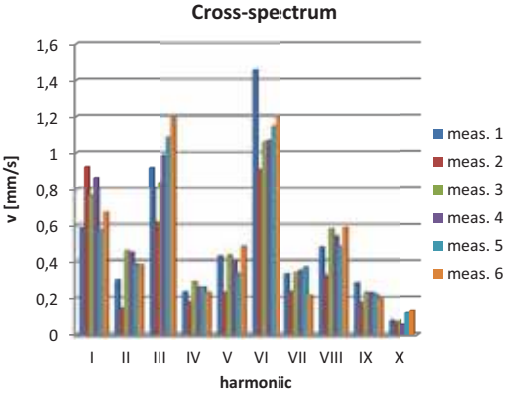

Fig. 18. Values of the cross – spectrum function – damaged turbocharger

Simulating damage to 5th cylinder and turbocharger failure due to unbalance

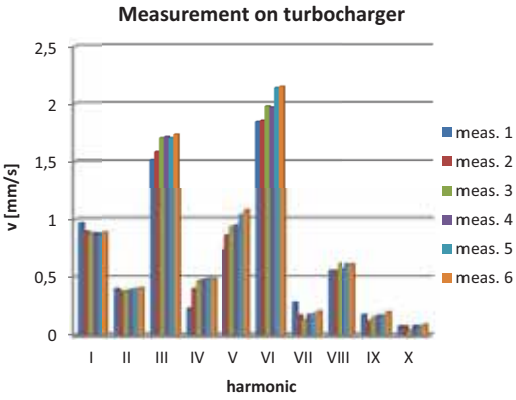

Fig. 19. Velocity amplitudes of the turbocharger vibrations – damaged turbocharger and 5th cylinder

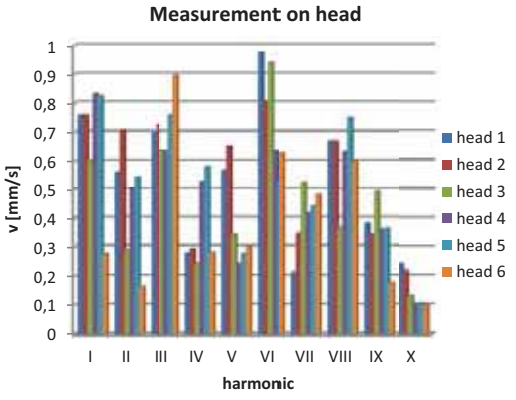

Fig. 20 Velocity amplitudes of the engine heads vibrations – damaged turbocharger and 5th cylinder

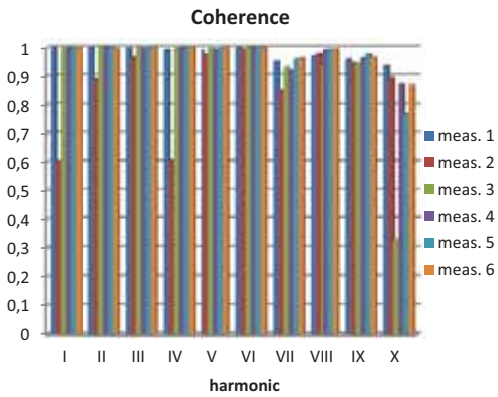

Fig. 21. Values of the coherent function – damaged turbocharger and 5th cylinder

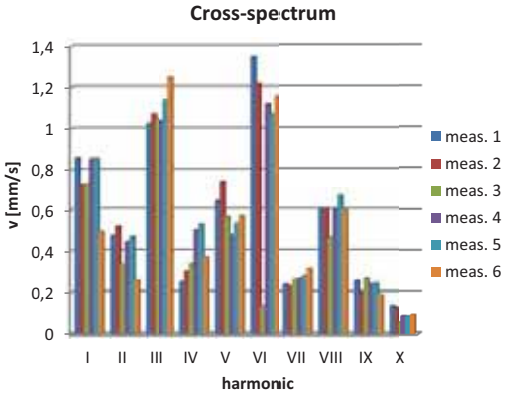

Fig. 22. Values of the cross – spectrum function – damaged turbocharger and 5th cylinder

Considering the situation in which the engine is running with a faulty turbocharger and damaged injector an increase in the value of the coherence function is observed - Figure 21.

Conclusions

The analysis provides a clear statement that the dominant harmonics in all spectra of the two measuring points are III and VI harmonic of vibration speed of the engine speed. The high value of the third harmonic is caused by gas-dynamic forces resulting from the combustion process taking place in the six-cylinder engine, while the VI harmonic is related to the forces of inertia of the crank-piston engine.

The read values of the coherence function vary quite considerably. It is therefore observed here that the fall in the value of the coherent function between the signal from the turbocharger and cylinder heads can mean that one of the cylinders has a faulty injector. Unambiguous quantification of this relationship is the subject of further ongoing research.

It should be noted that the lowest values of the coherence function occurred when the damage was the turbocharger rotor unbalance. It can therefore be a working hypothesis that the declining value of the coherence function between the signal from the turbocharger and cylinder head can mean a poor technical state of the turbocharger.

An essential symptom observed in the course of the analysis is the fact of a significant increase in the value of the coherence function at the frequency corresponding to subharmonic ½ of fundamental frequency of the rotation speed of the engine in cases where the engine is running with a malfunctioning injector (Figure 5 and 6). This phenomenon was observed regardless of the cause of deterioration of the engine condition. This will be further examined during a series of further laboratory tests and a simulation model implemented in a MatLab environment.

References

[1] Brüel & Kjær Pulse LabShop – *pruduct help.*
[2] Cempel, Cz., *„Diagnostyka wibroakustyczna maszyn”*, PWN, Warszawa 1989.
[3] Cempel Cz., *„Podstawy wibroakustycznej diagnostyki maszyn”*, WN-T, Warszawa 1982.
[4] Kałaczyński T., „The coherence method of technical state evaluation combustion engine”, Journal of KONES Powertrain and Transport, Vol. 17, No. 2 pp. 205-213, Warszawa 2010.
[5] Łutowicz, M., *Analizator pracy silnika” - instrukcja użytkownika.*

[6] Madej, H., *„Metody przetwarzania sygnałów wibroakustycznych w diagnozowaniu silników tłokowych”*, Zeszyty Naukowe Politechniki Śląskiej, seria: TRANSPORT z. 69 str. 97-104, Gliwice 2010.
[7] MatLab Signal processing toolbox – *product help.*
[8] Morel, J., *„Drgania maszyn i diagnostyka ich stanu technicznego”*, PTDT, Warszawa 1997.
[9] PN-ISO 10816., „*Norma międzynarodowa; Drgania mechaniczne – Ocena drgań maszyny na podstawie pomiarów na elementach niewirujących”.*
[10] Żółtowski B., *„ Diagnostyczny system eksploatacji silników spalinowych”,* Zeszyty naukowe Akademii Marynarki Wojennej, nr 4 (183), str. 133-142, Gdynia 2010.

Journal of Polish CIMAC
Gdansk University of Technology
The Faculty of Ocean Engineering and Ship Technology

MULTIDIMENSIONAL ANALYSIS AND ASSESSMENT OF COMBUSTION ENGINE TECHNICAL STATE BASIS ON SVD METHOD WITH MODERN ENGINEERS SOFTWARE APPLICATION

Tomasz Kałaczyński[1], Marcin Łukasiewicz[2]

University of Technology and Life Science
ul. S. Kaliskiego 7, 85-789 Bydgoszcz, Poland
tel.: +48 52 3408262
e-mail:kalaczynskit@utp.edu.pl[1], mlukas@utp.edu.pl[2]

Abstract

The changes of vibration estimators as a result of engine maladjustment, waste, damage or failure are the main idea of vibrodiagnostic investigation. Diagnostic investigations that use of vibration to determine the technical state of combustion engines are very difficult. Only a few proposed methods could have a wider technical use in diagnostics. This paper shows the validation of research results of the use of the Singular Value Decomposition (SVD) method.

The research object is combustion engine No. 138C.2.048 with 1.4l. swept capacity, power 55 kW / 75 KM, generally applied to Fiat. It is possible to introduce generated vibration signals as well as the investigation of its adjustment influence on the combustion engine vibration signals change. Thanks to SVD methods, it is possible to decide which symptom given in the observation matrix is the best to recognize the technical state of combustion engines. The results that are introduced in this paper are only the part of realized investigative project and they do not describe wholes of the investigative question, only chosen aspects.

Keywords: *combustion engine, diagnostic inference, damage, symptoms ,SVD*

1. Introduction

The technical state of objects, machine, and vehicles can be described as a set of the all parameters values that define the given object in a given moment of time t. The time sequences of these states could be considered as the time of existence of the device. The use of technical diagnostic methods makes possible the qualification of current technical states of studied objects, machines and vehicles [5, 6].

Diagnostic researches that use vibration to determine the technical state of combustion engines are very difficult to apply and only a few proposed methods could have wider technical use in diagnostics. This paper contains application of SVD methods focused to the identification of the technical state of combustion engines. The SVD method is the appropriate tool for analysing a mapping from one vector space into another vector space, possibly with a different dimension [2,3].

The object of research was a combustion engine No. 138C.2.048 with 1.4l. swept capacity, power 55 kW / 75 KM, generally applied to Fiat. It is possible to introduce generated vibration signals as well as the research of its adjustment influence on the combustion engine vibration signals change [2,3,4]. The necessity of estimating the technical state is conditioned by the

possibility of making decisions connected with object exploitation and the procedure methods to diagnose the technical state.

The present development of technical equipment and software creates new possibilities for diagnosing systems and monitoring technical condition of more folded mechanical constructions.[5,6]

2. Model of diagnostics signal generation

The research object was a combustion engine situated in the investigative laboratory of combustion engines in UTP Bydgoszcz. Based on this engine, a model of diagnostic signal generation was created during the investigations [2,3,4,5,6]. The proposed model of combustion engine diagnostic signal generation is shown on Figure 1.

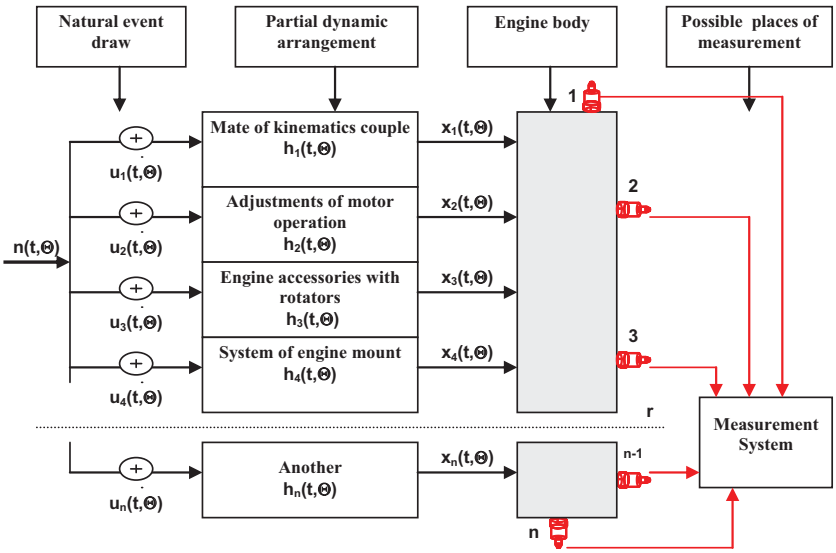

Fig.1. Combustion engine diagnostics signal generation model[4]

The received signals in any point of engine body are the sum of the answer at all elementary events un (t, Θ), outputs in individual partial dynamic arrangements with the pulse function of input hn (t, Θ). These influences after passing by proper dynamic arrangements are summed up on the engine body, on chosen points was measured by the vibration transducers. As a result of conducted measurements output signals was used to estimation. By n (t, Θ) was marked accidental influence stepping out from presence of dynamic micro effects such as friction [2,3,4,5,6].

Based on the Matlab environment the application diagnostics software "DM" was used for vibroacoustics signal analysis, serving to the processing and analysis of the investigative data.

This software enables the obtainment of symptoms from vibration signals and then it makes it possible to describe the technical state of the machine in matrix observation. A model of a machine in good state and another model of the same machine after certain period of usage gives an inference base about the state of the object and vibration predominant sources that allows machine modernization in the next step.

3. Singular value decomposition

The SVD method is the one of the newest diagnostic methods. It is the appropriate tool for analysing a mapping from one vector space into another vector space, possibly with a different dimension [1,6,7]. The SVD method was included in the diagnostics software "DM", the general programming structure of the Multivariable Diagnosis application developed by the Research Group on Industrial Maintenance (GEMI), Mechanical Engineering Department, Engineering School, EAFIT University and used for result validation. The SVD method algorithm is shown in Figure 2.

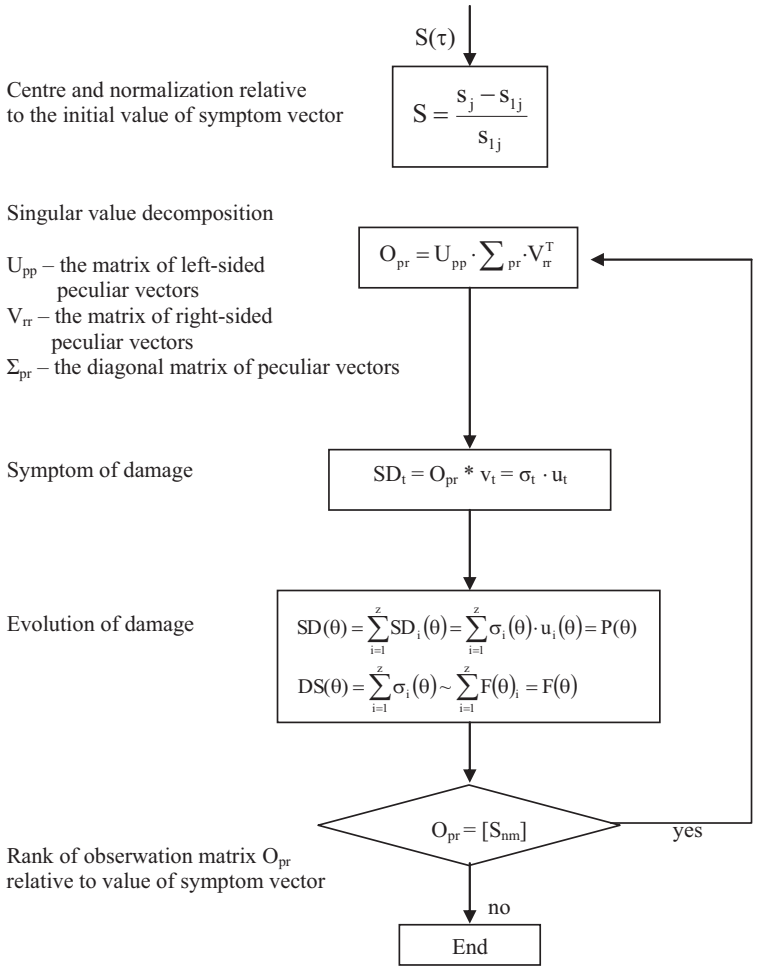

Fig.2. Singular Value Decomposition algorithm [1,6,7]

Figure 3 displays the main window of the SVD module that was used for analysis.

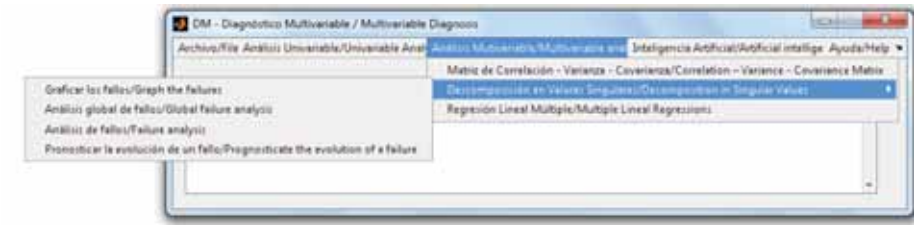

Fig.3. SVD module window

Percentage of damage in the object status description obtained in the "DM" software is shown in Figure 4. The red line marks a value of 50% failure of the principal failure.

Fig. 4. Graphical interpretation of failures in object

The program allows to present graphical interpretations:

- analysis of the principal failure - Figure 5,
- reliability analysis - Figure 6.

Figure 5 contains two graphs: the first is a graphic interpretation of a generalized state of the object with the specified limit, which is determined based on the configuration parameters. The generalized state of the object is presented using the main damage to its technical state. The second graph relates the analysis of discretion areas by presenting:

- limit,
- probability of success evaluation for a good state,
- probability of unnecessary repairs allowed,
- probability of undetected fault state,
- probability of success in the evaluation of the damage.

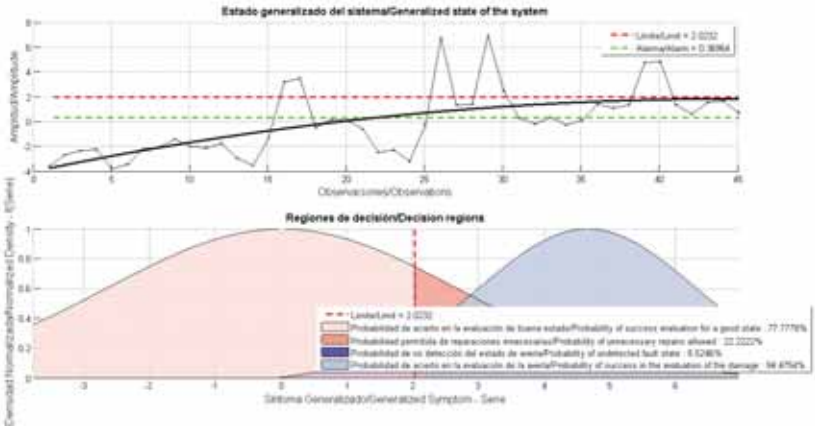

Fig. 5. Graphical interpretation analysis of the principal failure

Figure 6 shows the graphical interpretation of the reliability and damage assessment: speed development risk and its main damage, and speed development of global risk for all damages.

It also shows the histogram of the principal failure with: limits, probability of not exceeding the limit value, probability of exceeding the limit value, type of distribution together with the values of distribution parameters. The next stage of analysis is the graphical interpretation of the correlation symptoms with the selected failure as shown in Figure 7. The analysis of correlation symptoms with the selected failure allows to rank the symptoms due to the correlation coefficient value as shown in Figure 7. Figure 8 shows a graphic interpretation of the generalized object state with the specified limit and permissible value for the selected fault.

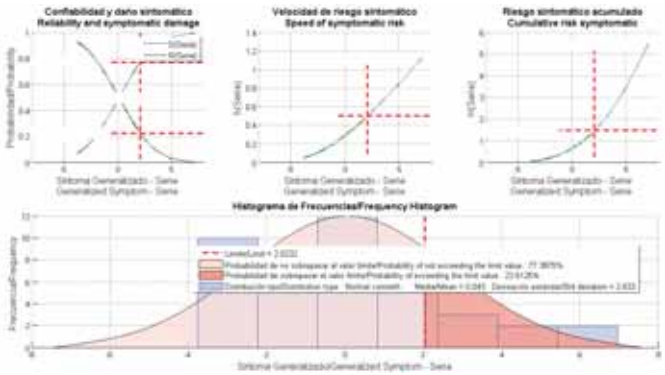

Fig. 6. Graphical interpretation reliability analysis

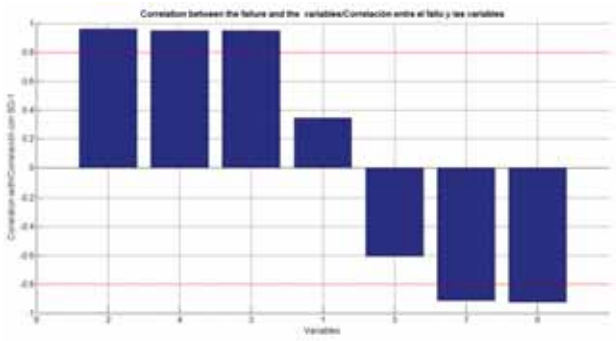

Fig. 7. Graphical interpretation correlation of symptoms with the selected failure

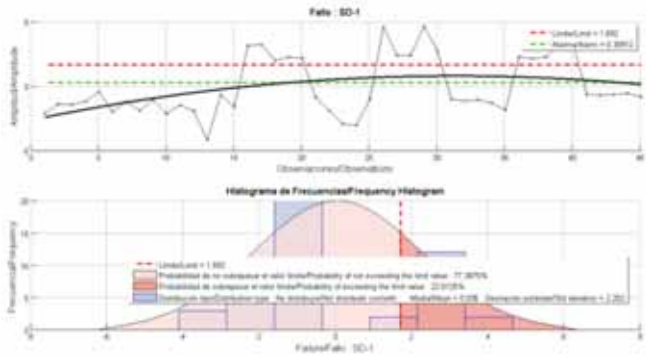

Fig. 8. Graphical interpretation analysis of the selected failure

The generalized state of the object is presented by a selected damage in relation to states of the object. Figure 8 shows the histogram of the selected fault value with:

- limits,
- probability of not exceeding the limit value,
- probability of exceeding the limit value,
- type of distribution together with the values of distribution parameters.

4. The results of research

With the object of research in the laboratory, 33 states were simulated with the damages to the spark plug and injectors on the individual cylinders of the engine and the combination of these damages. Figure 9 shows the failure to the spark plug electrodes modeled by removing the side electrode and the injector damage modeled by the release the signal cable.

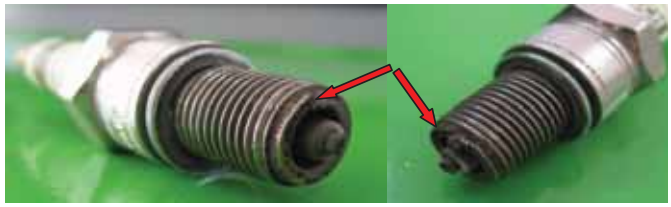

Fig. 9. Failure of removing the spark plug side electrode

During the experimental research uniform conditions in the engine are needed in order to guarantee the success of the analytical process. The research was performed under the following conditions:

- 830 r.p.m was executed measurements for the rotational speed of the engine,
- for neutral gear - temperature of the trunk of the engine carried out 71 degrees,
- the dynamic state of the engine is described 30 measuring files,
- the investigations were executed using two measuring channels for the fulfillment of the state of Fourier transformation.

The measuring track consisted of (Figure. 10) :

- two acceleration sensors ICP Model: 352C68,
- two leads series 002,
- data acquisition module VIBDAQ +.

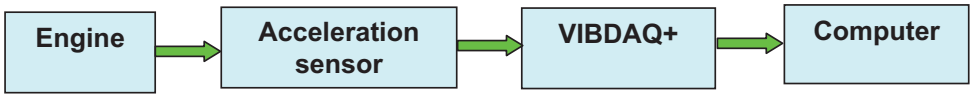

Fig. 10. Block diagram of the measuring system

The research allowed obtaining vibration signals in time response function from selected points on the engine for the simulated research object states.

The results obtained were analyzed in the software "SIBI". SIBI program was developed in the University of Technology and Life Sciences in Bydgoszcz, Faculty of Mechanical Engineering, Department of vehicles and diagnostics, and was used to validate the results of research [7].

The analysis in SIBI program allowed generating eight own measures and eight mutual measures. This measures were analysed by using the SVD method for assessing the diagnostic usefulness of the generated own and mutual measures.

5. The results of validation

Conducted researches on combustion engines depend on the delimitation of vibroacoustics measures of the engine and comparing them with measures appointed for damaged engines (eg. damaged spark plug, injector) to accomplish the assessment through operational vibroacoustic methods of how the received results influence the technical state of an engine.

The observation matrixes have eight own symptoms (χ_{ave} – Average, A_{RMS} – Root Mean Square. P_{MAX} – Pick max., σj – Standard deviation, K – Shape factor, C – Crest factor, I - Impulse factor, R_{xx} – Autocorrelation factor) and eight mutual symptoms $\gamma(f1)$ – value of coherence for a first characteristic frequency 12,63 [Hz], $\gamma(f2)$ – value of coherence for a second characteristic frequency 23,27 [Hz], $\gamma(f3)$ – value of coherence for a third characteristic frequency 46,96 [Hz], $\gamma(\Delta f)$ – value of the area under course of the coherence function for the range from the first to the third characteristic frequencies, $R_{xy}(\Delta f)$ – value of the area under course of the crosscorrelation function for the range from the first to the third characteristic frequencies, $FFTx(\Delta f)$ – value of the area under the course of signal spectrum from the first point between the first and the third characteristic frequencies, $FFTy(\Delta f)$ – value to the area under the course of signal spectrum from the second point between the first and the third characteristic frequencies $H_{xy}(\Delta f)$ – value of the area under course of the transmittance function for the range from the first to the third characteristic frequencies [2,3]. The final observation matrixes of engine performance given in Table 1 describe 8 own symptom and in the ones in Table 2 describe 8 mutual symptoms.

Table 1. The final observation matrix for own symptoms

Symptom / State	x_{ave}	A_{RMS}	P_{MAX}	σ_j	K	C	I	R_{xx}
damaged spark plug on cylinder 1	0,048	0,057	0,144	0,057	1,197	2,501	2,994	0,043
damaged spark plug on cylinder 2	0,052	0,060	0,152	0,060	1,155	2,535	2,927	0,045
damaged spark plug on cylinder 3	0,060	0,073	0,200	0,073	1,215	2,733	3,321	0,045
damaged spark plug on cylinder 4	0,013	0,014	0,028	0,014	1,131	1,971	2,229	0,043
damaged spark plug on cylinder 1 -2	0,054	0,065	0,191	0,065	1,213	2,936	3,561	0,047
damaged spark plug on cylinder 1 -4	0,076	0,090	0,218	0,090	1,195	2,412	2,882	0,045
damaged spark plug on cylinder 2-3	0,052	0,063	0,166	0,063	1,216	2,649	3,223	0,043
damaged spark plug on cylinder 3 - 4	0,038	0,046	0,107	0,046	1,193	2,342	2,794	0,043
dam. injector on cylinder 1	0,046	0,056	0,151	0,056	1,206	2,698	3,253	0,047
dam. injector on cylinder 2	0,304	0,365	0,815	0,365	1,201	2,235	2,684	0,050
dam. injector on cylinder 3	0,278	0,353	0,871	0,353	1,270	2,469	3,137	0,045
dam. injector on cylinder 4	0,279	0,354	0,912	0,354	1,271	2,575	3,272	0,047
dam. injector on cylinder 1-2	0,353	0,447	1,149	0,447	1,267	2,572	3,259	0,050
dam. injector on cylinder 1-4	0,354	0,424	0,961	0,424	1,198	2,269	2,719	0,045
dam. injector on cylinder 2-3	0,193	0,234	0,625	0,235	1,213	2,665	3,233	0,053
dam. injector on cylinder 3-4	0,235	0,317	1,081	0,318	1,352	3,405	4,605	0,055
dam. injector on cylinder 1 and spark plug on cylinder 2	0,355	0,411	0,868	0,411	1,160	2,111	2,449	0,045
dam. injector on cylinder 1 and spark plug on cylinder 3	0,352	0,403	0,833	0,403	1,146	2,069	2,371	0,047
dam. injector on cylinder 1 and spark plug on cylinder 4	0,376	0,432	0,829	0,433	1,149	1,916	2,201	0,045
dam. injector on cylinder 2 and spark plug on cylinder 1	0,273	0,319	0,700	0,319	1,169	2,193	2,563	0,040
dam. injector on cylinder 2 and spark plug on cylinder 3	0,188	0,215	0,619	0,216	1,144	2,874	3,286	0,050
dam. injector on cylinder 2 and spark plug on cylinder 4	0,272	0,311	0,718	0,311	1,142	2,311	2,639	0,050
damaged injector on cylinder 3 and spark plug on cylinder 1	0,103	0,133	0,431	0,133	1,292	3,234	4,177	0,018
dam. injector on cylinder 3 and spark plug on cylinder 2	0,347	0,398	0,889	0,399	1,146	2,231	2,558	0,047
dam. injector on cylinder 3 and spark plug on cylinder 4	0,188	0,214	0,539	0,214	1,136	2,518	2,861	0,053
dam. injector on cylinder 4 and spark plug on cylinder 1	0,348	0,400	0,827	0,400	1,147	2,069	2,373	0,045
dam. injector on cylinder 4 and spark plug on cylinder 2	0,359	0,413	0,868	0,413	1,152	2,101	2,420	0,045
dam. injector on cylinder 4 and spark plug on cylinder 3	0,223	0,252	0,551	0,252	1,131	2,190	2,477	0,050
dam. injector on cylinder 1 and spark plug on cylinder 1	0,361	0,412	0,851	0,412	1,141	2,067	2,357	0,047
dam. injector on cylinder 2 and spark plug on cylinder 2	0,152	0,182	0,509	0,182	1,197	2,799	3,351	0,047
dam. injector on cylinder 3 and spark plug on cylinder 3	0,082	0,102	0,300	0,102	1,232	2,955	3,639	0,045
dam. injector on cylinder 4 and spark plug on cylinder 4	0,050	0,064	0,220	0,064	1,275	3,448	4,394	0,045

Table 2. The final observation matrix for mutual symptoms

Symptom / State	$\gamma(f_1)$	$\gamma(f_2)$	$\gamma(f_3)$	$\gamma(\Delta f)$	$R_{xy}(\Delta f)$	$FFT_x(\Delta f)$	$FFT_y(\Delta f)$	$H_{xy}(\Delta f)$
damaged spark plug on cylinder 1	0,439	0,982	0,691	7,576	12,402	0,007	0,007	16,680
damaged spark plug on cylinder 2	0,797	0,987	0,308	6,167	18,817	0,006	0,027	23,493
damaged spark plug on cylinder 3	0,893	0,972	0,125	6,573	19,924	0,007	0,008	15,729
damaged spark plug on cylinder 4	0,576	0,906	0,207	5,043	1,495	0,003	0,005	23,397
damaged spark plug on cylinder 1 -2	0,292	0,989	0,339	4,416	7,067	0,035	0,041	22,863
damaged spark plug on cylinder 1 -4	0,335	0,987	0,961	5,784	4,064	0,044	0,047	20,212
damaged spark plug on cylinder 2-3	0,947	0,992	0,852	7,443	5,886	0,060	0,072	21,766
damaged spark plug on cylinder 3 - 4	0,746	0,975	0,328	4,924	6,335	0,044	0,057	20,140
dam. injector on cylinder 1	0,606	0,123	0,058	4,498	0,533	0,012	0,104	16,897
dam. injector on cylinder 2	0,914	0,986	0,143	5,292	0,467	0,013	0,057	15,316
dam. injector on cylinder 3	0,969	0,989	0,905	4,800	0,357	0,011	0,049	13,977
dam. injector on cylinder 4	0,970	0,993	0,711	4,406	0,304	0,010	0,056	23,070
dam. injector on cylinder 1-2	0,813	0,980	0,966	9,941	5,758	0,418	0,132	6,060
dam. injector on cylinder 1-4	0,990	0,998	0,543	10,458	8,054	0,286	0,084	5,796
dam. injector on cylinder 2-3	0,957	0,931	0,513	10,143	10,479	0,265	0,056	4,475
dam. injector on cylinder 3-4	0,998	0,941	0,909	7,798	6,570	0,386	0,101	4,204
dam. injector on cylinder 1 and spark plug on cylinder 2	0,623	0,993	0,497	7,027	9,149	0,273	0,208	21,748
dam. injector on cylinder 1 and spark plug on cylinder 3	0,699	0,990	0,870	3,771	0,940	0,197	0,130	13,359
dam. injector on cylinder 1 and spark plug on cylinder 4	0,773	0,995	0,943	4,130	0,825	0,254	0,139	8,254
dam. injector on cylinder 2 and spark plug on cylinder 1	0,981	0,888	0,851	4,374	0,847	0,253	0,178	13,147
dam. injector on cylinder 2 and spark plug on cylinder 3	0,929	0,707	0,819	6,516	15,671	0,203	0,165	15,254
dam. injector on cylinder 2 and spark plug on cylinder 4	0,845	0,848	0,843	5,497	15,647	0,183	0,160	14,334

damaged injector on cylinder 3 and spark plug on cylinder 1	0,880	0,984	0,619	4,538	9,495	0,250	0,173	13,718
dam. injector on cylinder 3 and spark plug on cylinder 2	0,754	0,985	0,347	15,695	17,729	0,189	0,192	26,972
dam. injector on cylinder 3 and spark plug on cylinder 4	0,938	0,344	0,771	7,616	14,901	0,169	0,127	15,253
dam. injector on cylinder 4 and spark plug on cylinder 1	0,808	0,996	0,226	5,605	13,350	0,195	0,194	17,487
dam. injector on cylinder 4 and spark plug on cylinder 2	0,859	0,997	0,487	8,947	15,324	0,210	0,193	23,706
dam. injector on cylinder 4 and spark plug on cylinder 3	0,792	0,628	0,850	7,746	8,431	0,172	0,151	17,617
dam. injector on cylinder 1 and spark plug on cylinder 1	0,613	0,976	0,922	5,342	7,884	0,180	0,140	12,710
dam. injector on cylinder 2 and spark plug on cylinder 2	0,964	0,918	0,533	6,337	10,451	0,096	0,061	10,632
dam. injector on cylinder 3 and spark plug on cylinder 3	0,974	0,990	0,907	5,689	4,026	0,109	0,078	9,978
dam. injector on cylinder 4 and spark plug on cylinder 4	0,992	0,993	0,883	5,518	3,455	0,091	0,092	10,789

For the purposes of analysis the technical states were classified into 3 groups:

- first group - damage spark plug,
- second group - damage the injector,
- third group - damage the injector and spark plug.

The following illustrations shows the graphical interpretation of own symptoms revealed through the analysis research results with the SVD method (failures in the engine, the histogram of values the principal failure, the correlation between of individual symptoms of root damage). For the first group of states:

Fig. 11. Graphical interpretation of the failures in objects for the first group of states

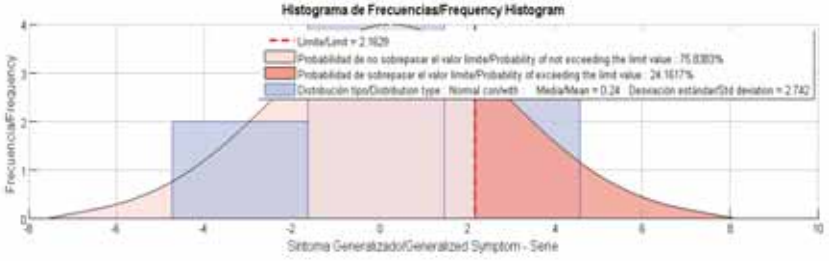

Fig. 12. Graphical interpretation histogram value of the main failure for the first group of states

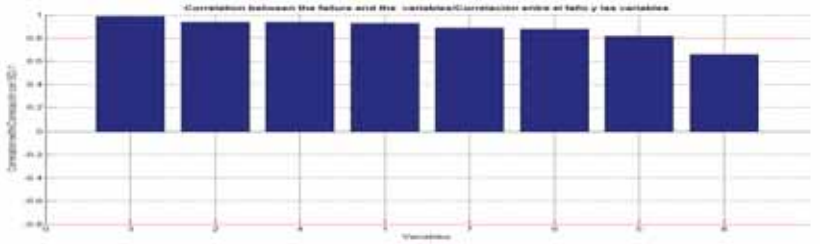

Fig. 13. Graphical interpretation of the correlation of own symptoms with the main failure for the first group of states

For the second group of states:

Fig. 14. Graphical interpretation of the failures in objects for the second group of states

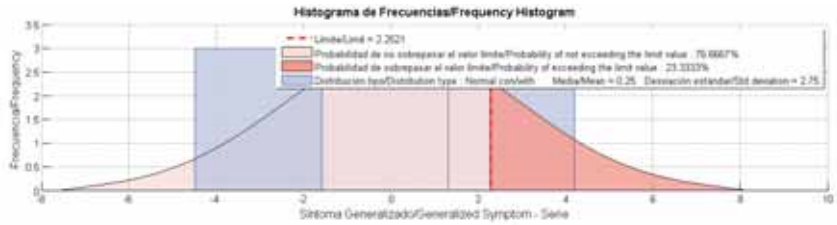

Fig. 15. Graphical interpretation histogram value of main failure for the second group of states

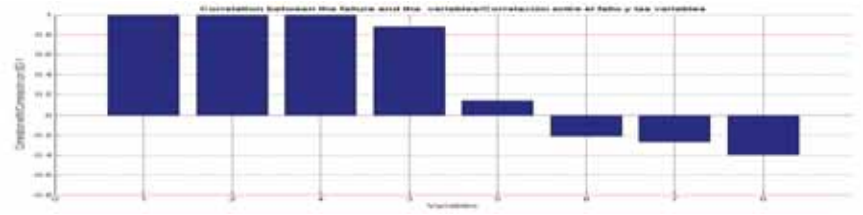

Fig. 16. Graphical interpretation of the correlation of own symptoms with the main failure for the second group of states

For the third group of states:

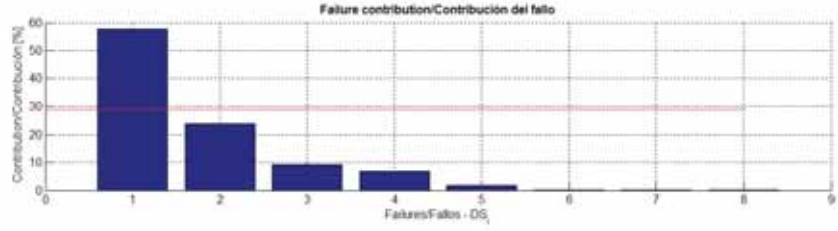

Fig. 17. Graphical interpretation of the failures in object for the third group of states

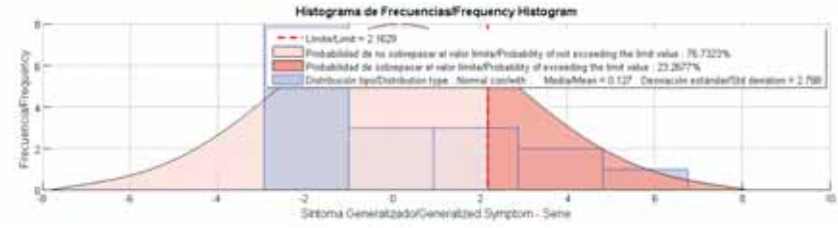

Fig. 18. Graphical interpretation histogram value of main failure for the third group of states

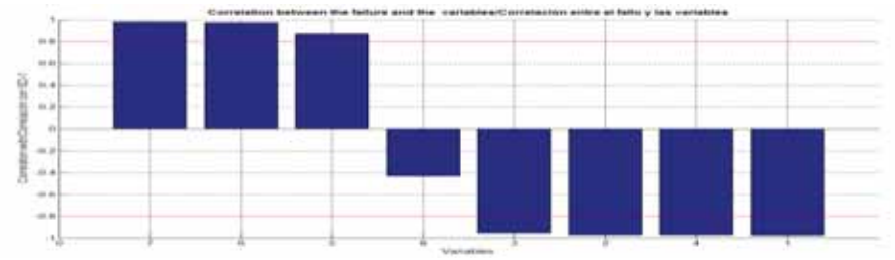

Fig. 19. Graphical interpretation of the correlation of own symptoms with the main failure for the third group of states

The following illustrations shows the graphical interpretation of mutual symptoms revealed through the analysis research results with the SVD method (failures in the engine, the histogram of values the principal failure, the correlation between of individual symptoms of root damage).

For the first group of states:

Fig. 20. Graphical interpretation the failures in object for the first group of states

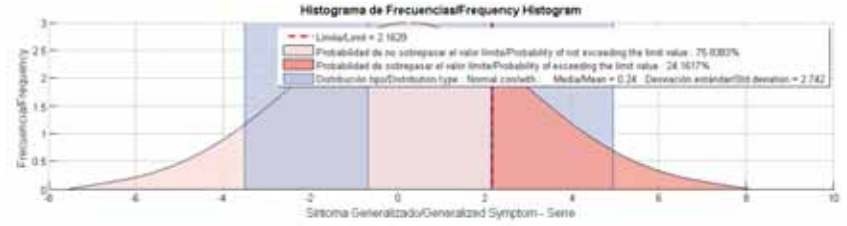

Fig. 21. Graphical interpretation histogram value of main failure for the first group of states

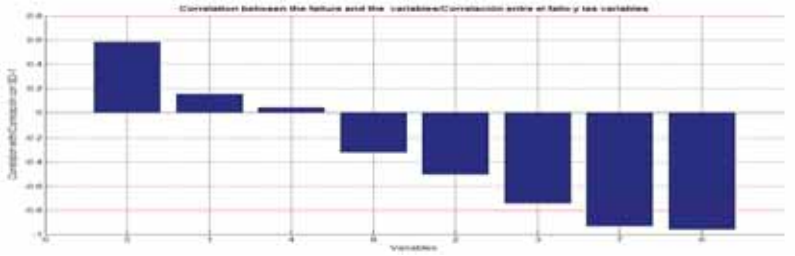

Fig. 22. Graphical interpretation correlation of symptoms with the main failure for the first group of states

For the second group of states:

Fig. 23. Graphical interpretation the failures in object for the second group of states

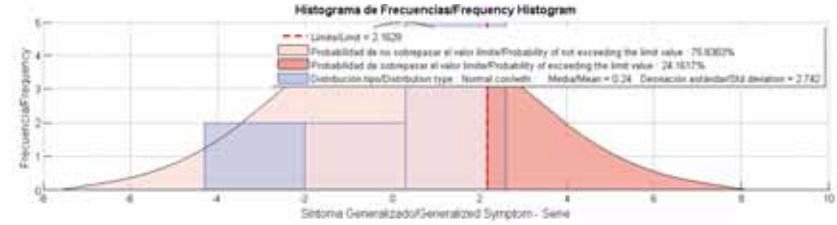

Fig. 24. Graphical interpretation histogram value of main failure for the second group of states

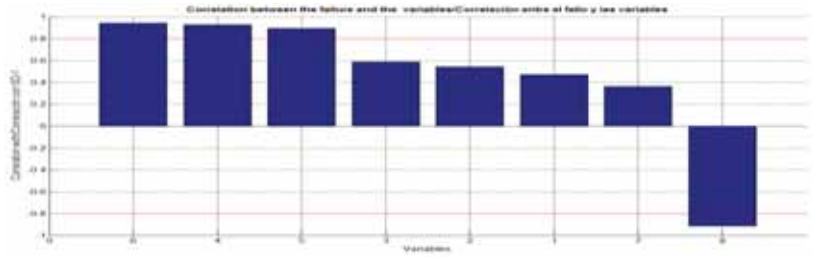

Fig. 25. Graphical interpretation correlation of own symptoms with the main failure for the second group of state

For the third group of states:

Fig. 26. Graphical interpretation the failures in object for the third group of states

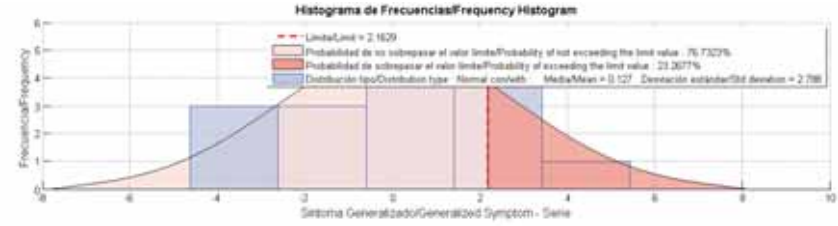

Fig. 27. Graphical interpretation histogram value of main failure for the third group of state

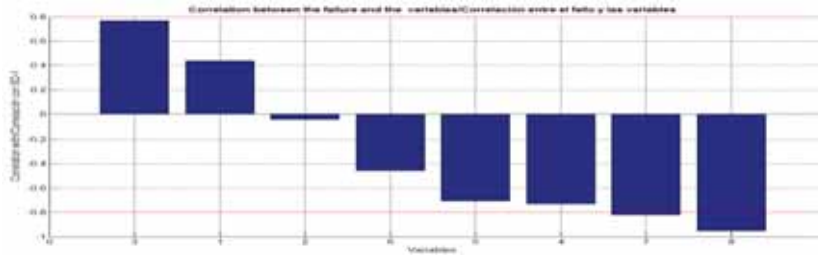

Fig. 28. Graphical interpretation correlation of own symptoms with the main failure for the third group of state

The result of the analysis with SVD method obtained five own and five mutual symptoms that best describe the states of the internal combustion engine. The summary of selected symptoms are presented in Table 3.

Table 3. Results of SVD method with five own and mutual symptoms that best describe the states of the internal combustion engine

GROUP STATE	OWN SYMPTOMS				
First group	P_{MAX}	A_{RMS}	σ_j	x_{ave}	I
Second group	x_{ave}	A_{RMS}	σ_j	P_{MAX}	K
Third group	I	C	K	A_{RMS}	P_{MAX}
GROUP STATE	MUTUAL SYMPTOMS				
First group	$R_{xy}(\Delta f)$	$\gamma(f_1)$	$\gamma(\Delta f)$	$FFT_x(\Delta f)$	$\gamma(f_2)$
Second group	$FFT_x(\Delta f)$	$\gamma(\Delta f)$	$R_{xy}(\Delta f)$	$\gamma(f_3)$	$\gamma(f_2)$
Third group	$\gamma(f_3)$	$\gamma(f_1)$	$\gamma(f_2)$	$FFT_x(\Delta f)$	$R_{xy}(\Delta f)$

The analysis indicates the need to assess the technical state of using mutual symptoms. The SVD method indicated that mutual symptoms have greater stability to describe the technical state of the engine. Own symptoms play an advisory role, based on which it is not possible to make a clear description of mutual symptoms.

The next step of the quantitative and qualitative analysis description of participation symptoms in the assessment of technical state is modelling engine cause - effect relationships using multiple regression [7]. Modelling makes it possible to identify the relationship between symptoms.

SVD method allows the selection symptoms for modelling because it is multidimensionality.

5. Conclusion

In modern technical systems, taking into account technological progress and the great opportunities available for acquisition and signal processing makes it possible to obtain a lot of information from the signals recorded in different parts of the machine. This information must be processed and interpreted in most cases by staff to determine the status of the machine. In the practice of diagnostic investigations, the utilization of vibrations allows describing the dynamic condition of the machine by set of estimators from various vibration symptoms. Received symptoms in the vibroacoustics signal experiment unambiguously show the different technical state of the combustion engine. The diagnosis of complex systems based on a multidimensional analysis, gives the opportunity to evaluate the relationship between symptoms whose values have

changed as a result of damage. SVD methods marked the most important symptoms for describing the technical state of engines- the best symptoms are: $\gamma(f1)$ – value of coherence for a first characteristic frequency 12,63 [Hz], $\gamma(f2)$ – value of coherence for a second characteristic frequency 23,27 [Hz], $\gamma(f3)$ – value of coherence for a third characteristic frequency 46,96 [Hz], $\gamma(\Delta f)$ – value of the area under course of the coherence function for the range from the first to the third characteristic frequencies). Among the possible techniques that use the relationship between symptoms is the SVD method. SVD method can be used to eliminate symptoms that do not provide important information about the state of the machine that is being tested. This method allows to generate a new set of independent symptoms that may be useful for the diagnosis of technical systems. This is why the SVD method is useful in many applications, such as statistics, control theory, compression, processing a lot of information and evaluation of technical state of complex objects. This paper is a part of investigative project **WND-POIG.01.03.01-00-212/09**

References

[1] Cempel, Cz., *SVD Decomposition Of Symptom Observation Matrix As The Help In A Quality Assessment Of A Group Of Applications,* Diagnostyka v.35, PTDT Warszawa 2005.
[2] Kałaczyński T., Łukasiewicz, M., *Technical state evaluation of combustion engine using diagnostic properties of the coherence function*, Materiały Seminarium Twórczość inżynierska dla współczesnej europy, Bydgoszcz - Białe Błota 2007.
[3] Kałaczyński T., Żółtowski, B., *Properties of the coherence function in technical state evaluation of combustion engine*, 12th International conference on Developments in Machinery Design and Control, Nowogród 2008.
[4] Łukasiewicz M., *Investigation of the operational modal analysis applicability in combustion engine diagnostics*, Journal of Polisch CIMAC, vol.3 no.2 Gdańsk 2008.
[5] Żółtowski, B., *Badania dynamiki maszyn,* ATR, Bydgoszcz, 2002.
[6] Żółtowski, B., Cempel, Cz., *Inżynieria diagnostyki maszyn,* Polskie Towarzystwo Diagnostyki Technicznej, Warszawa, Bydgoszcz, Radom 2004.
[7] Żółtowski B., Kałaczyńsk, T., Łukasiewicz, M., *The investigations aid in exploitation,* 11th International Technical Systems Degradation Conference, Liptovsky Mikulas 2012.

Journal of Polish CIMAC
Gdansk University of Technology
The Faculty of Ocean Engineering and Ship Technology

TURBO DIESEL 5 – THE NEW SIMULATOR FOR MARITIME ENGINEERING TRAINING

Stefan Kluj

Gdynia Maritime University
Department of Engineering
Morska Street 81-87, 81-225Gdynia, Poland
tel.: +48 5 8 6901439
e-mail: kluj@wm.am.gdynia.pl

Abstract

The specialized diesel engine simulator named Turbo Diesel 5 is the subject of this paper. The mathematical model simulates an engine operation under various conditions and introduces various defects. This model has been implemented in a software, which is used for teaching of the relation between the diesel engine technical state and its operating parameters. The software can be also used for the maintenance strategy teaching. The most popular marine diesel engine faults like a faulty fuel injector, a leaky cylinder, a worn fuel pump, the broken piston rings, a dirty turbocharger, a dirty air filter, a dirty air cooler (and many others) were simulated. Each fault can be simulated in the certain range which can be observed in the practical operation of marine diesel engines. Not only faults, but also the improper adjustment of the fuel injection advance angle were simulated. First the single faults were simulated and their influence on the NOx emission was analyzed. The simulation research has shown that the interaction of several typical engine faults can cause the NO_x emission far above the emission limit defined by IMO MARPOL convention. It has been also observed that the simulation of multiple mixed faults gives in many cases the different results that the simple multiplication of the single faults simulation.

Keywords: *engine room simulators, marine diesel engines, NO_x emission*

1. Introduction

STCW 2010 has introduced several significant enhancements in management level training when compared with its previous version – STCW 1995 [7]. The requirement for the maintenance planning, repair planning and non-destructive examination have been added together with the requirement that the appropriate simulator training should be used for examination and assessment. The majority of the existing engine room simulators currently available on the market are aimed principally at operational training, even if some of them include the tools and means for management analysis as well. The availability of the indicator diagrams and the possibility of the multiple fault simulation is are rarely combined with the choice of the appropriate maintenance and repair so the management level trainees have usually have no chance to plan and apply different maintenance strategies. Exceptionally, the trainees have the possibility of choosing not only the proper, but also the cost effective, maintenance strategy and most of them are not aware of the additional cost caused by the improper technical state including also environment pollution.

MARPOL convention on the other hand, especially its Annex VI [2, 4], introduces the new higher requirements not only for SO_x and NO_x emission but also for greenhouse gas emission. Under the

"NO_x Technical Code", the ship operator is responsible for in-use compliance which means that not only the adequate training but also the assessment methods for the chief and second engineers have to be provided.

Bearing in mind all abovementioned requirements, the new diesel engine simulator named Turbo Diesel 5 has been developed. This simulator is based on its earlier version 4 [5, 6], which has been successfully used for many years by numerous maritime training centres, academies and owners.

2. Simulator Model

The model simulates the engine operation under selected initial conditions (for example: torque, revolution speed, ambient air pressure) and the variable technical state (Tab. 1). The model will react naturally under almost any combination of factors, but sometimes the engine operation will be impossible. Faults introduced by the user or by the computer will lead to a progressive deterioration in system conditions if maintenance action is not taken at an appropriate stage.

Tab. 1. Diesel engine fault simulations available in Turbo Diesel 5

Simulation Name	Units	Min. Value	Max. Value
Injection advance angle change	deg	10	26
Fuel effective quantity decrease	%	0	20
Gas leak through the piston rings or valves	%	0	20
Injector nozzle cross section change	%	80	120
Decrease of the air filter cross section	%	0	40
Air blower - decrease of the air flow efficiency	%	0	4,5
Air cooler - decrease of the cross section at air side	%	0	40
Decrease of the exhaust duct cross section	%	0	40
Gas turbine – decrease of the cross section at gas side	%	0	4,5
Decrease of the water flow in the air cooler	%	0	20
Decrease of combustion chamber cooling efficiency	%	0	20
Cooling water temp. change at inlet to the engine	°C	40	80
Engine friction coefficient increase	%	0	40
Increase of the pressure drop at the oil filter	MPa	0	0,2
Lub. oil temp change at inlet to the engine	°C	30	70
Ambient air temperature change	°C	20	60
Ambient air pressure change	hPa	950	1050

Great care has been paid to the mathematical modelling of the fuel injection and the combustion process (Fig. 1) [5]. In general, the technique is to solve the governing equations of state and of conservation of energy and mass on a step-by-step basis, using small crank angle increments (2 degrees). The calculation sequence invariably divides itself into two major portions, for closed and open period, starting with assumed trapped conditions of the cylinder charge at the beginning of compression. The stable values of these conditions are obtained only after several successive cycles have been evaluated.

The air flow rate through a turbocharged diesel engine has been simulated as a function of the engine speed, compressor delivery air density and the pressure difference between intake and manifolds during the period of a valve overlap. The digitized turbocharger characteristic has been used in order to simulate its operation. Making suitable simplifying assumptions concerning the

diesel cycle, as well as for a compressor and turbine efficiency, it is possible to construct curves of specific power for engine, compressor and turbine as a function of a boost pressure. Such a mathematical modelling, based on the details of the diesel engine and the compressor map, has made possible the determination of the operating points for both an engine and a turbocharger.

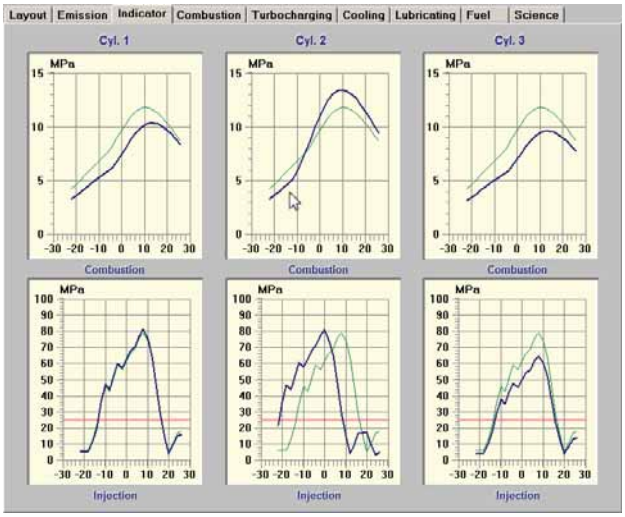

Fig. 1 The example of the combustion and injection diagrams calculated for the different faults (medium speed diesel engine Sulzer3AL25)

Special attention has been paid to the digital simulation of an exhaust gas emission including the concentration of O_2, CO_2, CO, SO_2 and NO_x (Fig. 2) [1, 2, 3]. The mathematical model was validated during the tests at the actual diesel engine in the laboratory, but the actual model illustrates how the single faults and the multiple mixed faults influence the exhaust emission. The numerous additional combustion parameters like the maximum combustion temperature, air/ fuel ratio and even the thermal load can be presented on request in order to make the relation between engine technical state and the caused environment pollution more readable und understandable.

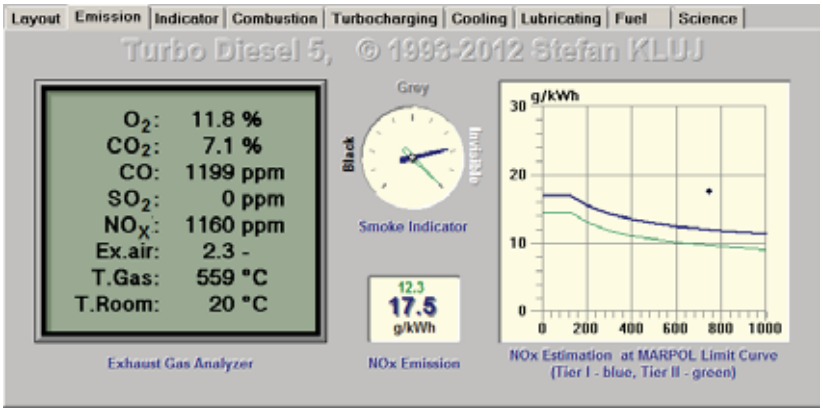

Fig. 2 The example of the exhaust gas content simulation and its immediate evaluation in reference to MARPOL

3. Operation Modes

Turbo Diesel 5 has three operation modes:

Evaluation mode (default): the trainee can freely change the technical state of the engine elements as well as the engine load and operation conditions. This includes the possibility of inspecting the present technical state of the engine elements. This mode can be used for testing the relation between the engine operation conditions or the technical state on one side and the engine operation parameters on the other side. The evaluation mode is necessary at an early stage of the engine operation education.

Live Run mode: Changes in the engine technical state are simulated automatically "in the background" by the computer. The trainee can only perform maintenance and repair activity and change the engine speed, but he cannot control directly the present technical state. The maintenance tasks have their conventional prices and all these expenses will be taken into account later while calculating the final results. The duration of successful diesel operations renders the player certain incomes; so the final result is actually the difference between the global income and the global cost. The final result will depend also on the cost of all necessary (but required) maintenance. The Live Run is very useful for ~~the~~ management level assessment.

Replay Run mode: The Live Run when finished can be saved on a disk. The saved Run can be re-played in Run Replay mode. The user can navigate between the single run steps using the set of recorder-like keys. The main purpose of this mode is for debriefing and student error discussion. This can be useful both with and without an instructor's assistance, but an instructor can usually better comment on all errors by the student reported automatically in this mode.

The Live Run mode is most interesting for the maritime training because the operator has to act as the qualified user against the computer with its dangerous situations, faults, etc. The trainee can freely inspect all the available engine parameters, perform maintenance and repair and change the engine speed. Each maintenance and repair has its specific price (in US $) which the engineer has 'to pay' and which has to be deducted from the total income (Fig. 3).

Fig. 3 The choice of available maintenance and repair with their prices

The present status of the Live Run can be seen in the Summary window where the following information (Fig. 4) is presented together with other data.

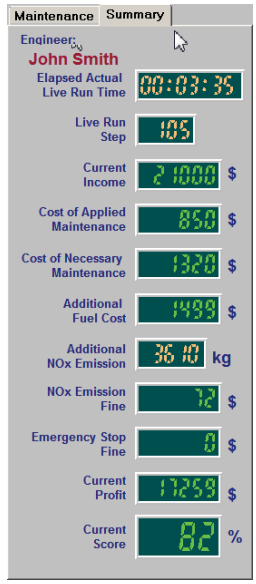

Fig. 4 The example of the Live Run current status

- *Current Income* field shows Live Run Step number multiplied by a Income in a single Live Run Step which is by default $ 200/day but can be changed any time by a person with the full rights (instructor) in Options | Preferences dialog window. Increasing Step Income causes that all Live Runs will be easier, decreasing it causes that they are more difficult (not recommended).
- *Cost of Applied Maintenance* is the sum of the applied maintenance cost till now. This cost depends only on the kind of applied maintenance (and its quantity). The cost of each maintenance cannot be changed.

- *Cost of Necessary Maintenance* shows the cost of all maintenance which should be applied right now and it depends only on the current technical state.

- *Additional Fuel Cost* is a cost of the additional fuel (i.e. over the normal consumption) burned since the beginning of a Live Run. This value depends on the MDO Fuel Cost which can be changed in Options | Preferences dialog window.

- *Additional NOx Emission* displays the additional NOx in kg caused only by the improper engine technical state since the beginning of Live Run. This value cannot be changed.

- *NOx Emission Fine* is calculated by multiplying the Additional NOx Emission (in tons) by NOx Emission Fine in $/t. The NOx Emission Fine per ton can be customized in Options | Preferences dialog window.

- *Emergency Stop Fine* is calculated by multiplying the number of emergency stops (since the beginning of Live Run) by the Emergency Stop Fine per single stop which can be edited in Options | Preferences dialog window.

- *Current Profit* is calculated as follows. The Current Income minus Cost of Applied Maintenance minus Cost of Additional Maintenance minus NOx Emission Fine minus Emergency Stop Fine.

- *Current Score* shows the relation of the Current Profit to Current Income shown in %. The Current Score must be higher than 60% in order to pass the assessment.

The current Live Run results (Fig. 5) will be saved automatically in the file and can be viewed or printed on request. The result shows also the evaluation of completed (premature or unnecessary) maintenance and required maintenance. This feature enables very precise debriefing of the Live Run and learning about proper engine operation depending on its technical state.

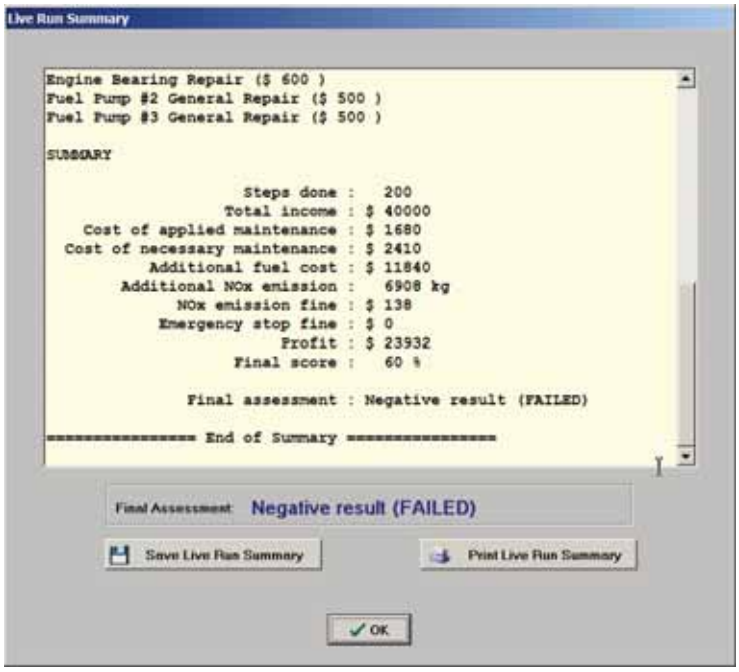

Fig. 5 The example of Live Run results.

4. Mixed Faults Simulation

Turbo Diesel 5 offers the possibility to observe the influence of mixed engine faults on numerous operational parameters. As an example, the influence of the single and multiple (mixed) engine faults on NO_x emission will be discussed. Fig. 6 shows, how does NO_x emission and concentration in the exhaust gases depend on the injection advance angle. It is easy to conclude

that the recommended by an engine producer injection timing (18 deg before TDC) offers the lowest NO_x emission.

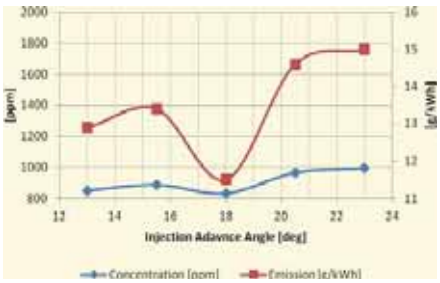

Fig. 6. NOx emission and concentration as a function of an injection advance angle

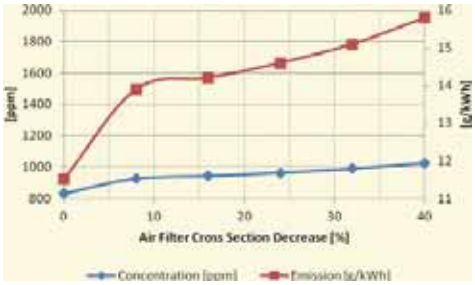

Fig.7. NOx emission and concentration as a function of an air filter cross section decrease

On the other hand, the air filter cross section decrease which simulates the dirty air filer causes a decreased air flow through the engine, lower air/fuel ratio and the significant increase of NO_x emission (Fig. 7) what it is well known from the literature [2, 3, 8].

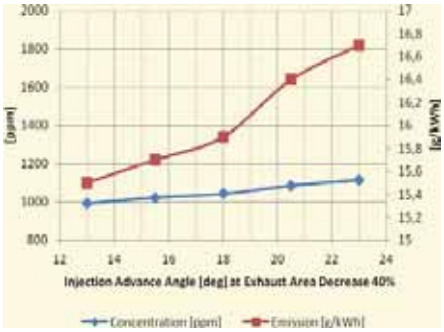

Fig. 8. NOx emission and concentration as a function an injection advance angle and dirty exhaust

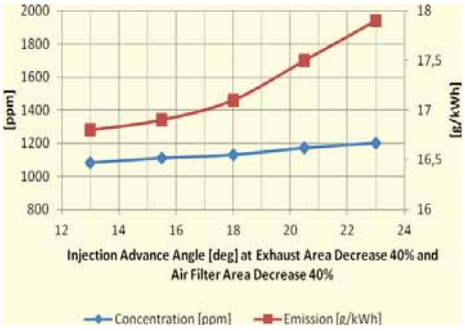

Fig. 9. NOx emission and concentration as a function of an injection advance angle, dirty exhaust and dirty air filter

When the dirty exhaust duct is simulated and the injection advance angle is changed (Fig. 8) the lack of an air dominates the influence of the optimal injection timing and the total NO_x emission is higher than when both single faults are simulated. The emission is much higher and far above even the MARPOL - Tier I limits when the third fault i.e. dirty air filer simulation is mixed in (Fig. 9). The above described observations imply the need to care of the turbocharging system cleanliness as an important measure to prevent the environment pollution by NO_x emission. On the other hand, when the proper flow of the turbocharging air is provided, it is necessary take care about the injection adjustment as an effective measure of the environment protection.

5. Conclusion

The presented simulator, based on the mathematical model of the high power, medium speed, four stroke diesel engine, is particularly suited for management level training, providing the instructors with a powerful teaching tool and the trainees with an increased understanding of the relation between the engine technical state and its operating parameters. The possibility to test the engineer's diagnostic knowledge and to try out the different maintenance strategies is another

feature of this simulator. It is especially important that the assessment rules are based on the financial results of the engine operation, the fuel costs and the cumulated NO_x emission.

This kind of a simulator offers not only the training in marine diagnostics and maintenance strategy but also increases the awareness of the environment pollution problems caused by the diesel engine technical state.

References

[1] Challen B., Baranescu R., *Diesel Engine Reference Book*, Elsevier, Oxford 2003.

[2] Genesis Engineering Inc. & Levelton Engineering Ltd., *Non-road Diesel Emission Reduction Study*, prepared for Puget Sound Clean Air Agency, Oregon Department of Environmental Quality and U.S. Environmental Protection Agency 2003.

[3] Habib M.A., Elshafei M., Dajani M., *Influence of Combustion Parameters on NO_x Production in an Industrial Boiler*, Elsevier, Oxford 2007.

[4] *International Convention for the Prevention of Pollution from Ships (MARPOL) Annexes I – VI*, International Maritime Organization, London 2011.

[5] Kluj S., *Symulowanie wybranych niesprawności na symulatorze Turbo Diesel 4*, Zeszyty Naukowe Akademii Morskiej w Gdyni, Zeszyt nr 60/2009.

[6] Kluj S., *The application of a diagnostic simulator Turbo Diesel 4 for maritime engineering training,* Joint Proceedings Akademia Morska Gdynia - Hochschule Bremerhaven, Gdynia - Bremerhaven, 20/2007.

[7] Kluj S., Cwilewicz R., *The Influence of STCW Manila Amendments on Engine Room Simulator Training*, Proceedings of 10th International Conference on Engine Room Simulators, Sankt Petersburg, 2011.

[8] Westlund A., *Simplified Models for Emission Formation in Diesel Engines During Transient Operation*, Doctoral thesis, Department of Machine Design, Royal institute of Technolgy, Stcokholm, 2011.

Journal of Polish CIMAC
Gdansk University of Technology
The Faculty of Ocean Engineering and Ship Technology

MODEL OF PROFIT IMPROVEMENT IN MAINTENANCE SYSTEM

Leszek Knopik

University of Technology and Life Science
Faculty of Management Science
Fordonska st. 424, 85-790 Bydgoszcz, Poland
Email: knopikl@utp.edu.pl

Abstract

The objective of this paper is to study a profit maximization model under decreasing the number of instantaneous failures. We derive the objective function (profit from work of the technical object) under general assumptions. The method is illustrated by a two numerical examples. In the first example the times between two instantaneous failures have two point distribution, in the other two parameters Weibull distribution

Keywords: *lifetime, mixture of distribution, Weibull distribution, exponential distribution, reliability function, instantaneous failures, profit.*

1. Introduction

In the real maintenance system the reduction of the number of the failures of a technical objects causes the growth of the profit from the work of an object. Reduction of the number of the failures depends on the expenditure on the diagnostic and improvement of the organization of the repairs. However, it is known that elimination of all failures is impossible or demands high cost. In this paper, we construct the profit model under reduction of the instantaneous failures.
The lifetime distribution is very important in reliability studies. An important topic in the field of lifetime data analysis is based on the selection of the most appropriate lifetime distribution for statistical data coming from an experiment. This distribution is to describe the time of a component failure, a subsystem or a system. Some failures result from natural damages of the machines, while the other ones may be caused by an inefficient repair of the previous failures, resulting from an incorrect organization of the repairs. The analysis of the results of the operation and maintenance investigations, regarding the moments the failures occurrence proves that the set of the failures may be divided into two subsets, namely into the set of primary failures and the set of secondary failures. It follows the fact that the population of times to failure is often heterogeneous. In this case, the resulting population of lifetimes can be described by using statistical concept of a mixture of two distributions.

2. The model of the profit maximization

We consider a mixture of the lifetimes T_1 and T_2 with the densities $f_1(t)$, $f_2(t)$, the reliability functions $R_1(t)$, $R_2(t)$, the failure rate functions $\lambda_1(t)$, $\lambda_2(t)$ and the weights p and $1 - p$, where $0 < p < 1$. The mixed density function is then written as

$$f(t) = p\, f_1(t) + (1 - p)\, f_2(t)$$

and the reliability function is

$$R(t) = p\, R_1(t) + (1 - p)\, R_2(t) \tag{1}$$

The failure rate function of mixture can be written as the mixture [1]:

$$\lambda(t) = w(t)\, \lambda_1(t) + (1 - w(t))\, \lambda_2(t),$$

where $w(t) = R_1(t) / R(t)$.
The mean value of the mixture is following:

$$ET = p\, ET_1 + (1-p)\, ET_2, \tag{2}$$

where ET_1 and ET_2 are the mean values of T_1 and T_2. We assume that $ET_1 < ET_2$.
Reduction of the number of the instantaneous failures is realized by decreasing the value of the parameter p. We assume, that the profit from the work of the technical object is proportional to the expected value of time to failure. This profit, we describe by $g_1(t) = d\, ET$, where $d > 0$. It can be easily seen that $g_1(0) = d\, ET_1$, $g_1(1) = d\, ET_2$. By $h_2(t) = - g_2(t)$, we describe the expenditure on elimination of instantaneous failures. We assume that the function $g_2(t)$ is twice differentiable on (0, p) and the following assumptions are fulfilled:

$$g_2(t) < 0,\ g_2(0^+) = -\infty,\ \ g_2(p^-) = 0, \tag{3}$$

$$g_2'(t) > 0,\ g_2'(0^+) = +\infty,\ g_2'(p^-) = 0, \tag{4}$$

$$g_2''(t) < 0, \tag{5}$$

The objective function expresses the profit from the work of the technical object:

$$g(t) = g_1(t) + g_2(t)$$

The first derivative of the objective function g(t) is

$$g'(t) = d\,(ET_1 - ET_2) + g_2'(t)$$

The first derivative $g_2'(t)$ decreases from $+\infty$ to 0 at point p, whereas $d\,(ET_1 - ET_2) < 0$. Now we conclude, that the equation $g'(t) = 0$ has exactly one solution. By assumption (5), the function g(t) approaches exactly one maximum on the interval (0, p). Consequently, we proved:
Proposition 1. If $ET_1 < ET_2$ and the assumptions (3), (4) and (5) are fulfilled, then the objective function g(t) approaches the exactly one maximum on the interval (0, p).

3. Examples

Example 1. In this example, we assume that the lifetime o T_1 has two-point distribution

$$P\{T_1 = 0\} = r,\ \ P\{T_1 = 1\} = 1 - r,$$

and T_2 has an exponential distribution with the density function

$$f(t) = \lambda \exp(-\lambda t) \text{ for } t \geq 0$$

The expected value of T is following:

$$ET = p(1-r) + (1-p)/\lambda$$

We assume that the function $g_2(t)$ has the form: $g_2(t) = -a/t - b\,t + c$
It can be seen that $g_2(0^+) = -\infty$ and

$$g_2(p^-) = 0 \text{ if and only if } -a/p - b\,p + c = 0 \qquad (6)$$

The first derivative of $g_2'(t)$ is $g_2'(t) = a/t^2 - b$
It can be seen that $g_2'(0^+) = +\infty$ and $g_2'(p^-) = 0$ if and only if $p = \sqrt{a/b} \leq 1$, hence $a \leq b$.
Substituting $p = \sqrt{a/b}$ to (6), we obtain $c = 2\sqrt{ab}$.
It is easily seen that: if $a > 0$, $b > 0$, $c = \sqrt{ab}$, then the function $g_2(t)$ fulfills the assumption (3), (4) and (5). The objective function approaches the maximum at the point t_0,

$$t_0 = \sqrt{\frac{a}{b + d/\lambda - (1-r)d}}$$

Fig. 1 demostrates the dependence of profit on the the value parameter p for the different values of the parameter a.

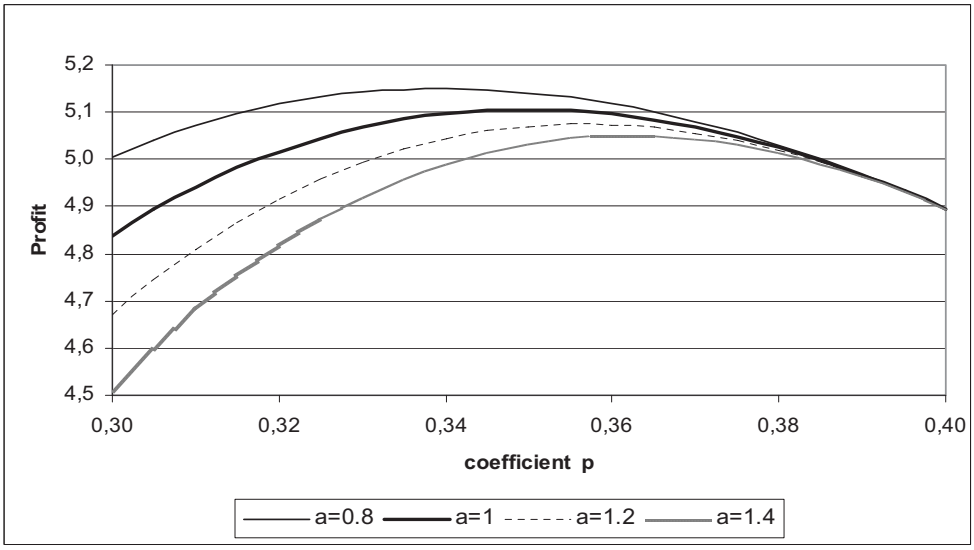

Fig. 1. The profit as function of the parameter p for different values of parameter a

Example 2. We assume that the lifetime T_1 is two parameters Weibull distribution with the reliability function

$$R(t) = \exp(-\alpha\, t^{\beta}) \text{ for } t \geq 0$$

and T_2 has an exponential distribution with $ET_2 = 1/\lambda$. For the expected value of T, we have

$$ET = p\alpha^{-\frac{1}{\beta}}\Gamma\left(\frac{1}{\beta}\right)/\beta + (1-p)\lambda,$$

where $\Gamma(q)$ is gamma function $\Gamma(q) = \int_0^{\infty} t^{q-1} e^{-t} dt$.

We assume that the function $g_2(t)$ has the form: $g_2(t) = -a \ln(t) - b\,t + c$. If $b > 0$, $a = b\,p$, $c = b\,p \ln(e/p)$, then the function $g_2(t)$ fulfills the assumption (3), (4) and (5). The function $g_2(t)$, we can describe in the form: $g_2(t) = (b / p)(\ln(t) - t / p + \ln(e / p))$. In this example the objective function has the form:

$$g(t) = td\alpha^{-\frac{1}{\beta}}\Gamma\left(\frac{1}{\beta}\right)/\beta + d(1-t)/\lambda - a/t - bt + c$$

Fig. 2 shows a graphics of the objective function for the different values of the parameter a.

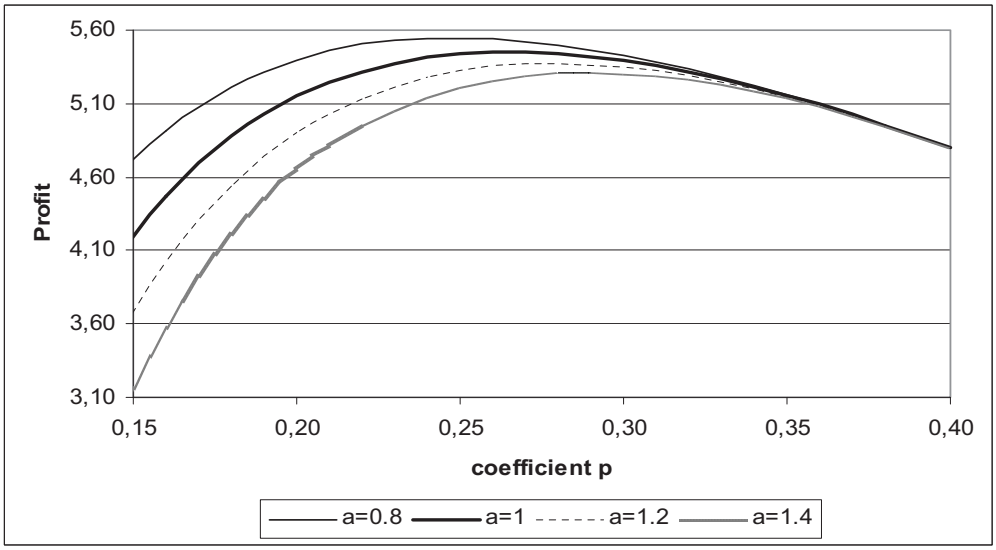

Fig. 2. The profit as function of the parameter p for different values of parameter a

4. Conclusions

In this paper, we study the profit maximization model while the number instantaneous failures is decreasing. The objective function is the profit from the work of a technical object. We show under general assumptions that this function approaches the maximum. Two numerical examples show that this model may be applicable in practice. In both causes of the objective function approaches exactly one maximum.

References

1. Knopik L., *Mixture of distributions as a lifetime distribution of a technical object*, Scientific Problems of Machines Operation and Maintenance, vol.45, 2(165), 2010, pp. 53-60.

2. Wdzięczny A. Woropay and M. Muślewski Ł., *Division and investigation of damages to technical object and their influence on the reliability of operation and maintenance systems* Scientific Problems of Machines Operation and Maintenance, vol.44, 2, 2008, pp. 31-43.

Journal of Polish CIMAC
Gdansk University of Technology
The Faculty of Ocean Engineering and Ship Technology

STATISTICAL ANALYSIS OF FAILURES

Leszek Knopik

University of Technology and Life Science in Bydgoszcz
Faculty of Management Science
Fordonska 424 st, 85-789 Bydgoszcz, Poland
e-mail: knopikl@utp.edu.pl

Abstract

The lifetime distribution is important in reliability studies. There are many situations in lifetime testing, where an item (technical object) fails instantaneously and hence the observed lifetime is reported as a small real positive number. The investigation in this article was motivated by an extended and generalized Weibull distribution. We suggest a mixture of a singular distribution and Weibull distribution. We apply the maximum likelihood method to estimate the parameters of the mixture. The method is illustrated by a numerical example for the time between the failures of bus engines.

Keywords: *Weibull distribution, mixture of distributions, maximum likelihood method, confidence interval, early failures*

1. Introduction

In reliability and quality control, the probability density and failure rate function provides the valuable information about the distribution of the failure times. The important thing in the field of the lifetime analysis is the most appropriate lifetime distribution that describes the time to a failure of a component, assembly or system.
Occurrence of instantaneous or early failures in lifetime testing is observed in sets of failures of machines. These occurrences may be due to faulty constructions or inferior quality. Some failures result from natural damages of the machine while the other failures may be caused by inefficient repairs of previous failures resulting from incorrect organization of the repairs. These situations can be modeled by modifying commonly used parametric models such as exponential, gamma and Weibull distributions.
In the papers [9], [10] the set of failures of a machine is divided into two subsets, namely into the set of primary failures and the set of secondary failures. This division suggests that the population of lifetime is heterogeneous. The population of time before failures can be described by using the statistical concept of mixture. This mixture, in a particular case, has the unimodal failure rate function. In the paper [9], special attention has been paid to determination of shape of the failure rate function from mixture of the exponential distribution and distribution with linear increasing failure rate function. It is clear that instantaneous failures can be primary failures or secondary failures. In this paper, the mixture of a singular and Weibull distributions is considered.
In this paper, we show that the mixture of a singular and Weibull distributions is useful to describe the lifetime of the machines. The numerical example is also provided to illustrate the practical

impact of this approach. In this example n = 193 failures of the bus engine is studied. This example shows that in this case a mixture of the singular distribution and the exponential distribution is sufficient.

2. The model of lifetime distribution

We consider the continuous time failure cumulative distribution function F(t, a, b) with F(0, a, b) = 0. In this paper we assume that F is two parameter Weibull distribution with parameters (a, b). The distribution function is the following:

$$F(t, a, b) = 1 - \exp(-x^{b} / a) \qquad \text{for } x \geq 0 \tag{1}$$

and the density function

$$f(t, a, b) = (b/a)\, t^{b-1} \exp(-t^{b})$$

We assume that the early failures are recorded as a class with notational failure time c so that the modified distribution has the density function given by

$$g(t,p,a,b) = \begin{cases} 0 & \text{for } x < c \\ 1 - p + pF(c,a,b) & \text{for } x = c \\ pf(t,a,b) & \text{for } x > c \end{cases} \tag{2}$$

The purpose of this paper is to consider the probability density function given by (2), when F is two parameters Weibull distribution. The problem of statistical inference about (Θ, p) has received considerable attention particularly when T is exponential. Some of the early references are: Aitchison [1], Kleyle and Dahiya [4], Jayade and Parasad [2], Muralidharan [5, 6], Kale and Muralidharan [3] and the references contained therein. Muralidharan and Kale [7] considered the case where F is a two parameters gamma distribution with shape parameter β and scale parameter α, and they obtained confidence interval for δ = pαβ assuming α as being known and unknown respectively.

3. The maximum likelihood estimation

In the paper [8] these distributions are considered and the maximum likelihood estimation of parameters (p, a, b) is obtained. Here, we give the equations for the maximum likelihood estimate for (p, a, b).

$$\hat{p} = \frac{n - n_0}{n} \exp(c^{\hat{b}} / \hat{a}), \tag{3}$$

where n_0 is the number of observations reordered as c.

$$\hat{a} = \frac{1}{n - n_0} \sum_{x_i > 0} x_i^{\hat{b}} - c^{\hat{b}} \tag{4}$$

and $\hat{b}$ is the solution of the equation

$$\frac{n_1 c^b \ln c - s_3}{s_1 - n_1 c^b} + \frac{1}{b} + \frac{s_2}{n_1} = 0 \qquad (5)$$

where

$$n_1 = n - n_0$$

$$s_1 = \sum_{x_i>0} x_i^b$$

$$s_2 = \sum_{x_i>0} \ln x_i$$

$$s_3 = \sum_{x_i>0} x_i^b \ln x_i$$

The Fisher information matrix is given by

$$I(p,a,b) = \begin{bmatrix} I_{pp} & I_{pa} & I_{pb} \\ I_{ap} & I_{aa} & I_{ab} \\ I_{bp} & I_{ba} & I_{bb} \end{bmatrix} \qquad (6)$$

where

$I_{pp} = A/(p\,B)$

$I_{pa} = I_{ap} = (c^b A)/(a^2 B)$

$I_{pb} = I_{bp} = -\,c^b A/(aB^2)$

$I_{aa} = (p\,A/a^2)\,(c^{2b}/(a^2 B)+1)$

$I_{ab} = I_{ba} = (-p/a)(c^{2b}\ln(c)\,A/(a^2(1-B) + A(\ln(c) + 1/b - I_1/b))$

$I_{bb} = p\,A\,((c^b \ln(c))^2 / (a^2 B) + 1/b^2 + \ln(c)/b + (\ln(c))^2) + (p/b^2)\,(I_1 + I_2)$,

where

$A = \exp(-c^b / a)$

$B = 1 - \exp(-c^b / a)$

$$I_1 = \int_{c^b}^{\infty} y^{-1} \exp(-y/a)\,dy = -\sum_{j=0}^{\infty} \frac{(-1)^j}{j!} \left(\frac{c^b}{a}\right)^j$$

$$I_2 = \int_{c^b}^{\infty} y^{-1} \ln y \exp(-y/a)\,dy = \sum_{j=0}^{\infty} \frac{(-1)^j}{j!} \left(\frac{c^b}{a}\right)^j \left[\frac{1}{j} - b\ln c\right]$$

By $I^{-1}(p, a, b)$ we denote the inverse of the matrix $I(p, a, b)$.
Let

$$K(p,a,b) = \frac{1}{n} I^{-1}(p,a,b)$$

Using the matrix $K(p, a, b)$ we estimate the confidence interval for (p, a, b). The approximate $1 - \alpha$ confidence interval for p is the following:

$$(\hat{p} - u_\alpha \sqrt{K_{pp}}, \hat{p} + u_\alpha \sqrt{K_{pp}})$$

for a

$$(\hat{a} - u_\alpha \sqrt{K_{aa}}, \hat{a} + u_\alpha \sqrt{K_{aa}})$$

for b

$$(\hat{b} - u_\alpha \sqrt{K_{bb}}, \hat{b} + u_\alpha \sqrt{K_{bb}})$$

where K_{pp}, K_{aa}, K_{bb} are the diagonal elements of the invert matrix K(p, a, b), and u_α is the value of standard Gauss random variable U such that

$$P\{|U| < u_\alpha\} = 1 - \alpha .$$

4. Numerical example

The object of the investigation is a real municipal bus transport system within large agglomeration. The analyzed system operates and maintains 190 municipal buses of various types and makes. In this section, we consider a real time data on failure of bus. The data set contains n = 193 times between failures of a bus. This set contains $n_0 = 50$ times equal to one and we assume that c=1.

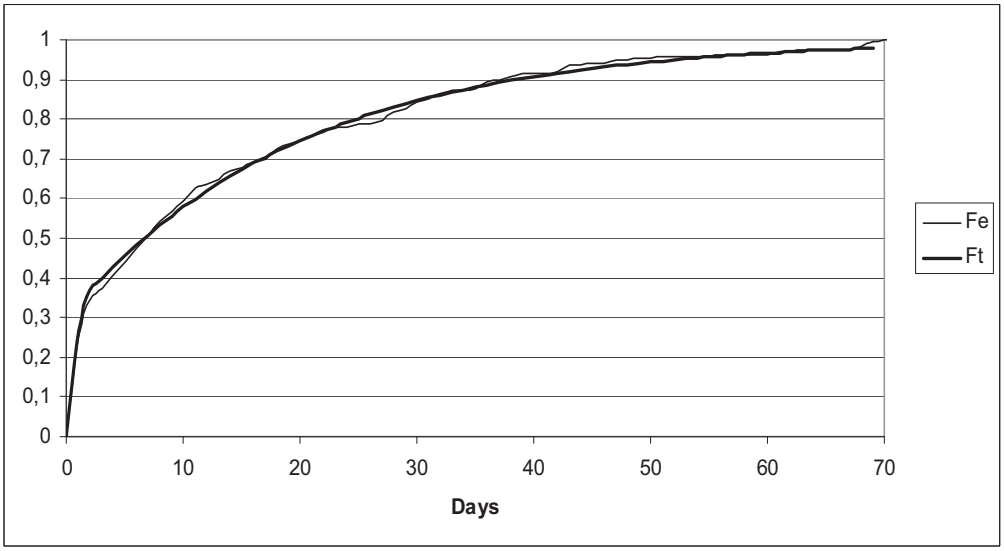

Fig. 1. Plots of empirical and mixture distribution functions

We apply the maximum likelihood estimates of the parameters p, a and b. As the initial solution of the equation (5), we give b = 1.We calculate the values of the parameters p = 0.26, b = 1.02 and a = 17.4, and the corresponding confidence interval, for p we obtain (0.23, 0.29), for b (0.94, 1.2) and a (10.2, 11.2). For these values of parameters, we prove the Pearson's test of fit and compute the associated p-value = 0.54. It shows a good conformity of the empirical data with the mixture distributions. Fig. 1 shows the empirical distribution function (Fe) and mixture distribution function (Ft) for this example.

5. Conclusions

In this paper, we study the lifetime model for instantaneous and early failures of bus engines. The

estimation of parameters is approached by the method of maximum likelihood and the expected information matrix is derived. The estimate for b can be obtained as the solution of equation (5). The confidence intervals for p, a and b depend on the information matrix
I(p, a, b). Furthermore, these confidence intervals can be used for large sample. When the parameters are estimated, it is possible to apply for further calculations, such as MTTF (Mean Time to Failure), burn-in time, the failure rate function and the replacement time. The development of efficient parameters estimation methods for this mixture distribution and their application for times to failure modeling are topics for further study. An application to a real data set shows that this model may be applicable in practice.

References

1. Aitchison I.: (1955) On the distribution of a positive random variable having a discrete probability mass at origin, Journal of the American Statistical Associations, vol. 50, pp. 901-908.
2. Jayade V. P. and Parasad M. S.: (1996) Estimations of parameters of mixed failure time distribution. Communications Statistics, Theory and Method, vol19, pp. 4667-4677.
3. Kale B. K. and Muralidharan K.: (2000) Optimal estimating equations in mixture distributions accommodating instantaneous or early failures, Journal Indian Statistical Associations, vol. 38, pp.317-329.
4. Kleyle R.M. and Dahiya R.L.: (1975) Estimation of parameters of mixed failure time distribution from censored data, Communications Statistics, Theory and Method, vol.4, pp. 873-882.
5. Muralidharan K.: (1999) Test for mixing proportion in mixture of a degenerate and exponential distributions, Journal Indian Statistical Associations, vol. 37, pp. 105-119.
6. Muralidharan K.: (2000) The UMVUE and Bayes estimate of reliability of mixed failure time distribution, Communications Statistics, Simulation Computer, vol. 29, No 2, pp. 603-158.
7. Muralidharan K. and Kale B.K.: (2002) Modified gamma distribution with singularity at zero, Communications Statistics, Simulation Computer, vol. 31, No1, pp.143-158.
8. Muralidharan K. and Lathika P.: (2006) Analysis of instantaneous and early failures in Wiebull distribution, Metrika vol. 64, pp.305-316.
9. Knopik L.: (2010) Mixture of distributions as a lifetime distribution of a technical object, Scientific Problems of Machines Operation and Maintenance, 2010, vol.45, 2(165), pp. 53-60.
10. Wdzięczny A., Woropay M. and Muślewski Ł.: Division and investigation of damages to technical object and their influence on the reliability of operation and maintenance systems Scientific Problems of Machines Operation and Maintenance, 2008, vol.44, 2(154), 2008, pp. 31-43.

Journal of Polish CIMAC
Gdansk University of Technology
The Faculty of Ocean Engineering and Ship Technology

STRESS IN A SALVAGE FAYING FACE OF A SUBMARINE WHILE MOORING A RECOVERY VESSEL

LesławKyzioł

Gdynia Maritime University, The Faculty of Marine Engineering
Str. Morska 81 – 87,81-225 Gdynia
e – mail: lkyz@am.gdynia.pl

Abstract

The article presents stress distribution in a seat face of a submarine while docking a submergence recovery vessel. Rescue faces (salvage faying faces) in submarines are used to dock emergency vehicles. Both submergence recovery vessels and submarines possess special seat faces which enable the transition of a crew from a sunken ship to an emergency vehicle. Due to corrosion environment, seat faces in submarines undergo degradation, which requires periodic inspection of their condition. With accordance to the valid standards, the minimum thickness of faying faces cannot be less than 25,4 mm on account of the stresses and dislocations. Seat measurements made it possible to carry out simulation studies to determine their strength, distribution of stresses and displacements. The obtained results of seat strength allow for a submersion of a submarine to a maximum depth according to the current standards.

Keywords: *salvage (rescue) faying face, thickness of contact plate, measurements of seat face condition, simulation calculations of seat strength, permissible submergence of a submarine*

1. Introduction

Submarines of the Polish Navy were built in the 70's. Later, the ships were modified by changing components used in their construction, as well as changing the shape of the hull, conning tower and location of rudder. These units have one emergency scuttle that allows the crew to evacuate in case of failure of the ship. Evacuation of crew takes place through scuttles of the ship and the rescue vessel that are opened when an the vehicle seat face connects with the salvage faying face of a submarine. The next step is to pump out water from the space between faces and pressure equalization. After this, the scuttles can be opened and the crew is evacuated to an emergency vehicle (Fig. 1) [11].

Due to the poor technical condition of the submarines it was necessary to check the surface adhesion of the submarine seat face to the face of the rescue vehicle [5 ÷ 8, 11]. In order for the faces to adhere properly to each other, they must meet the requirements of the International Standard NAVSEA and the Polish Defence Standard NO-42-A2007 [9, 10]. The main parameters regarding the condition of a seat are its thickness, roughness and geometry. Fig. 1 shows the rescue seat location on a submarine.

Salvage faying face is exposed to the maritime environment, hence its thickness gradually decreases [5 ÷ 8, 11]. Changing the thickness of the seat is a consequence of the removal of corrosion by grinding the ship when in the harbor.

The main purpose of this study is to make strength calculations of a rescue seat face to determine its capacity. Therefore, it was necessary to carry out numerical simulations involving

the analysis of stresses and displacements in order to determine the current capacity of the seat and to indicate the minimum thickness of the seat at the maximum depth submergence of the submarine.

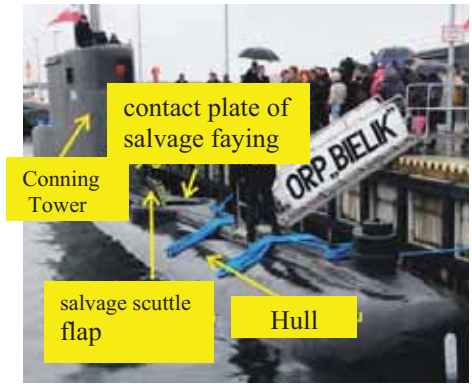

Fig. 1. The location of a salvage (rescue) scuttle on a submarine

2. Geometric and strength requirements of the rescue seat

Both the American NAVSEA Standard and Polish Defence Standard NO-42-A2007 identify the location and dimensions of the seat face (Fig. 2, 3):

- minimum outside diameter 1676,4 mm, maximum inner diameter 1143 mm,
- thickness of contact plate 25,4 mm, surface roughness should be no more than $R_a = 6{,}3$ μm,
- the location of the seat face should be centered relative to the vertical centering line of the emergency scuttle.

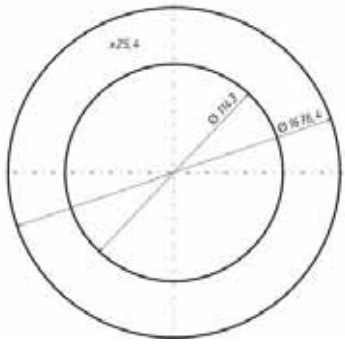

Fig. 2. Principal dimensions of submergence recovery vessel

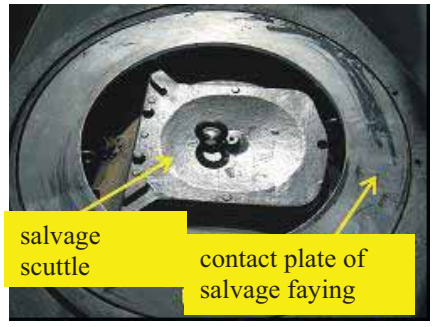

Fig. 3. View of submarine seat face

Measurements of contact plate thickness is performed along 8 measuring lines at 24 measuring points (Fig. 4). In each measurement line from A to H there are made three measurements of thickness. The measurements were made using an ultrasonic method with an approved measuring instrument SONO M310. Fig. 5 shows the dimensions of the face flange of an emergency vehicle docked on a seat of a submarine.

In the absence of data concerning the steel the faces are made of, further calculations were based on 10GHMBA steel parameters [13]. Flange of the adapting basket has dimensions of shown in Fig. 5. The standard also illustrates the distribution of the forces acting on the surface of the seat (Fig. 6).

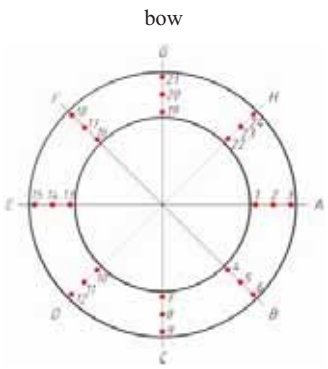

Fig. 4. View of the measuring points of the seat contact plate thickness bow

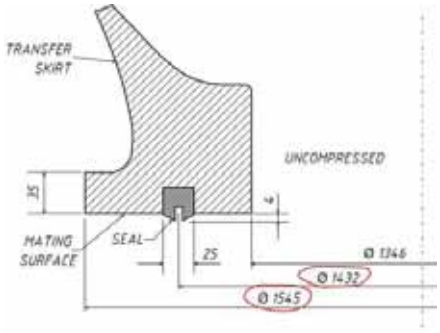

Fig. 5. Flange dimensions of emergency vehicle seat

Dead load caused by hydrostatic pressure P_c *Additional load caused by side current P_L* *Total load*

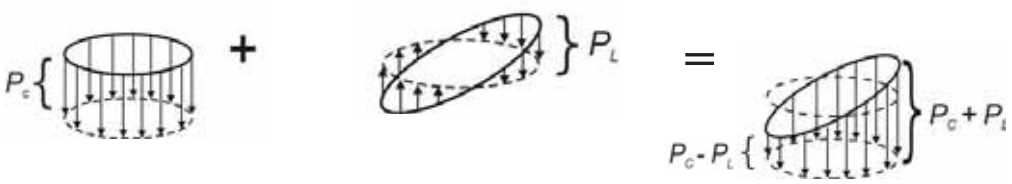

Fig. 6. Distribution of surface forces on the seat face

3. The results of measurements of a salvage faying face of a submarine

NAVSEA Standard contains detailed information on the construction of emergency vehicles, their dimensions and how to dock such vessels. Table 1 shows the results of measurements of the thickness of the seat of one submarine in accordance with NAVSEA and the Polish Defence Standard, using the scheme presented in Fig. 4.

Tab. 1. List of seat face thickness in characteristic points

No of point	Thickness, mm	No of point	Thickness, mm
1	24,5	13	25,8
2	-	14	-
3	23,8	15	25
4	25,1	16	26,6
5	-	17	-
6	23,1	18	24,6
7	25,4	19	24,2
8	-	20	-
9	22,4	21	21,3
10	25,2	22	24,4
11	-	23	-23,9
12	23,3	24	-

In characteristic points 2, 5, 8, 11, 14, 17, 20 and 23 no measurements were made due to the high roughness of the surface. The average thickness of the plate was 24,29 mm. On average, reduction in thickness of the contact plate was 1,11 mm, while the largest point reduction in seat plate thickness was more than 4 mm. Thus, it became necessary to carry out the numerical analysis for determining the actual seat face capacity and to determine the minimum thickness of the contact plate for particular submergence depth of the submarine.

4. Geometric representation of the submarine salvage faying face

Based on the ship's documentation, sketches and photographs, there was formed the basis for the seat, on which the contact plate is attached. Next the geometry of the pressure hull was mapped using CAD software [1, 2]. Then the geometry of the scuttle was mapped, which was followed by creation of geometry of contact plate reinforcement. The final step was creating frames strengthening the pressure hull from the inside (Fig. 7).

Fig. 7. Top view of faying face

When creating the geometry of the seat some simplifications were used to facilitate the creation of the computational model. In the geometric model of the face the weld seams were omitted. In the course of the work aiming at mapping the faying face, it was found that all the welds were in perfect condition [5 ÷ 8]. In addition, some of the dimensions in the geometric model were averaged (e.g. a constant contact plate thickness was adopted, assuming the worst option).

An analysis of free vibration of the system was carried out to determine the continuity of the geometry. The notion of free vibration of the system means that the structure deflected out of balance is affected only by the internal forces caused by the deflection. Analysis of free vibration frequency allows to predict the behavior of the structure during motion [3, 4].

In MES free vibrations of the system are described by the following relation:

$$K \cdot U + M \cdot \ddot{U} = 0 \,, \tag{1}$$

where:

K – stiffness matrix,
U – node displacements vector,
Ü – self-acceleration vector,
M – inertia matrix for one element represented in the formula:

$$M^e = \rho \int_V N^T \cdot N dV \,, \tag{2}$$

where:
N – form function matrix,
ρ – density,
V – volume of element.

In equation (2) the following substitution shall be applied:

$$U = X \cdot \sin \omega t \ , \tag{3}$$

where:

U – displacements vector,
X – amplitude vector,
ω – ring frequency.

$$\lambda = \frac{1}{\omega^2} \ , \tag{4}$$

where:
λ – proper value.

The above equations are solved with Lanczos method [3, 4]. In order to verify the continuity of the geometry of the 3D model, free vibrations of the first 10 forms were analyzed. To do this, the analysis of free vibration built-in the CAE environment was used.

Geometry of the face was made as one element and before calculations for the simulation it was divided into 101 parts (partitioning). The division was made to achieve an independent digitization of individual seat elements. First, the base of the seat was separated from the pressure hull, thus getting two parts. Then, the contact plate was separated from the base and the strengthening brackets, dividing it into two parts. In subsequent steps individual brackets were separated I order to get independent elements. Besides, the base was divided into 26 parts. In the final stage the internal strengthening elements with a holder were divided into two elements. The division of a face model resulted in independent digitization of its individual components. It was possible to make calculations in a solver [12]. The model was digitized with 31693 tetragonal 4-nodal elements, and 42261 hexagonal 8-nodal elements [1, 2, 4]. The constructed model of pressure hull sector together with the construction of salvage face were supported along the edge of the cutoff part of the pressure hull, thus depriving the nodes lying on it all degrees of freedom (Fig. 8). The salvage faying face of a submarine was loaded with pressure exerted by the contact surface of the submergence recovery vessel while docking at a depth of 100 to 400 m with regard to the forces induced by side sea currents (Fig. 6) that must be taken into consideration according to the guidelines included in the standards [9, 10].

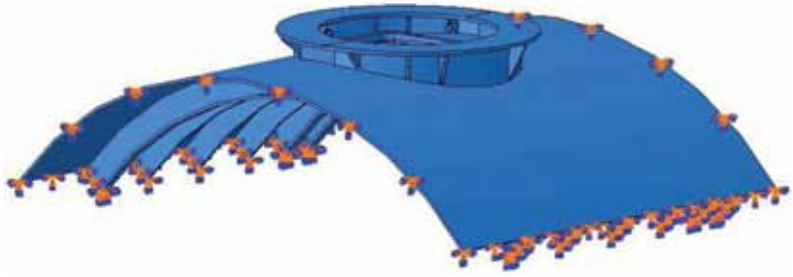

Fig. 8. View of faying face support with regard to boundary conditions

In the moment of connecting an emergency vehicle seat with the contact plate of a submarine rescue seat (salvage faying face), the buoyancy force balances the gravity. When pumping out water from the space between the faces, the force acting on the seat is determined by a simple relation.

$$p_w \cdot \Delta S = p_h \cdot S_k, \text{ thus } p_w = \frac{p_h \cdot S_k}{\Delta S}. \tag{5}$$

Section of internal surface of a face measured from the end of the seal $S_w = \frac{\pi \cdot d_w^2}{4}$,

Surface area of the contact plate of an emergency vehicle seat $S_k = \frac{\pi \cdot d_k^2}{4}$, thus the ring area $\Delta S = S_k - S_w$,

where:

p_h – hydrostatic pressure at the depth of submergence,
p_w – pressure in the space between the faces,
S_w – internal area (to the outside edge of the seal),
S_k – surface area of an emergency vehicle seat contact,
d_w – diameter of a wheel limited by the circle to end the seal,
d_z – outside diameter of the contact plate seat of an emergency vehicle.

The calculations omitted salinity of the Baltic Sea and adopted specific weight of water equal 10.000 N/m^3. Table 2 shows load of the faces at a given depth of submarine submergence.

Tab. 2. Load of the faces at a given depth of submarine submergence

Depth of docking, m	Pressure at the depth, MPa	Load of face, MPa
100	1	6,21
200	2	12,41
300	3	18,62
400	4	24,82

5. Numerical calculations of the strength of the submarine rescue seat

Numerical simulations of reduced stresses were determined with use of Huber's Strength Hypothesis for the thickness of contact plate of 25,4 and 23 mm, and the submarine submergence at a depth of 100 ÷ 400 m. Exemplary stress and displacement patterns in a face of 25,4 mm thickness, loaded with pressure at a depth of 100 m is presented in Fig. 9 and 10. Table 3 includes results of the conducted simulations for a 25,4 mm thick contact plate.

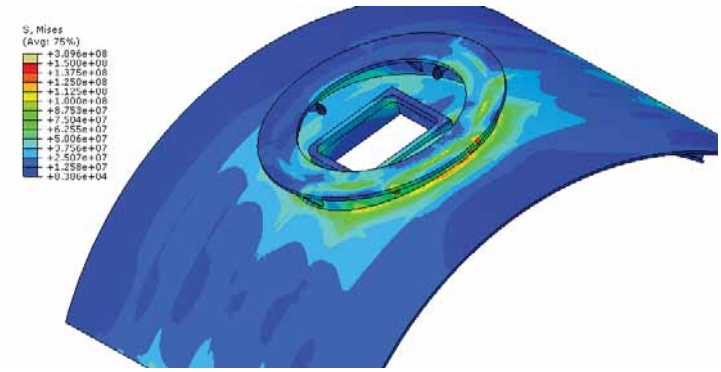

Fig. 9. Reduced stresses pattern in a submarine faying face of 25,4 mm thickness at a depth of 100 m

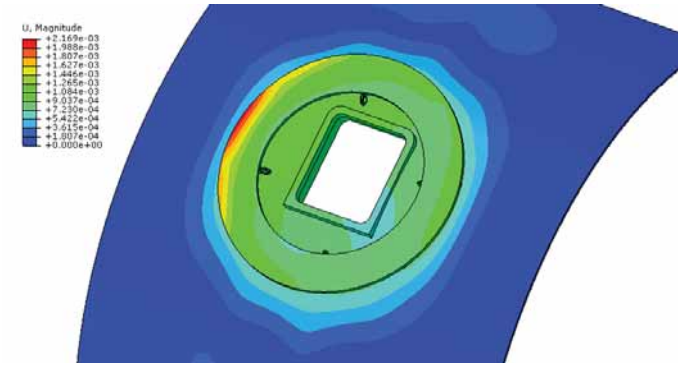

Fig. 10. Displacements pattern in a submarine faying face of 25,4 mm thickness in vertical direction at a depth of 100 m

Tab. 3. Results of numerical simulations for a contact plate of 25,4 mm thickness

Depth of docking submergence recovery vessel, m	Load value, MPa	Reduced stress, MPa		Relative vertical displacement, mm
		max	local extremum	
100	6,21	150	310	0,621
200	12,41	330	618	1,434
300	18,63	450	928	2,165
400	24,82	600	1237	2,892

Value of stresses in a submarine faying face at a depth 100 m amounted 0,008 ÷ 310 MPa, while displacements in vertical direction achieved 0,621 mm (Fig. 9, 10). At a depth of 400 m local value of reduced stresses exceeded 1200 MPa, and the displacements were close to 3 mm (Table 3). Results of simulation calculations of stresses and displacements for a contact plate of 23 mm thickness while docking submergence recovery vessel at depths of 100, 200, 300, 400 m are presented in table 4.

For the thickness of contact plate of 23 mm, and the depth of docking submergence recovery vessel of 100 ÷ 400 m, reduced stresses amount 0,172 ÷ 1536 MPa, and the displacements exceed 3 mm for the submergence depth of 400 m.

Table 4. Results of numerical simulations for a contact plate of 23 mm thickness

Depth of docking submergence recovery vessel, m	Load value, MPa	Reduced stress, MPa		Relative vertical displacement, mm
		max	local extremum	
100	6,21	179	384	0,671
200	12,41	370	767	1,538
300	18,63	550	1152	2,307
400	24,82	700	1536	3,077

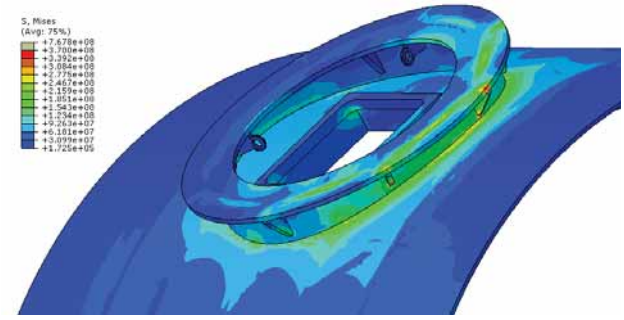

Fig. 11. Reduced stresses pattern in a submarine faying face of 23 mm thickness at a depth of 200 m

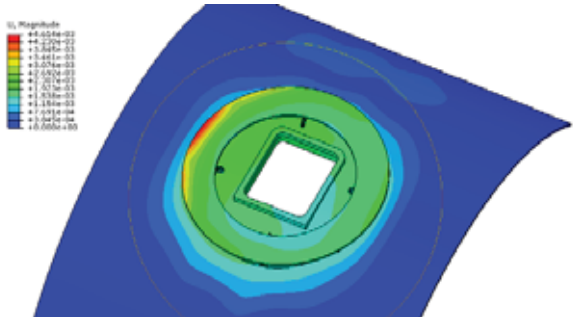

Fig. 12. Displacements pattern in a submarine faying face of 23 mm thickness in vertical direction at a depth of 200 m

Exemplary stress and displacement patterns in a face of 23 mm thickness, loaded with pressure at a depth of 200 m is presented in Fig. 11 and 12.

6. Conclusions

1. Simulation calculations proved that docking a submergence recovery vessel on a submarine faying face (when its thickness complies with the applicable standards) is safe at a depth up to 200 m. Nevertheless, at a depth of 200 ÷ 300 m the locally appearing stresses exceed the yield point of the matter.
2. For 23 mm thick contact plate it is safe to dock an emergency vessel at a depth up to 100 m. Docking a submergence recovery vessel at a depth up to 100 ÷ 200 m may result in permanent local deformations of the faying face construction. In the case of docking at a depth above 200 m the stresses significantly exceed the yield point of the matter.

3. More than forty years of operation of submarines caused a wear of the seats (faying faces) and thus limited the secure depth of submergence, taking into account safety conditions of the crew.
4. In order to maintain safety conditions a submarine should not submerge to a depth exceeding 200 m.

7. References

[1] Skrzat, A., Modelowanie liniowych i nieliniowych problemów mechaniki ciała stałego i przepływów ciepła w programie ABAQUS, Politechnika Rzeszowska, 2010.
[2] Skrzat, A., Ćwiczenia z metody elementów skończonych w programie ADINA, Politechnika Rzeszowska, 2003.
[3] Rakowski, G., Kacprzyk, Z., Metoda elementów skończonych w mechanice konstrukcji, Wydawnictwo OWPW, 2005.
[4] Zagrajek, T., Krzesiński, G., Marek, P., Metoda elementów skończonych w mechanice konstrukcji, Ćwiczenia z zastosowaniem systemu ANSYS, Wydawnictwo OWPW, 2005.
[5] Kyzioł, L., Szturomski, B., Świątek, K., Bohn, M., Ekspertyza przylgni okrętu podwodnego – 294 projekt 207, 2009.
[6] Kyzioł, L., Szturomski, B., Świątek, K., Bohn, M., Ekspertyza przylgni okrętu podwodnego – 295 projekt 207, 2009.
[7] Kyzioł, L., Szturomski, B., Świątek, K., Bohn, M., Ekspertyza przylgni okrętu podwodnego - 296 projekt 207, 2009.
[8] Kyzioł, L., Szturomski, B., Świątek, K., Bohn, M., Ekspertyza przylgni okrętu podwodnego - 297 projekt 207, 2009.
[9] Norma Obrona NO-42-A207, Okręty podwodne, Przylgnie ratownicze, Wymagania, Ministerstwo Obrony Narodowej, 2001.
[10] Norma SS700-AA-INS010, International Submarine Rescue Requirements and Instruction Manual for Mating with U.S. Navy Rescue Assets, Naval Sea Systems Command, 2001.
[11] Bohn, M., Projekt pierścienia do dokowania pojazdu ratowniczego na powierzchni przylgni okrętu podwodnego, Praca inżynierska, 2010.
[12] http://www.knse.pl/publikacje (z dnia. 18.01.2012 r.).
[13] Kyzioł, L., Czapczyk, K., The Analysis of the Parameters of the Materials used for Antiterrorist safety shields in Marine Vessels, Journal of KONES Powertrain and Transport, vol. 18, No 1, 2011, pp. 185 ÷ 193.

Journal of Polish CIMAC
Gdansk University of Technology
The Faculty of Ocean Engineering and Ship Technology

APPLICATION OF MARKOV PROCESS FOR MODELING CHANGES OF TRANSPORT MEANS OPERATION STATES

Bogdan Landowski, Daniel Perczyński, Piotr Kolber

University of Technology and Life Sciences in Bydgoszcz
Faculty of Mechanical Engineering
ul. Kaliskiego 7, 85-796 Bydgoszcz, Poland
tel.:+48 52 3408495, fax: +48 52 3408495
e-mail: lbogdan@utp.edu.pl, perkol@utp.edu.pl

Abstract

The article deals with selected problems connected with modeling, prognosis and control of the operation process of a certain class of technical objects used in a complex operation system. The research object is an urban bus transportation system. The authors present assumptions be used for developing a model of the process carried out within the research object. A model of the operation process (Markov process) of an urban transportation bus has been presented. On the basis of identification of the research object and the operation process carried out in it, there has been built a graph of the transport means operational states and possible transitions between these states have been determined. The mean 'life time' of the system in which the modeled operation process is carried out has been established The whole study has been illustrated by a computational example. Values of the model parameters have been estimated on the basis of results of the initial tests performed in areal transport means operation system.

Keywords*: maintenance process, modelling, Markov process, urban public transport, lifetime of system*

1. Introduction

Supporting people, responsible for making decisions on the control of complex operation processes, can involve prognosis of the operation system and assessment of the impact of selected decision variants on the operation process course [3].

Vehicles involved in the operation process go through many operational states which make up a space of S states. A random process with a finite number of states S and a set of parameters R+ is a natural model of the operation process [7]. An assumption has been accepted that a homogenous Markov model is the one which describes the real process of the vehicle operational states changes [1,2,3,5,6,8]. In practical application, it is necessary to verify if there occur any reasons to reject the assumptions resulting from the related mathematical apparatus.

The purpose of this elaboration is to present the possibilities of using Markov model of the technical object operation process for an analysis of the operation system behavior after changing the model initial parameters. A Change in the model initial parameters values can simulate the impact of different factors on the system behavior and characteristics of the vehicle operation process (duration times of the operation states, probabilities of the state change, numbers of entrances to states). In order to illustrate the discussion, a simplified computational example, concerning the initial prognosis of the system "life time" with the assumption that the objects withdrawn from operation have been replaced by new ones, has been demonstrated. For this

purpose, the so called absorption state has been specified in the model of the transport means operation. In such a case the vehicle "lifetime" is the expected value of a random variable, standing for the time period, after which process X(t), being a model of the transport means operation process, will be found in the absorption state.

In the analyzed system of operation, determination of the "life time" of the system, viewed as the length of time interval after which the system stand-by is exhausted (stand-by vehicles), and the number of vehicles being in the state of serviceability is too small to perform fully the accepted range of transport tasks.

2. Research Object

The research object is a complex system of transport means operation (technical objects) including the process of technical objects operation. The process of operation is referred to as all the processes concerning technical objects in the phase of operation, thus determining advisability of their application and efficiency of the related system.

An urban bus transportation system used in a big urban agglomeration is an example of a complex system of technical objects operation which has been used for illustration of the study presented in this work.

The main goal of the examined system operation is safe and efficient performance of transport tasks in a defined quantity and over an assigned territory. Transport task are directly performed by elementary socio-technical subsystems of the type O-TO (operator –technical object). Elements of these subsystems, that is, the driver (operator) and a vehicle (technical object), are coupled in the by a series structure in the sense of reliability. Transport tasks are performed with the use of buses. Further, in this work, an assumption is accepted that in the set of operated buses there can be distinguished systems of objects, homogenous from the point of view of the analysis purpose.

The main processes carried out in the research object include, apart from transport means operation processes, processes connected with ensuring serviceability of the vehicles.

In the analyzed system there can be distinguished a subsystem responsible for providing the vehicles with serviceability which includes: [3,8]:

- servicing station with stands for current repairs – in which the damaged vehicles are provided with serviceability,
- subsystem of, the so called, teams for maintenance of traffic during performance of transport tasks- it provides damaged vehicles with serviceability while performing transport tasks (definite range of carried out processes).

In order to guarantee efficient performance of transport tasks, in the accepted quantity and over the assigned territory, it is necessary to have m fit for use vehicles. Ensuring the continuity of tasks performance in case of the vehicle damage is possible through maintenance of k stand-by vehicles. In the considered object there are used n=m+k number of buses. They perform transport tasks during a 24 hour-cycle.

3. Simplified model of the vehicle operation

For further studies it has been assumed that there can be distinguished the technical object operation states that are significant from the point of view of the research goal. In a given time the object can be only in one of the analyzed operational states.

A stochastic model describing changes of the vehicle operational states has been accepted to be its operation process model.

On the basis of an analysis of the space of the transport means operational states it is possible to distinguish states which are significant in terms of these systems operation efficiency analysis. The size of the distinguished state spaces depend, among others, on the goals of the carried out

analyses and studies. Due to the character of the research, five operational states of a city bus transportation system have been analyzed. However, the presented approach to the model description enables its use for objects with different, than the analyzed, space of states. In works [3,4,7,8,9,10,11] models of an urban bus transportation operation process are analyzed for more complex spaces of states.

In result of identification of the research object and the related operation process, the following operation states of vehicle have been distinguished:

- S_1 – performance of transport tasks,
- S_2 – performance of, the so called, servicing processes, on the day of operation,
- S_3 – servicing the vehicle at the station,
- S_4 – withdrawal of the vehicle from operation (the so called liquidation of the vehicle, in the analyzed example in result of damage whose removal is economically unjustified, e.g. being the effect of a road collision),
- S_5 – standby of the vehicle at the premises of the depot (according to the schedule of transport tasks).

It has been assumed that duration time of state S_4 approaches infinity (the vehicle is crossed out from the vehicle register and is not replaced by a different one).

On the basis of an analysis of the operation process realized within the research object, there have been determined transitions between the vehicle operation states – fig. 1.

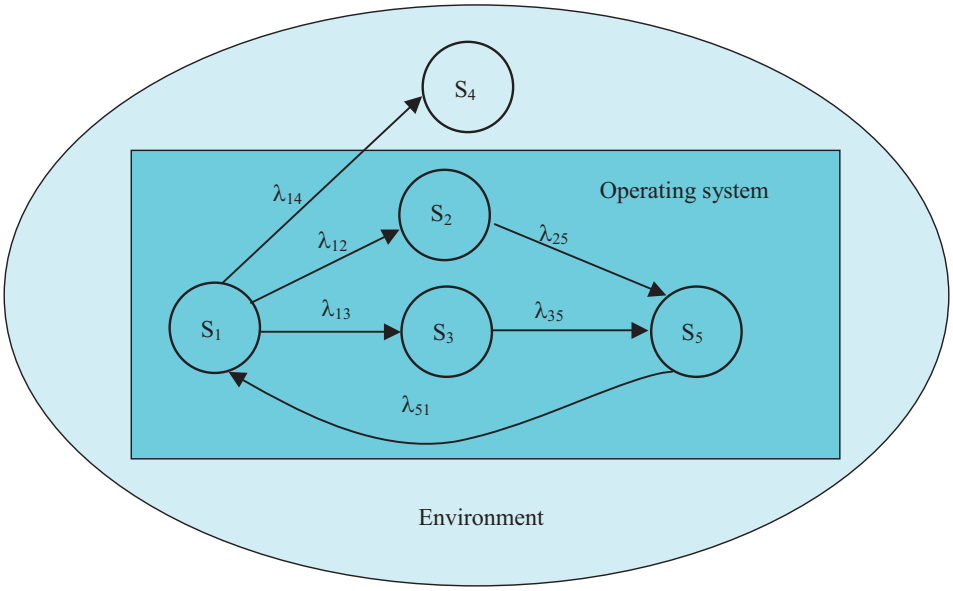

Fig 1. Directed graph of operational states

A homogenous Markov process X(t) has been accepted to be a model of the vehicle operation process. The analyzed process X(t) has an infinite phase space $S=\{ S_1 ,S_2, S_3, S_4, S_5\}$. If $X(t) = S_i$, $i = 1, 2, 3, 4, 5$, then the vehicle is in state Si, in time t. For the analyzed model of the vehicle operation process, state S4 is an absorption one.

Let $P_i(t) =P\{X(t) =S_i\}$ denote probability that process X(t) is in state S_i, i=1,2,3,4,5. State S_1, is assumed to be the initial one which means that the initial distribution is in the form:

$$P\{X(0)= S_1\}=1,$$
$$P\{X(0)= S_i\}=0, \text{ dla } i=2,3,4,5.$$

Intensity of transitions from the process state to state has been accounted for in matrix Λ:

$$\Lambda = \begin{bmatrix} -(\lambda_{12}+\lambda_{13}+\lambda_{14}) & \lambda_{12} & \lambda_{13} & \lambda_{14} & 0 \\ 0 & -\lambda_{25} & 0 & 0 & \lambda_{25} \\ 0 & 0 & -\lambda_{35} & 0 & \lambda_{35} \\ 0 & 0 & 0 & 0 & 0 \\ \lambda_{51} & 0 & 0 & 0 & -\lambda_{51} \end{bmatrix}. \quad (1)$$

For the purpose of simplification notation $\lambda = \lambda_{12}+\lambda_{13}+\lambda_{14}$ has been introduced.
Matrix of intensity of transitions Λ allows to build the differential equations layout as form [2]:

$$\begin{aligned} P'_1(t) &= -\lambda P_1(t) + \lambda_{51}P_5(t), \\ P'_2(t) &= \lambda_{12}P_1(t) - \lambda_{25}P_2(t), \\ P'_3(t) &= \lambda_{13}P_1(t) - \lambda_{35}P_3(t), \\ P'_4(t) &= \lambda_{14}P_1(t), \\ P'_5(t) &= \lambda_{25}P_2(t) + \lambda_{35}P_3(t) - \lambda_{51}P_5(t). \end{aligned} \quad (2)$$

System of differential equations (2), in a matrix notation, assumes the form:

$$\begin{bmatrix} P_1'(t) \\ P_2'(t) \\ P_3'(t) \\ P_4'(t) \\ P_5'(t) \end{bmatrix} = \begin{bmatrix} -\lambda & 0 & 0 & 0 & \lambda_{51} \\ \lambda_{12} & -\lambda_{25} & 0 & 0 & 0 \\ \lambda_{13} & 0 & -\lambda_{35} & 0 & 0 \\ \lambda_{14} & 0 & 0 & 0 & 0 \\ 0 & \lambda_{25} & \lambda_{35} & 0 & -\lambda_{51} \end{bmatrix} \begin{bmatrix} P_1(t) \\ P_2(t) \\ P_3(t) \\ P_4(t) \\ P_5(t) \end{bmatrix}. \quad (3)$$

In order to provide the above system of equations with a unique solution it is necessary to accept the initial conditions. On the basis of the initial distribution of X(t) process, it can be noted:

$$\begin{aligned} P_1(0) &= 1, \\ P_2(0) &= 0, \\ P_3(0) &= 0, \\ P_4(0) &= 0, \\ P_5(0) &= 0. \end{aligned} \quad (4)$$

It is convenient to solve the systems of linear differential equations by means of Laplace transform which with accounting for initial condition (4) has the form:

$$\begin{aligned} s\widetilde{P}_1(s)-1 &= -\lambda \widetilde{P}_1(s) + \lambda_{51}\widetilde{P}_5(s), \\ s\widetilde{P}_2(s) &= \lambda_{12}\widetilde{P}_1(s) - \lambda_{25}\widetilde{P}_2(s), \\ s\widetilde{P}_3(s) &= \lambda_{13}\widetilde{P}_1(s) - \lambda_{35}\widetilde{P}_3(s), \\ s\widetilde{P}_4(s) &= \lambda_{14}\widetilde{P}_1(s), \\ s\widetilde{P}_5(s) &= \lambda_{25}\widetilde{P}_2(s) + \lambda_{35}\widetilde{P}_3(s) - \lambda_{51}\widetilde{P}_5(s). \end{aligned} \quad (5)$$

Taking into consideration notation (1) system of equations (5) can be written as follows:

$$P'(t) = \Lambda^T P(t), \tag{6}$$

where:

$P'(t) = [P'_1(t), P'_2(t), P'_3(t), P'_4(t), P'_5(t)]^T$,
$P(t) = [P_1(t), P_2(t), P_3(t), P_4(t), P_5(t)]^T$.

The matrix notation of linear system of equations for transforms has the following form:

$$\begin{bmatrix} -\lambda+s & 0 & 0 & 0 & \lambda_{51} \\ \lambda_{12} & -\lambda_{25}+s & 0 & 0 & 0 \\ \lambda_{13} & 0 & -\lambda_{35}+s & 0 & 0 \\ \lambda_{14} & 0 & 0 & s & 0 \\ 0 & \lambda_{25} & \lambda_{35} & 0 & -\lambda_{51}+s \end{bmatrix} \begin{bmatrix} \widetilde{P}_1(s) \\ \widetilde{P}_2(s) \\ \widetilde{P}_3(s) \\ \widetilde{P}_4(s) \\ \widetilde{P}_5(s) \end{bmatrix} = \begin{bmatrix} 1 \\ 0 \\ 0 \\ 0 \\ 0 \end{bmatrix}. \tag{7}$$

It is convenient to solve equation system (7) by Cramer's method. The prime determinant of the equation system is as follows:

$$W(s) = \begin{vmatrix} s+\lambda & 0 & 0 & 0 & -\lambda_{51} \\ -\lambda_{12} & s+\lambda_{25} & 0 & 0 & 0 \\ -\lambda_{13} & & s+\lambda_{35} & 0 & 0 \\ -\lambda_{14} & 0 & 0 & s & 0 \\ 0 & -\lambda_{25} & -\lambda_{35} & 0 & s+\lambda_{51} \end{vmatrix}. \tag{8}$$

After performance of successive developments and computing of 3-degree determinant, we receive:

$$W(s) = s(s+\lambda)\,(s+\lambda_{51})\,(s+\lambda_{25})\,(s+\lambda_{35}) - s\lambda_{51}[\lambda_{12}\lambda_{25}\,(s+\lambda_{35}) + \lambda_{13}\lambda_{35}\,(s+\lambda_{25})]. \tag{9}$$

Similarly specified were determinants:

$$\begin{gathered} W_1(s) = s(s+\lambda_{51})\,(s+\lambda_{25})\,(s+\lambda_{35}), \\ W_2(s) = s\lambda_{12}(s+\lambda_{35})\,(s+\lambda_{51}), \\ W_3(s) = s\lambda_{13}(s+\lambda_{25})\,(s+\lambda_{51}), \\ W_4(s) = \lambda_{14}(s+\lambda_{25})\,(s+\lambda_{35})\,(s+\lambda_{51}), \\ W_5(s) = s[\lambda_{12}\lambda_{25}\,(s+\lambda_{35}) + \lambda_{13}\lambda_{35}\,(s+\lambda_{25})]. \end{gathered} \tag{9a}$$

In order to determine the mean "life time" of the system it is necessary to determine the expected value of the sum of times during which the vehicle is in non absorbing states. Without determination of return transforms which enable determination of probabilities $P_i(t)$, where i=1,2,3,4,5 it is possible to establish the expected values of the vehicle being in particular states. It is known [1] that:

$$E(T_1+T_2+T_3+T_5) = \lim_{s\to 0^+}\left[\frac{1}{s} - \widetilde{P}_4(s)\right], \tag{10}$$

where:

T_i - denotes time of being in state i, i=1,2,3,5,
and:

$$\widetilde{P}_4(s) = \frac{W_4(s)}{W(s)} = \frac{\lambda_{14}(s+\lambda_{25})(s+\lambda_{35})(s+\lambda_{51})}{s\left[(s+\lambda)(s+\lambda_{51})(s+\lambda_{25})(s+\lambda_{35}) - \lambda_{51}\left[\lambda_{12}\lambda_{25}(s+\lambda_{35}) + \lambda_{13}\lambda_{35}(s+\lambda_{25})\right]\right]}. \quad (11)$$

Let W(s) = sM(s), then:

$$\frac{1}{s} - \widetilde{P}_4(s) = \frac{1}{s} - \frac{W_4(s)}{sM(s)} = \frac{M(s) - W_4(s)}{sM(s)}. \quad (12)$$

After computing values M(s) and $W_4(s)$ we receive:

$$M(0) = \lambda_{51}\lambda_{14}\lambda_{25}\lambda_{35}, \quad (13)$$

$$W_4(0) = \lambda_{51}\lambda_{14}\lambda_{25}\lambda_{35}. \quad (14)$$

Boundary

$$\lim_{s\to 0^+} \frac{M(s) - W_4(s)}{sM(s)} \quad (15)$$

is of the type [0/0], where M(s) is a polynominal of fourth degree in relation to s, and $W_4(s)$ is a polynominal of third degree.

Coefficient near s for M(s) is equal to:

$$\lambda\lambda_{51}\lambda_{25}+\lambda\lambda_{51}\lambda_{35}+(\lambda+\lambda_{51})\lambda_{25}\lambda_{35}-\lambda_{51}\lambda_{12}\lambda_{25}-\lambda_{51}\lambda_{13}\lambda_{35}, \quad (16)$$

and for $W_4(s)$:

$$\lambda_{14}(\lambda_{25}\lambda_{35} + \lambda_{51}\lambda_{25} + \lambda_{51}\lambda_{35}). \quad (17)$$

In relation to the above, we receive:

$$\lim_{s\to 0^+}\left[\frac{1}{s} - \widetilde{P}_4(s)\right] = \frac{\lambda_{25}\lambda_{35}(\lambda + \lambda_{51} - \lambda_{14}) + \lambda_{51}\lambda_{13}\lambda_{25} + \lambda_{51}\lambda_{12}\lambda_{35}}{\lambda_{51}\lambda_{14}\lambda_{25}\lambda_{35}}. \quad (18)$$

The expected value of system ET life time can be determined from dependence (18).

In table 1 there are values of the model parameters, estimated on the basis of initial results of tests performed in the analyzed system. In fig. 2 the dependence between the mean "life time" and the intensity value λ_{14} has been presented.

Tab. 1. Estimated values of the model parameters

λ_{12}	λ_{13}	λ_{14}	λ_{25}	λ_{35}	λ_{51}
0,055351	0,002768	0,000017	1,500000	0,344828	0,163043

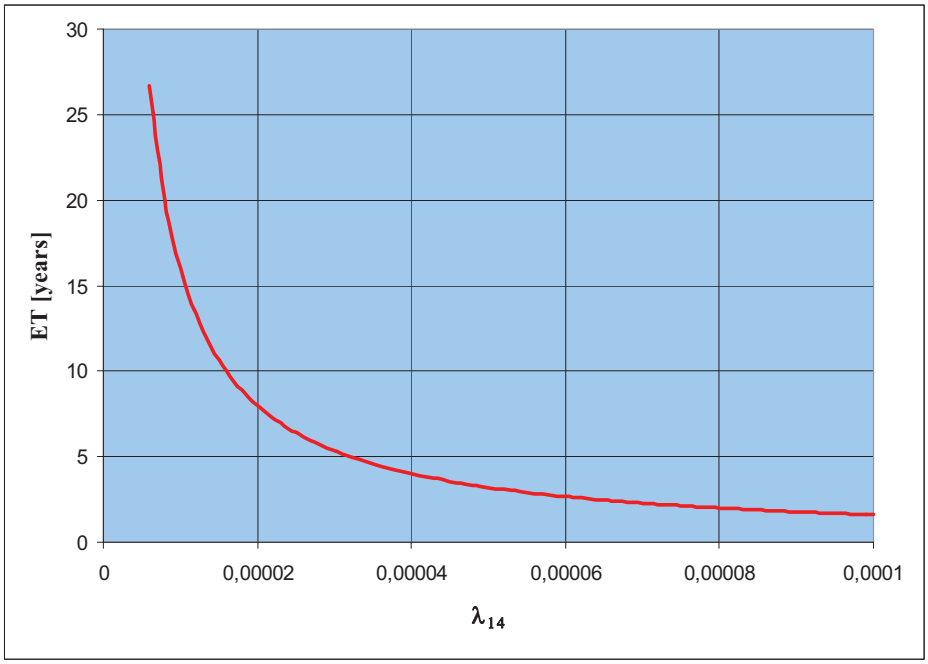

Fig. 2. Mean time of the system "life" in dependence on the intensity value λ_{14}

4. Summary

One of the purposes of the research presented in this work is to show the possibility of using selected stochastic processes for mathematical modeling of the vehicle operation system and process.

The assessment and prognosis of efficiency in complex systems of transport means operation is connected with mathematical modeling of the technical objects operation processes. It involves a necessity of providing a formalized description of the processes connected with the transport means operational states changes. Changes of operational states are caused by changes in the vehicle technical states and the processes of their operation and utilization. These processes are of random character and depend on each other. Their mathematical models will naturally be simplified. The analysis of these models tests results, made for the value of their parameters, determined on the basis of experimental tests performed in a real transportation system, makes it possible to formulate conclusions and assessments of both qualitative and quantitative (in a limited scope) character. Practical conclusions resulting from these models tests should be formulated carefully.

The discussed computational example is characterized by a significant simplification degree. Estimation of the values of the model parameters, simulating a change of control impacts of the operation process is an important problem (analysis of different decision variants). Assessment of the influence of the number of stand-by vehicles is difficult in the analyzed example due to the change of transitions intensity values occurring along with the stand-by exhaustion.

Solution of differential equation system (5) and introduction of a non-zero value λ_{51} of (purchase of new vehicles) matrix (1) enables an analysis of a wider range of issues concerning the analyzed system.

The presented approach to building models of the vehicle operational states changes and application of Markov for modeling the process of an urban transportation buses operation can be

relatively easily applied for an analysis of, different than the considered, characteristics of the process and for other operation systems.

References

[1] Bobrowski D., *Mathematical models and methods of reliability theory in examples and exercises*, WNT, Warsaw 1985.

[2] Buslenko N., Kałasznikow W., Kowalenko I., *Theory of complex systems*, PWN, Warsaw 1979.

[3] Landowski B., Woropay M., Neubauer A., *Controlling reliability in transport systems*, Library of Maintenance Problems, ITE, Bydgoszcz-Radom 2004.

[4] Landowski B., *Maintenance model of a certain class of technical objects*, Scientific Journals No. 229, Mechanics 48, University Publishing House ATR, Bydgoszcz 2000.

[5] Mine H., Osaki S., *Markowskije processy priniatija reszenij*, Science, Moscow 1977.

[6] Sołowiew A.D., *Analityczne metody w teorii niezawodności*, WNT, Warszawa 1983.

[7] Woropay M., Grabski F., Landowski B., *Semi-Markov model of the vehicle operation and maintenance processes within an urban transportation system*, Scientific Publishers PTNM, The Archives of Automotive Engineering, Vol. 7, No. 3, 2004.

[8] Woropay M., Knopik L., Landowski B., *Modelling the maintenance and operation processes in a transport system*, Library of Maintenance Problems, ITE, Bydgoszcz - Radom 2001.

[9] Woropay M., Landowski B., *Metoda symulacji procesu eksploatacji pojazdów poddawanych obsłudze profilaktycznej*, Wydawnictwo Naukowe PTNM - Archiwum Motoryzacji, Vol. 7, Nr 2, 2004.

[10] Woropay M., Landowski B., *Simulation Model for Maintenance Process of Passenger Transport Vehicles Operated within Urban Areas,* Archives of Transport, Volume 14, PAN, Warszawa 2002.

[11] Woropay M., Landowski B., *Simulation analysis of the maintenance and operation processes in an urban transport system*, Scientific Journals No. 212, Mechanics 42, University Publishing House ATR, Bydgoszcz 1998.

Journal of Polish CIMAC
Gdansk University of Technology
The Faculty of Ocean Engineering and Ship Technology

RISK CRITERIA FOR SEA-GOING SHIPS ARISING FROM THE OPERATION OF THE MAIN ENGINES' CRANKSHAFT – CONECTING ROD – PISTON SYSTEMS

Roman Liberacki

Gdansk University of Technology
ul. Narutowicza 11/12, 80-950 Gdańsk, Poland
tel.: +48 58 3471850, fax: +48 58 3472430
e-mail: romanl@pg.gda.pl

Abstract

In the article the risk criterion for sea-going ships arising from the operation of the main engines' crankshaft – connecting rod – piston systems is proposed. This criterion is based on the procedures recommended in the Formal Safety Assessment method developed under the auspices of International Maritime Organization (IMO). First of all the collective risk criterion for ship has been proposed. In the next step, the share of the main engines' crankshaft – connecting rod – piston systems, as the causes of marine accidents has been estimated. Then the risk criteria for ships arising from operation of those systems have been created. Additionally the reliability requirements for main engine components have been established.

Key words: *risk criterion, ship, main engine, crankshaft – connecting rod – piston system.*

1. Introduction

Safety in shipping is the object of interest of many people professionally connected with this branch of transportation, but also of the general public, because every one of us can be a passenger on the watercraft or we can be affected by an accident at sea for example in the case of environmental disaster caused by the loss of the ship's hull integrity or ship sinking.

Special responsibility for the safety in shipping is laying on the ship designers, ship builders, ship owners and crew members. Marine accidents and disasters can cause a loss of human life, serious damage in the environment and of course in every case financial loss.

There are numerous rules governing the principles of proper design, construction, operation and disposal of vessels. The examples of that are the rules of classification societies, international conventions on safety in navigation and protection of the marine environment. However, all those norms and regulations are of deterministic character. Still there are no widely used probabilistic rules in shipping, as it take place in inland nuclear power plants, chemical industry and some sectors of aviation.

Attempts to non - deterministic approach to the issue of safety at sea are undertaken. In particular it can be observed since 1997, when under the auspices of the International Maritime Organization the maritime community began to develop the method of Formal Safety Assessment.

In this article the special attention of the author is focused on the unreliability of main engines' crankshaft – connecting rod – piston systems components. Damage or failures of these elements

can lead to the need of reducing the main engine output power or in some cases to the need of stop main engine during sea travel. It can directly lead to the marine accident or disaster, especially under the difficult conditions of navigation.

Hence the idea: to create the risk criterion for a ship as a whole and the risk criterion arising from the operation of the main engines' components. These criteria are based on ALARP risk acceptability criteria concept. ALARP means that risk level should be as low as reasonably practicable. The proposed risk criteria relate to health and life of human beings and also losses of an economical and ecological nature.

2. Individual and societal risk criteria in maritime transportation

The definitions of individual and societal risk are given in [4]. Individual risk is the frequency at which an individual may be expected to sustain a given level of harm from realization of specified hazards. Societal risk is the relationship between the frequency and the number of people suffering from a specified level of harm in a given population from the realization of specified hazards.

As it has been already stated above, risk criteria are built using principles of ALARP concept widely described in the literature, for example in [1, 2, 3, 4, 5]. To build ALARP based risk criterion it is necessary to divide the risk spectrum area into three parts. To do that, two limits of risk have to be established: the lower limit of risk and the upper limit of risk. The area below the lower limit of risk is an acceptable risk area. The area above the upper limit of risk is an unacceptable risk area. The area between those two limits (ALARP region) is the subject of judgment between the risk and benefits and between possibility to reduce the risk level and costs of such reducing.

If the risk is in the acceptable area we needn't take any action to reduce the risk. If the risk is in the unacceptable area the object of interest (ship) can't be used as the mean of transportation, it is necessary to take steps to reduce the level of risk. In the ALARP region we should try to reduce the risk as far as it is reasonably justified and possible in practice. Individual risk criteria (frequency of loss of life by individual) proposed for ships are as follows [2, 5]:

- maximum tolerable risk for crew members 10^{-3} annually,
- maximum tolerable risk for passengers 10^{-4} annually,
- maximum tolerable risk for public ashore 10^{-4} annually,
- negligible risk 10^{-6} annually.

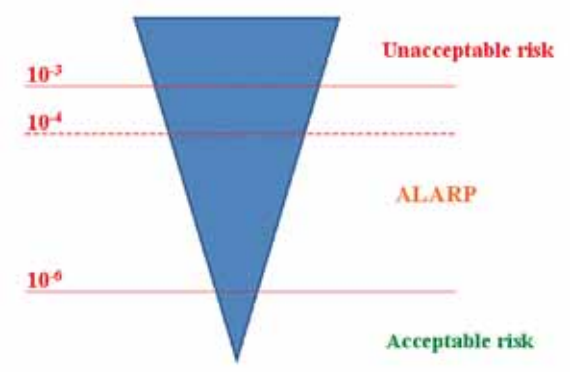

Fig. 1. Individual risk criteria for crew members and passengers on ships

Societal risk criteria are created to limit the risk from ships to whole groups of people containing crew members, passengers, and even local communities, which may be affected by ship

activities. According to [5] these criteria are used to limit the risks of catastrophes affecting many people at the same time. The criteria are given in the form of FN diagrams. F - means an annual frequency of N or more fatalities, N - means a number of fatalities. The diagrams are divided into three areas of risk: intolerable risk, ALARP, negligible risk. The examples of such risk criteria are given in Fig. 2.

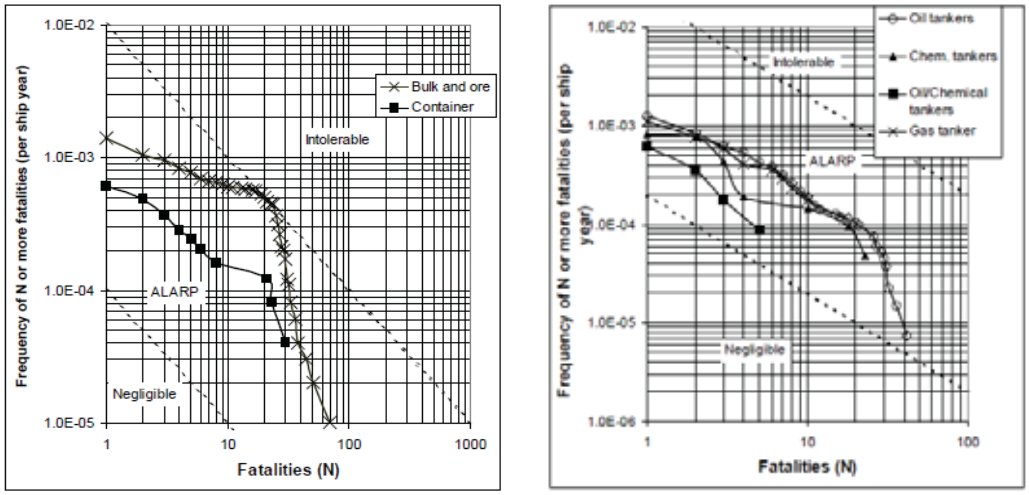

Fig. 2. FN curves for bulk carriers, container vessels and tankers shown together with risk evaluation curves [5]

As we can see above the historical data gives us FN curves for most examined ships in the ALARP region. More about the individual and societal risk criteria for ships one can find in [4, 5].

3. Set of risk criteria proposed for sea-going vessels

All the above presented risk criteria are related only to the loss of life. In this section the author's proposals of risk criteria for ships are presented. The graphical form of the criteria (three in one) is shown in Fig. 3.

Those criteria relate to health and life of human beings and also to losses of an economical and ecological nature. They were built using principles of risk assessment for the inland industrial plants, extensively described in [3]. The criteria are similar to those proposed on the forum of the International Maritime Organization and developed for the case of loss of human life. The similarity arises from the fact that IMO decision-makers also relied on procedures developed for land based installations.

To create a risk criterion is necessary to build a risk matrix. The risk matrix should contain the frequency of hazardous events per year and the potential consequences of the dangerous incident. In addition both of them (frequency and consequences) should be quantified. In the first step the quantification was made with the use of linguistic values. The frequency of hazardous events was identified by the following values: very often, often, quite often, occasionally, seldom, very seldom, almost never. The potential consequences of hazardous events are defined as follows: catastrophic, significant, moderate, small, minor.

The next, very difficult but also very important step is to convert the linguistic values into numerical values. It was decided, that the frequencies of hazardous events will be convert into numerical values in accordance with the rules described in [3]. The frequencies of hazardous events per year in accordance with these guidelines are:

- very often frequency of occurrence more than 10^{-1} per year,

- often — frequency of occurrence from 10^{-1} to 10^{-2} per year,
- quite often — frequency of occurrence from 10^{-2} to 10^{-3} per year,
- occasionally — frequency of occurrence from 10^{-3} to 10^{-4} per year,
- seldom — frequency of occurrence from 10^{-4} to 10^{-5} per year,
- very seldom — frequency of occurrence from 10^{-5} to 10^{-6} per year,
- almost never — frequency of occurrence less than 10^{-6} per year.

Determination of numerical values of the potential consequences of hazardous events is very debatable. A certain amount of financial losses for one ship owner may be a little fraction of his income. For another ship owner it can be very significant. That is why categories of losses should be developed with taking into account the individual situation of the owner of the ship, the type of the ship, the value of the cargo, the navigation area, etc.

It doesn't mean that's impossible to propose universal risk criteria. Such an attempt was made in this study. The three categories of losses were taken into account: loss of human life, financial losses and ecological losses.

The biggest problem, of course, is a reasonable scaling of the size of losses. The taxonomy of the losses is presented below with the explanation why such numerical values were established. It is worth noting, that in the risk analysis we use quite often order of magnitude rather than precise numbers to express the value of losses.

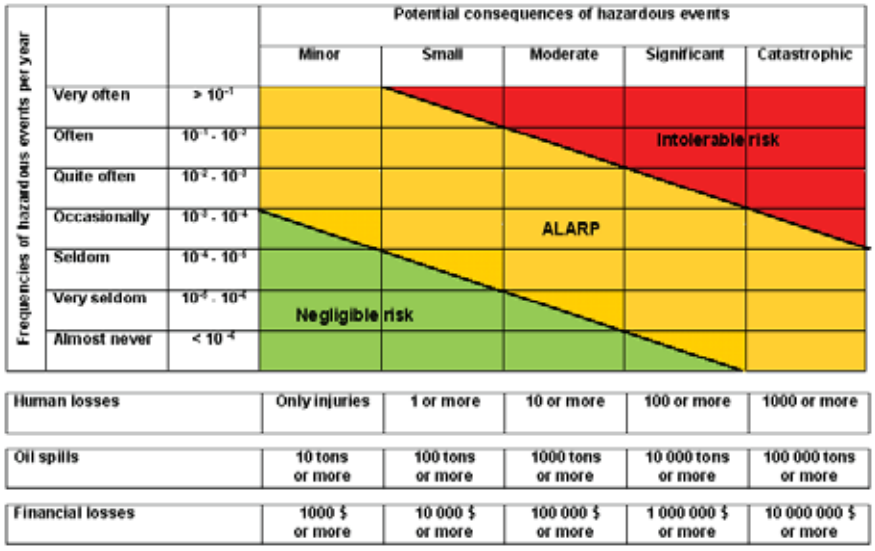

Fig. 3. The proposal of set of risk criteria for sea-going vessel

Human losses. The greatest number of people, even a few thousand (for example 4000 people) can stay aboard a luxury cruise ship. So as the result of accident at sea, in the most pessimistic scenario, may lose life several thousand people. Therefore the scale of fatalities will start from thousands of victims and will be vary by an order of magnitude. The scale will be than as follows: thousands of victims, hundreds of victims, tens of victims, individual victims, only injuries.

Financial losses. As the basis of financial losses it was taken the cost of purchasing of a typical vessel. The most expensive cargo ships cost is tens of millions of dollars (luxury passenger cruiser costs even hundred millions of dollars). So the scale of financial losses will be like this: tens of millions of dollars, millions of dollars, hundreds of thousands of dollars, tens of thousands of dollars, thousands of dollars. Of course in the event of total loss of the ship, the financial loss will be higher than the current value of the ship (value of the cargo, compensation payment etc.).

Ecological losses. Environmental losses depend on the type of vessel and the cargo. It is therefore hard to offer a universal measure of potential damage in the environment. So, as the example, the environmental risk measure for crude oil tankers has been proposed, in the form of the potential size of the oil spill. The largest tankers operated nowadays in the sea are able to carry hundreds of thousands of tons of cargo onboard one vessel. Such volume was taken then as the upper limit of oil spill.

4. Risk criteria arising from the operation of the main engines' crankshaft – connecting rod – piston systems

First of all let's try to determine a participation of the failure events of crankshaft – connecting rod – piston systems as the causes of accidents at sea. Because it was impossible to collect statistical data, by the author, directly showing the participation of such systems as the causes of accidents - an attempt was made to estimate the value according the indirect data.

In the article [6] the principal causes of ship accidents are as follows: deck officer error 26 %, crew error 17 %, shore error 9 %, pilot error 5 %, eng. officer error 2 %, structural failure 9 %, equipment failure 9 %, mechanical failure 5 %, under investigation 6 %, other 12 %.

According to this report the unreliability of mechanical systems is the cause of 5 % of all marine accidents.

Looking at the research results published in [7] we can find out, that the average number of the loss of propulsion event by the container vessel, equipped with direct propulsion system (no reduction gear), is m = 2.5 times per year with a standard deviation $\sigma = 1.1325$ times per year. The same research team has established and published in [7] the share of main participants in the loss of propulsion event probability: fuel oil subsystem $p_1 = 0.1330$; sea water cooling subsystem $p_2 = 0.0437$; low temperature fresh water cooling subsystem $p_3 = 0.0395$; high temperature fresh water cooling subsystem $p_4 = 0.0620$; starting air subsystem $p_5 = 0.0853$; lubrication oil subsystem $p_5 = 0.0687$; cylinder lubrication oil subsystem $p_6 = 0.0446$; electrical subsystem $p_7 = 0.1876$; main engine $p_8 = 0.1987$; remote control subsystem $p_9 = 0.1122$; propeller and shaft line $p_{10} = 0.0247$.

The above results show, that for the direct propulsion system, the main engine's failure share is approximately 20 % in the all causes of loss of propulsion.

Marine diesel engine component failure distribution is given in Fig.4.

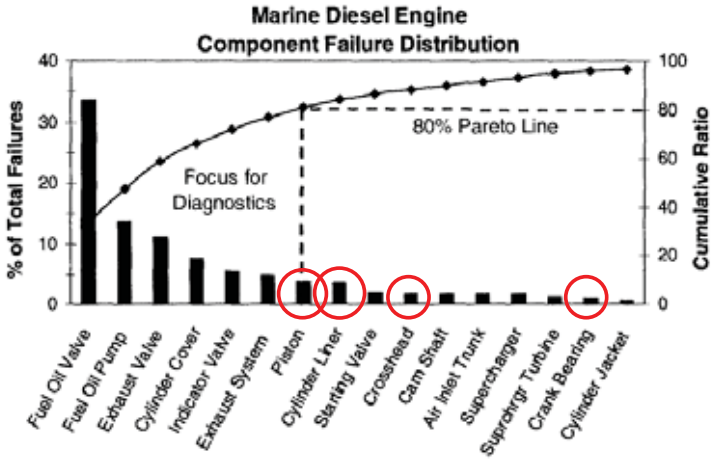

Fig. 4. Marine diesel engine component failure distribution [8]

Components like: piston, cylinder liner, crosshead, crank bearing together are responsible for about 15 % of the main engine failure events.

Based on all the data given above, the share of the main engines 'crankshaft – connecting rod – piston systems as maritime accidents causes can be estimated like this: mechanical failure as the cause of accident 5 %, main engine as the cause of loss of propulsion by ship 20 %, selected components of the main engine as the cause of engine failure 15 %.
So, finally the share is $0.05 \cdot 0.20 \cdot 0.15 = 0.0015 = 0.15$ %.

Failures of the main engines' crankshaft – connecting rod – piston systems, assuming the correctness of the above considerations, have a small part in maritime accidents. However we shouldn't ignore them, because in each case they generate high costs connected with the repair of the engine and exclusion the ship from the operation.

The risk criterion for ships arising from operation of the main engines 'crankshaft – connecting rod – piston systems can be build with the help of the criteria given at Fig. 2. The goal is to not overstep the limits of frequencies of hazardous events involving a ship per year. As we can see the limits are 10^{-3} per year between negligible risk area and ALARP region and more then 10^{-1} per year between ALARP region and intolerable risk area.

Assuming that the considered elements of the main engine are responsible for 0.15 % of the marine accidents, the risk criteria for them should take the following form:
If the frequency of hazardous events for a ship caused by the elements per one year period of time:

- is lower or equal to $0.0015 \cdot 10^{-3}$ then the risk is negligible;
- is between $0.0015 \cdot 10^{-3}$ and $0.0015 \cdot 10^{-1}$ then we should make a risk analysis according to ALARP principle;
- is higher than $0.0015 \cdot 10^{-1}$ then the risk is intolerable.

Safety is a value itself. The need to take care of safety doesn't require justification. In order to improve the safety we can't ignore components of the main propulsion engines. Efforts should be made to improve their reliability in the future to a higher level than today and do not allow to reduce their quality. So, it is worthy to think about creating the relevant requirements of reliability of such elements. But the requirements need to be realistic.

Therefore, as the starting point of reliability level should be taken the mean time to failure of engine components, achieved by the leading manufacturers on the market today. The mean time to failure should be increased in the future. The proposal of reliability requirements for the future components is given in Fig. 5.

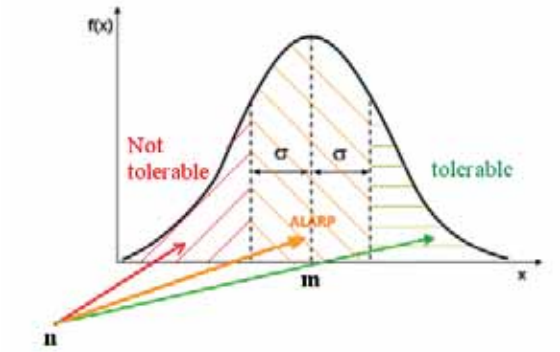

Fig. 5. Proposal of reliability requirements for the future main engines' components

m – the mean time to failure of component used today,
σ – standard deviation of the mean time to failure of component used today,
n – mean time to failure of component to be used in the future,

Following the example of ALARP risk criterion, the proposition of the author is: do not use in the future components with the mean time to failure shorter then $m - \sigma$; for components with the mean time to failure between $m - \sigma$ and $m + \sigma$ try to rise the reliability level, if it is economically justified; for components with the mean time to failure longer then $m + \sigma$ assume that their reliability is sufficient and doesn't require any action to improve it.

5. Final remarks

The considerations made above show, that the share of the main engines' crankshaft – connecting rod – piston systems as a cause of maritime accidents is relatively low. It is worthy to note, that not all of their failures ends with the disaster in the sea. But each serious failure of those elements generates very serious economical costs.

The "safety culture" requires that everyone in his own sphere of responsibility is obligated to take care for safety. Need to take care for safety is not negotiable. Fact that other factors (especially human factor) have a greater impact on the level of risk doesn't relieve the engine manufacturers and designers of ship power plants from responsibility for the safety of maritime transportation.

The aim is to minimize all risk factors. Effective risk management requires appropriate risk measures, procedures for determining the risk and risk criteria. That is why in the article a set of risk criteria, taking into account risk of loss of life, economical risk, and ecological risk has been proposed by the author.

However, the subject has not been closed. Conducted considerations may serve as the basis for further discussion.

References

[1] Brandowski A., *Nauka o bezpieczeństwie*. Warszawa, 1993.

[2] IMO, *Amendments to the guidelines for formal safety assessment (FSA) for use in the IMO rule – making process*. (MSC/Circ.1023 - MEPC/Circ.392). MSC-MEPC.2/Circ.5. October 2006.

[3] Borysiewicz M., Markowski A., *Kryteria akceptowalności ryzyka poważnych awarii przemysłowych.* Warszawa, 2002.

[4] Trbojevic V.M., *Risk criteria in EU*.

[5] Skjong R., *Risk Acceptance Criteria: Current proposal and IMO position*. Valencia. Spain, June 2002.

[6] Guedes Soares C. Teixeira A.P., *Risk assessment in maritime transportation*. Elsevier. Reliability Engineering and System Safety 74. 2001.

[7] Brandowski A., *Estimation of the probability of propulsion loss by a seagoing ship based on expert opinions*. Polish Maritime Research 1(59) 2009 Vol 16.

[8] Jeffrey Banks, Jason Hines, Mitchell Lebold, Robert Campbell, Colin Begg and Carl Byington., *Failure modes and predictive diagnostics considerations for diesel engines.* Defenses Technical Information Center Compilation Part Notice ADP013484.

Journal of Polish CIMAC
Gdansk University of Technology
The Faculty of Ocean Engineering and Ship Technology

EXHAUST EMISSIONS FROM THE PZL SW-4 PUSZCZYK HELICOPTER BASED ON THE MEASUREMENTS OF THE CONCENTRATIONS OF EXHAUST COMPONENTS IN THE EXHAUST GASES DURING A PRE-FLIGHT TEST

Jerzy Merkisz, Jaroslaw Markowski, Jacek Pielecha, Ireneusz Pielecha

Poznan University of Technology, Institute of Internal Combustion Engines and Transport
ul. Piotrowo 3, 60-965 Poznan, Poland
tel.: +48 61 665 2207, fax: +48 61 665 2204
e-mail: {jerzy.merkisz, jaroslaw.markowski, jacek.pielecha,
ireneusz.pielecha}@put.poznan.pl

Abstract

This paper presents the results of the tests on the exhaust emissions from a turboprop engine used for the propulsion of PZL SW-4 Puszczyk helicopter. The tests were conducted in pre-flight conditions. The paper presents the test results and their analysis that enabled the determining of the values of the brake-specific emissions at selected load points. The load values were determined based on the courses of the parameters recorded by an on-board flight recorder during the pre-flight test. The obtained values of the brake-specific emissions as assigned to the engine load conditions were used for the evaluation of the emissions of the helicopter under actual operating conditions. The load conditions of the powertrain were determined based on the analysis of the operating data as obtained from several archival flight records. The analysis enabled an obtainment of the values of the exhaust emissions generated during the actual operating conditions of the helicopter.

Keywords: *emissions, turbine engine, helicopter, pre-flight test*

1. Introduction

The increasing demand for transport tasks dedicated to helicopters is directly translated into growth of the number of such types of aircraft in use. This, in turn, is significant for the condition of the natural environment. The emission of carbon dioxide and particulate matter is still a severe threat and, at the same, time an obstacle in the development of contemporary combustion engines - turboprop engines in particular [1, 2, 4, 5]. The current provisions relating to the effects of the aviation transport upon the environment as introduced by the Environmental Protection Agency and International Civil Aviation Organization mainly relate to noise and exhaust emissions with particular consideration of nitric oxides [3, 6]. They relate to turboprop, turbofan and jet engines and include requirements for apparatuses and stationary testing procedures depending on the operating conditions of an engine [6]. Turboprop engines used in helicopters are classified with respect to all standards, but no limits of exhaust emission are determined. Therefore, an attempt was made to evaluate the exhaust emissions generated by engines of PZL SW-4 Puszczyk helicopter in its actual operating conditions.

2. Methodology

Object of tests

The tests on the exhaust emissions generated by a helicopter turboprop engine were performed on PZL SW-4 Puszczyk (Fig. 1) with its powertrain composed of two turboshaft Rolls-Royce 250-C20R/2 engines (Fig. 2). The exhaust emission tests were performed in real operating conditions of the helicopter during a pre-flight test. PZL SW-4 Puszczyk was fitted with an on-board flight parameter recorder that not only records such parameters as flight velocity and altitude, but also the position angles of the helicopter and the operating parameters of the engines.

Fig. 1. PZL SW-4 Puszczyk helicopter

Fig. 2. Turboshaft Rolls-Royce 250-C20R/2 engines

The basic technical parameters have been shown in Table 1.

Tab. 1. Basic technical parameters of the Rolls-Royce 250-C20R/2 engine

Name	Symbol	Range	Unit of measure
1	2	3	4
Power output	N_e	380	kW
Unit fuel consumption	g_e	0.465	g/kWh
Mass flow rate	G_p	1.7	kg/s
Compression rate	Π	7.9	–
Engine weight	m	78	kg

The exhaust emission tests were preformed in the actual conditions of the helicopter operation during a preflight test. The PZL SW-4 Puszczyk helicopter is fitted with a flight recorder whose purpose is recording airspeed, altitude and helicopter angles as well as the operating parameters of the engines.

Measurements equipment

The exhaust emissions were measured in the actual operating conditions of the helicopter. This approach required installing a system of exhaust gases uptake in the helicopter near its exhaust in such a manner as to make it possible to operate the helicopter (Fig. 3).

Fig. 3. Placement of the exhaust gases probe

A duct feeding the exhaust gas sample to the analyzer was conducted through an open window in the loading space of the helicopter. Semtech-DS portable analyzer manufactured by Sensors was used for the measurement of the concentration of the exhaust components (Fig. 4).

Fig. 4. View of the exhaust emission analyzer

The analyzer enabled a measurement of the concentration of carbon monoxide, hydrocarbons, nitric oxides and carbon dioxide. The exhaust gases were introduced into the analyzer through a measuring probe that maintained the temperature of 191°C and then were filtered out of the particulate matter (only in the case of diesel engines) and the concentration of hydrocarbons was measured through a flame ionization detector. Next, the exhaust was cooled down to the temperature of 4°C and the concentrations of the following were measured respectively NO_x, CO, CO_2 and oxygen [2]. The analyzer measures the concentration of carbon monoxide, hydrocarbons, nitric oxides and carbon dioxide as per the characteristics given in Table 2.

Tab. 2. Characteristics of Semtech DS (a portable exhaust emission analyzer) [6]

Parameter	Measurement method	Accuracy
1	2	3
CO	NDIR, measurement range 0–10%	±3% of the measurement range
HC	FID, measurement range 0–10,000 ppm	±2.5% of the measurement range
NO_x	NDUV, measurement range 0–3000 ppm	±3% of the measurement range
CO_2	NDIR, measurement range 0–20%	±3% of the measurement range
O_2	Electrochemical, measurement range 0–20%	±1% of the measurement range
Exhaust flow rate	Mass flow rate	±2.5% of the measurement range
Exhaust temperature	Up to 700°C	±1% of the measurement range
Warm up time	900 s	
Response time	$T_{90} < 1$ s	

3. Emission tests results and analysis

During the pre-flight test of the helicopter, concentrations of the exhaust components were measured. The results of the measurements of the concentration of CO_2, CO, HC, NO_x were presented as measurement values for several minutes' measurement initiating from the moment before engine startup until several seconds following the stopping of the engines. The test course was additionally recorded by the flight parameter recorder. The obtained courses were compared and, then, used for further analysis of instantaneous values of engine loads (Fig. 5).

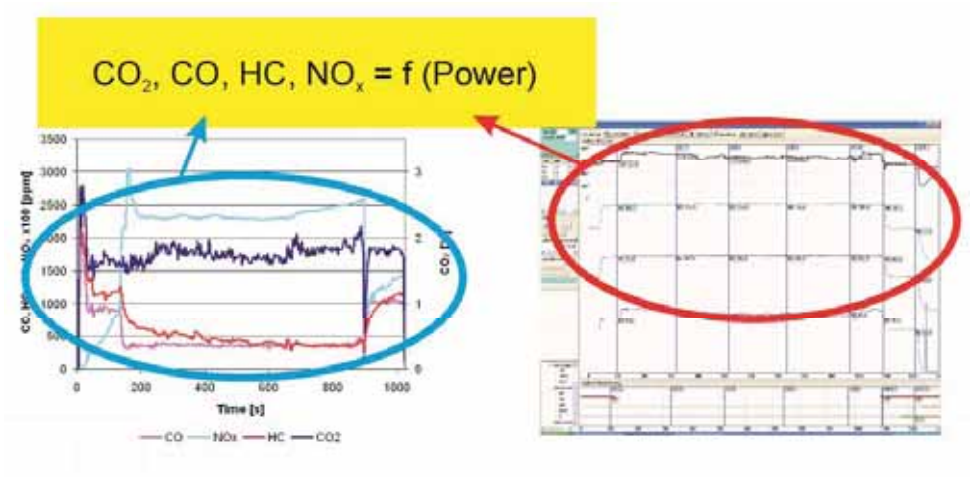

Fig. 5. The compared courses of concentration of individual exhaust components and the course of the operating parameters of engines as recorded by the flight parameter recorder during the pre-flight test of the helicopter

On the basis of the recorded course, engine loads in time were determined. During the pre-flight test engines work under approximately 10% of maximum load for 7% time of the test, under the loads ranging from 60÷65% of the maximum load for approximately 13% of time and under 95 % of maximum load for approximately 80% of the test (Fig. 6).

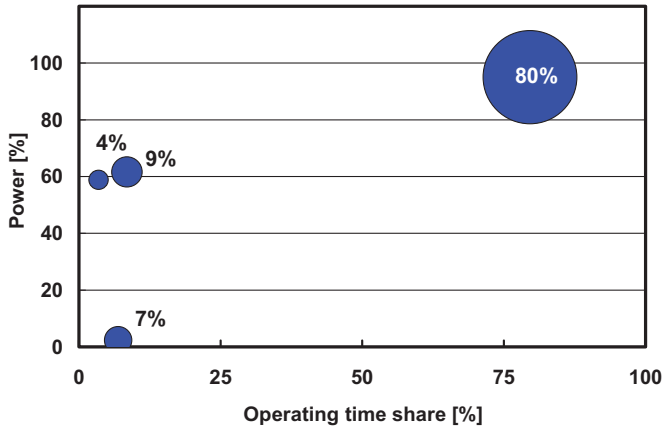

Fig. 6. Test operating time share of the powertrain of the PZL SW-4 Puszczyk helicopter during the preflight test

On the basis of the available flow characteristics of Rolls-Royce 250-C20R/2 engine and the measured instantaneous value of air excess coefficient, exhaust gas rate in individual points of load was measured.

The obtained values of instantaneous exhaust flow rate, multiplied by the measured instantaneous value of the concentration of a given exhaust component yielded the instantaneous emission of the individual exhaust components during the test (Fig. 7–10).

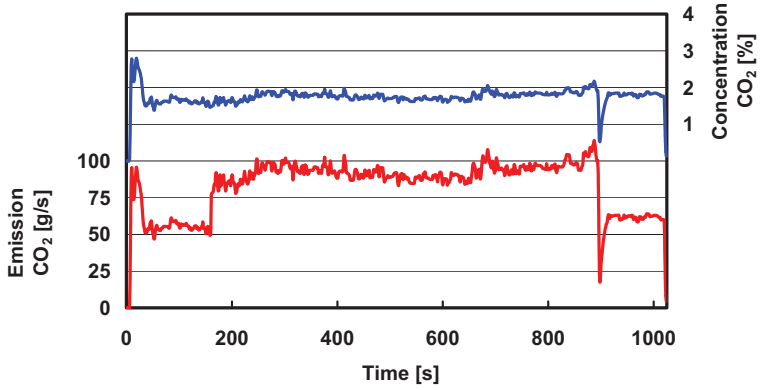

Fig. 7. The course of the instantaneous concentration and emission rate of CO_2 in the exhaust gases during the test

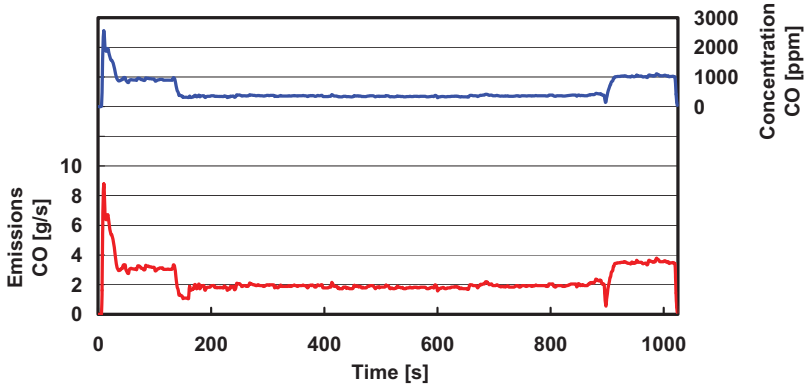

Fig. 8. The course of the instantaneous concentration and emission rate of CO in the exhaust gases during the test

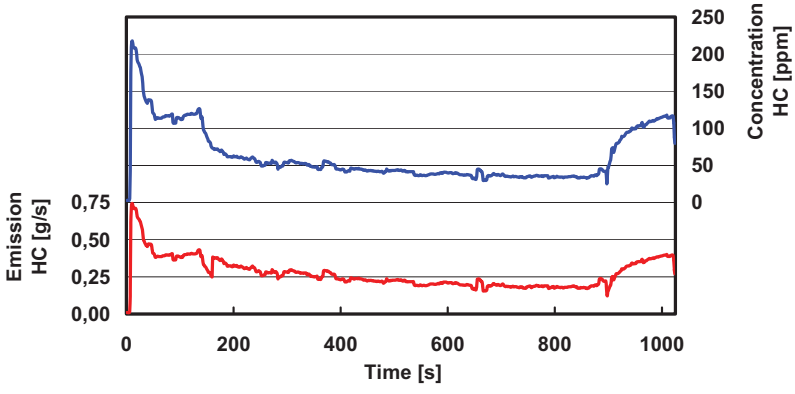

Fig. 9. The course of the instantaneous concentration and emission rate of HC in the exhaust gases during the test

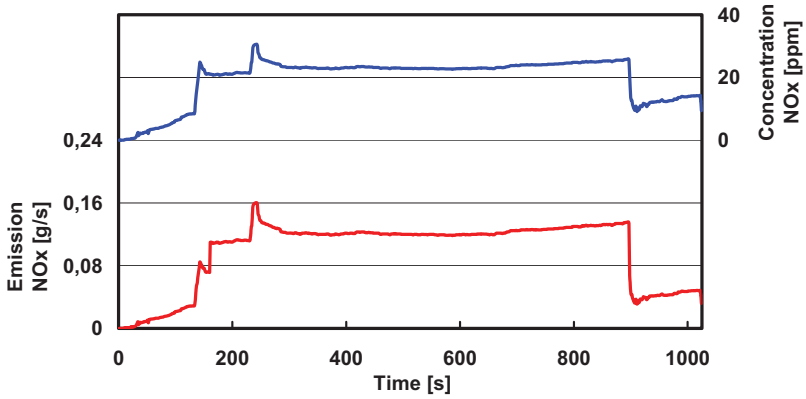

Fig. 10. The course of the instantaneous concentration and emission rate of NO_x in the exhaust gases during the test

The obtained values of the exhaust gas concentration as multiplied by the instantaneous value of concentration of an exhaust component resulted in instantaneous values of emission rate of particular exhaust gas components during the performed test. The obtained courses of instantaneous value of the concentration of the individual exhaust gas components were compared to the instantaneous values of the engine loads recorded by the on-board flight parameter recorder. The comparison resulted in obtaining of values of unit-based emissions of exhaust gas components for individual points of engine loads (Fig. 11). It results from the obtained data that the largest ecological nuisance is the stage of starting up and warming of the engine under small loads. With an increase of load, one may observe a decrease in the values of brake-specific emissions. It is particularly the case in the emission of carbon monoxide and hydrocarbons. The values of unit-based emission of carbon dioxide and nitric oxides change insignificantly for 75÷95% of the maximum engine load.

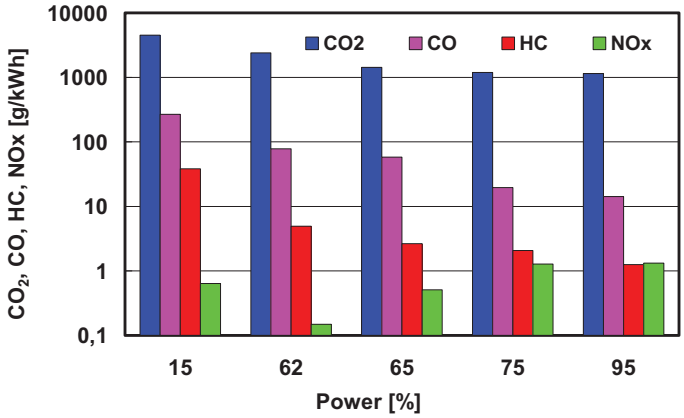

Fig. 11. The values of brake-specific emissions generated by the powertrain of PZL SW-4 Puszczyk helicopter during the pre-flight test and for individual load values

The values of unit-based exhaust emissions as determined for individual engine loads may be multiplied by the percentage share of time of engine load during the pre-flight test performed. This allows obtaining values of unit-based exhaust emissions constituting individual characteristics for a given engine in a given pre-flight test (Fig. 12).

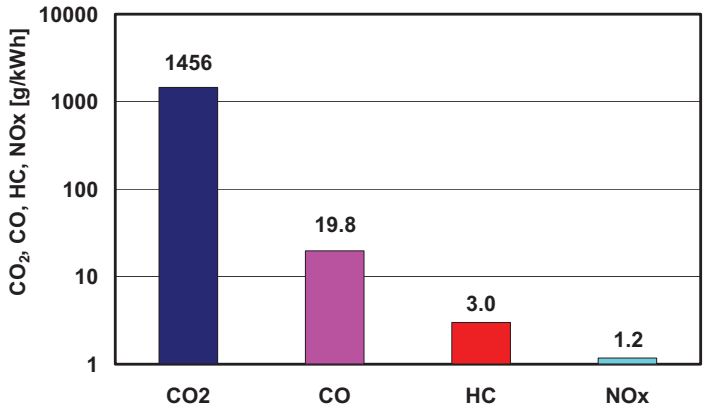

Fig. 12. The values of unit-based exhaust emissions as generated by the powertrain of the helicopter during the pre-flight test

The unit emission of CO_2 was approximately 1456 g/kWh, CO approximately 19.8 g/kWh, HC approximately 3 g/kWh and NO_x approximately 1.2 g/kWh.

4. Conclusions

The conducted exhaust emissions tests from PZL SW-4 Puszczyk during the pre-flight test enabled an obtainment of data on the concentration of exhaust gas components in the exhaust gases of a helicopter turboprop engine. A further analysis of the results as compared to the engine operating parameters provided values of brake-specific emissions generated by the powertrain for individual engine loads. Based on the obtained values, actual exhaust emissions from the powertrain of the helicopter during the pre-flight were determined. The here-discussed evaluation constitutes a part of a larger work aimed at the evaluation of negative impact of operation of transport helicopters upon the natural environment. The work is also connected with the development of a universal test facilitating the determination of exhaust emissions generated by helicopters.

References

[1] Antas, S., *Determination of performance and parameters for turboprop and turboshaft engine for modification through change of gas temperature before turbine*, Combustion Engines, 4/2006, pp. 34-43, Dec. 2006.

[2] Dzierzanowski, P., Kordzinski, Otys, W.J., Szczecinski, S., Wiatrek, R., *Turbinowe silniki smiglowe i smiglowcowe*, Wydawnictwa Komunikacji i Lacznosci, Warszawa 1985.

[3] Kotlarz, W., *Turbine Driving Systems as Pollution Sources at Military Airports*, Air Forces Academy, Dęblin 2004.

[4] Peitsch, D., *Propelling the future – the meaning of Aare VISION 2050 for the future development of propulsion systems for aircraft*, Combustion Engines, 4/2011, pp. 3-13, Dec. 2011.

[5] Merkisz, J., Markowski, J., Pielecha, J., Babiak, M., *Emission Measurements of the AI-14RA Aviation Engine in stationary test and under Real Operating Conditions of PZL-104 'Wilga' Plane*, SAE Paper 2010-01-1563.

[6] *Anex 16 – Environmental Protection, Vol. II – Aircraft Engine Emissions*, ICAO.

Journal of Polish CIMAC
Gdansk University of Technology
The Faculty of Ocean Engineering and Ship Technology

APPLICATION OF SEMI-MARKOV'S PROCESS FOR CONTROL OF AVAILABILITY OF EXECUTIVE SUBSYSTEM WITH A THRESHOLD STRUCTURE

Klaudiusz Migawa

University of Technology and Life Sciences
Prof. S. Kaliskiego Street 7, 85-789 Bydgoszcz, Poland
tel.: +48 52 340 84 24
e-mail: klaudiusz.migawa@utp.edu.pl

Abstract

The article presents the method for control of availability of executive subsystem with the threshold structure, consisting of elementary subsystems of the type <driver-vehicle>. The whole of the consideration was presented using the example of a chosen authentic system of the operation and maintenance of transport means. The basic objective of the operation of transport systems is fulfilling the transportation needs as a result of the carrying out of transport on particular routes. The effectiveness of the operation of transport system depends on the possibility of correct carrying out of the assigned transport task. Among many significant criteria used for assessment of a transport system operation there is one of special importance, that is availability of the executive subsystem to perform the assigned tasks. Availability of the executive system to perform the assigned tasks depends on availability of particular technical objects (transport means) used in the system of transportation and their number. The presented method consists of determining and comparison of the values of the required and actual availability of the executive subsystem. The article deals with the way of determining the required availability of an individual technical object (means of transport) as well as the required number of technical objects used in the system, in order for the obtained value of the availability of the executive subsystem to exceed the value of the required availability determined by the parameters of transport task. The availability of the individual technical object was defined on the basis of a constructed mathematical model of operation and maintenance process realized in the tested transport system. Exemplary results have been presented on the basis of experimental data, obtained from the tests carried out in a real operation and maintenance system of transport means.

Keywords: *transport system, availability, operation and maintenance process, threshold structure*

1. Introduction

In general, the transport system consists of two main subsystems: logistics and executive. In the logistics subsystem, the processes carried out are supposed to assure task-based efficiency of the used technical objects. The goal of the executive subsystem is to perform the assigned transport tasks over set routes, with a given frequency, according to a set schedule. A proper accomplishment of the transport task is possible only if the required number of technical objects (transport means) is prepared to perform the assigned task in a given time.

The effectiveness of the operation of transport system depends on the possibility of correct carrying out of the assigned transport task. In the executive subsystem, the direct carrying out of the transport task is performed by elementary subsystems such as operator – means of transport, linked by an appropriate structure. One of the factors strongly influencing the possibility of correct

carrying out of the transport task is the availability of the executive subsystem to carry out the task. The executive subsystem availability for the carrying out of the assigned transport task depends on many factors, such as:

- availability of the technical objects (means of transport) used in the system,
- number of technical objects used in the system,
- the structure with which the technical objects are linked,
- reliability and receptivity to servicing and repair of technical objects used in the system,
- availability and efficiency of the logistics subsystem.

On the basis of the above statement, it can be said that control of the executive subsystem availability can be carried out both by selecting technical objects with the required availability and matching the required number of the objects which are to be used in the system in order to ensure proper accomplishment of the transport tasks.

In this work there has been discussed a method for determination of the required availability of a single object as well as the required number of technical objects indispensable to perform appropriately the assigned transport task, on the basis of the transportation system availability assessment. The method consists of determining and comparison of the values of the required and actual availability of the executive subsystem for the carrying out of the assigned transport task and choosing the required availability of technical objects and the required number of objects used in a transport system, so that obtained value of actual availability of the executive subsystem is higher than the value of required availability, determined by the parameters of the transport task. The value of actual availability of the executive subsystem is defined for a given availability of a single technical object as well as a given structure which links the individual technical objects. The actual availability of the technical objects (transport means) was defined based on a mathematically built model of the operation and maintenance process carried out in the tested transport system.

2. The method for control of availability of executive subsystem with a threshold structure

In order to assure the correct realization of the assigned transport task it is necessary for the value of the availability of the executive subsystem G^{PW} to be at least equal to the value of required availability G_w^{PW} :

$$G^{PW} \geq G_w^{PW} . \tag{1}$$

In the tested transport system the individual technical objects (means of transport) are coupled the threshold structure of the k_w of N type, where k_w marks the required number of technical objects available for the carrying out of the assigned transport task, while N the number of all technical objects used in the system. Then the availability of the executive subsystem with a threshold structures marked by the formula [2, 6]:

$$G^{PW} = \sum_{i=k_w}^{N} \binom{N}{i} \cdot \left(G^{OT}\right)^i \cdot \left(1 - G^{OT}\right)^{N-i} . \tag{2}$$

Taking into consideration the fact that the required minimum number of objects available for the particular transport task is constant $k_w = const.$, the availability of the executive subsystem G^{PW} depends on the number N of technical objects used in the system as well as the availability of a single technical object G^{OT} .

Availability of a single technical object defined on the basis of the semi-Markovian model of operation and maintenance process is determined as the sum of limit probabilities p_i^* of remaining at states S_i of proces $X(t)$, belonging to the availability states set S_G [2, 5]:

$$G^{OT} = \sum_i p_i^*, \quad dla \quad S_i \in S_G \,. \tag{3}$$

The required availability of the executive subsystem for the realization of the assigned transport task is determined depending on the required minimum number of available technical objects k_w, defined in the description of the assigned transport task as well as the number of all technical objects used in the transport system N, according to the following formula:

$$G_w^{PW} = \frac{T_w^{PW}}{T_w^{PW} + U_w^{PW}} = \frac{k_w \cdot \tau_z}{k_w \cdot \tau_z + n_w \cdot \tau_z} = \frac{k_w}{N}, \tag{4}$$

where for the given assigned transport task:

T_w^{PW} – required time of availability of the executive subsystem,
U_w^{PW} – required time of non-availability time of the executive subsystem,
k_w – the required minimum number of available technical objects,
n_w – the required maximum number of non-available technical objects,
N – the number of all technical objects used in the transport system,
τ_z – required time for the realization of the assigned transport task.

In the presented method the evaluation of executive subsystem, is done on the basis of the comparison of its value and the value of the required availability which the executive subsystem should have for the assigned task to be carried out correctly. Then for the evaluation of the availability of the executive subsystem for the realization of the assigned task the following criteria were adopted:

– facilitating the definition of the required number of technical objects used in the transport system N_w for a given value of the availability of a single technical object G^{OT} :

$$N = N_w \Leftrightarrow \sum_{i=k_w}^{N} \binom{N}{i} \cdot \left[G^{OT}\right]^i \cdot \left[1 - G^{OT}\right]^{N-i} \geq \frac{k_w}{N}, \tag{5}$$

– facilitating the definition of a required value of availability of a single technical object G_w^{OT} for a given number of technical objects used in the transport system N:

$$G^{OT} = G_w^{OT} \Leftrightarrow \sum_{i=k_w}^{N} \binom{N}{i} \cdot \left[G^{OT}\right]^i \cdot \left[1 - G^{OT}\right]^{N-i} \geq \frac{k_w}{N}. \tag{6}$$

3. Semi-Markovian model operation and maintenance process of transport means

In result of carried out analysis of assumptions and restrictions, semi-Markov's process $X(t)$ was assumed to be the model operation and maintenance process of technical objects. Using semi-

Markov's process for the operation and maintenance process mathematical modeling, the following assumptions have been accepted:

- semi-Markov's process $X(t)$ reflects the modeled real process properly enough from the point of view of the tests,
- the modeled process of operation and maintenance has a finite number of states S_i, i=1,2,….,16,
- random process $X(t)$ which is a mathematical model of operation and maintenance process is a homogenous process,
- in time t=0 the process is in state S_1 (S_1 is the initial state).

The model of operation and maintenance process was created on the basis of the analysis of state space as well as operational events pertaining to technical objects (municipal buses) used in the analyzed real transport system. Due to the identification of the analyzed transport system and the multi-state process of technical object operation utilized in it, crucial operation states of the process as well as possible transfers between the defined states were designated. Based on this, a graph was created, depicting the changes of operation and maintenance process states, shown in Fig. 1.

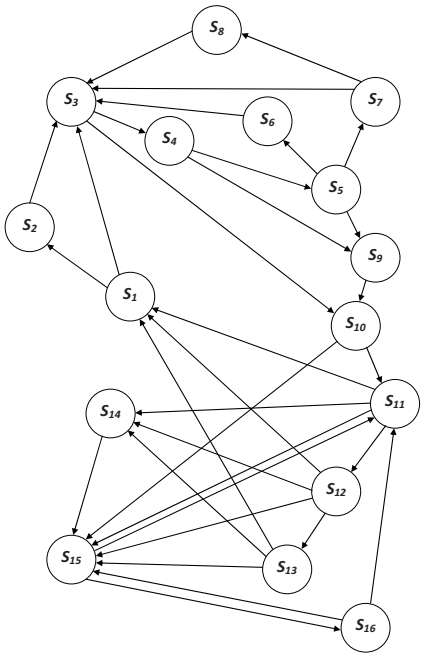

Fig. 1. Directed graph representing the operation and maintenance process of transport means S_1 – awaiting the carrying out of the task at the bus depot parking space, S_2 – repair at the bus depot parking space without losing a ride, S_3 – carrying out of the transport task, S_4 – waiting for the decision of the traffic controller after occurrence of the vehicle damage, S_5 – diagnosing by the emergency service unit, S_6 – repair by technical support unit without losing a ride, S_7 – repair by the emergency service with losing a ride, S_8 – awaiting the start of task realization after technical support repair, S_9 – emergency exit, S_{10} – waiting for action of the maintenance subsystem, S_{11} – refueling, S_{12} – maintenance check on the operation day, S_{13} – realization of periodical servicing, S_{14} – prior to repair diagnosing in the serviceability assurance subsystem, S_{15} – repair in the serviceability assurance subsystem, S_{16} – diagnosing after the repair in the serviceability assurance subsystem

The homogenous semi-Markovian process is unequivocally defined when initial distribution and its kernel are given [1, 2, 3]. Form our assumptions and based on the directed graph shown in figure 1, the initial distribution $p_i(0)$, i = 1,2,…,16 takes up the following form:

$$p_i(0) = P\{X(0) = i\} = \begin{cases} 1 & when \quad i = 1 \\ & \\ 0 & when \quad i \neq 1 \end{cases}, \tag{7}$$

whereas the kernel of process $Q(t)$ takes up the form:

$$Q(t) = \begin{bmatrix}
0 & Q_{1,2}(t) & Q_{1,3}(t) & 0 & 0 & 0 & 0 & 0 & 0 & 0 & 0 & 0 & 0 & 0 & 0 & 0 \\
0 & 0 & Q_{2,3}(t) & 0 & 0 & 0 & 0 & 0 & 0 & 0 & 0 & 0 & 0 & 0 & 0 & 0 \\
0 & 0 & 0 & Q_{3,4}(t) & 0 & 0 & 0 & 0 & 0 & Q_{3,10}(t) & 0 & 0 & 0 & 0 & 0 & 0 \\
0 & 0 & 0 & 0 & Q_{4,5}(t) & 0 & 0 & 0 & Q_{4,9}(t) & 0 & 0 & 0 & 0 & 0 & 0 & 0 \\
0 & 0 & 0 & 0 & 0 & Q_{5,6}(t) & Q_{5,7}(t) & 0 & Q_{5,9}(t) & 0 & 0 & 0 & 0 & 0 & 0 & 0 \\
0 & 0 & Q_{6,3}(t) & 0 & 0 & 0 & 0 & 0 & 0 & 0 & 0 & 0 & 0 & 0 & 0 & 0 \\
0 & 0 & Q_{7,3}(t) & 0 & 0 & 0 & 0 & Q_{7,8}(t) & 0 & 0 & 0 & 0 & 0 & 0 & 0 & 0 \\
0 & 0 & Q_{8,3}(t) & 0 & 0 & 0 & 0 & 0 & 0 & 0 & 0 & 0 & 0 & 0 & 0 & 0 \\
0 & 0 & 0 & 0 & 0 & 0 & 0 & 0 & 0 & Q_{9,10}(t) & 0 & 0 & 0 & 0 & 0 & 0 \\
0 & 0 & 0 & 0 & 0 & 0 & 0 & 0 & 0 & 0 & Q_{10,11}(t) & 0 & 0 & 0 & Q_{10,15}(t) & 0 \\
Q_{11,1}(t) & 0 & 0 & 0 & 0 & 0 & 0 & 0 & 0 & 0 & 0 & Q_{11,12}(t) & 0 & Q_{11,14}(t) & Q_{11,15}(t) & 0 \\
Q_{12,1}(t) & 0 & 0 & 0 & 0 & 0 & 0 & 0 & 0 & 0 & 0 & 0 & Q_{12,13}(t) & Q_{12,14}(t) & Q_{12,15}(t) & 0 \\
Q_{13,1}(t) & 0 & 0 & 0 & 0 & 0 & 0 & 0 & 0 & 0 & 0 & 0 & 0 & Q_{13,14}(t) & Q_{13,15}(t) & 0 \\
0 & 0 & 0 & 0 & 0 & 0 & 0 & 0 & 0 & 0 & 0 & 0 & 0 & 0 & Q_{14,15}(t) & 0 \\
0 & 0 & 0 & 0 & 0 & 0 & 0 & 0 & 0 & 0 & Q_{15,11}(t) & 0 & 0 & 0 & 0 & Q_{15,16}(t) \\
0 & 0 & 0 & 0 & 0 & 0 & 0 & 0 & 0 & 0 & Q_{16,11}(t) & 0 & 0 & 0 & Q_{16,15}(t) & 0
\end{bmatrix}, \tag{8}$$

where:

$$Q_{ij}(t) = P\{X(\tau_{n+1}) = j, \tau_{n+1} - \tau_n \leq t | X(\tau_n) = i\}, \quad i, j = 1,2,...,16, \tag{9}$$

means that the state of semi-Markovian process and the period of its duration depends solely on the previous state, and does not depend on earlier states and periods of their duration, where τ_1, τ_2, ..., τ_n, are arbitrary moments in time, so that $\tau_1 < \tau_2 < ... < \tau_n$, as well as

$$Q_{ij}(t) = p_{ij} \cdot F_{ij}(t), \tag{10}$$

where:

p_{ij} – means that the conditional probability of transfer from state S_i to state S_j, as well as

$$F_{ij}(t) = P\{\tau_{n+1} - \tau_n \leq t | X(\tau_n) = i, X(\tau_{n+1}) = j\}, \quad i, j = 1,2,...,16, \tag{11}$$

is a distribution function of random variable Θ_{ij} signifying period of duration of state S_i, under the condition that the next state will be state S_j.

Limit probability p_i^* of staying in states of process were assigned on the basis of limit theorem for semi-Markovian processes [2]:

If hidden Markov chain in semi-Markovian process with finite state S set and continuous type kernel contains one class of positive returning states such that for each state $i \in S, f_{ij} = 1$ *and positive expected values* $E(\Theta_i), i \in S$ *are finite, limit probabilities:*

$$p_i^* = \lim_{t\to\infty} p_i(t) = \frac{\pi_i \cdot E(\Theta_i)}{\sum_{i\in S} \pi_i \cdot E(\Theta_i)}, \tag{12}$$

where probabilities $\pi_i, i \in S$ *constitute a stationary distribution of a hidden Markov chain, which fulfills the simultaneous linear equations:*

$$\sum_{i\in S} \pi_i \cdot p_{ij} = \pi_j, \quad j \in S, \quad \sum_{i\in S} \pi_i = 1. \tag{13}$$

4. Results

Based on the source data obtained from operational research carried out in an existing municipal bus transport system, with the use of the MATHEMATICA software, the limit probability p_i^* of staying in states of semi-Markov process were determined. Results are given in Tab. 1.

Tab. 1. Values of probability p_i^* *and border semi-Markov process distribution*

$p_1^* = 0{,}30282$	$p_2^* = 0{,}00042$	$p_3^* = 0{,}54035$	$p_4^* = 0{,}00052$
$p_5^* = 0{,}00204$	$p_6^* = 0{,}00039$	$p_7^* = 0{,}00117$	$p_8^* = 0{,}00085$
$p_9^* = 0{,}00163$	$p_{10}^* = 0{,}09614$	$p_{11}^* = 0{,}00614$	$p_{12}^* = 0{,}00518$
$p_{13}^* = 0{,}00281$	$p_{14}^* = 0{,}00149$	$p_{15}^* = 0{,}03668$	$p_{16}^* = 0{,}00137$

In order to define availability of technical objects (means of transport) based on the semi-Markovian model of operation and maintenance process, the states of the process of technical object should be divided into availability states S_G and non-availability states S_{NG} of the object for the carrying out of the assigned task. The states of availability of the technical objects are such states, when the object, including the operator remains in the operational system, is efficient and supplied, or will be repaired and/or supplied in a period of time shorter than the period of the time reserve assigned for the task. Non-availability states are such states, when the object or the operator remain outside of the operational system (efficient or not) as well as when an inefficient and/or unsupplied object remains within the operational system. In the presented model, the following technical object availability states were enummerated:

state S_1 – awaiting the carrying out of the task at the bus depot parking space,
state S_2 – repair at the bus depot parking space without losing a ride,
state S_3 – carrying out of the transport task,
state S_6 – repair by technical support unit without losing a ride,
state S_8 – awaiting the start of task realization after technical support repair.

Then, the availability of technical objects of the transport system were determined:

$$G^{OT} = p_1^* + p_2^* + p_3^* + p_6^* + p_8^* = 0{,}84483\ . \tag{14}$$

Then for the values of parameters describing assigned to the executive subsystem transport task (k_w = 159), the values of actual availability G^{PW}, required availability of the executive subsystem G_w^{PW} and the graphs $N_w = f(G_w^{PW})$, $N_w = f(G^{OT})$, $G_w^{OT} = f(G_w^{PW})$, $G_w^{OT} = f(N)$ were determined. Results are presented in Fig. 2 to 5.

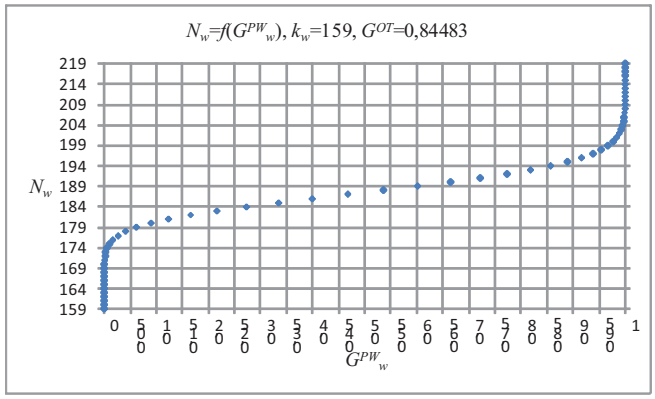

Fig. 2. Required number of the technical objects used in the system of transport N_w in the function of required availability of the executive subsystem $G^{PW}{}_w$, for given value k_w and G^{OT}

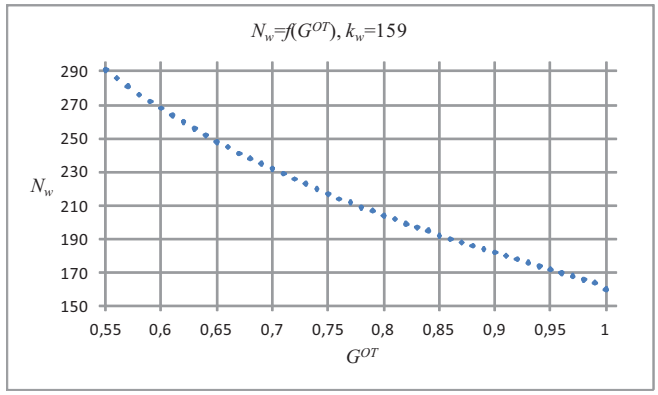

Fig. 3. Required number of the technical objects used in the system of transport N_w in the function of availability of the technical objects G^{OT}, for given value k_w

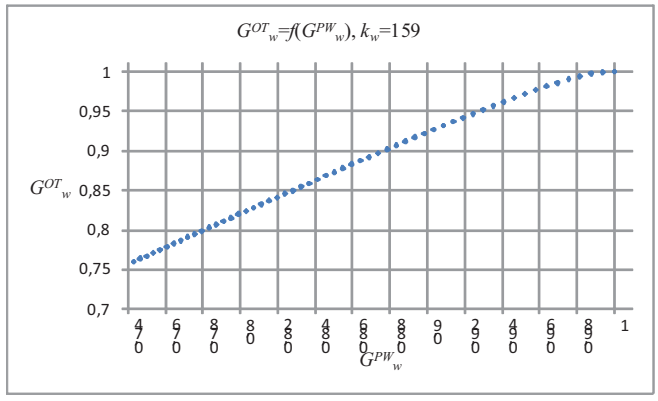

Fig. 4. Required availability of technical object $G^{OT}{}_w$ in the function of required availability of the executive subsystem $G^{PW}{}_w$, for given value k_w

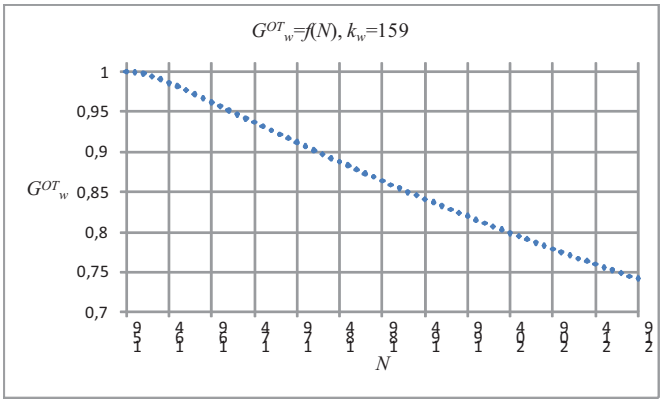

Fig. 5. Required availability of technical object G^{OT}_w in the function of number of the technical objects used in the system of transport N, for given value k_w

5. Conclusions

The presented method enables the selection of the required availability G_w^{OT} and the required number N_w of technical objects coupled the threshold structure so as to ensure proper realization of the tasks assigned to a transport system.

The method can be used both for designing or upgrading the transport system (selection of the required values G_w^{OT} and N_w) and for the assessment and selection of variants for transport tasks that can be implemented (for determined values G^{OT} and N).

On the basis of the graphs drawn, for given number of technical objects, that should to realize the assigned transport tasks, eg k_w = 159, it is possible to determine:

a) required number N_w of technical objects used in the system:
   - depending on the required availability of executive subsystem G_w^{PW} (Fig. 2),
   - depending on the actual availability of technical objects G^{OT} (Fig. 3);

b) required availability G_w^{OT} of technical objects used in the system:
   - depending on the required availability of executive subsystem G_w^{PW} (Fig. 4),
   - depending on the number of all technical objects used in the transport system N (Fig. 5).

References

[1] Grabski, F., *Semi-markowskie modele niezawodności i eksploatacji*, Badania systemowe, Tom 30, Warszawa 2002.

[2] Jaźwiński, J., Grabski, F., *Niektóre problemy modelowania systemów transportowych*, Instytut Technologii Eksploatacji, Warszawa-Radom 2003.

[3] Koroluk, V. S., Turbin, A. F., *Semi-Markov processes and their application*, Naukova Dumka, Kiev 1976.

[4] Kulkarni, V. G., *Modeling and analysis of stochastic systems*, Chapman & Hall, New York 1995.

[5] Migawa, K., *Semi-Markov model of the availability of the means of municipal transport system*, Zagadnienia Eksploatacji Maszyn, 3(159), Vol. 44, Radom 2009.

[6] Praca zbiorowa pod red. J. M., Migdalskiego, *Inżynieria niezawodności. Poradnik*, Wydawnictwo ZETOM, Warszawa 1992.

Journal of Polish CIMAC
Gdansk University of Technology
The Faculty of Ocean Engineering and Ship Technology

INFLUENCE OF GAS CHANNELS OF MEDIUM SPEED MARINE ENGINES ON THE ACCURACY OF DETERMINATION OF DIAGNOSTIC PARAMETERS BASED ON THE INDICATOR DIAGRAMS

Rafał Pawletko, Stanisław Polanowski

Gdynia Maritime Univeristy
ul. Morska 81-87, 81-226 Gdynia, Poland
tel.: +48 586901319
e-mail: pawletko@am.gdynia.pl, stpolanowski@gmail.com

Abstract

Analysis of the indicator diagram is the basis of technical state evaluation of marine diesel engines. The indicator diagram contains a large amount of diagnostic information. A major problem for the diagnostic use of the indicator diagrams in case of medium speed engines are distortion caused by the gas channels between the cylinder and the pressure sensor. Indicator channel and valve may introduce significant distortions which increases with increasing engine speed. The paper presents results of results of the analysis of the indicator diagram of engines in onboard service, and research conducted on the medium speed laboratory engine Al 25/30. These engines are characterized by gas channels of high complexity. During laboratory research pressure measurement (indication) was made by the sensor placed directly in the cylinder (instead of starting air valve), before the indicator valve (with special Kistler adapter) and on the indicator valve. Distortion of heat release characteristics for the sensor placed on the indicator valve is important, but it is estimated that diagnostic information is not erased. For medium speed engines is to be expected the use of a portable pressure sensors placed on the indicator valve. For this reason, further research is needed to assess the impact of channels and valves on different cylinders. During the research the course of heat release rate q and the heat released Q were determined. The curve of heat release rate q is a full equivalent to fuel injection pressure curve in the fuel pipes. It allows identification of the failure of the injection system. The curve of Q allows such determination and assessment of internal efficiency of the cylinder.

Keywords: *marine combustion engines, indicator valve, indicator diagram analysis*

1. Introduction

Medium speed engines are used principally in shipbuilding as generators in a power plant of low speed engines and in power plant with gear drive systems, or as the main source of electrical power in a diesel-electric power plants.

Engine speed for the Wartsilla company smallest power engines (cylinder diameter from 200 mm to 260 mm) is amounts to 1000 rpm. For the other engines of those company the range of speeds is from 750 to 330 rpm for Wartsila 64 engine.

In generating sets from MAN company, because of the lower cylinder bores, speeds range are from 1200 rpm for the smallest diameter cylinders (160 mm) to 500 rpm for the largest diameter of the cylinder (600 mm).

Medium speed marine engines are mostly equipped with indicator valves which are used both for decompression and for cylinder pressure measurement (indication).

Gas channels in the indicator valves and channels which connects the valve to the cylinder causing the delay and distortion of the indicator diagrams, which increase with engine speed. For engines A25/30 and A20/24 ignition angles can range from 3 ° CA to 11 ° CA before TDC and receive variable values depending on the engine load.

Table 1 shows the TDC determination errors calculated on the basis of zero point of first order derivative estimated by extrapolation.

Tab. 1. Examples of values of TDC determination errors $\Delta\alpha_{G1}$ for the selected engine 6A25/30: n = 750 obr/min; engine idling

	Cyl. 1	Cyl. 2	Cyl. 3	Cyl. 4	Cyl. 5	Cyl. 6
$\Delta\alpha_{G1}$ [deg]	-0,85	-1,10	0,00	0,00	-0,80	-0,50

As shown in table 1 TDC determination error exceeded a value of -1 ^{o}CA, which is very high value. Analysis of indicator diagrams of many medium speed engines show similar values of TDC errors.

Several investigations have already been done on problem of indication valve influence on pressure curve. According to the authors of [1, 2] the main source of distortion is the geometry of the indicator valve. The problem is know but in this paper, its impact on the diagnostic usefulness of the pressure signal will be assess.

Difficulties with the TDC position location on the indicator diagrams cause, that only one diagnostic parameter, which is the maximum combustion pressure is considered to be reliable [3, 4, 5]. In addition, this parameter should be related to the average from all cylinders due to the expected high value of the measurement error. In order to determine the level of errors and possible diagnostic use of mean indicated pressure and heat release characteristics, experimental research on the engines were carried out.

2. The object and subject of research

The objective of research was to determine the influence of the indicator channel and indicator valve on the form of cylinder pressure diagram. Research was carried out on the medium speed ship's engine Sulzer Al 25/30 in the laboratory. The tests were made at engine speed 750 rpm. In Sulzer Al engine, gas channel, which connect indicator valve with the combustion chamber, has considerable complexity and length (Fig. 1).

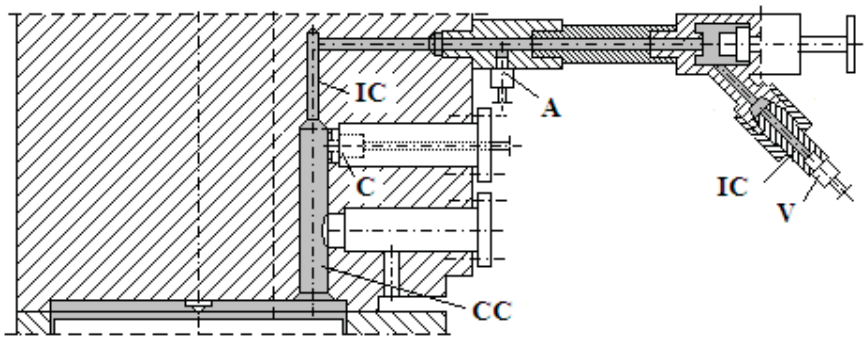

Fig. 1. The design of the gas channel, pressure sensors location of the test engine Al 25/30: CC – cylinder channel, IC - indicator channel, C - pressure sensor location in the cylinder, A - pressure sensor location in the adapter Kistler 7523A10 , V - pressure sensor location on the indicator valve

The measurement sensors Kistler type 6353A24 were used during the test. The measurements were performed for three loads. Pure compression diagram were also registered by cutting-off fuel injection pump on the test cylinder. All measurements were performed for the engine speed 750 rpm.

3. Distortion and delay of pressure graphs

Comparing the indicator diagrams (Fig. 2) the following symptoms of gas channels impact can be observed: delay of pressure diagrams p_A and p_V compared with reference p_C, oscillations and distortions of the pressure curves and higher maximum pressures values p_V and p_A, compared with the maximum values of pressure in the cylinder p_C.

Pressure distortions are particularly well observable on the graphs of pure compression.

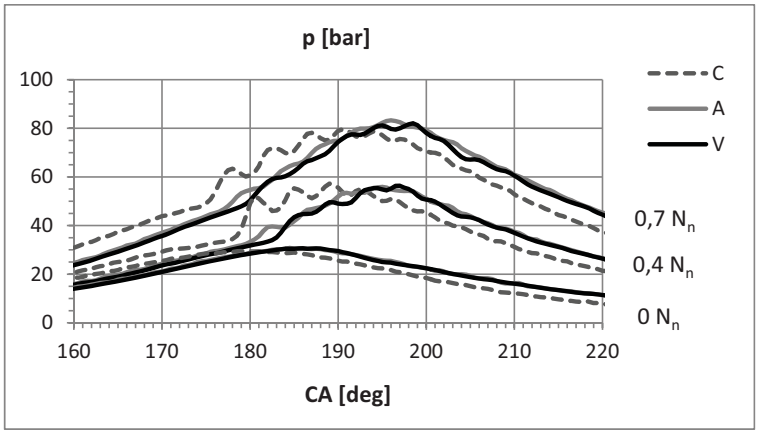

Fig. 2. Comparison of the indicator diagram in the range of the end of the compression and combustion: C - pressure in the cylinder, A – pressure in the adapter, V – pressure after the indicator valve. Coordinate 180°CA (Crank Angle) corresponds to thermodynamic TDC on C pressure curve (in the cylinder)

Especially large distortions visible on the curves are caused by fading standing wave, excited at the moment of ignition in the channel CC (Fig. 1) and spreading to the indicator channel.

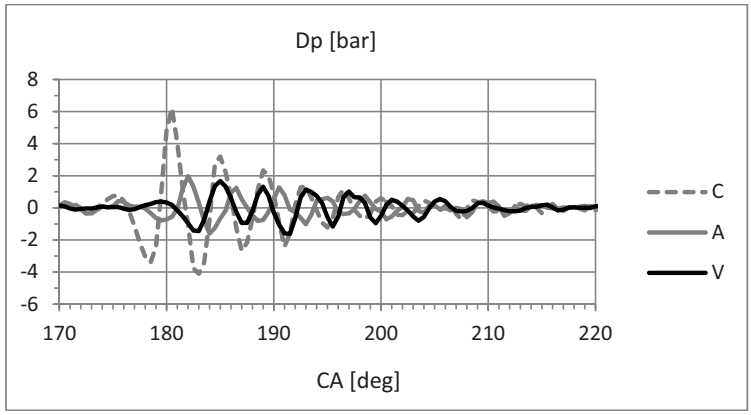

Fig. 3. Dp pressure curves oscillation at the open indicator valve (Fig. 1): C - in the cylinder channel, A - in the adapter, V - on the indicator valve

The initial amplitude of observed waves in the channel CC exceeds 10 bar, which is about 18% of maximum pressure. The period of oscillation is about 4.5 ^{o}CA for engine speed 750 rpm. This wave does not change its form after closing the indicator valve when the space (channel) of indicator valves is cut off (Fig. 4).

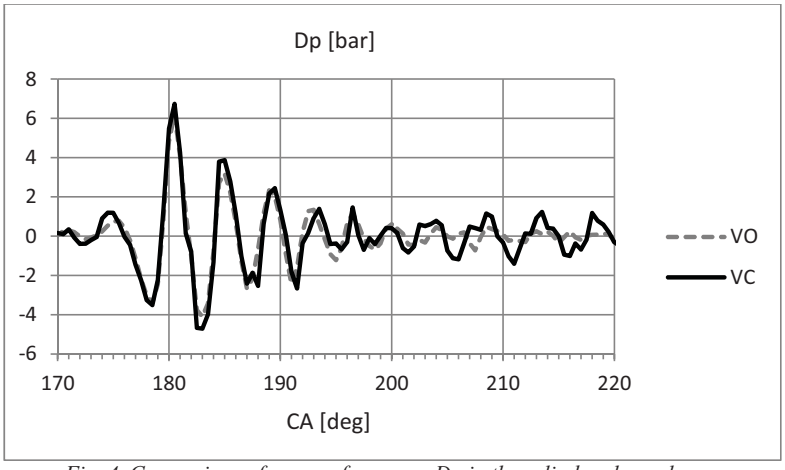

Fig. 4. Comparison of waves of pressure Dp in the cylinder channel: VO – indicator valve open, VC – indicator valve closed

The results confirm the above observation is that the main source of pressure distortion is cylinder channel. If the engine load increases, waving phase changes with respect to TDC, but does not change its frequency. Phase shift is caused by a change of injection start, together with the engine load.

The analysis of indicator diagrams carried out for different type of medium speed engines shows that the wave phenomena for engine cylinders have the similar nature (Fig. 5).

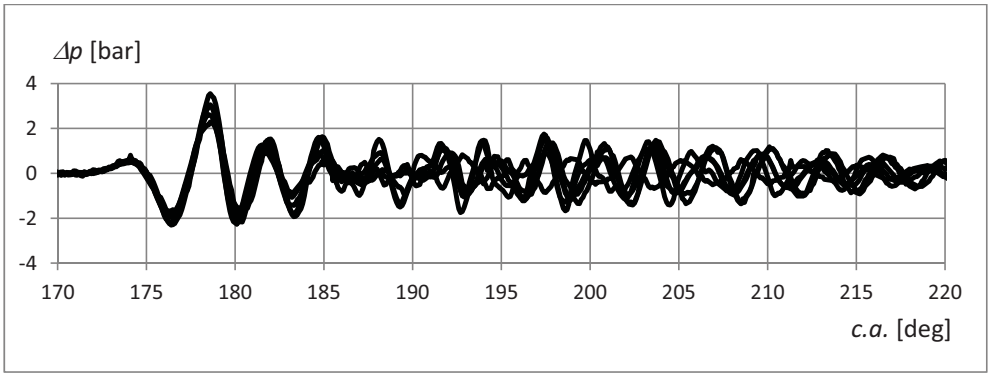

Fig. 5. Comparison of the oscillation of the indicator diagrams of 6A25/30 engine in service: n = 750 rpm, MIP = 13.94 bar

It is expected that indicators diagrams of the same type of engines will be burdened with systematic errors of the same value and the same course, which will enable the diagnostic use of mean indicated pressure and heat release characteristics.

4. Gas channel influence on TDC designation errors, indicated work designation errors and the mean indicated pressure designation errors

The main source of errors of determination of the indicated work and the mean indicated pressure are errors of TDC positioning on the indicator diagram. Sometimes, in order to determine TDC positioning errors, a position of maximum of pure compression are used. The maximum of pure compression can be find with the zero point of the first order derivative of pressure curve.

The study assumed a TDC position as a thermodynamic TDC determined using the original method [4]. The difference between the position of TDC in the cylinder (C), and the position of TDC in the adapter (A) was 6°CA. The difference between the TDC in the cylinder (C) and the position at TDC on the indicator valve was 5.9°CA.

Positions of designated TDC based on the zeros point of the first order derivatives were respectively: 108.4 °CA for the cylinder (C), 179.3 °CA for the adapter (A) and 179.8 °CA for the indicator valve. These are significant values. To determine the mean indicated pressure, indicated work and heat release characteristics, thermodynamic TDC were designated individually for each pressure curve.

Comparison of the indicated work (related to the volume of a cylinder) (Fig. 5) shows their high similarity.

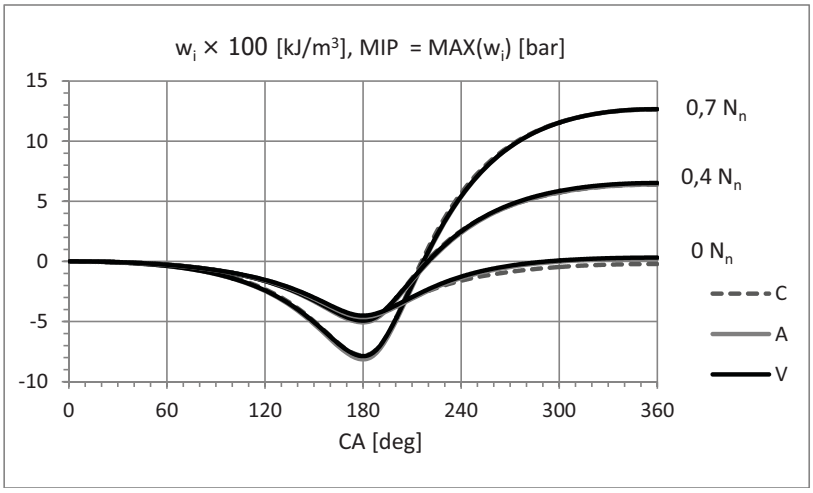

Fig. 5. Comparison of the indicated work curves w_i (referred to the volume of a cylinder), mean indicated pressure MIP for different values of the engine power N_n: C - in a cylinder channel, A - in the adapter channel, V - on the indicator valve

Deviation of the MIP to the value measured in the cylinder (C) did not exceed 0.3% for nominal load (Table 1).

Table 1. Values of mean indicated pressure MIP and their percentage deviations for each of the measurement points, referenced to the values measured in the cylinder (C)

Engine load	MIP [bar]			δMIP [%]	
	C	A	V	AC	VC
0,7 N_n	12,04	12,09	12,08	0,30	0,27
0,4 N_n	6,38	6,39	6,52	0,14	2,08
0 N_n	- 0,22	0,22	0,31		

Very good convergence of results were obtained despite the high similarity level of interference. This follows from the integral nature of the values and the relatively small signal lost following the signal delays and waving.

5. Gas channel influence on net heat release characteristics

Net heat release characteristics were determined based on a simplified model for an ideal gas, based on thermodynamic TDC [4].

First order derivative of pressure curves was determined using a polynomial Savitzkiego-Golay filter for three passages and wide range of different approximations in each passage. The filter were built according to individual original study [5].

Despite considerable noise a good convergence of heat release rate q and heat released Q were obtained (Fig. 6).

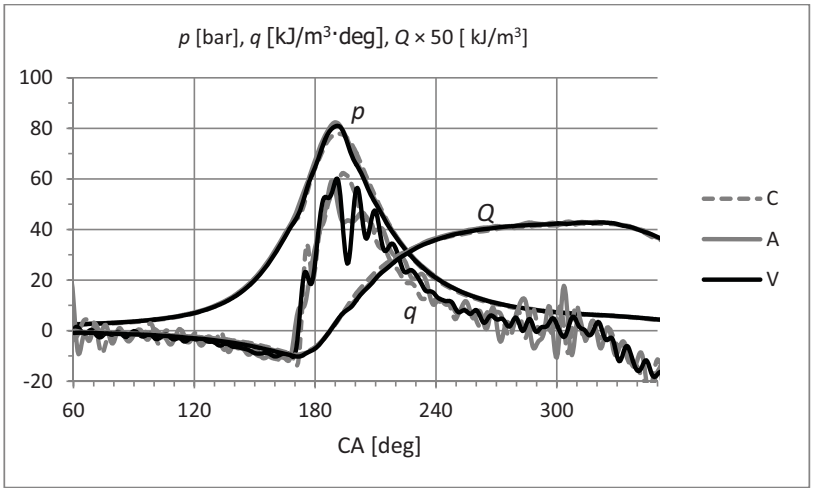

Fig. 6. Comparison of heat release characteristics designate for the set of indicator diagrams for the load 0.7 N_n: q – heat release rate, Q – heat released, C – for the measurement in the cylinder, A – for the measurement in the adapter, V – for measuring on the indicator valve

A similar results were obtained for the other engine loads - the difference between the values of heat released for the various loads are small (Table 2) and have a systematic nature.

Tab. 2. Values of the maximum of heat released Q and their percentage deviations for each of the measurement, referenced to the those specified for the cylinder: C (C)

Engine load	Q ×50 [kJ/m^3]			δQ [%]	
	C	A	V	AC	VC
0,7 N_n	21,16	21,56	21,39	1,88	1,09
0,4 N_n	13,45	13,61	13,59	1,19	1,05
0 N_n	- 0,54	0,12	0,18		

Heat released curves Q are something distorted. Smoothing can be improved by developing a special filter. Further smoothing with applied filter (subsequent transition to wider intervals) lead to excessive phase deformation. It should be noted, however, that the systematic errors of comparable values do not affect the diagnostic usefulness of the signals.

Figure 7 shows the curves δq and δQ designated for marine engine 40DM with advanced wear (before main repair).

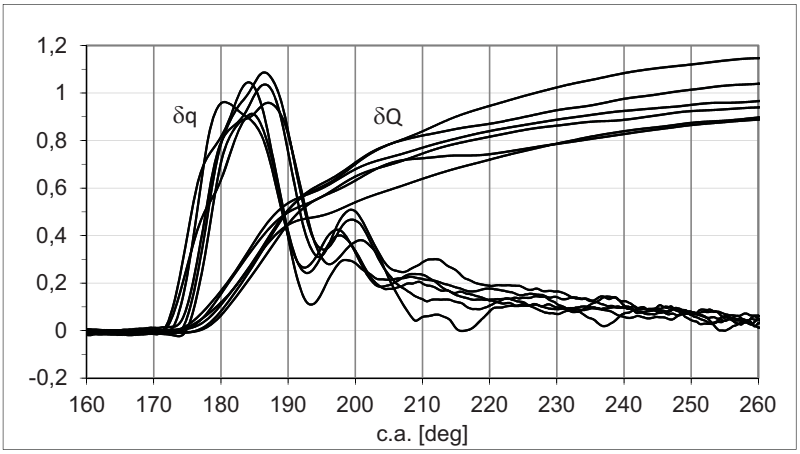

Fig. 7. Dimensionless (related to the average maximum values for the motor) the heat release rate δq and heat released δQ for the medium speed marine engine 40DM working on nominal load (750 rpm)

The presented examination of the heat release characteristics allows the diagnostic inference about condition and quality of control injection equipment, which is practically impossible on the basis of direct comparison of the pressure curves.

The design of gas channel in 40DM engine is different from Al type (straight channel directly from the cylinder), but can easily be seen waving arising to the right from coordinate 190°CA.

In the case of low-speed engines such interference gas channels are not present, or are practically negligible.

Conclusions

Gas channels of medium speed engines bring significant delay and deformation of the indicator diagram. In the case of the test engine, the signal delay on the indicator valve reached 6 °CA at 750 rpm, compared with the measurement in the cylinder channel. In the cylinder channel (C) of test engine fading standing wave is formed with a large amplitude, which distorts the pressure curves on the adapter and on the indicator valve.

Deviation of the mean indicated pressure, maximum of heat release rate and a maximum of heat released does not exceed 2% on the surveyed engine loads.

It is expected that disturbances in the gas channels are systematic and derived characteristics will reproducible and diagnostic useful.

It is not excluded to improve the results of analyzes by increasing the accuracy of the determination of TDC, detecting changes in the characteristics of the measuring channels and the development of improved methods of the disturbed signals processing.

References

[1] Trunen, R., Kaario, O., Liljenfeldt, G., *Cylinder pressure measurement via indicating Cock*, CIMAC 2007.

[2] Oezatay, E., Onder, C., *Model based sensor reconstruction of in-cylinder pressure trace using indicator cock pressure information*, Cimac Congress 2010, Bergen paper no. 166.

[3] Pawletko, R., Polanowski, S., *Influence of TDC determination methods on mean indicated pressure errors in marine diesel engines*, Journal of KONES, Vol. 18, No. 2, Warsaw 2011.
[4] Pawletko, R., Polanowski. S. *Research of the influence of marine diesel engine Sulzer Al 25/30 load on the TDC position on the indication graph,* Journal of Kones Powertrain and Transport, Vol. 17, No. 3, p. 361-368 , Warsaw 2010.
[5] Polanowski, S, *Determination of location of Top Dead Centre and compression ratio value on the basis of ship engine indicator diagram*, Polish Maritime Research № 2(56), 2008, Vol. 15.
[6] Polanowski, S. Pawletko, R., *Application of multiple moving approximation with polynomials in curve smoothing*, Journal of Kones Powertrain and Transport, Vol. 17, No. 2, p. 395-402, Warsaw 2010.

Journal of Polish CIMAC
Gdansk University of Technology
The Faculty of Ocean Engineering and Ship Technology

THE SELECTED CHARACTERISTICS OF FUEL INJECTION IN THE SYSTEMS OF MARINE COMBUSION ENGINE COMMON RAIL TYPE

Leszek Piaseczny, Mirosław Walkowski

Polish Naval Academy
ul. Śmidowicza 69, 81 – 103 Gdynia, Poland
tal. +48 58 6262603
e–mail: piaseczny@ptnss.pl
University of Warmia and Mazury
ul. Oczapowskiego 2, 10-719 Olsztyn, Poland
tel. +48 602833175
e–mail: mwal@interia.eu

Abstract

The injection Systems of Common Rail type are becoming widely used in marine combustion engines. The research and development of these systems aims to multi-criterial optimization of the injection process. The authors of the paper present the results of tests on the fuel supply system of the common-rail marine engine. The study was conducted on a special laboratory stand for nominal, average and minimum engine speed. For the analysis were accepted three variants of fuel supply – a single dose, two-piece dose and three-piece dose. There were presented the received characteristics of injection and discussed their most important aspects.

Keywords: *common rail, fuel injection characteristics, single dose and multi-piece dose*

1. Introduction

The need to obtain the relevant characteristics of the fuel injection process which ensure the desired course of the combustion process resulted in applying the electronic control of fuel injection into the cylinders of combustion engines. There has occurred a rapid development of systems of electronically controlled fuel injection [1 ÷ 9], which also found its place in relation to marine combustion engines. For several years, low-speed (n = 70 ÷ 240 rpm) engines from Wärtsilä RT-flex type and MAN B & W LM-E with electronically controlled fuel injection are used on ships. This last company replaced the fuel injection pump equipped with adjustable overflow valve with the electronically controlled hydraulic cylinder supplying the traditional power injectors. The Wärtsilä Company applied the tank system of Common Rail type by electronically controlling of the injector operation by means of the Wärtsilä Engine Control System – 9500 (WECS-9500), which also controls the operation of exhaust valves and motor starters, pumps operation and lubrication of the cylinders. Input values of the control system are: given and actual engine speed and angular speed of the crankshaft, type of fuel and its maximum dose limited by the setting carried out by the operator.

Medium-speed engines (n = 240 ÷ 1200 rpm) also are being equipped with the fuel injection systems of CR type. Injectors of these engines have electromagnetically controlled needle lift (for the fuel delivery less than 45 mm^3/ms) or traditional – hydraulic controlled.

In the high-speed engines (n = 1200 ÷ 2500 rpm) are used CR systems analogous to those used in the automotive industry. Because of the value of injection pressure and the distribution of the fuel dose into several sections (phases) are used piezo-quartz injectors.

Each of the electronic control system of fuel injection has usually the possibility of controlling both the injection advance angle, fuel dose and the distribution of dose in the injection process – in the time domain (CA). This new quality of fuel supply has been achieved not only by the electronic control system, but also through using new executive elements, such as high-pressure plunger pump, electronically controlled safety valves, hydraulic tank and electronically controlled fuel injectors.

These factors allow to a radical change in the processes of controlling the fuel injection into the cylinders and to development of optimal (e.g. according to the criterion of minimum specific brake fuel consumption or required specific brake emission of nitrogen oxides) conditions of the course of combustion process. It has become an important multi-dimensional characteristics of injection, taking into account ex. pressure in the tank, the distribution of the nominal dose into parts, time interval or crank angle (CA) successive parts of injection, etc.

The research described in [3] found that at the distribution on the pilot injection and main injection the biggest changes of total fuel dose occur at small crank angles between the successive phases of injection and at lower pressures in the tank (Fig. 1).

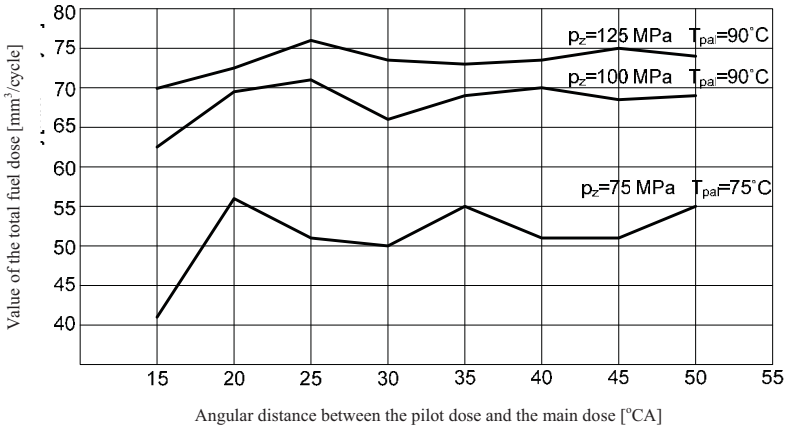

Fig. 1 Influence of distance between the beginning of the pilot dose and the main dose to the total dose at T_w=1 ms T_1=0,5 ms i T_2=0,5 ms; [3]

In these studies was found that the fluctuation of the fuel dose decreases with an increase of its total amount, which can be noticed by comparing Figures 1 and 2.

The pilot injection dose causes the pressure wave in the fuel system, which can not be suppressed before the main injection between too low angular distance between the successive phases of injection. As a result of this phenomenon (despite the continuous time of injection) there are changes in the total value of fuel dose, which course depends on the wavelength at which the injector opens.

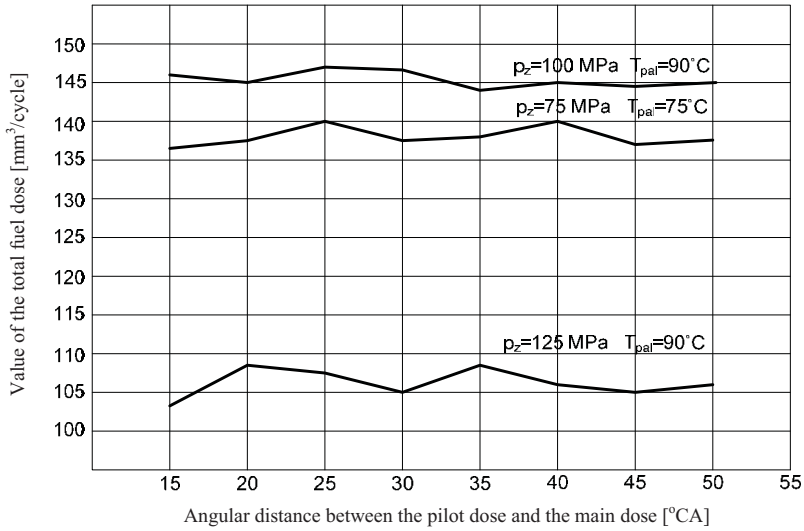

Fig. 2 Influence of distance between the beginning of the pilot dose and the main dose to the total dose at T_w=3 ms T_1=0,5 ms i T_2=2,5 ms; [3]

For small angles CA between the pilot dose and the main dose changes the actual beginning of the injection (Fig. 3). This is due to the fact that at the start of the main injection the needle is still in motion caused by the injection of pilot dose, and changes in pressure above and below the needle cause the advance stroke in relation to a single injection [3].

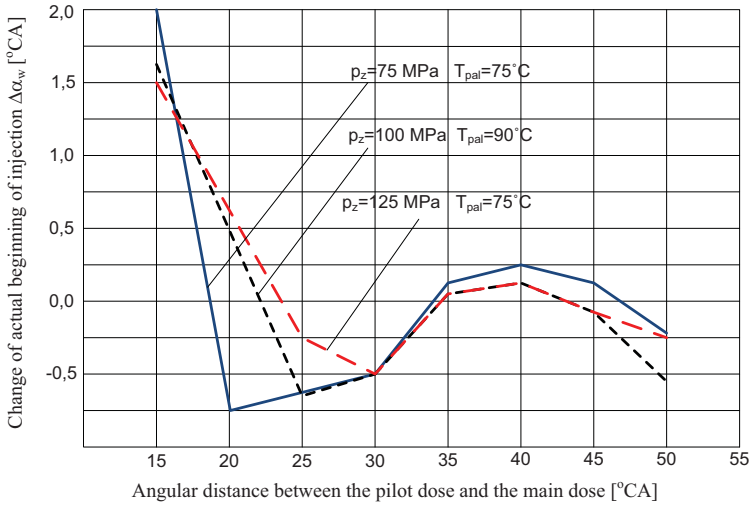

Fig. 3 Influence of distance between the beginning of the pilot dose and the main dose on the change of actual beginning of injection of main dose at n_p = 2000 rpm; [3]

It was established that too low angle between the pilot dose and the main dose is the main reason of reduced accuracy of fuel delivery and change of actual beginning of injection and as a result the energy and environmental indicators of diesel engine operation may deteriorate [3].

The paper [10] described the results of a mathematical model of the process of fuel injection and combustion in classical engine and equipped with a CR system. For this system were assumed

the initial injection pressure p_{ow} = 90 MPa, because after taking into account the course of characteristics of the pressure waveform the maximum injection pressure will be p_{wmax} = 125 MPa. Calculations were carried out for a constant advance angle of main dose injection θ = 15ºCA and constant participation of the pilot dose in the total dose of fuel m_d = 0.6 g / cycle.

Distribution of fuel injection on the pilot dose and the main dose significantly increased the pressure in the cylinder (Fig. 4), which is synonymous with an increase in engine power and decrease of unit fuel consumption.

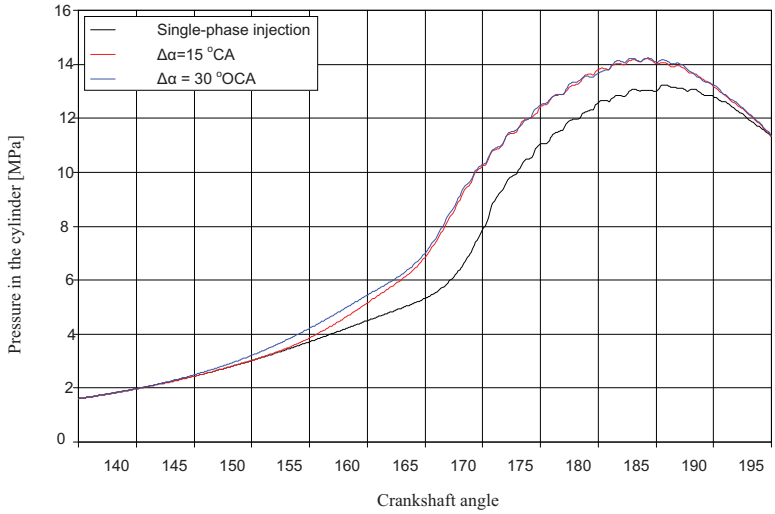

Fig. 4 Pressure waveforms of working medium at various angles between the pilot dose CA and the main dose Δα [10]

a)

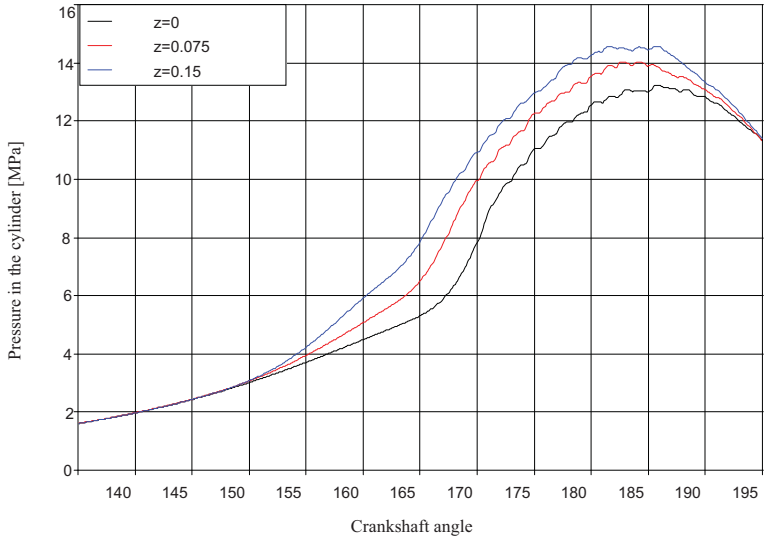

b)

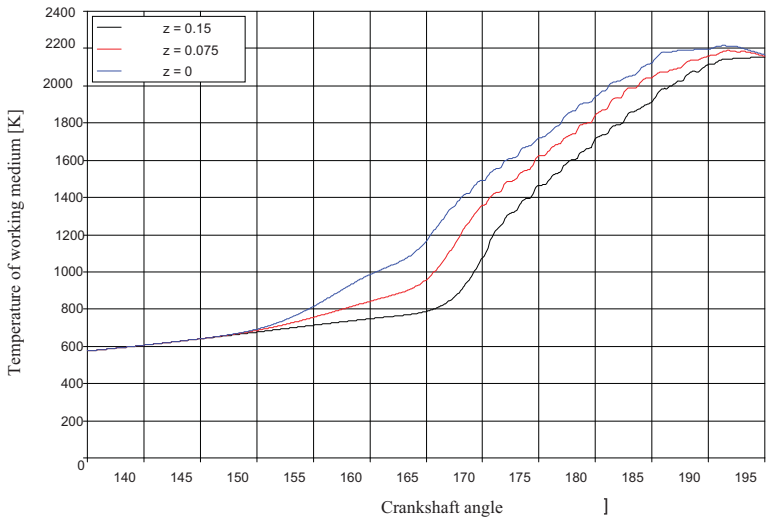

Figure 5 Influence of change of the pilot dose „z" share in the total dose of fuel on the course of: a – pressure; b – temperature of the working medium in the cylinder [10]

On the basis of obtained results of the model, it was found that increase of the pilot dose share increases the maximum pressure and the maximum combustion temperature (Fig. 5). Increasing the share of a pilot dose (as in the case of increasing the angular distance between the phases of injection) resulted in increased level of nitrogen oxides in the exhaust gas (Fig. 6).

From the given examples of the research on injection process in CR systems result that further development of the applying fuels requires knowledge of many of the characteristics of the course of injection process. Such tests are carried out in a number of national and international centers with special stands – fuel dose indicators or directly on the research engines [3,4,10,11].

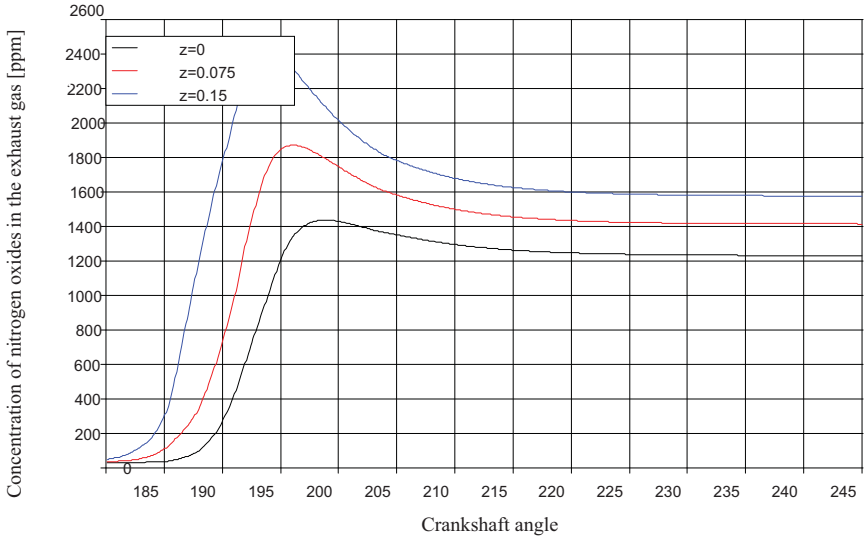

Fig. 6 Impact of changes in the pilot dose share "z" in the total dose on the concentration of nitrogen oxides in the exhaust gas [10]

The authors conducted such tests on the test stand made by a ATH team of Bielsko-Biała. This test stand with fuel dose indicator was made according to the design intent of the authors of the publication, according to the laboratory research of existing AMW dynamometer stand of engine Sulzer 6AL20/24 type.

2. Own research

2.1. Description of the test stand

The test stand, which scheme is shown in Figure 1 differs from the supply system of the engine that instead of the combustion chamber was used the fuel dose indicator. The indicator enables to measure the volume of fuel dose and record wave phenomena associated with fuel supply. The second additional device is controller which enables to program the volume of dose and multiplicity of its distribution, the time of injection and the interval between various stages of injection (design of controller allows the distribution of dose in five parts). The controller also allows the measurement and recording of: fuel pressure in the manifold, engine speed, fuel temperature in different parts of the power supply system, duration of injection angle CA, the volume of a single dose.

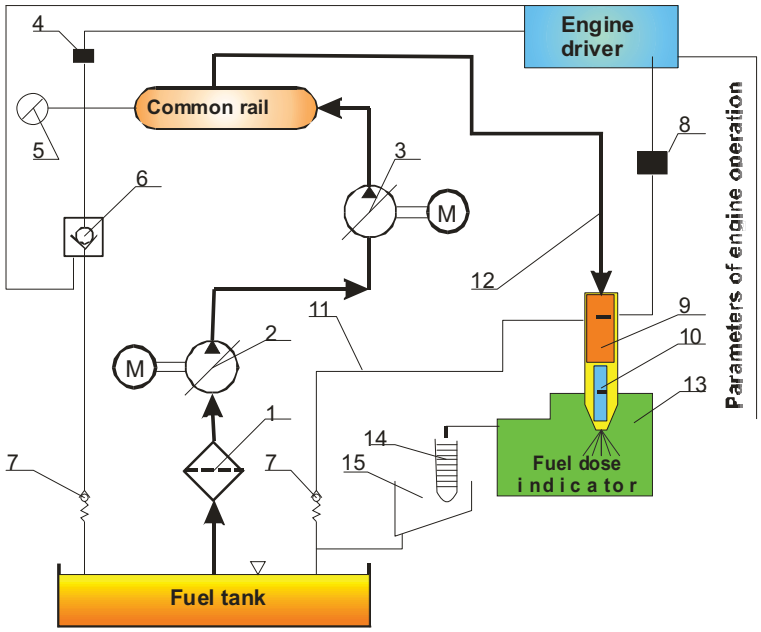

Fig. 7 Scheme of the test stand of electronic control fuel injection process: 1 – filter, 2 – low pressure pump, 3 – high pressure pump, 4 – pressure sensor in the hydraulic accumulator, 5 – pressure gauge, 6 – back-pressure valve with opening control, 7 – overflow valve, 8 – amplifier, 9 – fuel dose controlling valve, 10 – atomizer, 11 – low-pressure fuel pipe (overflow), 12 – high pressure fuel pipe, 13 – fuel dose indicator, 14 – buret to measure the amount of fuel, 15 – cumulative trough

2.2. The program of research

Research on the fuel delivery by injector depending on the distribution of the nominal dose into parts, the hydraulic pressure in the container and the injection time are conducted according to the following schedule:

- tests were carried out at three values of hydraulic pressures in the hydraulic tank having 150, 135 and 120 MPa;
- a single dose of fuel was adequate to the minimum engine speed, average and nominal - that is respectively - 850, 1025 and 1200 rpm;
- each engine speed, which was adopted for the analysis, corresponded to the maximum speed of the fuel injection time equivalent to approximately 25° CA, so for the assumed engine speed it fits in the range 3470 ÷ 4900 s^{-6};
- for the above assumptions were adopted three variants of power supply, the first - the single dose, the second - a two-piece dose in the proportion 1/3 + 2/3 of the nominal dose, and the third - the three-piece dose in the proportion - 0.1 + 0.8 + 0.1 of the nominal dose;
- for the two-piece dose was adopted constant interval of valve overdrive equal to 850 μs, while for the three-piece dose the interval between the pilot dose and the main dose was 700 s^{-6} and between the main dose and the supplementary dose of 600 s^{-6} – due to time constraints resulting from the completion of the full dose at the nominal engine speed.

There was used the electromagnetic injector CR with control valve with mass expenditure of approximately 0.1054 g/cycle. As was shown by preliminary studies, if the time interval between doses is less than 700 μs, the fuel flow through the nozzle needle is not fully closed.

2.3. The results of research

Graphs which is shown in Figure 8 to 16 presents the qualitative relations between basic parameters of the fuel injection in the presented system CR for assumed engine speed, hydraulic pressure in the tank and time intervals for the completion of fuel supply process of considered marine engine.

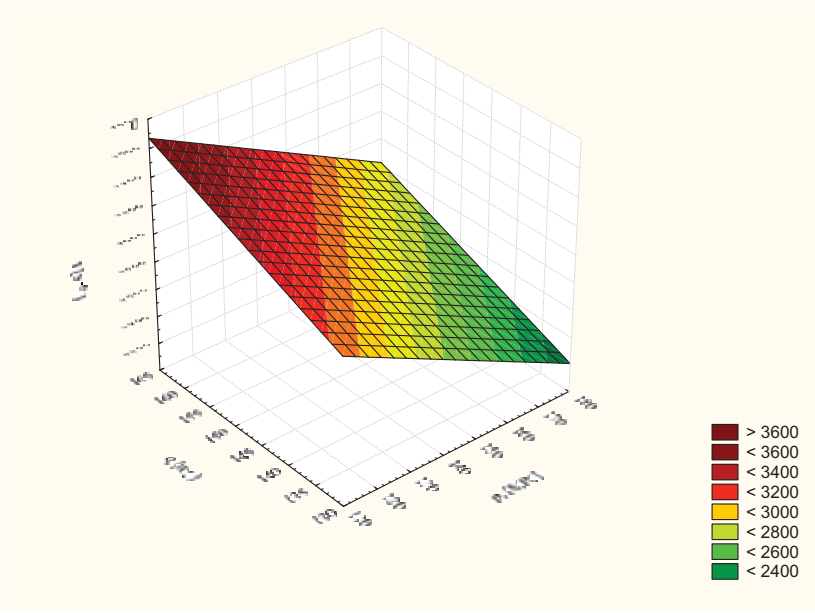

Fig. 8 Dependence of the nominal fuel dose q tank on the hydraulic pressure p_z and the total time of injection t for a single fuel dose

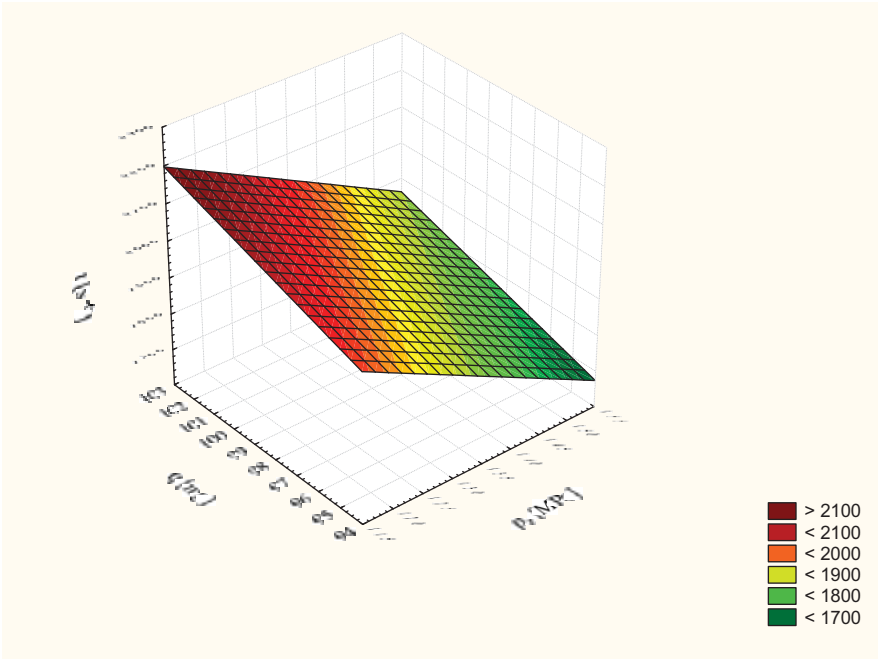

Fig. 9 Dependence of the average fuel dose q on the pressure in the tank hydraulic p_z and the total time of injection t for the a single fuel dose

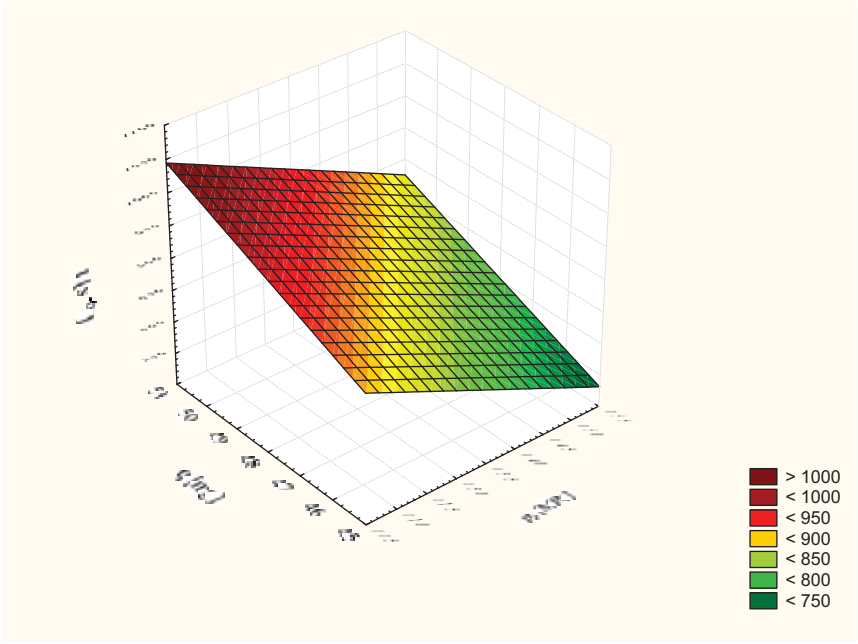

Fig. 10 Dependence of the minimum fuel dose q on the pressure in the hydraulic tank p_z and total time of injection t fuel for a single dose

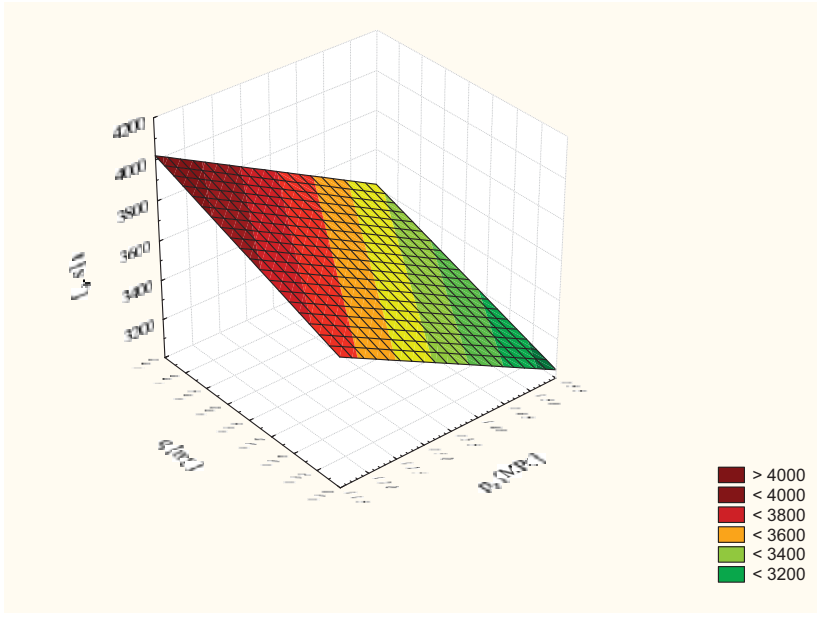

,

Fig. 11 Dependence of the nominal fuel dose q on the pressure in the hydraulic tank p_z and the total time of injection t for the two-piece fuel dose

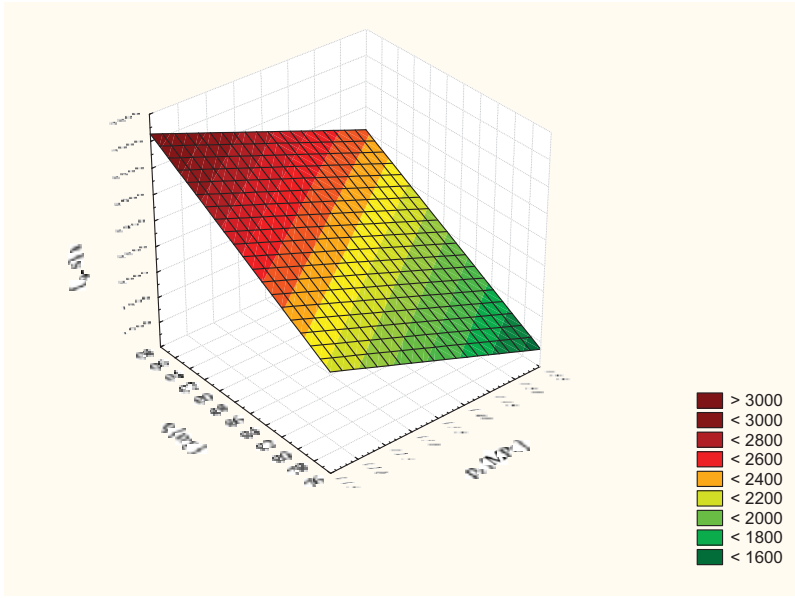

,

Fig. 12 Graph of dependence of the average fuel dose q on the pressure in the hydraulic tank of p_z and the total time of injection t for the two-piece fuel dose

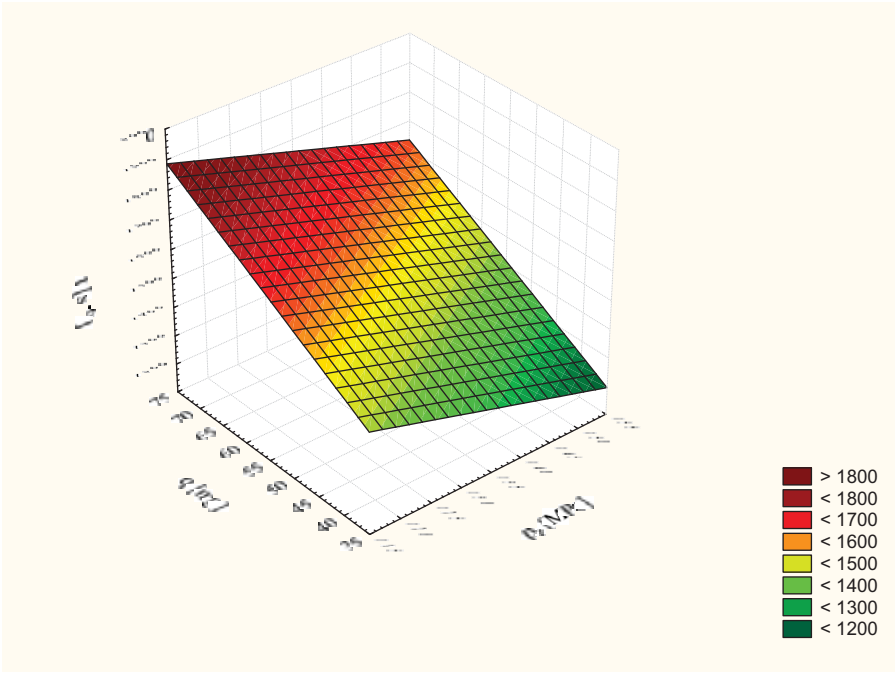

,

Fig. 13 Dependence of the minimum fuel dose q on the pressure in the hydraulic tank p_z and the total time of injection t for the three-piece fuel dose

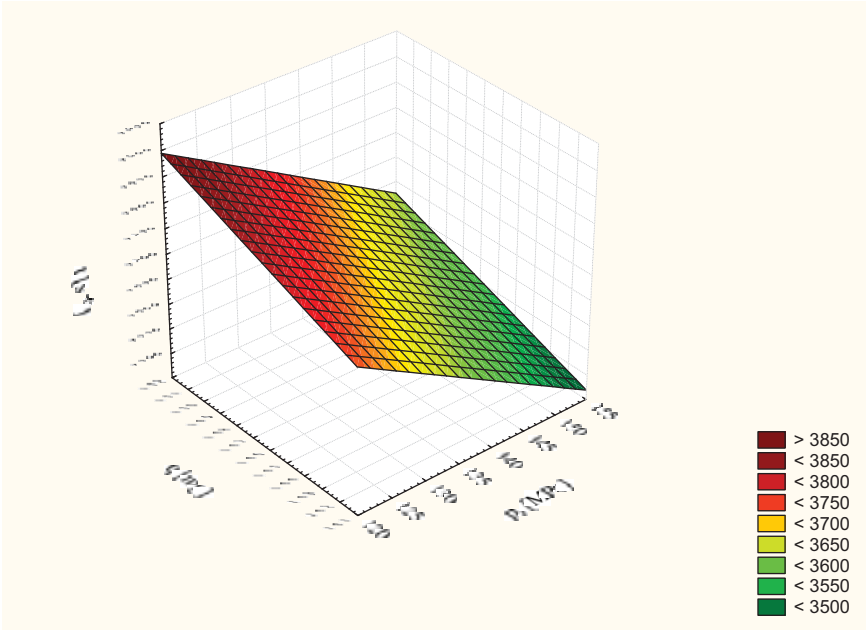

,

Fig. 14 Dependence of the nominal fuel dose q on the pressure in the hydraulic tank p_z and the total time of injection t for the three-piece fuel dose

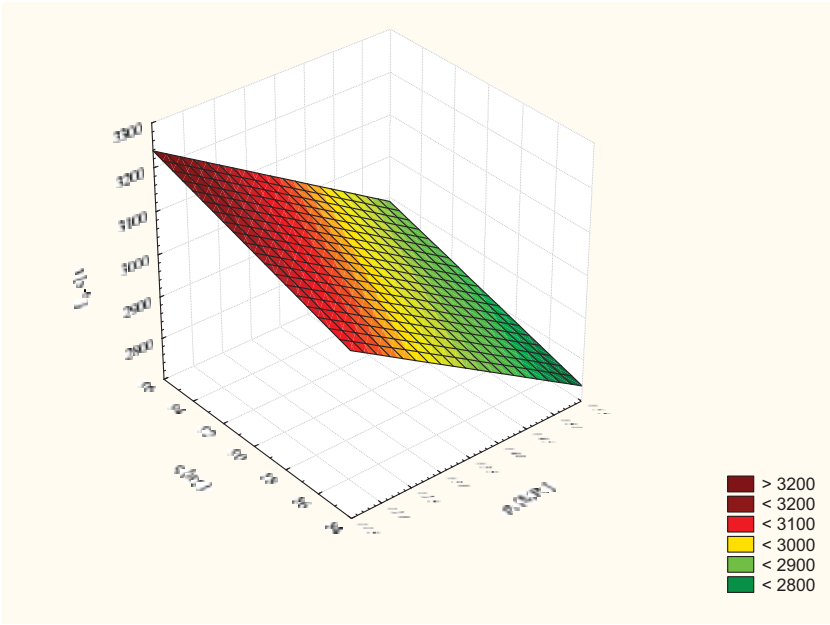

Fig. 15 Dependence of the average fuel dose q on the pressure in the hydraulic tank p_z and the total time of injection t for three-piece fuel dose

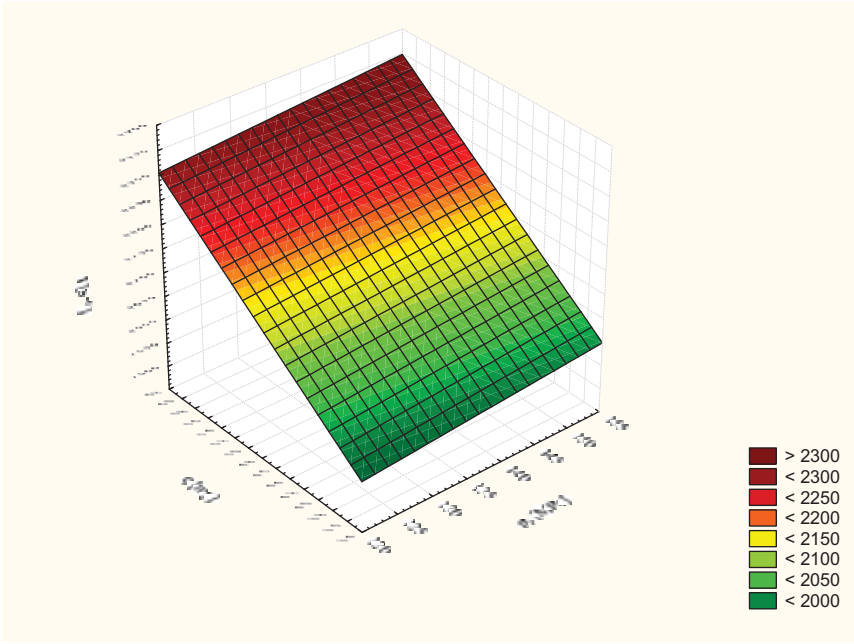

Fig. 16 Graph of dependence of the minimum fuel dose q on the pressure in the hydraulic tank p_z and the total time of injection t for three-piece fuel dose

Figures 17 ÷ 19 shows graphs of sequential basic parameters necessary to ensure the stable operation of the engine at minimum, medium and nominal engine speed. Posted graphs present in a comp manner the relationship of considered parameters.

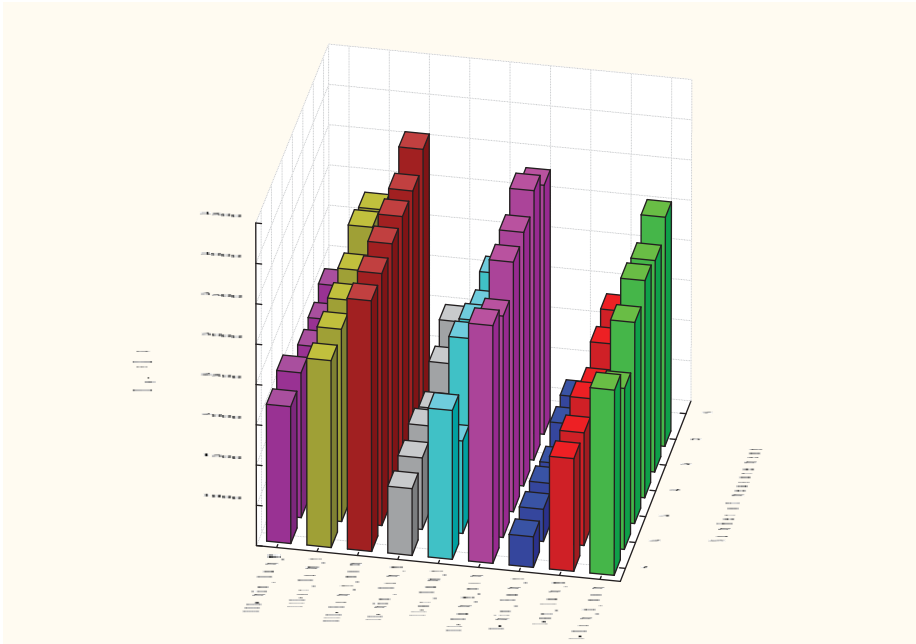

,

Fig. 17 Dependence of multiplicity of fuel dose on the time required for the completion of comparable fuel doses and assumed for research engine speed at different values of pressures in the hydraulic tank p_z (measurement 1,2 – the highest pressure, 3,4 – average pressure, 5,6 – the lowest pressure)

Fig. 17 contains the sequence graph of the total time required to complete the fuel delivery at a nominal dose, medium and minimum speed (eg II-Sum_t_nom – the total time of fuel injection for the two-piece nominal dose, I, II, III – multiplicity of the distribution of fuel dose), adequately one-, two-and three-piece for comparable doses of the three assumed to the research values of pressures in the hydraulic tank. As it can be remarked the time required to carry out the necessary fuel delivery depends both on the pressure in the hydraulic tank and the dosage multiplicity.

Fig. 18 shows the range of volumes of fuel doses for the considered variants of fuel injection (e.g. III-q_min - three-piece fuel dose at minimum engine speed).

Fig. 19 shows the value of pressure in the hydraulic tank for the considered variants of fuel injection (e.g. I-pz_sr - pressure in the hydraulic tank for a single fuel dose and medium engine speed).

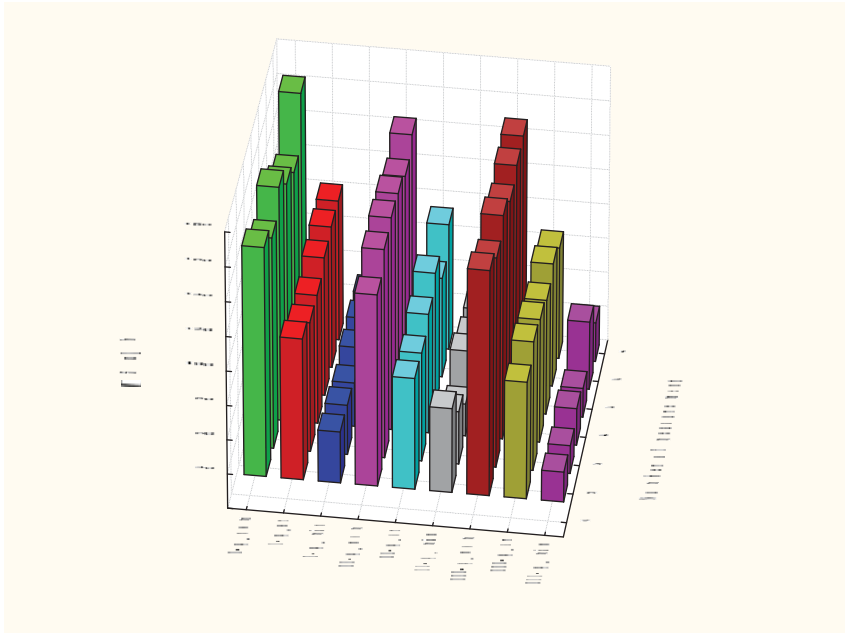

,

Fig. 18 Diversity of fuel delivery q for the considered multiplicity, engine speed (nominal, medium and minimum), and injection at different values of pressure p_z (measurement 1,2 – the highest pressure, 3,4 – average pressure, 5,6 – the lowest pressure)

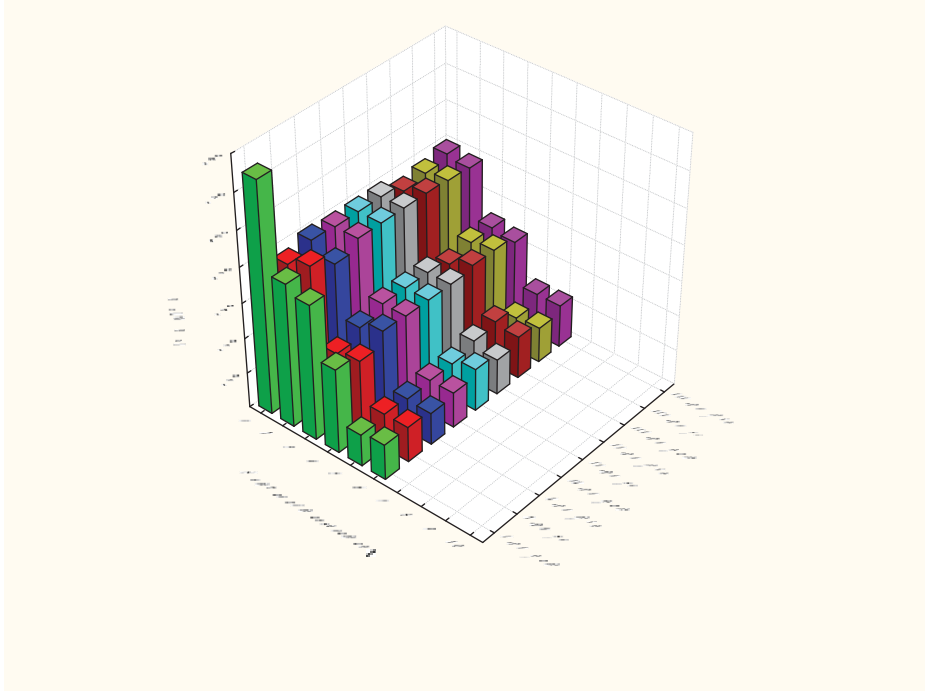

,

Fig.19. Values of pressure in the hydraulic tank p_z for the considered multiplicity of injection and nominal engine speed, average and minimum (measurement 1,2 – the highest pressure, 3,4 – average pressure, 5,6 – the lowest pressure)

5. Summary

Analyzing the obtained results it can be concluded that:

- for the analyzed nominal engine speed for which falls the shortest time to completion the full fuel dose the essential parameter that can be used to select the dose considering its quality is the pressure in the hydraulic tank;
- in case of medium and minimum engine speed there is available the longer time to carry out the necessary dosage of the fuel at adequate CA, and consequently at the same injection ratio, it is possible to control the injection timing;
- the total time for the completion of comparable doses of fuel at the same pressure but different multiplicities of dose distribution was much different;
- selecting multiplicity of the dose at specified pressure in the hydraulic tank it is possible to change the angle of the beginning and end of the fuel injection in dependence to engine load;
- the considerable dispersion of fuel doses: nominal, average and minimum is the result of complex wave phenomena, hydraulic impacts, turbulence, cavitation, etc., which are caused by rapid (about ms) overdrives in control valves, fuel injectors and hydraulic tank.

6. References / Literatura

[1] Sobieszczański M.: Modelowanie procesów zasilania w silnikach spalinowych. Zagadnienia wybrane. WKŁ, Warszawa 2000.

[2] Merkisz J.: Kierunki rozwoju spalinowych zespołów napędowych. Czasopismo Techniczne, Zeszyt 6-M/2004, str. 9 – 32.

[3] Balawender K., Kuszewski H., Lejda K., Ustrzycki A.: Wpływ wielofazowości wtrysku na wybrane parametry systemu zasilania Common rail. Combustion Engines, 2008, No. 4, p. 22 – 28.

[4] Kuszewski H., Lejda K., Ustrzycki A.: Determinanty dokładności dawkowania paliwa w systemie zasobnikowego układu zasilania Common Rail. Czasopismo Techniczne, Zeszyt 8 – M/2008, str. 161 – 172.

[5] Informator Bosch: Zasobnikowe układy wtryskowe Common Rail. WKiŁ, Warszawa 2009.

[6] Janiszewski T., Mavrantzas S.: Elektroniczne układy wtryskowe silników wysokoprężnych. WKiŁ, Warszawa 2009.

[8] Zbierski K.: Układy wtryskowe Common Rail. Oficyna Wydawnicza, Łodź 2001.Krupa A.: Silniki sterowane elektronicznie – zaawansowane wdrożenia. Combustion Engines, 2004, No. 1, p. 20 – 27.

[9] Bocheński C.: Możliwość sterowania procesami termodynamicznymi w silnikach wysokoprężnych przy zastosowaniu akumulatorowego (Common Rail) systemu paliwa. Journal of KONES Internal Combustioon Engines, 2000, str. 38 – 44.

[10] Kafar I., Merkisz J., Piaseczny L.: Model rozpylania paliwa w średnioobrotowym silniku okrętowym i jego badania symulacyjne. Combustion Engines, 2006, No. 3, pp.63 – 76.

[11] Smolarz J., Walkowski M.: The model of steady fuel flow in the injector channels in the Common Rail systems. Scientific Journals. Maritime University of Szczecin. 2009, 17(89) pp. 80 – 86.

Journal of Polish CIMAC
Gdansk University of Technology
The Faculty of Ocean Engineering and Ship Technology

LOW SPEED MARINE DIESEL ENGINE DIAGNOSIS BASED ON PASSIVE EXPERIMENT

Stanisław Polanowski, Rafał Pawletko

Gdynia Maritime Univeristy
ul. Morska 81-87, 81-226 Gdynia, Poland
tel.: +48 586901319
e-mail: stpolanowski@gmail.com, pawletko@am.gdynia.pl,

Abstract

Analysis of the indicator diagram is the basis of technical state evaluation of marine diesel engines. The indicator diagram contains a large amount of diagnostic information. In most cases, analysis of the graph is reduced to determination only the maximum pressure or mean indicated pressure. It seems appropriate to determine the possibility of use heat release characteristics for the diagnostic purpose. The paper presents results of studies related to the use of indicator diagrams for the diagnosis of high power marine diesel engine. The results include a comprehensive approach to problems of use of the cylinder pressure curves for the evaluation of the technical condition of the engine. The problem of dynamic adjustment of the GMP position, smoothing distortions due to the impact of the channel and indicator valve were considered. Diagnostic analysis includes also the designation of the heat release characteristics on the basis of the curves pressure in the engine cylinder. The algorithms allow to determine both the curves of heat release rate q and the heat released Q. The curve of heat release rate q is a full equivalent to fuel injection pressure curve in the fuel pipes. It allows identification of the failure of the injection system. The curve of Q allows such determination and additional assessment of internal efficiency of the cylinder. The analyzed indicator diagrams were obtained during the sea voyage with the use of the stationary electronic indicator PREMET. The pressure sensor were placed on the indicator valves.

Keywords: *marine combustion engines, heat release characteristics, indicator diagram analysis*

1. Introduction

Modern cargo ships are distinguished by considerable tonnage freight, requiring considerable power propulsion systems, which is associated with significant fuel consumption and generation of combustion products by a single object.

The cargo ship propulsion systems are primarily used the slow and medium speed diesel engines with power exceeding 80 MW. If we use the example of the marine engine MAN 9K90MC (41162 kW/94 rpm), improving its efficiency by 1%, at 75% load would reduce fuel consumption by 0.05 t/h. At a year scale, such improvements, would save about 250 t, assuming a specific fuel consumption of at SFOC = 169 g/kWh. Getting savings is possible with a good engine technical condition and with optimal settings and regulation of fuel and propulsion system.

For this reason, there is a need in shipping, to use diagnostic systems to monitor the working process in the cylinders and diagnostic reasoning based on indicator diagrams. In general, the greatest expectations in relation to diagnostic systems are associated with failure detection and forecasting of the technical condition. This follows from the need to maintain sailing safety and

environmental protection. In shipbuilding there are still widely used indicators of both mechanical and automatic measurement and the on-line diagnostic systems.

The indicator diagrams of marine engines are considered to be one of the major sources of diagnostic information about the work and condition of engine cylinder sections. There are still widely used on ships mechanical and electronic maximum pressure meters, mechanical and electronic indicators for measurements in the time domain, and the more complex indicators in the field of the crank angle. Pressure measurement in the crank angle domain is the one of the condition of the automation of data processing.

The still actual problem is a selection of diagnostic information contained in the indicator diagrams and evaluation of the reliability of obtained information. Despite the rapid development of measuring techniques, in the field of methods and scope of obtaining diagnostic information from the indicator diagram there is a stagnant.

Diagnosis, in these types of systems, is based on comparing the values of the maximum compression pressure, the maximum combustion pressure and the mean indicated pressure (MIP). Pressure curves and parameters listed above or their deviation from the mean value are compared between the engine cylinders at a given load. In more advanced systems, trends of observed diagnostic parameters are created, which allows obtaining additional diagnostic information. In order to obtain the trends of diagnostic parameters, it is necessary to use pressure sensors that maintain long-term measurement characteristics. An additional condition is the creation of diagnostic parameters independent of the load.

It seems that a significant increase in diagnostic capacity of indicator diagrams, can be obtained by heat release characteristics. These characteristics, despite the high diagnostic potential, are still not used to assess the condition of marine engines.

2. The experiment methodology

The paper analyzed the diagnostic information obtained on the one type of container vessel with a capacity of 67 682 DWT (4612 TEU). Measurement information are related to main engine MAN B&W 9K90MC, which uses on-line diagnostic system of known company widely used in the ships. The study cover six test sessions, which are performed by the crew within three months of sea voyage. Test results includes information about detected malfunctions and maintenance activities performed during this period (Table 1).

Tab. 1. Measurement sessions (indications), detected failures and maintenance operations on main engine MAN B&W 9K90MC

Measurement session (date)	Detected failures, symtpoms	Maintenance operations
A (12.07.2011)		
B (23.08.2011)		
C (30.08.2011)		
	Cyl. 9 - exhaust valve leakage (high temperature of exhaust gas, a large amount of fuel)	Cyl. 9 – exhaust valve replacement
	Cyl. 2 - blocked two upper piston rings (detected by performing other procedures)	Cyl. 2 – piston rings launched
	Cyl. 7 – fuel pump damage (VIT setting 8,1; should be about 6,7)	
D (23.09.2011)		
E (07.10.2011)		
		Cyl. 7 – fuel pump replacement

		(VIT in operation)
		Cyl. 1;3;5 – eliminated leaks inAIR SPRING (large pressure drops indrop test)
F (20.10.2011)		

It should be noted that most of the diagnostic observations were not based on indicator diagrams and the results of the test reports of indication, but on different diagnostic parameters and symptoms. In this paper an analysis of whether any malfunction can be detected using the previously used indicator diagram processing methods, and using the heat release characteristics.

3. Assessment of the diagnostic usefulness of pressure curves and MIP values

Direct comparative analysis of the indicator diagram, as well as the MIP values allows diagnostic inference only in case of significant deviations from the mean values. Even in such cases there are diagnostic interpretation difficulties. The example is illustrated in Figure 1, where in session C, in the case of cylinder 2 there was a significant deviation of the MIP about 15 %.

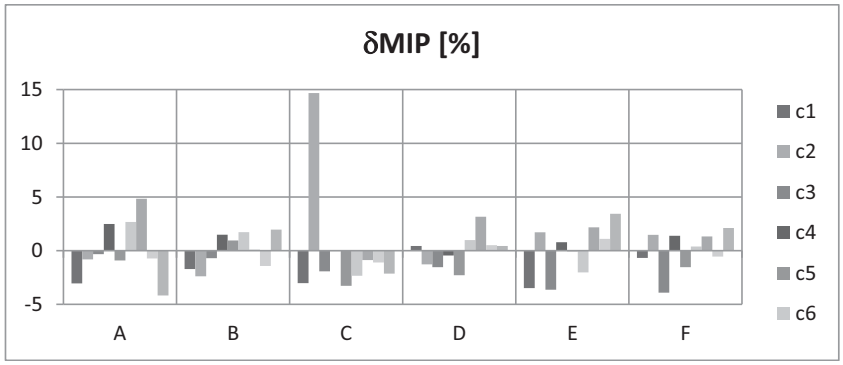

Fig. 1. Percentage deviations from mean δMIP for the cylinder for all test sessions A ÷ F

A significant deviation of the cylinder 2 with respect to the course of an average is seen on the imposed pressure curves (Figure 1).

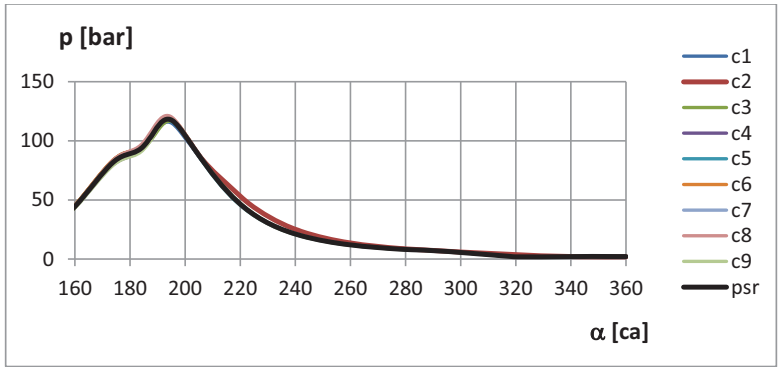

Fig. 2. Comparison of the pressures in the cylinders and their averaged in the session C

The identification of reasons of deviation of cylinder nr 2 is very difficult. Is known only that the amount of fuel is higher.

4. Assessment of the diagnostic utility of the maximum combustion pressure

The maximum combustion pressure p_m is the parameters which can be measured even by the simplest maxi meters or mechanical indicators. This parameter is usually used in the operation for the overall evaluation of the technical condition of cylinders and fuel injection systems regulation. It is believed that the maximum combustion pressure can be used to assess on the engine load balance between the cylinders in place of the mean indicated pressure (MIP).

Analysis of measurement data obtained during the operation (Table 1) showed that the use of the maximum combustion pressure for the loads regulation assessment of marine engines, in this case, is not eligible. The indicator diagrams were smoothing before analysis to reduce the impact of large measurement noise. The values of correlation coefficients between the values of the maximum combustion pressure p_m and p_{wm}, and the values of p_i, for each measuring session (Table 2) indicate no significant relationship at the level of variation at a given level of loads.

Tab. 2. The values of correlation coefficients between the mean indicated pressure pi, and maximum combustion pressures: p_{max} – designated from original pressure curve, p_{wmax} - designated from pressure curve after smoothing

Correlation coefficients	Measurement session					
	A	B	C	D	E	F
$K(p_{max};p_i)$	0,23	0,21	0,24	0,00	0,10	-0,09
$K(p_{wmax};p_i)$	0,24	0,18	0,16	0,06	0,02	0,07

As can be seen (Table 2) smoothing slightly affected the values of correlation coefficients. The results obtained in both cases indicate a lack of correlation between p_m, p_{wm}, and p_i. Thus, for a given load level for the maximum pressure deviations below 5% should not be guided by the value of the maximum combustion pressure for the assessment of the cylinder load. The reasons may be different.

5. The heat release characteristics and their possible diagnostic use

Determination of the heat release dynamics is a complex mathematical and measuring problem [3, 4]. For diagnostic purposes it is advisable to use a simplified model of the net heat release rate q_n for an ideal gas [3].

This formula can be written as follows:

$$q_n = \frac{dQ_n}{d\propto} = (\kappa - 1)^{-1}\left[\kappa p \frac{dV}{d\alpha} + V\frac{dp}{d\alpha}\right] \quad (1)$$

where:
Q_n – net heat release,
κ – isentropic exponent,
V – current volume of the cylinder,
α – crank angle.

Determination of released heat Q requires the integration of the value of q in the field crank angle, from the piston BDC.

In this work the net heat release rate and net heat released are related to a cylinder volume. In this case the unit of heat release is pressure.

In order to determine the heat release characteristic as well as MIP values thermodynamic TDC was used which was calculated with the original method based on polynomial model of compression curve exponent [1, 2].

Figure 3 shows an example of a significant deviation of heat release Q is easy to see that in the case of cylinder 2 appeared much higher Q value than for the other cylinders.

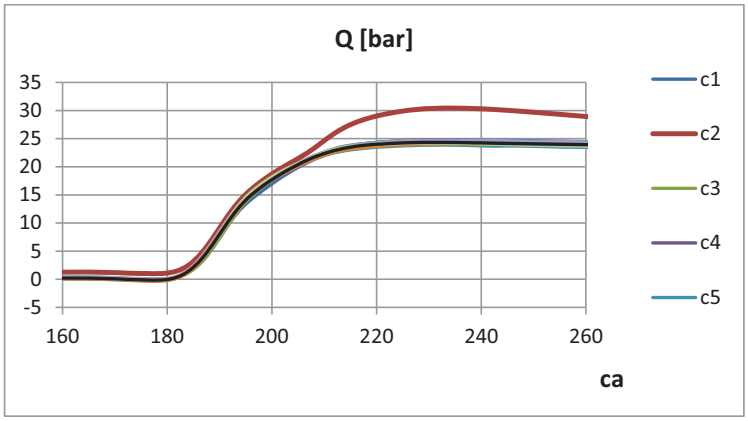

Fig. 3. Curves of net heat released in the cylinder Q for the measurement session C

The fault symptoms visible on cylinder nr 2 are results of faulty operation of the fuel injection system. The identification of fault can greatly facilitate with the analysis of the curve the heat release rate (Fig. 4), which is correlated with the process of fuel injection into the cylinder and the injection pump operation.

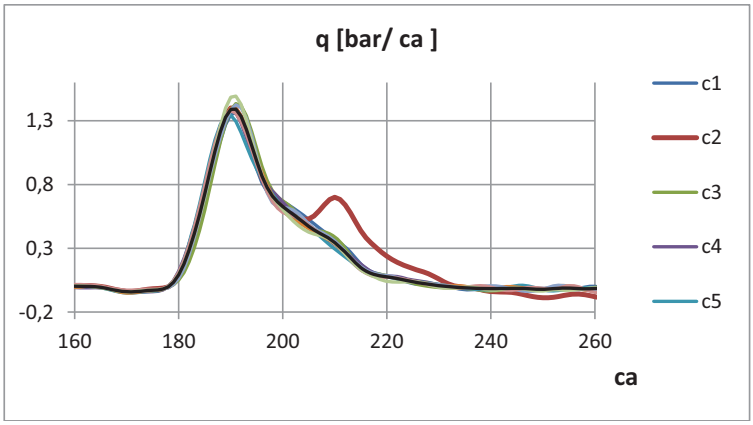

Fig. 4. The curve of heat release rate in the cylinders for the session C

By analyzing the observed curve of q in the cylinder 2, in conjunction with the principle of operation of the injection system, it's easy to perform diagnostic reasoning. In total, the analyzed test sets identified several cylinders for which there were various derogations from the normal curve of q. It is appropriate to create a catalog for the failure of symptom-injection systems. For this purpose, it's plans to establish wider cooperation with the crews machine, which will enable

the development of diagnostic methods of injection systems based on the heat release characteristics.

Summary

Diagnostic reasoning based on a comparison of indicator diagrams and the variation of maximum combustion pressure within the 5% and even 10% is very difficult. The diagnosis in this case is limited to an occurrence of significant deviations without specifying of its reasons. This conclusion is confirmed by the results of analyzes of indicator diagrams taken for other engines, ships and pressure analyzers.

Similar problems have occurred with regard to the use of the MIP for diagnostic purposes, which further requires a sufficiently precise determination of TDC position of the piston, and in particular the thermodynamic TDC determination. Most electronic indicators used on ships, are characterized by inadequate methodology and poor accuracy of determination of TDC. The absolute values of TDC position errors sometimes exceed 1 ° OWK, apart from systematic errors. Designation error of MIP values, which results from the accuracy of the determination of TDC at the nominal engine load can exceed 8%.

Improvement of diagnostic inference based on indicator diagrams, can be obtained by analyzing the characteristics of the net heat release rate, determined on the basis of indicator diagrams. Heat release characteristics allows the observation of the angular amplitude variation associated with the operation of the injection systems and cylinder loads. Since there is no possibility of carrying out active research on this type of object, methods of diagnosis based on heat release characteristics will be written in the passive mode experiment based on measurement data provided by the crews of merchant ships.

References

[1] Pawletko, R., Polanowski, S., *Research of the influence of marine diesel engine Sulzer AL 25/30 load on the TDC position on the indication graph*. Journal of Kones Powertrain and Transport, Vol. 17, No. 3, Warsaw 2010.

[2] Polanowski, S., *Determination of location of Top Dead Centre and compression ratio value on the basis of ship engine indicator diagram*, Polish Maritime Research № 2(56), 2008, Vol. 15.

[3] Rychter, T., Teodorczyk, A., *Modelowanie matematyczne roboczego cyklu silnika tłokowego*, PWN Warszawa (1990) – in polish

[4] Heywood, J.B., *Internal Combustion Engine Fundamentals*, McGraw-Hill, 1988 – 930.

Journal of Polish CIMAC
Gdansk University of Technology
The Faculty of Ocean Engineering and Ship Technology

THE EVALUATION OF THE VIBRATION MEASUREMENT USABILITY OF ELECTRONIC INDICATOR LEMAG „PREMET® C"

Jacek Rudnicki

Gdansk University of Technology
ul. Narutowicza 11/12, 80-233 Gdańsk, Poland
tel.: +48 58 3472973, fax: +48 58 3471981
e-mail:jacekrud@pg.gda.pl

Abstract

The measuring possibilities of modern compression and combustion pressure analyzers are extended with additional functions. One of them is parallel to the pressure measurement, the measurement of vibrations in the region of the cylinder head. The paper presents a general assessment of the vibration measurement function of the electronic indicator LEMAG „PREMET® C". This feature is very rarely offered by manufacturers of these devices. Based on experience summarizes the advantages and disadvantages of this method with the use of this device.

Keywords: *vibration, engine timing, diesel engine indicator*

1. Introduction

Since the service life every complex system, which is a piston diesel engine (in particular - the main drive) cannot be a clear measure of the use of its components and the high reliability of this engine ensures eg. the safety of a ship, rational exploitation requires flow of information on the current state of technical and development in this area relevant predictions.

In recent years, in spite of the remaining formal - legal restrictions concluded min. in the classification rules, the concept of exploitation of marine energy systems changes. Due to the increasing running costs of maritime transport trends to implement at least the elements of condition based maintenance strategy are becoming increasingly clear.

This is not possible without existing operating system monitoring tool. Implementation of hardware - software diagnostic system allows you to control the process of ownership by [3]:

- the possibility to change the current power state of the engine according to the current state of technical and external conditions e.g. hydrometeological,
- identification of the servicing needs through understanding the diagnosis and prognosis of engine condition,
- the possibility of quality assessment of the service.

The basic indicators of engine performance on his property, environmental and ergonomic are largely determined by physical and chemical processes that make up the operating circuit. Therefore, in the research on the functioning of marine diesel engines as well as during use, a key role in the evaluation of the implementation of each operation circuit of the piston diesel engine play indicator diagrams and their analysis.

Information pictured in the indicator graph (Fig.1) enable to assess the quality of implementation of the conversion of the chemical energy of fuel into mechanical energy, and apply for the engine condition.

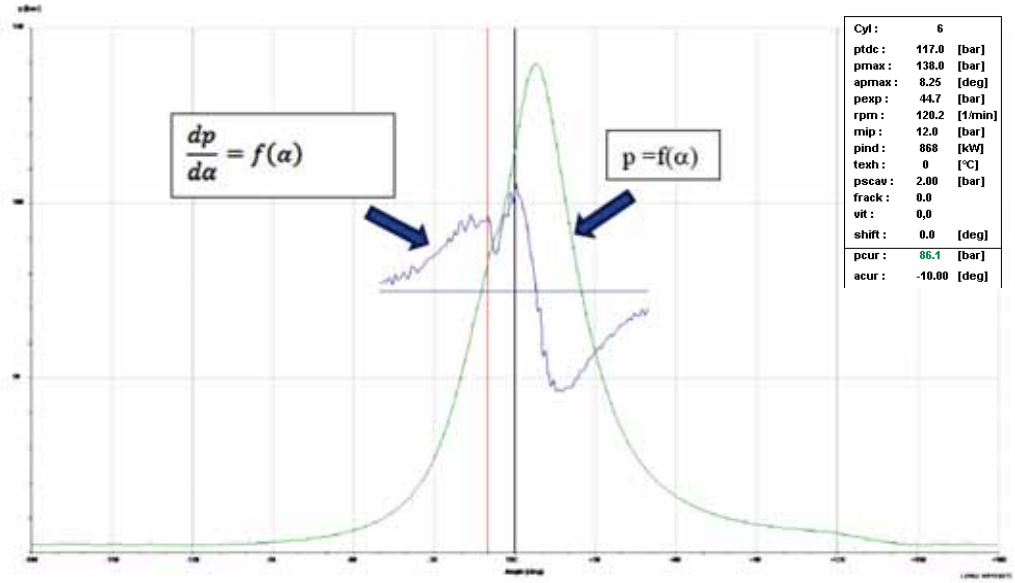

Fig. 1 Sample indicator diagram obtained using LEMAG „PREMET C"

Measurement capabilities of contemporary indicators are complemented by integrated software tools that enable the processing of measurements obtained during the data measurement and derive the basic indicators to assess the implementation of the operating circuit, such as mean indicated pressure - p_i (Fig. 2a), or the deviation from the mean value (Figure . 2b) in a clear and readable form, usually graphically with marked values relating to all of the engine cylinders.

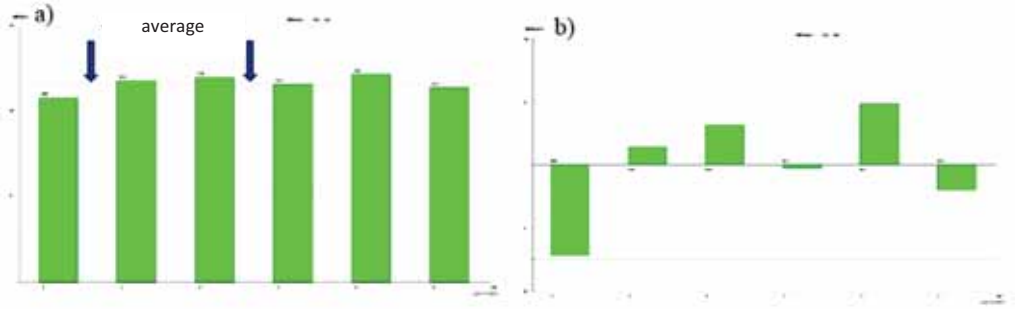

Fig. 2 Mean indicated pressure values (a) and the deviation from the mean (b) for specific cylinder of 6-cylinder engine .

The market offers a lot of this type of pressure analyzer as [7], [8], [9], [10], [11], [12], and all exhibit similar capabilities, which typically include:

- measurement of the pressure in the working space and optional fuel injection pressure,
- measurement of the speed of the crankshaft, pressure sync with TDC,
- similar pressure measurement accuracy,
- option to archive the results of measurement,
- the possibility of manual adjustment of TDC point for each cylinder,

- user-friendly interface
- interface (USB or RS232) to export the data to a computer,
- adapted software
- battery power.

The basic advantage of this kind of solution is it's mobility and wide range of use, non-limited to one type of engine.

The need for a number of additional activities during indication cylinder, above all, pressure sync with the current position of the piston, and the growing requirements for obtaining a variety of information in a single diagnostic test using the mobile system, encourages the manufacturers to equip the additional features. One of them seems to be very useful but rarely offered the ability to measure vibrations in the vicinity of the cylinder head.

2. The use of vibration signals in the evaluation of the technical condition of the timing gear

Vibroacoustic processes are the result of activation of the different types of equilibria disorders in mechanical functioning of the technical system. Disorders may be the result of periodic excitations at the input of the system or part of a utility process [1], [2]. Phenomena characterizing these processes are emitted at the output of the system that represents the device and they are manifested mainly in the form of mechanical vibration and acoustic, as well as a time-varying dynamic loads and deformation of the device.

The reciprocating diesel engine the implementation of operating circuit are accompanied by physical and chemical processes that cause the vibration pulses. From the point of view of operational diagnostics for the most important of these phenomena should be considered [2], [4], [5]:

- movement of the piston rings in the grooves of the ring,
- opening and closing of the injectors,
- impact valves in valve seats
- combustion process.

The nature of these phenomena and engine design make the vibration signal, eg. in the form of vibrations registered includes information about their conduct. From the operational point of view, particularly valuable are diagnostic information about the engine camshaft. It thus seems fairly simple matter, to complete a routine measurement of pressure inside the cylinder by an additional measurement channel, which in turn will significantly increase the utility of these diagnostic tests.

Additional prerequisites pleading for using such a solution should be a number of scientific publications on this topic and a very high demand from users (especially older structurally marine engines) for this type of testing the technical condition of the engine.

Making therefore the analysis of the availability of such analyzers in commercial solutions appears a kind of surprise. Leading manufacturers of marine engines dedicated devices (eg. Leutert, Kongsberg Maritime) generally do not offer anything in this regard. The few exceptions to use in a wider scale, you may encounter (eg. diagnostic system developed at the Naval Academy in Gdynia [6]) do not change the situation fundamentally.

If the criteria of the effectiveness of diagnostic methods are the widespread use of the method, the acceleration measurements in the region of the head during the cylinder indication time prove to be highly ineffective method, limited to individual and experimental applications.

The statement above will, of course, cause the appearance of a natural object, due to the existing state of knowledge about the of the vibroacoustic diagnosis and it's applications. Does not it change the fact that the unit uses these tools in the diagnosis of marine diesel engines operating.

3. Description of measurement abilities of electronic indicator LEMAG PREMET® C XL

Electronic indicator PREMET® C in XL version [8] is a modern, mobile, very solid and reliable pressure analyzer offered with adapter software WPREMET (tab. 1, fig. 3).

Tab. 1 Basic information about PREMET C XL electronic indicator

Ignition pressure range	0 – 25 MPa
Speed range	40 – 1800 rpm
Max. number of cylinders	20
Max. number of measurements/cylinder	30
Manufactured according to ISO 9001	yes
Compensation of temperature	yes
PC connection	USB
Stainless steel housing with isolated thermogrip	yes
High resolution colour display	yes
Accuracy	better than 1,6

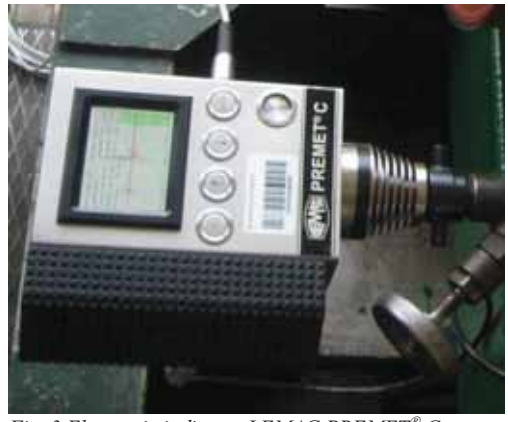

Fig. 3 Electronic indicator LEMAG PREMET® C

In terms of options for measuring and analyzing the pressure inside the cylinder the device allows standard features that determine the value of common indicators to assess the course of operating in the cylinder e.g. the average indicated pressure. The distinguishing feature of the analyzer is described equipment manufacturer offer it in accelerometer (typically mounted on the engine with a magnet – fig. 4), which allows parallel, synchronized with the position of the piston, the measurement of vibrations.

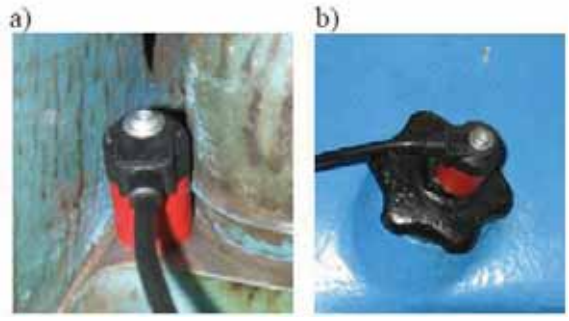

Fig. 3 Magnetic mounting of sensor: a) cylinder head mounting, b) valves cover mounting

Tab. 2 Basic information about Bosch 0261231118 accelerometer

Frequency range	0 – 20 kHz
Measuring range	0 – 400 g
Sensitivity at 5 kHz	26 ±8 mV/g
Dominant resonant frequency	> 25 kHz
Self - impedance	> 1 MΩ
Operating temperature range	-40 – 150 ^{o}C

In view of the statements of the previous chapter it is so important difference compared with other commercial devices of this type that should decide a kind of monopoly in the market of universal analyzers.

As can be seen from the experience of the author, indeed indicators of this type are quite commonly used by engineering crew on board, (not without influence in this case, so-called. the certificate of approval of the indicator, the leading classification societies such as Germanischer Lloyd), whereas the use of the monitoring function vibration is minimal.

The question therefore arises - why so useful additional feature that allows for more complete information in a standard cylinder indication is so reluctant to use by users.

4. The evaluation of the results of the research

As the featured in the previous section of the article indicator PREMET® C in XL version, is since 2009, the scientific equipment - Research and Teaching Department of Ship and Land Power Department of Ocean Engineering and Ship Technology Gdansk University of Technology, it was complemented by the possibility of measuring the vibration acceleration measurement function.

Diagnostic tests of engines already in service and laboratory tests on experimental engine made it possible to collect the expertise, which to some extent are the answer to the question asked in the previous chapter.

The first thing that appears before you use the analyzer is the lack of any guidance on the use of this function in the technical unit. In fact, there is only mention of such a possibility. This probably indicates a slight experience of the manufacturer in this field and makes the average user does not realize how big the potential opportunities may involve the use of additional measurement channel.

Another essential problem is a way of displaying the results. Figure 5 shows a sample screenshot of the recorded data.

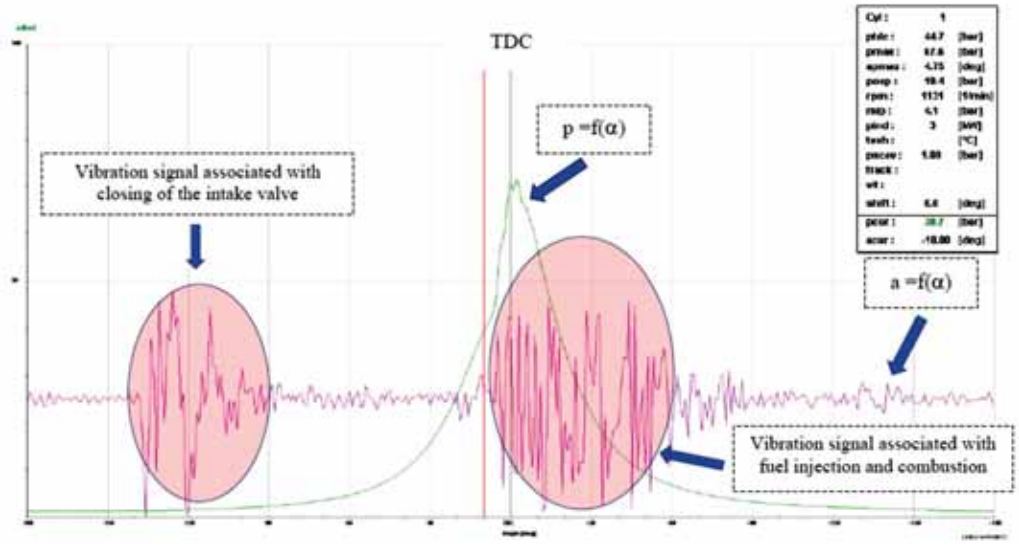

Fig. 5 WPREMET screenshot of the results of the recorded pressure p = f(α) and the vibration acceleration in the region of the head a = f(α) for diesel engine Farymann laboratory type D as a function of the angle of rotation of the crankshaft - α during compression and expansion strokes , TDC - top piston position feedback, an accelerometer installed magnetically on the screw fixing the head, from the side of the intake valve

Because as you can see in fig. 5 the results are presented in the form of "raw", very noisy, probably without any processing, their usefulness in diagnostic reasoning basically comes down to statements such as: injection took (or was not) place, the inlet valve closed at the beginning of the compression stroke, etc.

Another issue related to the use of the accelerometer is the way and the place of installation. Manufacturer standard equipped accelerometer with a magnetic holder (fig. 4), which is of course very practical and convenient way. At the indicated time, the realities of engine room, however, often turns out to be the most unreliable way, introducing significant signal attenuation or more of its components under certain conditions.

Figure 6 shows an example of extreme situation, where initially it can be concluded that neither closing the intake valve or injection and combustion in the cylinder does not happen.

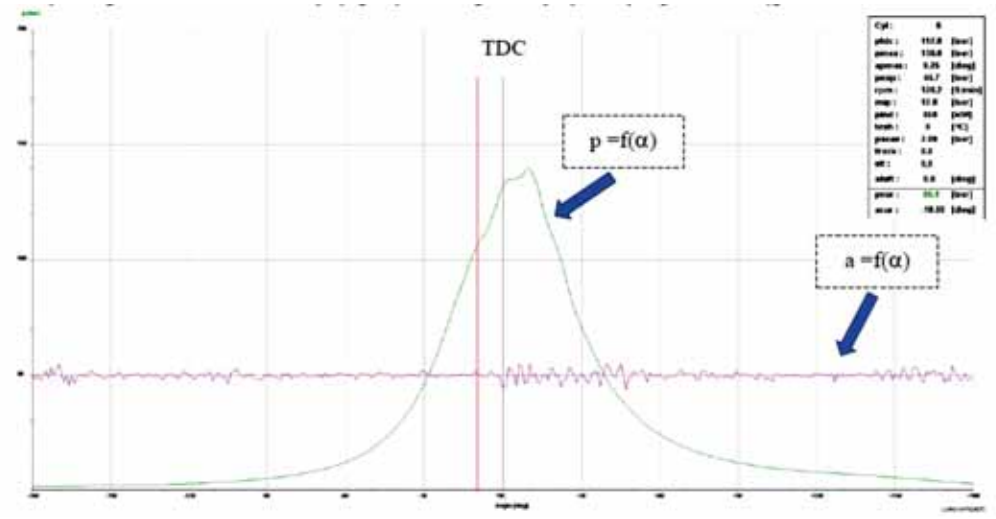

Fig. 6 WPREMET screenshot of the results of the recorded pressure p = f(α) and the vibration acceleration in the region of the head a = f(α) on the engine type SULZER 12ZAV40 S as a function of the angle of rotation of the crankshaft - α during compression and expansion strokes; TDC - top piston position feedback, an accelerometer installed magnetically on the screw fixing the valve cover from the intake valves

To avoid such cases it is advisable to modify method of installation the accelerometer. The most preferred method, which does not lose its practicality in relation to the magnetic clamping while devoid of its drawbacks, it seems as proposed in elaboration (for example, [4]) with a suitable mounting bracket. An example of such solution is shown in fig. 7.

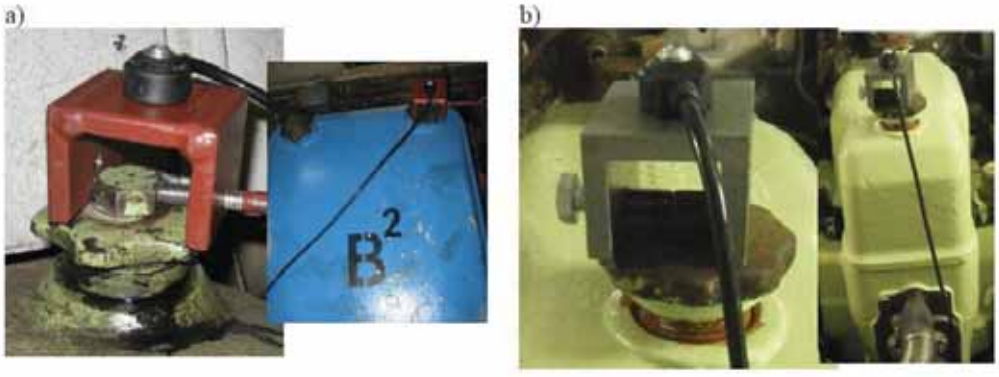

Fig. 7 Installing accelerometer of an indicator PREMET® C with mounting brackets on the covers of engine valves: a) a 12ZAV40 SULZER S, b) type 8ATL SULZER 25/30

5. Summary

In view of the results, it appears that the potential for simultaneous measurement of vibration and a cylinder indication were not used by the manufacturer of the indicator, which is recognized in the market shipping company LEHMANN & MICHELS GmbH. It can be assumed that the way to present the results

of measurements and the lack of information in the technical documentation simply discourages potential user to practical application.

On the other hand, because the measurement results are stored in plain text it is always possible to process and analyze them using digital signal processing methods (eg [1]). Data obtained in this way is much more meaningful and allow for diagnostic reasoning by a user of an average knowledge in this area.

REFERENCES

[1] Antoniou A.: *Digital Signal Processing. Signals, Systems and Filters.* McGraw – Hill Companies Inc., New York 2006.

[2] Cempel Cz.: *Wibroakustyka Stosowana*, PWN, Warszawa 1989.

[3] Girtler J.: *Sterowanie procesem eksploatacji okrętowych silników spalinowych na podstawie diagnostycznego modelu decyzyjnego*. Zeszyty Naukowe AMW, nr 100A, Gdynia 1989.

[4] Lus T.: *Analiza przydatności kątowej selekcji drgań w diagnostyce zaworowego rozrządu okrętowych silników spalinowych*. Rozprawa doktorska. Wydział Mechaniczno – Elektryczny AMW, Gdynia 1992.

[5] Polanowski S.: *Zastosowanie metod drganiowych w diagnostyce tłokowych silników spalinowych*. Materiały XXVII Ogólnopolskiego Sympozjum „Diagnostyka Maszyn", Węgierska Górka 2000.

[6] Polanowski S., Łutowicz M., Bruski S., Wontka L., Żuralski Cz.: *Nowa wersja analizatora cisnień i obwiedni drgań do pomiarów i diagnostyki silników okrętowych*. Materiały XVIII Sympozjum Siłowni Okrętowych, Gdynia 1996.

[7] http://www.leutert.com/docs/maritime/Products_Maritime.htm

[8] http://www.lemag.de/

[9] http://www.imes.de/epm-xp.html

[10] http://www.km.kongsberg.com/

[11] http://dimar-tec.com/product.php?pid=CBM&pcode=CBM003

[12] http://www.ultima-automatyka.pl/

Journal of Polish CIMAC
Gdansk University of Technology
The Faculty of Ocean Engineering and Ship Technology

METHOD OF DIAGNOSING THE POWER TRANSMISSION SYSTEM IN A TARPAN HONKER MILITARY VEHICLE[1]

Rychlik Arkadiusz, Szczyglak Piotr

University of Warmia and Mazury in Olsztyn, Faculty of Technical Sciences
Department of Vehicle and Machine Design and Operation
Address: Oczapowskiego 11, 10-719 Olsztyn
Tel: (48 89) 523 37 51 Fax: (48 89) 523 34 63
e-mail: rychter@uwm.edu.pl

Abstract

This paper presents a diagnostic system for monitoring the operation of the Tarpan Honker military vehicle, referred to as the Autonomous Logistics System (ALS). The diagnostic model, the structure and tasks of ALS and selected diagnostic algorithms were discussed. The structure of the diagnostic system was analyzed in detail with special emphasis on communication between system modules. The description of the diagnostic model defines diagnostic monitors implemented in the memory of the on-board diagnostic system. The ALS system comprises transmission-receiver modules connected as part of an RS-485 type communication and data transmission system. The modules were individually designed and provided with measuring sensors using multipin plugs and connectors. All measuring sensors were installed in the vehicle, and most of them were not part of built-in equipment. Every module has a diagnostic connection for entering data into processor memory (programming) and for module self-testing. The implemented system is fully independent of external circuits, therefore, if damaged or not activated, it does not affect mission performance.

Keywords: *transport, diagnostics, transmission system, transmission topology, RS-485*

1. Introduction

The contemporary battlefield is characterized by dynamic operational, tactical and technical requirements. Those requirements are met through the acquisition of real time data, high operational and tactical mobility of troops and warfare, distribution and movement in terrain, maneuverability performance and safe combat operations under all circumstances and at all times.

Contemporary combat requirements necessitate the choice of modern warfare and military equipment, in particular vehicles with effective operating and diagnostic systems. The contemporary military vehicle should be prepared for network-centric warfare [7], therefore, it has to meet the highest reliability and safety standards. Damage resistance is one of the key criteria in evaluations of a military vehicle's reliability and safety.

[1] This study was carried out as part of research project No. O N509 008336

2. Diagnostic model of the power transmission system in a military vehicle

The functionality of a military vehicle is described by a set of tasks which have to be performed under all circumstances, both outdoors and in the battlefield. The vehicle's objective function should be determined to indicate whether the vehicle's current technical condition supports the achievement of planned tasks.

According to [3], the objective function of a military vehicle is defined as a specific interaction between the following variables: H_o – transformation vector, $\boldsymbol{U}(t)$ – input signal vector, $\boldsymbol{X}(t)$ – status parameter vector, t – dynamic time, and Θ - operating parameters. The number of input functions ($\boldsymbol{U(t)=const}$) is strictly defined in diagnostic tests to ensure that every change in diagnostic signal results from changes in the vehicle's technical condition.

In tests analyzing the technical condition of mechanical vehicles, state vector $\boldsymbol{W(t)}$ can be determined by measuring the components of vector $\boldsymbol{Y(t)}$ of diagnostic signals. In simple terms, the state vector is a function of independent and complete numerical values of diagnostic parameters (status parameters) and the transformation operator [6].

The Tarpan Honker military vehicle was analyzed to diagnose, prognosticate and generate its operating states [5]. As part of the diagnostic process, the power transmission system of the military vehicle was split into five decomposition levels. The 5-level structural model of the investigated vehicle is discussed in [4]. A homogenous 5-level structural model of the studied vehicle has been developed. Level 5 combines basic components, and it describes the depth of structural penetration. Damage localization takes place at level 5. A set of basic components has been created on the assumption that a diagnosis of all vehicle elements is possible but not justified. The set accounts for basic components which, in the authors' opinion, need be diagnosed to determine the vehicle's general ability to perform a combat mission. The methodology for developing vectors of diagnostic parameters, describing information models and their characteristics is presented in [1, 4]. In the modeled diagnostic system, faults are identified in a binary classification system which is identical for all symptoms.

Diagnostic algorithms

Diagnostic algorithms are core concepts in technical diagnostics. In the discussed system, they are referred to as diagnostic tests which analyze the operation of diagnostic system components:

- operability test of electric measuring and actuating elements,
- passive test of metrological traceability of actuating elements,
- functional tests of actuating elements,
- active tests of metrological traceability of measuring elements.

In measuring and actuating elements, algorithms of electrical operability are applied to analyze: circuit continuity, short circuit of the signal line and actuating elements to ground or supply voltage. A passive algorithm for evaluating measuring elements tests the accuracy of sensor readouts. A functional algorithm uses a model signal to test actuating elements. An active algorithm for testing the metrological traceability of measuring elements is similar to a functional algorithm. In an active test, the control signal is used to analyze the actuating element by monitoring changes in measured values.

The developed system relies on diagnostic algorithms (tests) where the operability criterion has been formulated as follows:

An element or a system is regarded as damaged if its characteristic parameter or diagnostic signal (symptom/s) exceed boundary values or allowable values, thus obstructing or disabling task performance. The element is regarded as operational if the above requirements are not met.

In this paper, diagnostic tests (algorithms) are referred to as monitors based on standard OBD-I [2]. Every monitor (algorithm, test) supports only one system which affects vehicle operation and

task performance. The monitors implemented in the on-board diagnostic system have been classified as follows (Tab. 1.2):

- discontinuous (conditional) monitors which require the implementation of other monitors and/or prolonged observations of changes in parameter values under given driving conditions, i.e. temperature, dynamic behavior of the engine and the power transmission system;
- continuous (unconditional) monitors which support elements that can be tested under any driving conditions and whose performance is not dependent on testing requirements for other monitors.

A model for communicating the status of selected subassemblies of the power transmission system and the accompanying fault symptoms, without identifying boundary and admissible states, is presented in Tab. 1.1.

Tab. 1.1. Diagnostic information model for identifying the status of selected elements of the power transmission system based on registered symptoms, without identifying boundary states

Subassembly	**State (W_m)**	**Symptoms (Y_n)**
Gearbox + reduction gear	$W_{3,1}$ – gearbox and reduction gear are operational	not ($W_{3,2}$), not ($W_{3,3}$) and not ($W_{3,4}$)
	$W_{3,2}$ – excessive wear of gearbox, reduction gear or clamping mechanisms	contact shorting in a binary vibration sensor of the gearbox and reduction gear after an *n* number of gear shifts (checked 1-2 s after gear shift) (signal S_6)
	$W_{3,3}$ – low oil or seizure of gearbox or reduction gear elements	$T_{sb-r} \geq T_{gr3}$ where: T_{sb-r} – temperature of gearbox and reduction gear [°C] T_{gr3} – boundary temperature of gearbox and reduction gear [°C]
	$W_{3,4}$ – damaged elements of gearbox, reduction gear or clutch	open contact in the gear shift position sensor (signal S_3)
		open contact in the gearbox clearance sensor (signal S_4)
		$n_e > 0$ where: n_e – rotational speed of crankshaft [rpm]
		$n_r = 0$ where: n_r – rotational speed at reduction gear outlet [rpm]

The discussed diagnostic system was equipped with diagnostic monitors. A list of monitors and monitor types are presented in Table 1.2.

Tab. 1.2. List of diagnostic monitors implemented in the memory of the diagnostic system of the Tarpan Honker military vehicle

No.	Diagnostic monitor	Type / Description
1	Circuit temperature monitor	continuous – for determining boundary and admissible temperatures of operating systems and materials
2	Fluid level monitor	continuous – for determining operating fluid levels
3	Engine cooling monitor	discontinuous – for determining engine temperature at low driving speeds
4	Battery and electrical installation monitor	discontinuous – for determining battery status, charging parameters and electrical installation status
5	Fuel consumption monitor	continuous – for determining fuel consumption and driving distance on current fuel reserve
6	Engine power monitor	discontinuous – for determining instantaneous engine power
7	Power transmission system monitor	discontinuous – for determining wear/clearance of the power transmission system (clutch, gear box, reduction gear, crankshaft, final drive) and transmission clamp damage
8	Monitor of front axle wheel spin	continuous – for determining the relative spin of front axis wheels
9	Monitor of rear axle wheel spin	continuous – for determining the relative spin of rear axis wheels
10	Tire pressure monitor	discontinuous – for determining the loss of tire pressure
11	Power transmission system efficiency monitor (gear shift assistant)	continuous – for optimizing the gear-shifting sequence subject to crankshaft load

3. Structure of the diagnostic system

The communication and data transmission system in the discussed monitoring and diagnostic system relies on an RS-485 type transmission system with linear (serial) half-duplex technology. The receiver and the transmitter communicate as follows: the transmitter has differential output voltage of minimum 1.5 V, whereas the receiver picks up differential signals with the minimum value of 200mV (Fig. 1). Those values guarantee reliable transmissions, even if significant signal loss is reported along different components of the transmission path.

The functional structure of the developed diagnostic system and data transmission topology are presented in Figure 1. The data transmission structure relies on the RS-485 standards for which four receiver modules (modules No. 1, 2, 3 and 4) and one receiver-transmission module (module No. 5) have been designed.

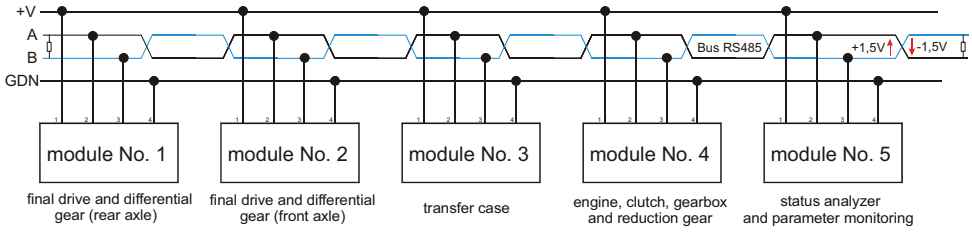

Fig. 1. Functional structure of the diagnostic system and the data transmission system with an indication of the main system components, +V – *12 V power supply,* GDN – *ground,* A, B – *RS485 bus signal line*

The structure of the above modules relies on the Atmega 250 8-bit control processor with 256 kB memory and 16 MHz clock rate.

RS-485 is a standard data transmission system designed for multipoint transmission lines (Fig. 1). Unlike other standards, RS-485 defines and limits only the electrical characteristics of the transmitters and receivers connected to a shared data bus. Based on the data (information) supplied by the internal protocol (RS 485 standard), each module (receiver and transmitter) generates an electrical signal which is transmitted to the data bus (data bus bar or data transmission network). In the designed system, data is transmitted to the data bus every 250 ms. According to the authors, in the monitored systems, this time interval is sufficient to identify the fault and the observed parameters. According to estimates, the computing power of the Atmega2560 control processor in each module will be deployed in 50%.

The data protocol generated by any module connected to the bus is fed to both bus cables (Fig. 1) with opposing signals to protect the signal from interruptions caused by other electrical devices or magnetic fields. The data transmission protocol comprises several fields (data frames). A graphic interpretation of the data protocol for module No. 1 is presented in Figure 2.

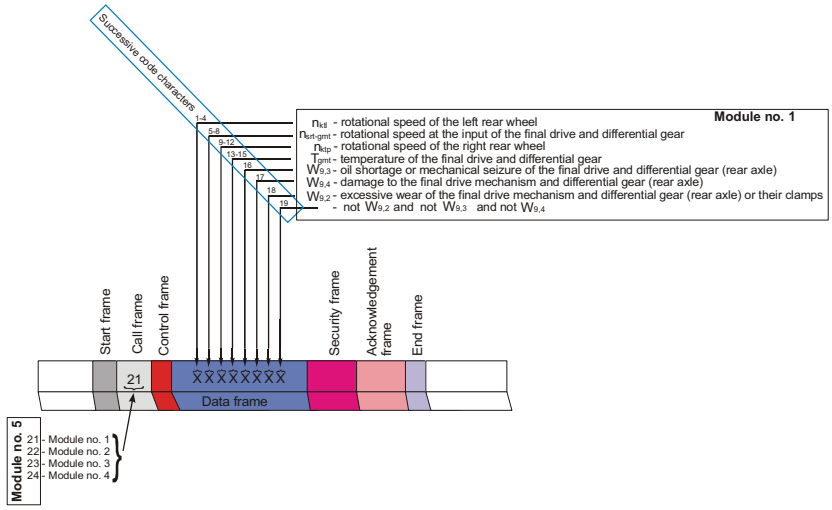

Fig. 2. Principal structure of the data protocol generated by module No. 1 (described in the text) [4]

The information confirming that data can be transmitted to a selected module is sent via the call frame. In the analyzed example, module No. 5 fills the data frame with code "21" and sends the inquiry to module No. 1. Code "21" means that module No. 1 can transmit data, and a data frame comprising a sequence of 19 characters describing the parameters or statuses monitored by module No. 1 appears in the data signal frame. The code is encrypted by receiver-transmitter module No. 5, and the relevant information is displayed in the graphic interface. The length of the frame code is determined by the volume of data transmitted by the data frame. The frames shown in Figure 2 which are not described above are part of the internal structure of the RS-485 transmission standard, and they are not programmable.

4. Physical model of the diagnostic system

A physical model of an on-board diagnostic and monitoring system for the Tarpan Honker military vehicle, referred to as the Autonomous Logistics System (ALS v1.0), was developed. The location of actuating modules and measuring sensors in the vehicle is presented in Figure 3.

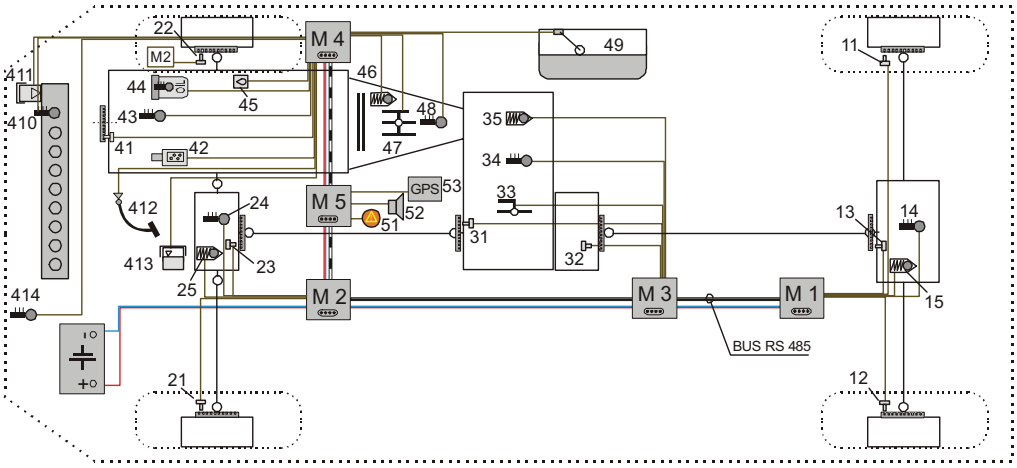

Fig. 3. Graphical presentation of the Autonomic Logistics System v. 1.0. M1 in the Tarpan Honker military vehicle. M1 – module of the final drive and differential gear in the rear axle (with a diagnostic connection); M2 – module of the final drive and differential gear in the front axle (with a diagnostic connection); M3 – transfer case and reduction gear module (with a diagnostic connection); M4 – engine and gearbox module (with a diagnostic connection); M5 – status analysis and data visualization module; 11, 12 – motion sensor of rear axle wheels; 13 – motion sensor of the final drive (rear axle); 14 – temperature sensor of the final drive (rear axle); 15 – vibration sensor of the final drive (rear axle); 21, 22 – motion sensor of front axle wheels; 23 – motion sensor of the final drive (front axle); 24 – temperature sensor of the final drive (front axle); 25 – vibration sensor of the final drive (front axle); 31 – motion sensor at reduction gear output (front axle); 32 – motion sensor at reduction gear output (rear axle); 33 – reduction gear activation sensor; 34 – temperature sensor of reduction gear; 35 – vibration sensor of reduction gear; 41 – crankshaft speed sensor; 42 – fuel injection sensor; 43 – engine coolant temperature sensor; 44 – oil temperature sensor (measurement at the filter); 45 – engine lubricant level sensor; 46 – gearbox vibration sensor; 47 – gear shift position sensor; 48 – gearbox temperature sensor; 49 – fuel level sensor; 410 – engine coolant temperature sensor (measurement at the radiator); 411 – coolant level sensor; 412 – clutch position sensor; 413 –brake fluid level sensor; 414 – ambient temperature sensor; 51 – fault signal pilot lamp; 52 – fault acoustic signal speaker; 53 – GPS module

Receiver-type actuating modules (modules 1, 2, 3 and 4) were placed in aluminum boxes and mounted under the chassis. Receiver-transmitter module (No. 5) was placed in the driver's cab (Fig. 4). The modules were linked by a network of data transmission and feed buses. The modules were also connected to measuring sensors with multipin plugs and connectors. All measuring sensors were installed separately, and they did not constitute built-in vehicle equipment.

Every module has a diagnostic connection for entering data into processor memory and for module self-testing. A manual tester has been developed for self-diagnosing individual modules. System software and the ALS control panel have been designed to produce a clear and intuitive user interface. The main goal of the optimization process was to maximize the information content of displayed data. Efforts were made to reduce to the minimum the number of panel keys required to operate the system, and visual and audio signals were deployed.

Fig. 4. View of the control panel in the prototype of the ALS v1.0 system (module No. 5)

Owing to the vehicle's functional characteristics (all-terrain vehicle), an LCD touch screen was abandoned during preliminary tests. When the vehicle is driven in uneven terrain, screen buttons are difficult to control, and they are almost impossible to operate at low temperatures.

5. Conclusions

An analysis of the physical model of the Autonomic Logistics System (ALS) in the Tarpan Honker military vehicle leads to the following conclusions:

- diagnostic information obtained from the data transmission system was used to develop a diagnostic model, algorithms for identifying the status of various circuits, algorithms for monitoring and displaying operating parameters on the control panel of the diagnostic system;
- a physical model of an on-board diagnostic and monitoring system for the Tarpan Honker military vehicle was developed;
- the ALS system comprised transmission-receiver modules which form an RS-485 type communication and data transmission system. The modules were individually designed and provided with measuring sensors using multipin plugs and connectors. All measuring sensors were installed in the vehicle, and most of them were not part of built-in equipment;
- every module has a diagnostic connection for entering data into processor memory and for module self-testing. A manual tester has been developed for self-diagnosing individual modules;
- the algorithm developed for module No. 5 features mechanisms for diagnosing individual models, but a tester can be used to diagnose any module without the need to activate the entire system. This is a highly useful option for diagnosing sensor and connection socket damage;
- the main goal of the optimization process was to maximize the information content of displayed data. Efforts were made to reduce to the minimum the number of panel keys required to operate the system, and visual and audio signals were deployed;
- the implemented system is independent of the vehicle's internal circuits, therefore, if damaged or not activated, it does not affect the mission performance;
- the ALS system was tested by the Military Institute of Armor and Automotive Technology in Sulejówek, and the results of the inspection confirmed that it is a useful and functional system (with regard to ease of use, metrological traceability of actuating elements and diagnostic

algorithms) characterized by high durability (system elements are resistant to low temperatures, dust and mechanical vibration).

References

[1] Kościelny J. M., *Diagnostyka zautomatyzowanych procesów przemysłowych*, Akademicka Oficyna Wydawnicza EXIT, Warszawa 2001.

[2] Merkisz J., Mazurek S., *Pokładowe systemy diagnostyczne pojazdów samochodowych,* WKŁ, Warszawa 2002.

[3] Młokosiewicz J. R., *Metoda wielopoziomowego badania stanu obiektów technicznych i synteza systemu diagnostycznego*, Nr 1734/87, Wojskowa Akademia Techniczna, Warszawa 1987.

[4] Niziński S. i inni, *Systemy diagnostyczne wojskowych pojazdów mechanicznych*, ITE Radom 2011.

[5] Niziński S. Michalski R., *Diagnostyka obiektów technicznych*, Instytut Technologii Eksploatacji, Radom 2002.

[6] Niziński S. Rychlik A., *Hierarchiczny model diagnostyczny wojskowego pojazdu mechanicznego*, Biuletyn WAT, Vol. LX, Nr1,Warszawa 2011, s. 196÷209.

[7] Wołejszo J., Siedlicki M., *Walka sieciocentryczna wyzwaniem XXI wieku*, Zeszyty Naukowe AON, Nr 3/68/A, Warszawa 2007.

Journal of Polish CIMAC
Gdansk University of Technology
The Faculty of Ocean Engineering and Ship Technology

FORMING RECOMMENDATIONS OF DIGITAL RECORDING DEVICES

Marcin Rychter

Motor Transport Institute
80 Jagiellonian St., 03-301 Warsaw, Poland
phone: + 48 22 330 4385; fax: + 48 22 4385 235
e-mail: rychter@poczta.fm

Abstract

The tachograph is the oldest recording device, which belongs to the Group of ORD (On Board Recording Devices). It was introduced in the USA in 1939. Digital tachograph, the new advanced type of recording device in road transport, was introduced by Council Regulation No 2135/98 of 24 September 1998 with the beginning of May 2006, in the area of the European Union. "In contrast to its analogue predecessors the digital tachograph was introduced to facilitate the control of rest and driving times and to prevent manipulation attempt" [1]. In order to prevent abuse, it has been made the system of cryptologic keys and certificates stored in cards and devices, allowing to create an explicit laws of users and authentic data recorded in, cards and devices. Despite the usage of the most advanced keys and protection systems, it has been observed that, in relation to the elements of the digital tachograph system, there are many ways to register invalid data. The European Union has taken action to prevent them, however, they must be implemented in daily life.

Keywords: *the tachograph card, control, digital tachograph, manipulation, technical inspection.*

1. Introduction

Tachograph (from Greek *tachos* – speed and *grapho*-writes) is a device combining the functions of speed indicator and clock. Tachograph records in the function of time the distance travelled by the vehicle, speed, as well as the driver's activity, i.e. periods of work or of availability, breaks from work and daily rest periods.

Due to the safety on the roads, many countries have introduced restrictions on working time for drivers of vehicles used in road transport of goods and passengers. Vehicles and sets of vehicles with a maximum permissible total mass above 3,5 t and vehicles which are constructed or permanently adapted for carrying more than nine persons including the driver, are covered by the monitoring of the driver activity by tachographs. The second aspect of the use of recording equipment in road transport was and is currently to ensure the safety of participants in road traffic as one of the main problems of present times. Number of vehicles involved in road traffic continuously increases. Despite the actions, aimed at designing and building increasingly safer means of transport, the scale of accidents is very high.

In the current situation of the functioning of digital tachograph system there are the following constituent elements: the inclusion in the TACHOnet system, the process of issuing of tachograph cards, approving of workshop conducting inspection of digital recording equipment, preparedness of States which will introduce the system of digital tachographs (fig. 1-2).

Digital recording devices use the same type of encryption protocol of signal as electronic tachographs, but with a greater degree of speed signal encryption transmitted between the motion sensor and the on-board unit. Such devices are much more safety than the equipment used previously, i.e. analogue tachographs, because of data once written in their memory cannot be changed or deleted. However, it was discovered the opportunity of very easy recording the forged information, which are stored in very safety way. Such proceedings totally changes the concept of safety.The loss of information about speed and distance, recorded in the memory of the digital tachograph, as well as the loss of data describing places of starting and finishing driver's work are quite difficult for the services authorised to inspection of digital recording equipment.

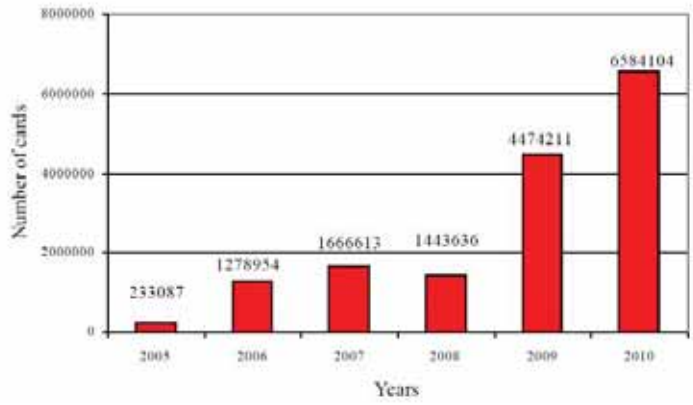

Fig. 1. Number of tachograph cards issued over the functioning of the digital tachograph system [2]

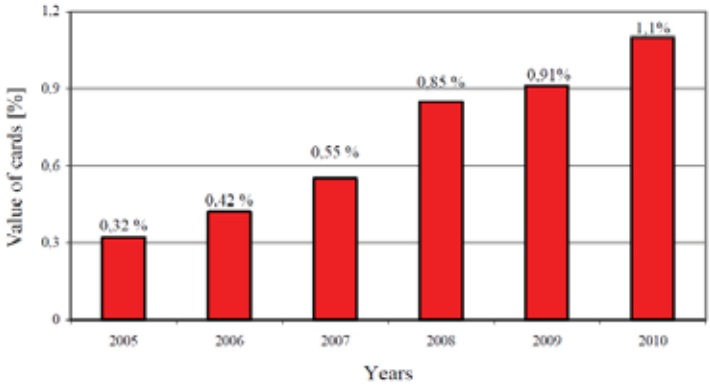

Fig. 2. Part of tachograph cards stolen and lost during the functioning of digital tachograph system [2]

2. Possibilities of manipulating the registers in recording devices.

Due to the effects of the impact, there are two types of ways to intervene in the functioning of the digital recording equipment. Invalid records may arise:

- from improper programming of on-board unit in terms of the transmission of the information concerning the vehicle speed to the vehicle unit,
- with the incorrect use of the switches of choice of the undertaken activity,
- with the adjustment of the clock or its stopping,
- with the invalid manual records,
- with the changes of recording method.

However, incomplete entries or their lack may result from:

- the possible retrospective nature of devices,
- the absence of vehicle speed signal,

- the lack of registers,
- not using the driver card,
- failure to comply with the manual entries.

Forging is not always due to performance driving in breach of the rules. Enter any kind of restrictions have created the need to hide the entries revealing their crossing. In terms of the functioning of digital recording equipment there would be no problems if the workshops carrying out checks, including calibration of digital recording equipment, implemented properly the tasks delegated to them, the drivers entered and took off the tachograph cards in good time, and the data saved in the memory cards were stored for the required period of one year, the drivers correctly used switches of changes the type of activity and correctly made records of other information and also properly stored the manual records in cases, when they do not have the possibility of creating the records by on-board unit.

Despite the benefits of greater security for the application of the digital tachographs in comparison with analogue tachographs, once saved data in the memory card as well as the on-board memory units cannot be changed. In addition, all data will be saved in the memory of the driver card and entries made on it kept manually by the driver and stored on the driver card memory, can no longer be changed. In the case of new equipment, it is very difficult to make unauthorized changes to the on-board unit, and individual driver activities are recorded by on-board unit even in the period when the driver card is left outside the on-board unit.

In the course of the functioning of the digital tachograph system it was also observed significant deficiencies in the elements concerning the safety of:

- records in the memory of the driver card and on-board units can be easily forged by saving the invalid data,
- printouts made from digital recording equipment do not contain any security (may be forged or altered),
- there is no justification for driving a vehicle, equipped with analogue tachograph without its own and valid driver card,
- although the type of the driver's work can be set without a driver card introduced to digital recording equipment, in many cases there may occur problems with the assignment to accurate driver,
- there is no obligation to make the manual records by the driver.

The data saved in the memory of driver card driver, carries large shortcomings resulting that the exact speed of the vehicle is recorded only in the on-board unit, and the record includes only last 24 hours of driving. Then, this information is deleted, and new information is written in this place. Place describing the beginning and end of each daily activity is written on driver cards until the moment of reaching the nearest city or another important place. These places, in conjunction with the written proceedings of the speed of the vehicle on the driver card, are used regularly by persons entitled to inspection in order to confirm the correctness of the recorded activity of the driver (e.g. change the vehicle speed signal often results in that recorded distance between two points is shorter than the actual distance between these two points). In the case of analogue tachograph unusual activities of the driver are written on the sheets and are stored together with other information about the driver. However, in the case of digital recording equipment, it is possible to write it on the printouts.

Digital recording devices use the encoded signal between the motion sensor and the on-board unit. The use of the encoded signal may not be treated as the improvement introduced with digital recording equipment, because these solutions have been already used in analogue tachographs. During the functioning of digital recording equipment it was observed the methods of avoiding the signal coding by using magnet or electromagnet on motion sensor, allowing to forge the signal sent to the on-board unit, so that the digital tachograph cannot record the driving activity (fig 3).

Fig. 3. Magnet on a motion sensor placed to manipulate the records of digital recording equipment

Magnets or electromagnets with different strength may cause reduction of vehicle speed signal strength by 10, 20 or 50% (figure 4–5). An additional element is the use of the plugs ("jack" type), causing grounding of the signal transmitted to the digital tachograph (fig. 6).

Fig. 4. The location of the magnet used to manipulate the indications of digital recording equipment

Fig. 5. The size of the magnet used for counterfeiting the indications of digital recording equipment

Manipulating of the records of digital recording equipment may also be made by changing the size of the wheels; its increase can cause the change about 8-10 km/h. Solutions can be checked on the basis of:

- installation table, which should be placed on the vehicle after the periodic inspection of digital recording equipment,
- the information saved in the memory of the digital recording equipment concerning the last calibration,
- technical data printout, in which the size of the wheels fixed in the car during the calibration was written.

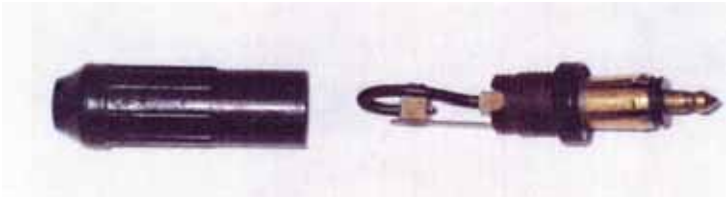

Fig. 6. Plug ("jack" type) acting on the indications of the digital tachograph

System of recording equipment may be exposed, due to its nature, to manipulation. All systems of tachograph cards, despite their numerous security equipment, are and will be exposed on

different types of manipulation to falsehood of data logged in their memory.

The use of recording equipment in road transport is necessary due to recording the driving and rest periods of drivers, and also to ensure the possibility to carry out by the competent authorities the effective inspections checking if the social rules are respected. To ensure the correct and reliable operation of these devices, and also to guarantee the possibility of recording and storing data, it is required to carry out periodic road checks and technical inspections, concerning the installed devices. Any attempt of the manipulation on records of digital recording equipment constitute a serious danger to road safety. They have also a negative impact on fair competition and the working conditions of road transport drivers, and also may cause unfair competition. In addition, they creates a serious threat to the security of the system of digital tachographs.

Authorities of the Member States should develop and implement procedures, together with the methods of research based on technological *know-how* that may contribute to the increase of the detection of the different way of manipulation of the digital recording equipment.

In addition, the drivers and companies who respect the social provisions in road transport should have the opportunity to trust the indication of digital recording equipment, and national control authorities throughout the European Union should have certainty as to the credibility and integrity of the data recorded and stored by the device, regardless of whether they come from the memory on-board unit or memory of the driver card. In order to guarantee the reliability of the data, it is necessary to keep equipment periodic inspections to ensure proper operation and use.

Member States are required to ensure that the checks were carried out in such a way as to ensure the effective implementation of community social legislation relating to road transport, however, this type of periodic checks cannot guarantee that devices for manipulation will not be installed and applied after finishing the inspection. Observations and experience demonstrate that possible detection of such devices is much greater during carrying out roadside checks, if a vehicle can be more precisely inspected.

3. Control of digital recording devices

Introduction of the digital tachograph in road transport had undeniably ensured:

- improving the efficiency and effectiveness of control of road haulage companies in road transport,
- the relevant standards in the field of social legislation and its harmonization in all the Member States of the European Union,
- strengthening the principles of fair competition,
- improving safety in road traffic.

The digital tachograph is a very important on-board device, used in road transport, due to control possibilities and enforcement of compliance with the legal provisions concerning the conditions of transport and social rules for drivers. Control of the road carriage (road transport and non-commercial carriage by road) it is the statutory task of the Road Transport Inspection (Article 50 of the Act of 6 September 2001 on road transport, Law Journal 2007, No 125, position 874, with changes). Additionally, police officers, Customs officers, border police inspectors and inspectors of the National Labour Inspection are also entitled to conduct the control of road haulage in area of the installation of tachographs in vehicles and the registration of the working time of drivers. The procedure of control on compliance with the provisions on periods of driving, minimum breaks and rest periods in road transport (both during roadside checks and checks in undertaking premises), as well as the required standard equipment of controlers and the list of basic elements which must be checked are determined by the regulation of Minister of Infrastructure of 2 September 2009 on the control of the carriage of goods by road (Law Journal No 145, position 1184). This regulation implements the directive 2006/22/EC of the European Parliament and of the Council of 15 March 2006 on minimum conditions for the implementation

of Council Regulations (EEC) No 3820/85 and (EEC) No 3821/85 concerning social legislation relating to road transport activities and repealing Council Directive 88/599/EEC **(***Official Journal L 102 , 11/04/2006, p. 0035 – 0044).*

According to these acts checks must be organized in such a way that:

- at least 3% of days worked by drivers of vehicles falling within the scope of Regulation (EEC) No 3821/85 and Regulation (EC) No 561/2006 are checked,
- not less than 30% of the total number of working days shall be checked at the roadside and not less than 50% of the total number of working days shall be checked at the premises of undertakings.

When performing inspection operations regarding compliance with the rules on periods of driving, minimum breaks and rest periods, the inspectors shall be equipped with the following devices able to:

- copy data from the digital tachograph installed in the vehicle and the driver card,
- read the downloaded data and its analysis or transmit the results of reading data to the office to make the analysis,
- make checks and detailed analysis of the confirmation of the digital signature attached to the data,
- analyze in order to determine the specific profile of the speed before the inspection of the registered equipment,
- check the sheets.

Optional equipment of the inspector includes especially devices able to make photocopies and photographic documentation.

The list of basic points which should be covered by roadside checks was defined in annex 5 to the mentioned above regulation of the Minister of Infrastructure on the control of road carriage and it includes the following elements:

- daily driving periods, breaks and daily rest periods,
- weekly driving periods and weekly rest periods,
- sheets from previous days, which should be in the vehicle in accordance with article 15, paragraph 7 of Council Regulation (EEC) No 3821/85 or data from the same period on the driver card, in memory of the digital tachograph or print with this device,
- cases exceeded the permitted speed of the vehicle,
- instantaneous speed reached by the vehicle, saved by the digital tachograph by not more than the previous 24 hours of use of the vehicle,
- correctness of operation and use of analogue equipment and digital recording equipment or record sheets or driver card.

In addition to elements during roadside check, at the premises of undertakings should be checked:

- weekly rest periods and driving times between these rest periods;
- observance of the two-weekly limitation of driving times;
- record sheets, vehicle unit and driver card data and printouts.

Nevertheless, to the control of vehicle unit, driver card data and printouts of the digital tachograph shall apply the provisions of § 10 of the regulation of the Minister of Internal Affairs and Administration of 18 July 2008 on the control of road traffic (Official Journal No 132, position 84, with changes). Inspector should check data in the memory of the digital tachograph and driver card through the insertion of the control card to the digital tachograph, and then display and viewing them, print or download using devices for copy the information. If the driver does not have a driver card or it is unable to use due to the damage, the inspector checks the data contained in the memory of the digital tachograph on the basis of the printout. The driver is required for writing on copy of printout, made by the inspector, his name and surname, driver card or driving licence number and signature (tab. 1).

Tab. 1. The catalog of infringements dealt with digital tachograph according to Polish Act on road transport (part I)

Position	Infringement	Penalty [PLN]
1	2	3
6.1.1	Performing carriage by road using vehicle that does not have the digital recording equipment	3.000
6.1.2.	Performing carriage by road using vehicle with a digital recording device, which does not register all required elements	2.000
6.1.3.	Performing carriage by road using vehicle with digital recording device, which does not register, at the same time, data dealt with periods of activities of all drivers who drive the vehicle in checked period	1.000
6.1.4.	Performing carriage by road using vehicle with digital recording equipment without the required periodical check, control check or calibration	1.000
6.1.5.	Performing carriage by road vehicle with digital recording equipment, by the driver without his own, valid card	1.000
6.1.6.	Performing carriage by road by driver without the required printouts of the tachograph driver card in case of damage, failure or its lack-for each missing printouts	100
6.2.1.	The digital tachograph does not register on driver card speed of vehicle, activity of driver and distance of travel	5.000
6.3.4.	Using the same driver card by more than one driver	3.000
6.3.5	Using the same driver card by more than one driver in the same time	1.000
6.3.7.	Showing during check in premises of undertaking data from driver card, digital tachograph or document confirming the fact of not driving the vehicle – for each day	500
6.3.9.	Showing during check in premises of undertaking incomplete data on the periods of driver activity – for each day	300
6.3.11.	Not making a copy of data from driver card – for each driver	500
6.3.12.	Not making a copy of data from digital tachograph – for each vehicle	500
6.3.13	Not showing during check in premises of undertaking data copied from digital tachograph and driver card, stored in undertaking – for each day	300
6.3.14.	Interference with the data written in digital recording equipment, driver card and undertaking card	5.000

Transport undertaking is liable for infringement dealt with obligation of installation and usage of digital tachograph, found by inspections. The penalty is imposed on the transport undertaking by administrative decision. Amount of fines for such infringement are set out in the annex no 3 to the Act on road transport. Part 6 of annex no 3 specifies 15 infringements dealt with digital tachograph and assigned them a penalty ranging from 100 to 5.000 PLN. Below there is a modified extract from the annex no 3 to the Act on road transport for infringements of the provisions on the use of the digital tachograph.

It must be underlined that the driver is also liable for infringement dealt with improper usage of digital tachograph. The infringements and penalties are described in annex no 1 to the Act on road transport. For instance, for performing carriage by road using vehicle with digital recording equipment with illegal additional device influenced on incorrect function of digital tachograph the driver should be punished fine of 2000 PLN.

The ratio of issued decisions on the imposition of a penalty payment to the number of checked vehicles in the year 2010 equals 15.4% (14,4% according to inspections of vehicles registered in Poland and 17,6% - vehicles registered abroad). In view of the comparison of the results of the checks carried out by the Road Transport Inspection from the beginning of its existence, it should be underlined the systematic decline in the number of checks with the imposition of the penalty by administrative decision in proportion to the number of controlled vehicles. The following chart shows the increase in compliance with the provisions of the transport by carriers, which covers the period from the beginning of activity of the Road Transport Inspection by 2010 (fig. 7).

The results of the roadside checks carried out by inspectors of the Road Transport Inspection indicate a statement of more than 172 000 infringements (in accordance with the annex to the Act on road transport). Approximately 70% of infringements were related to the provisions concerning driving and mandatory breaks and rest periods of drivers, over 15% of infringements were related to improper use of the recording equipment, while 10% constituted a violation of the requirements for the possession of the required licenses, certificates of accomplishment of the non-commercial, or documentation of drivers. Violations related to not paying by carriers the mandatory tolls on national roads is about 2% of the total number of infringements. The structure of infringements shows the fig. 8.

Of the total number of approximately 65 000 of infringements related to the non-observance of rules on social legislation for drivers in road transport, the most common is not allowed reduction of daily rest periods and driving time without required break. A detailed list of the number of infringements noted in respect of the working time of drivers shows the fig. 9.

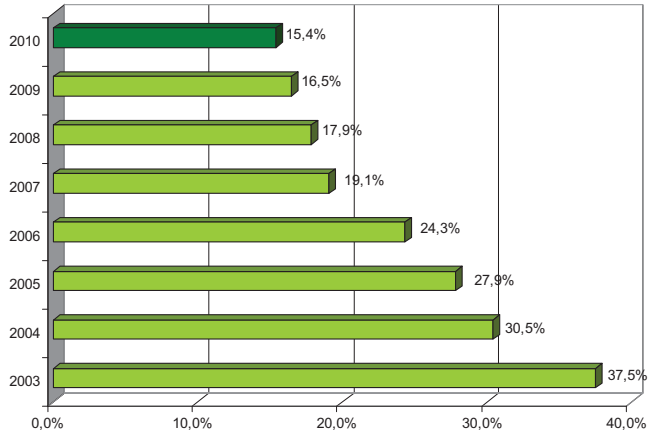

Fig. 7. The increase in compliance with the provisions of the transport

According to infringements referred to compliance by the drivers and traders with the provisions concerning the use of recording equipment cases of incorrect use of the recording equipment or the incorrect use of recorded sheets are very common. A detailed list of the number of infringements noted in the use of the recording equipment shows the fig. 10.

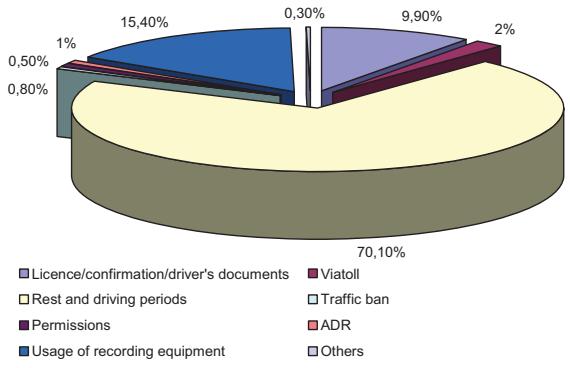

Fig. 8. The structure of infringements in road transport

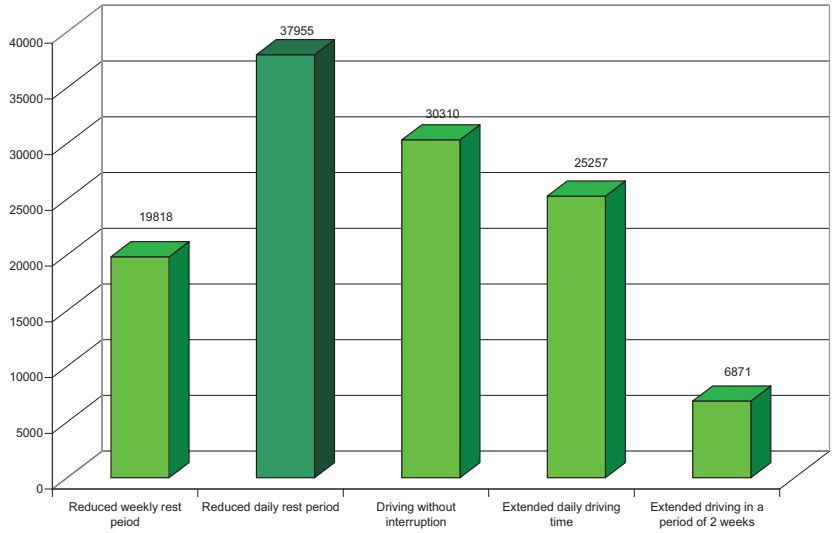

Fig.9. The number of infringements in road transport

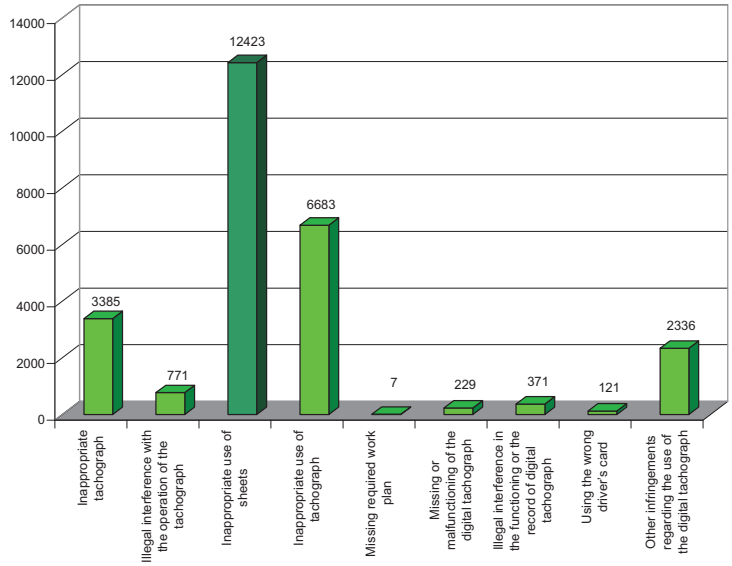

Fig. 10. The number of infringements in road transport in light of using recording equipment

Violations of the standards of the working time of drivers will also rise to the liability of the driver in the form of fines levied by the criminal mandate. This responsibility is independent of the responsibility of transport undertaking and aims to more effective compliance with the provisions concerning the standards of driving and mandatory breaks (fig. 11).

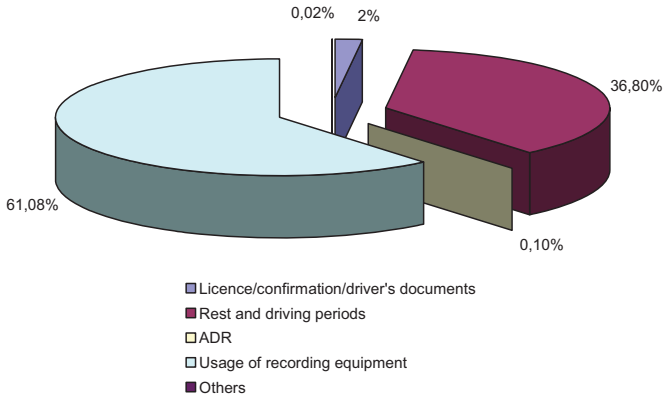

Fig. 11. The infringements number of standards of driving and mandatory breaks

As a result of the checks carried out in enterprises engaged in road transport in 2010 it was issued 2077 administrative decisions on the imposition of fines of value: 25 000 000 PLN.

As a result of checks carried out at the premises of undertakings, inspectors of the Road Transport Inspection claimed more than 243 000 infringements. More than 62% of the infringements concerned the incorrect use of the recording equipment, 36% of infringements related to the non-observance by the drivers of the provisions concerning driving and mandatory breaks and rest periods, but approximately 1% were infringements referred to the violation of the requirements for the possession of the required licenses, certificates of accomplishment of the non-commercial, or documentation of drivers.

4. Guidelines for prevention of tampering with a digital recording devices during roadside checks

One of the most important conditions of effective roadside checks is to ensure the proper training and full equipment for enforcement officers. "The digital tachograph is much like a burglar alarm in that the attacker only has to destroy confidence in it, by making it appear to be unreliable, in order to defeat it" [4] For that reason the inspectors should have a control card, and the appropriate tools to copy data from a memory on-board unit and the memory of driver card and analysis of these data or printouts, in combination with record sheets and any other documents relating to working time for drivers. Officers should also be provided with the necessary software enable quick and easy analysis of such data.

Regardless of whether the checks are carried out on the roadside, or in the premises and whether that they are related to compliance with periods of rest and driving, the roadworthiness or other aspects, officers of the control services could also be able to test the proper functioning and proper use of the equipment to detect cases of manipulation of these devices.

To achieve such tasks Member States should make the appropriate methodology and circumstances of conducting such additional checks. Therefore, the scope of these checks might be included in the national control strategy. Such methods as: method of two check points with the analysis of speed or distance, method of one check point with a detailed analysis of data or the method of one check point based on the technical inspection, increase the effectiveness of control. Ultimately, the officer could immediately order to carry out other vehicle inspection in the workshop.

The method of two check points with the analysis of the actual speed or distance. Using this method of inspection, officers could measure actual speed of the vehicle at a specific point using portable or installed in some place cameras, before stopping the vehicle. Then, they could copy file containing details of speed over the last 24 hours from on-board memory unit and compare registered speed in a given point with the speed measured several kilometres before. At the checkpoint, this method requires only the comparison of two numbers after reading a file containing details of speed over the last 24 hours.

Using the method of distance in time control, it is important to remember to select the point of inspection, located in a known distance from the specific place where officers have other means (bills of collected tolls, camera records, the protocols of border inspections) that enable to specify the moment, when a vehicle stopped in this place or not. Then, officers could copy a file containing details of the speed of vehicle for the last 24 hours from memory of on-board unit, and compare these data with the average vehicle speed, based on the known distance and time needed to reach the checkpoint.

Significant differences between read data and measured or calculated speed it is possible that the manipulation of the tachograph has been made. In that situation the vehicle could be directly checked in the workshop, without the need for additional inspection in the checkpoint.

In case of data read from the memory of on-board unit, it should be underlined that data was included with a digital signature, originally generated by the digital recording equipment or driver card in order to verify the authenticity and integrity of the data.

Method of one checkpoint with a detailed analysis of the copied data . In order to confirm the suspicions as to the presence of a device to manipulate, officers should compare data on driver's activity, copied from the memory of driver card and on-board unit with any documents in the vehicle and the driver's statement. Inconsistencies between these data could form the basis for suspicion and further action. In the next stage, it should be analyzed information about events and faults, including attempting to breach security, interruptions in power outage, move or sensor fault, especially registered within the last 5 days.

In addition, it should be analyzed the information including technical data, with particular regard to data concerning time adjustment or calibration data. The last group of data can be predominantly useful in finding too many cases of calibration, what may indicate that they have been carried out using the workshop card, which has been stolen or lost. Control officers should check the status of identified workshop cards, including their validity in days, when they have been used for the calibration of digital recording equipment.

If control officers continue to suspect irregularities after analysis of all the data, they could perform the copying file from the memory on-board unit, containing detailed data on speed for the last 24 hours and using specialized software to check whether there were unrealistic increases or decreases the acceleration of the vehicle, and whether the profile order is consistent with other documents in the vehicle, together with the statements of the driver (the number of breaks, speed in mountainous region or in urban areas).

Presented methods of inspection with obtained evidences may justify the suspicion of the use of the device in order to manipulate the indications of the digital recording equipment.

Method of one checkpoint with a special analysis of copied data requires disposal at the checkpoint an appropriate software to generate legible indications of speed changes in time, identify abnormal fluctuations in increasing speed and indicate automatically unrealistic rises or falls of the acceleration of the vehicle and any suspicious calibration of the recording equipment or any interruption of power.

Method of one checkpoint based on the technical control of seals . If it would be possible, officers should inspect the seals. If there is no seal or it is destroyed (damaged), then the driver should explain this fact. If the driver does not have a credible explanation, this may constitute the infringement and it is recommended to make directly an inspection of the vehicle in an authorised workshop.

Vehicle or data inspection in premises of undertaking. It is recommended that the competent authorities of the Member States use the possibility of controlling vehicles and on-board units, drivers with the cards drivers in the premises of transport undertaking. Data managed by the entity, must be kept for at least one year and must be available for inspection, on every request of control officers. For that reason, it could be checked any vehicle, which is located in the premises of transport undertaking. Additionally, it could be done any appropriate tests and activities, limiting to a minimum any delay, which driver could be exposed. Such controls could also cover the possibility of preparing and equipping control officers with suitable devices to enable verification of the recording equipment, in conformity with UE regulations [5] and [6].

5. Guidelines for prevention of manipulation of digital recording equipment during technical examination

If, after roadside check using the procedures of technical inspection, there is suspicion that it has been installed the device used to manipulate the indications of digital recording equipment, control officers would direct the vehicle to an authorised workshop. National authorities of the Member States may authorise to instruct the authorised workshop to make specific research to detect devices for manipulation.

In most cases, detailed examinations would enable the detection of erroneous pairing of the motion sensor and on-board units, which may indicate the presence of a device or equipment for manipulation. Such studies should include the control of seals and tablets of installation, testing a reference and an analysis of the copied data from the memory on-board unit.

In the case of detection of such devices, regardless whether they were actually used by the driver or not, the recording equipment should be removed from the vehicle and used as evidence. In addition, authorised workshops should be authorized to carry out the technical inspection for correct operation, correct recording and storage of data, and whether the calibration parameters are correctly set.

After all technical inspection and lack of detection of equipment used to manipulation of the indications, the recording equipment shall be subjected to a complete calibration and should be endorsed with a new measurement table together with the new seals, under the supervision of the regulatory authorities.

Detection of cases of the use of devices for the manipulation of the digital tachograph system and the prevention of their use is a continuous process, which requires constant engagement. With technological progress the quantity of possible interference in the system and possible risks increase. Consequently, all entities involved in ensuring the safety of the digital tachograph system, including control officers, authorized workshop, drivers and transport undertakings are very important in process of preventing the manipulation of digital tachograph.

Member States should aim to raise as much information and to develop their own strategies, threats, and also to provide a clear support in the dissemination of acquired knowledge, while a European Commission should be informed about new threats to the digital tachograph system.

Summary

Appropriate functioning of all elements of the system of digital tachographs enable to achieve the intended purpose. In general, the guarantee of security of the whole digital tachograph system is the closest cooperation of all elements of these system and the most correct functioning of each element. However, it must be underlined that in order to prevent the manipulation of the digital tachograph, first of all it is very important to provide for:

- a range of technical measures – the tachograph to be connected to a Global Navigation Satellite System device to automate the recording of the daily journey start and end location, a remote (wireless) communications function to provide a signal, only on request,

to allow an enforcement officer to assess whether to stop the vehicle for further checks and a harmonised interface to allow the use of Intelligent Transport Systems (ITS) with the tachograph;

- a requirement to ensure enforcement officers are appropriately trained, establishing the methodology for initial and continuing training.

References

[1] Blecker, T., Kersten, W., Meyer, M.: *High – Performance Logistics: Methods and Technologies*, Berlin 2009.

[2] Rychter, M.: *Budowa i zastosowanie systemu tachografii cyfrowej*, Warsaw 2010.

[3] Furgel, I., Lemke, K.: *A review of the digital tachograph system (in:) K. Lemke, Ch. Paar, M. Wolf, Embedded Security in Cars: Security Current and Future Automotive it Applications*, Birkhäuser 2006.

[4] Desworte, Y., Quiquater, J.J., Gollmann, C. Meadows, *Computer Security: Proceedings. Lourain-la-Neuve*, *5th European Symposium on Research in Computer Security,* Belgium, September 1998.

[5] Commission Regulation (EU) No 1266/2009 of 16 December 2009 adapting for the tenth time to technical progress Council Regulation (EEC) No 3821/85 on recording equipment in road transport (*Official Journal L 339 , 22/12/2009 P. 0003 – 0023).*

[6] Commission Regulation (EC) No 1360/2002 of 13 June 2002 adapting for the seventh time to technical progress Council Regulation (EEC) No 3821/85 on recording equipment in road transport (*Official Journal L 207 , 05/08/2002 P. 0001 – 0252).*

[7] MIDT documentation.

Journal of Polish CIMAC
Gdansk University of Technology
The Faculty of Ocean Engineering and Ship Technology

CHANGES OF OPTICAL PROPERTIES OF LUBRICATING OIL DURING ITS USE

Adam Stelmaszewski, Tadeusz Król

Gdynia Maritime University
ul. Morska 83-87, 81-225 Gdynia
tel.: +48 58 69 01 548
e-mails: a.stelmaszewski@wm.am.gdynia.pl; t.krol@wm.am.gdynia.pl

Abstract

The paper presents optical properties of mineral motor oil tested during its service in a car engine. The test was carried out in the question of oil detection and identification in water environment by means of optical methods. The light refraction and absorption coefficients were measured for the fresh oil and in particular state of its use. Light absorption as well as refractivity of oil increase during its use. The contrast, which the oil layer creates on the sea surfaces, slightly increases with oil use and this effect does not practical influence on the detection. Variations of light absorption disallow precise determination of the thickness of an oil layer. Furthermore, fluorescence spectra excited with ultraviolet radiation were measured. Both fresh and used oil has the greatest ability to photoluminescence in the range of wavelength between 300 to 400 nm. For all investigated wavelengths fluorescence increases with the time of oil use. Also shapes of spectra change. These changes disallow to determine the kind of oil by means of fluorescence methods.

Keywords: *oil, sea, identification, absorption, fluorescence, refraction*

1. Introduction

Petroleum is one of the most common pollutants of the marine environment and in some basins it is an almost constant component of seawater [4, 10]. Petroleum pollution is significant both in terms of magnitude, since the annual input of oil to global ocean is estimated at 1.3 million tons [10], and its adverse impact[1]. Petroleum occurs in various forms in seawater [6]. Each of these forms exerts its own individual influence on the environment. Among other, oil modifies the optical properties of the polluted water [7, 8, 12, 13, 14, 21]. These modifications are especially significant because of remote sensing, which makes it possible to collect data providing information for monitoring marine environment. Remote sensing is optical measurements based on the real physical relationship between the parameter of interest and the measured optical variable [16, 22]. Petroleum pollutant modifies results of these measurements. On the other hand, remote sensing is an primarily tool of the oil spill detection system nowadays [10, 22]. Moreover, remote sensing is used also for determination of petroleum pollutant in more details [1, 2], however this is limited by variability of oils. The oils – many kinds of crude oil and petrochemical products – vary

[1] Impact of the petroleum on the marine environment has been reported in many papers. A number of monographs [3, 4, 9, 10, 11] present lists of the relevant papers.

in their compositions and properties [5, 17]. The variability of oils is best reflected by their fluorescence spectra [20] and therefore fluorescence is a tool for identification of oil. Comparison of the total spectra allows even similar products of one kind to be distinguished [18].

Knowledge concerning optical properties of oil, especially its coefficients of light refraction and absorption, is the key to description its influence on any optical process. Lubricating oils create a separate group among many different petrochemical products [5]. The paper presents some results of investigations of the optical properties of a lubricating oil and changes of these properties occurring service in natural conditions. These investigations were carried out in the question of detection and identification of oil spills in marine environment and the current test is an extension of earlier work [19]. The refractivity and light absorption coefficient characterizing an oil in different stages of its use as well as its fluorescence spectra are presented here.

2. Methods

The aim of investigations was to determine changes, which occur in oil during its normal, constantly controlled service in a motor. The changes may be expressed as a dependence on the degree of oil use. The assumption was made that the changes would be followed during the whole period of oil service, without machine breakdowns and in the closed system (without oil leaks).

Such conditions satisfied the car FSO 125P (SUP115CC602119663), which was equipped with an engine FSO 115 (CC7652890278). This engine uses an all season mineral oil. The volume of oil in the motor was 3.6 dm^3. According to the instruction manual of the car, the oil should be changed after a year of exploitation or earlier – mileage could not exceed 5000 km. The decrease of oil amount resulted only from natural exploitation and after each sampling the same volume of fresh oil was supplemented. This procedure is similar as in ship motors, where also the same amount of oil is maintained in the lubricating system by supplementing. During the experiment the car was moderately used, in town (about 65 % of mileage) and outside town, almost entirely on hard roads. The engine most often worked at the average rotation velocity ranging from 35 s^{-1} to 50 s^{-1} and this speed never exceeded 70 s^{-1}. The average car speed was estimated at about 14 m/s (50 km/h). The car mileage served as a measure of oil use. The oil samples of volume 0.5 cm^3 were collected directly from the car engine.

The linear absorption coefficient describes the ability of medium to absorb light. The sense of this coefficient lays in the assumption that the relative decrease of intensity $-dI/I$ of monochromatic radiation as a result of its absorption by the homogeneous medium is proportional to the penetration path dl, which can be described as follows:

$$-\frac{dI}{I} = \alpha dl \,. \tag{1}$$

The constant α is a linear absorption coefficient and it depends on the radiation wavelength. In order to solve this equation, a function which combines radiation intensity I with the penetration path l in the medium must be applied:

$$I(l) = I^o \exp(-\alpha l), \tag{2}$$

where I^o denotes the radiation intensity which reaches the medium. In this shape the function expresses the Bouguer-Lambert Law. The length of the penetration path l is proportional to a number of absorption centers. If the medium is made of a solution of an absorbing of volume concentration C in a nonabsorbing solvent, then this function can be written as follows:

$$I(l) = I^o \exp(-\alpha C l), \tag{3}$$

which expresses the Bouguer-Lambert-Beer Law.

The determination of the linear absorption coefficient was made using the results of light transmission for oil or hexane solution, in the range of wavelengths from 210 nm to 730 nm. The

absorption coefficient was derived as follows:

$$\alpha = \frac{1}{C\,l} \ln \frac{T^o}{T}, \tag{4}$$

where T and T^o denote light transmissions for investigated solution and pure solvent.

The fluorescence spectra were measured for hexane oil solutions of constant concentration 10.0 ± 0.3 mg/dm^3. For each sample, measurements of 10 emission spectra, excited with light of wavelengths from 210 to 300 nm, every 10 nm, were made. Each spectrum was measured in the range of wavelengths from 240 to 500 nm, every 5 nm. According to the Bouguer Law, light intensity I_j^{em} of j-th wavelength (λ_j), emitted through the sample, is proportional to the intensity of the exciting light I_i^{ex} of i-th wavelength (λ_i):

$$I_j^{em} = \omega_{ij} I_i^{ex} \tag{5}$$

The proportionality coefficient ω_{ij} depends on the wavelength of the exciting radiation λ_i and emitted radiation λ_j:

$$\omega_{ij} \equiv \omega(\lambda_i, \lambda_j).$$

For a given exciting light wavelength λ_i the parameter ω is a function of the emitted light wavelength, which in the reminder of the paper will be called the spectral function. The dimensionless value W, which is proportional to the intensity of light emitted through the sample and the exciting light intensity, was measured directly:

$$W = k \frac{I_j^{em}}{I_i^{ex}} = k\,\omega_{ij}, \tag{6}$$

where k is a constant, independent of wavelength. Therefore, the spectrum measurement concerned the measurement of the spectral function ω for particular wavelengths, which were then multiplied by a certain constant.

The fluorescence and transmission spectra were measured using the spectrofluorimeter *Fluorat-02-Panorama*.[2] The measurements of light refraction coefficient n were made directly using the Abbe refractometer, for radiation of wavelength 590 nm and at stable temperature 20 ºC. The measurement accuracy was 0.0005.

3. Results

The test comprised the whole cycle of one year of oil exploitation. The car has driven 4734 km during this cycle. The all season mineral oil *Elf* type SAE 15W/40 SRI was tested in the experiment. Density of the fresh oil was 884 kg/m^3 (at temperature 20 ºC) and increased up to 892 kg/m^3 at the end of the test. During the exploitation the dynamic viscosity coefficient changed its value from 0.235 Pas to 0.146 Pas. In every time of the experiment the oil had not any contamination. Both fresh and used oil was entire dissoluble in hexane and gave a clear solution without any flock.

a. Fluorescence

For hexane solutions of the investigated oil the fluorescence is the most intense in the range of wavelengths from 300 to 400 nm. Chosen emission spectra (plots of spectral functions W) for fresh oil and used oil are presented in Figures 1 and 2. The spectra of the used oil vary significantly from spectra of fresh oil. These differences refer to both intensity of fluorescence and shape of the

[2] The set was made in the Research and Development Institute of Analytical Equipment *Lumex* in Sankt-Peterburg

spectra and they are noticeable after a short time of oil use. The most apparent differences in shapes are visible for spectra excited with light of wavelengths 240 and 250 nm.

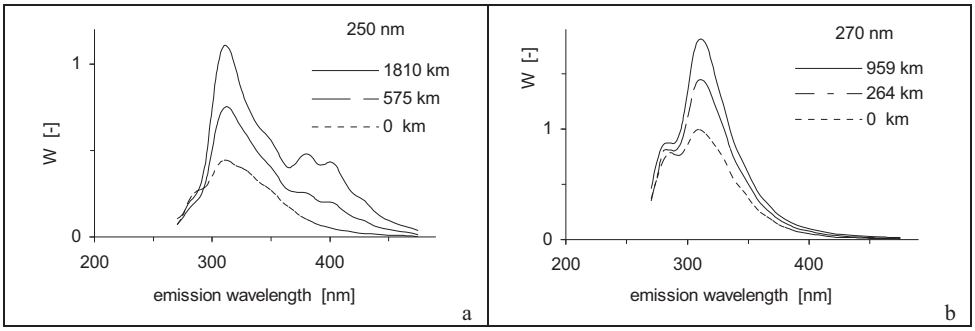

Fig. 1. Emission spectra W = W(λ) excited with radiation of wavelengths 250 nm (a) and 270 nm (b) of hexane solutions of oil after different mileage of the car, in kilometers

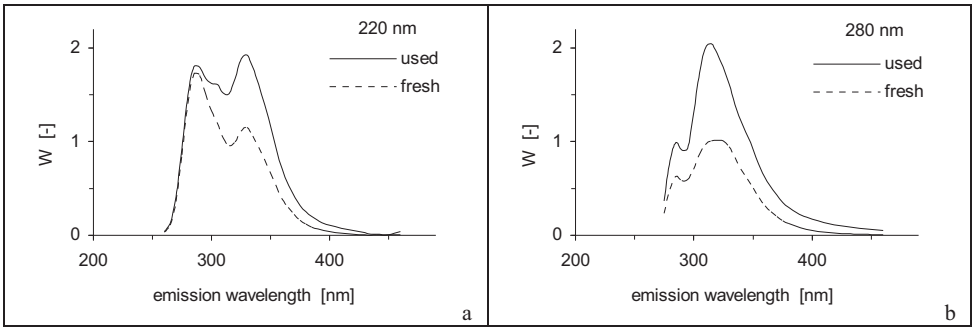

Fig. 2. Emission spectra W = W(λ) of hexane solutions of fresh oil (dashed line) and after mileage of 3320 km (solid line) excited with light of the wavelengths 220 nm (a) and 280 nm (b).

For all wavelengths of the exciting light the increase of fluorescence of the oil solution occurs with the longer oil use. Parameter ω, which is a function of the emitted light wavelength (λ) is also a function of energy quantum of this radiation. Therefore, fluorescence in the spectral area limited by the wavelengths λ_{min} and λ_{max} can be characterized by the radiation energy Ω, determined as follows:

$$\Omega = \int_{\lambda_{min}}^{\lambda_{max}} \omega(\lambda) \frac{h c}{\lambda^2} d\lambda \qquad (7)$$

where h is the Planck constant and c denotes the speed of light. Since only discrete values of function W have been determined, the total intensity of fluorescence Ω_i (for spectrum excited with light of i-th wavelength) may be evaluated as the following sum:

$$\Omega_i = \frac{2 h c \Delta\lambda}{k} \sum_j \frac{W_{ij} + W_{i(j+1)}}{\left(\lambda_{j+1} + \lambda_j\right)^2}, \qquad (8)$$

where $\Delta\lambda = 5$, λ_j has values 240 nm, 245 nm, ... 495 nm, and k is the constant from formula (4).

With oil use the increase of evaluated fluorescence energy of the oil hexane solution for all wavelengths of exciting light from the range 210 to 300 nm is observed. This increase is the best described by the power function of the car mileage x

$$\Omega(x) = \Omega_o(1 + ax^b), \tag{9}$$

where Ω_o is a fluorescence function for the fresh oil, while parameters a and b depend on wavelength of the exciting light. Figure 3 presents exemplary, relative fluorescence energies, related to energy of the solution of fresh oil ($\Omega^{rel} = \Omega/\Omega_o$), as a functions of car mileage.

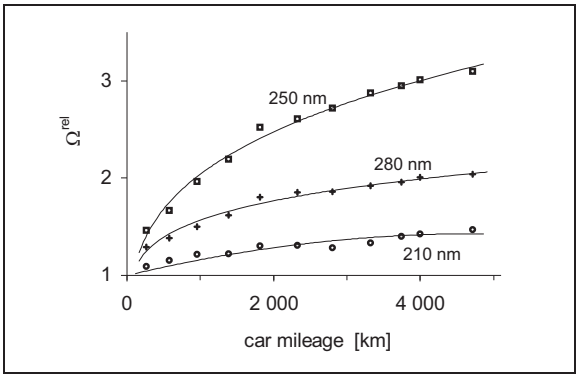

Fig. 3. Relative energy of fluorescence of oil hexane solutions Ω^{rel} (determined vs. energy of fresh oil solution) as a function of car mileage for spectra excited with light of the following wavelengths: 210, 250 and 280 nm.

b. Light absorption

Along with matter photoluminescence light is also absorbed. Absorption of the ultraviolet radiation in oil is very high and it decreases with the increase of light wavelength. The direct measurements of transmission in oil were possible for radiation of wavelengths $\lambda > 380$ nm. For shorter waves, the light intensity after passing through the cuvette, 1 mm thick, filled with oil, was negligible and thus in such cases the transmission in the hexane solutions was measured. Determination of the linear absorption coefficient from formula (4) requires that the light transmission was decreasing exponentially with an increase of the solution concentration (Beer Law). For tested oil this condition is satisfied for radiation of wavelengths longer than 400 nm (Fig. 4) and for such wavelengths the absorption coefficient was derived. For shorter wavelengths, the results of measurements of light transmission through solutions of the same concentration were used to determine the variations of the light absorption coefficient concerned with the oil use. A relative absorption coefficient A for particular samples of used oil versus the fresh oil was derived as follows:

$$A = \ln \frac{T_f - T}{T^o}, \tag{10}$$

where T_f, T and T^o denote the light transmission for a solution of the fresh oil, used oil and pure solvent, respectively.

Variations of light absorption coefficient for oil due to its use are presented in Fig. 5. The increase of light absorption by oil with its use is revealed. For radiation of wavelengths $\lambda < 500$ nm this increase is analogous to the increase of fluorescence energy (9). This dependence is not so obvious for longer wavelengths.

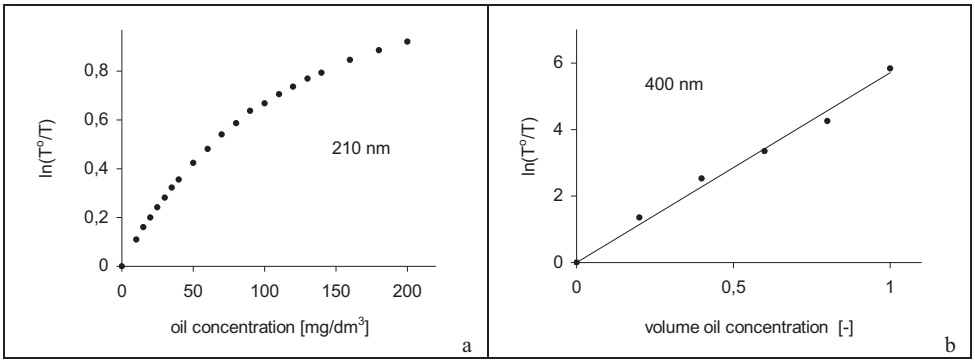

Fig. 4. Applicability of the Lambert-Beer rule: dependence ln(T°/T) on fresh oil concentration in hexane solution for light of wavelengths 210 (a) and 400 nm (b); T° – transmission through hexane, T – through solution

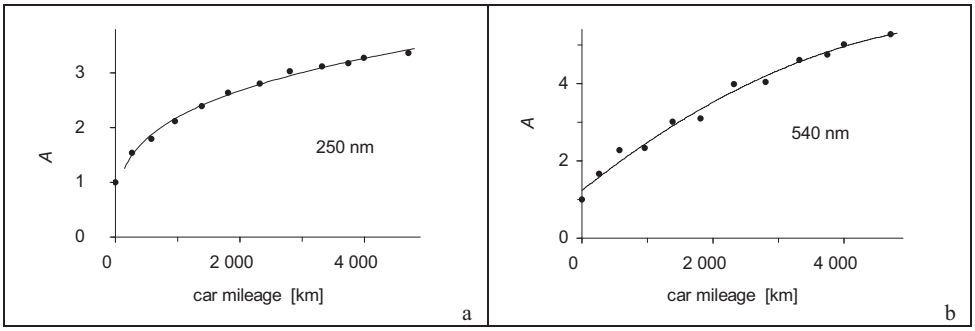

Fig. 5. Variations of relative light absorption coefficient A for Elf oil as a function of car mileage for radiation of the wavelengths 250 nm (a) and 540 nm (b)

c. Light refraction

The light refraction index n (refraction coefficient) for light of wavelength λ = 590 nm represents refractivity of a medium. Value of the index characterizing the fresh oil *Elf* is 1.4835. A small but systematic increase of this coefficient is observed along with the oil use. Value of n increased 0.001 per 1000 km of mileage during the test and the used oil have the index n = 1,489.

Along with increase of the light refraction coefficient the light reflection coefficient R increases. For perpendicular radiation the reflection coefficient R is combined with the refraction index n and the absorption coefficient α as follows:

$$R = \frac{4\pi(n-1)^2 + (n\lambda\alpha)^2}{4\pi(n+1)^2 + (n\lambda\alpha)^2} \quad (11)$$

For radiation of wavelength λ = 590 nm value of the absorption coefficient of the fresh oil α = 960 m^{-1} and increases with the oil use to 5100 m^{-1}, thus the product $n\lambda\alpha << n - 1$ and the dependence (11) may be written as follows:

$$R = \left(\frac{n-1}{n+1}\right)^2 \quad (12)$$

Contrast K between the oil and water surface is concerned with reflection coefficient. It is proportional to the difference in intensities of reflected radiation from both media related to total radiation intensity (with an assumption that the light intensity incident on both media is the same). Contrast is then a relative difference between both coefficients of light reflection from both media

$$K = \frac{I_o - I_w}{I_o + I_w} = \frac{R_o - R_w}{R_o + R_w}, \tag{13}$$

where: I_o and I_w denote intensity of light reflected from oil surface and water surface, and R_o and R_w denote coefficients of light reflection from oil and water, respectively. The assumed value of the refraction coefficient characteristic for sea water was accepted as 1.335. The contrast between water and oil, described as above, increases along with oil use, which is illustrated in Figure 6a.

Contrast between oil layer and water depends on the angle of light incident. For the angle of light incident $\varphi \neq 0$ light reflection coefficient is described by the Fresnel formula:

$$R = \frac{1}{2}\left[\frac{\sin^2(\varphi - \vartheta)}{\sin^2(\varphi + \vartheta)} + \frac{tg^2(\varphi - \vartheta)}{tg^2(\varphi + \vartheta)}\right];\ \vartheta = \arcsin\left(\frac{\sin\varphi}{n}\right). \tag{14}$$

For large angles light reflection coefficient increase and the contrast between oil and water decreases, however, the dependence of contrast on the use of oil remains unchanged (Fig. 6b).

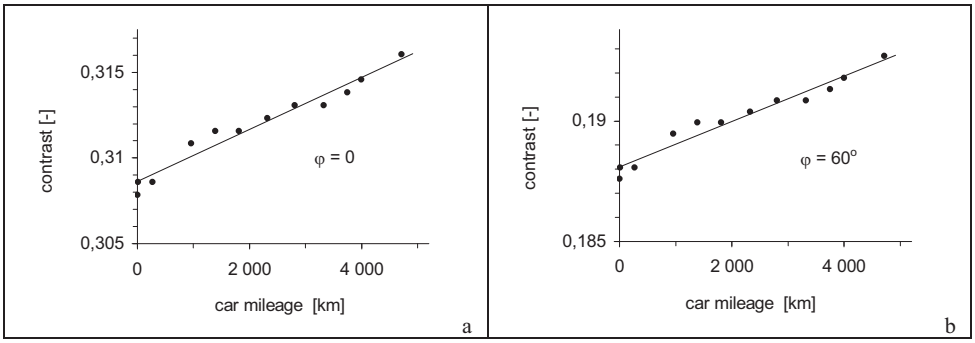

Fig. 6. Dependence of the contrast of the Elf oil layer vs. water on car mileage for radiation of wavelength 590 nm incident perpendicularly to the surface (a) and at an angle 60° (b)

4. Summary

During its use the lubricating oil changes and its optical properties change too. During use the following phenomena occur:

– linear absorption coefficient increases
– light refraction and reflection coefficients slightly increase
– the intensity of fluorescence increases and the shapes of its spectra change.

These phenomena generate concrete conclusions regarding application of optical methods to detect and identify oil spills based on the information about the properties of the oil spilled.

- Along with oil use the slightly increases the contrast, which the oil layer creates on the sea surface. This effects does not significantly influence the outcome of the detection.
- Variations of light absorption disallow precise determination of the thickness of the oil spilled by means of fluorescence method.
- Significant and increasing differences in oil spectra shapes along with oil use disallow to determine this substance, which is a derivative of the fresh oil by means of fluorescence methods.

References

[1] Drozdowska V., Zieliński T., Piskozub J., *Remote oil film thickness measurements on the water surface by means of water Raman signal attenuation*, Physicochemical Problems of Natural Waters Ecology, 5, 2007, 15-25.

[2] Gąsowski R., Mrozek-Lejman J., *Fluorometric method for determining the thickness of a crude oil film formed on the water surface*, Oceanologia, 36, 2, 1994, 121-135.

[3] GESAMP (IMO/FAO/UNESCOIOC/UNIDO/WMO/IAEA/UN/UNEP Joint Group of Experts on the Scientific Aspects of Marine Environmental Protection), *Impact of oil and related chemicals on the marine environment*, Reports and Studies 50, 1993, 180 pp.

[4] GESAMP *Estimates of oil entering the marine environment from sea-based activities*. Reports and Studies 75, 2007, 96 pp.

[5] Kajdas C., *Chemia i fizykochemia ropy naftowej*. WNT, Warszawa, 1979, 375.

[6] Kaniewski E., *Statek morski jako źródło zagrożeń ekologicznych*, Zagadnienia Eksploatacji Maszyn, 34, 1999, 151-163.

[7] Król T., *Absorption, scattering and attenuation of light by oil-in-water emulsions and other suspensions*, Physicochemical Problems of Natural Waters Ecology, 5, 2007, 8-10.

[8] Mrozek-Lejman J., Zieliński A., Król T., Witkowski K., *Light scattering in crude oil – sea water colloidal systems*, Oceanologia, 22, 1985, 21-33.

[9] NRC (National Research Council), *Oil in the Sea. Inputs, Fates and Effects*, The National Academy Press, Washington, 1985, 601 pp.

[10] NRC, *Oil in the Sea III: Inputs, Fates, and Effects*, The National Academies Press, Washington, 2003, 265 pp.

[11] NRC, *Assessing the Effects of the Gulf of Mexico Oil Spill on Human Health*: A Summary of the June 2010 Workshop, The National Academies Press, Washington, 2010, 185pp

[12] Otrmba Z., *The influence of an oil film covered sea surface on the reflection and upward transmission of light*, Oceanologia, 36, 1997, 137-154.

[13] Otremba Z., *Oil droplets as light absorbents in seawater*, Optics Express, 15, 14, 2007.

[14] Otremba Z., *Oil-in-water emulsion as a modifier of water reflectance*, Optica Applicata, 39, 1, 2009, 123-128.

[16] Parkinson C.L., Ward A., King M.D. (eds.), *Earth Science Reference Handbook – a guide to NASA's Earth science program and Earth observing satellite missions*, NASA, Washington, 2006, 277 pp.,

[17] Petrov A.A., *Petroleum hydrocarbons*, Springer-Verlag, Berlin, Heidelberg, New York, London, Paris, Tokyo, 1984, 255 pp.

[18] Stelmaszewski A.: *Fluorescence method for the determination of oil identity*, Optica Applicata, Vol. XXXIV, 3, 2004, 405-418.

[19] Stelmaszewski A.: *Badanie zmian właściwości optycznych oleju smarnego podczas jego eksploatacji*, Zeszyty Naukowe Akademii Morskiej w Gdyni, 54, 2005, 115-122.

[20] Stelmaszewski A.: *Discrimination of petroleum fluorescence spectra*. Luminescence, 22, 2007, 594-595.

[21] Stelmaszewski A., Król T., Toczek H.: *Light scattering in Baltic crude oil - seawater emulsion*, Oceanologia, 51, 3, 2009, 405-414.

[22] Zieliński A., 1983, *Zdalne metody pomiaru wybranych wielkości fizycznych morza*, Studia i Materiały Oceanologiczne, 42, 5-40.

Journal of Polish CIMAC
Gdansk University of Technology
The Faculty of Ocean Engineering and Ship Technology

DEVELOPMENT OF SHIP TECHNICAL REQUIREMENTS BY INTERNATIONAL MARITIME ORGANIZATION

Wieslaw Tarelko

Gdynia Maritime University
ul. Morska 81-87, 81-225 Gdynia, Poland
tel.: +48 58 6901331
e-mail: tar@wm.am.gdynia.pl

Abstract

The International Maritime Organization (IMO) is a specialized agency of the United Nations deals with international shipping. Its primary purpose is to develop and maintain a comprehensive regulatory framework for shipping and its remit today includes: safety, environmental concerns, legal matters, etc. In order to achieve its objectives, the IMO has promoted the adoption of some documents such as conventions, codes and recommendations concerning maritime safety, the prevention of pollution and related matters. Many of these documents include the ship safety requirements. In order to apply them to ships, they first should be generated, prepared and recorded. This paper deals exactly with the origins of ship safety requirements. Depending on the safety requirement origins, the IMO actions can get the reactive or proactive character. Reactive actions are used in response to a particular situation being observed, whereas proactive actions involve acting in advance of a future situation, rather than just reacting. It means taking control and making things happen rather than just adjusting to a situation or waiting for something to happen.
In the paper, development of safety technical requirements for ships is presented based on experience of the author as a chairperson of Polish department for Subcommittee of Ship and Equipment Design (DE) of International Maritime Organization.

Keywords: *safety, requirements, origination, ship*

1. Introduction

From the dawn of time, people had to reach agreements regarding various things, which facilitate their life. The Code of Hammurabi is one of the earliest known law codes and was probably compiled at the start of the reign of the Babylonian king Hammurabi (1792–1750 B.C.). It regulates in clear and definite the society organization. The Code is famous for demanding punishment to fit the crime (an eye for an eye) with different treatment for each social class. Its laws cover, inter alia: rent, the position of women, in inheritance, labour conditions. Such codification can be considered as a process of forming a legal code for example standards. They, in turn, have existed since the beginning of recorded history. Some of them were created by royal decrees. For example, King Henry I of England standardized measurement in 1120 AD by instituting the ell, which was equivalent to the length of his arm.
Agreements concerned ways of people communication appearing along with development of the human's civilization. In order to increase their quickness, the people had to unify them, for example railways. The invention of the railroad was a fast, economical and effective means of sending products cross-country. In fact, in the nineteenth century there were 70 railways with different gauges in England alone. For example, the Portland Company built and worked on cars

and locomotives of five or six different track gauges in the nineteenth century. This achievement was made possible by the standardization of the railroad gauge, which established the uniform distance between two rails on a track.
The first international bodies dealing with the unification and standardization of means of transport came into being in the nineteenth century. More or less in the same time it arose a need to establish international body dealing with a shipping especially its safety aspects. One of the most important tasks was to unify of tonnage measurement - a problem that had annoyed the shipping industry almost ever since ships were first constructed [1]. Another duty undertaken was to regulate safety aspects of maritime trade. Seafaring has always been one of the most dangerous occupations. The unpredictability of the weather and the vast power of the sea itself seemed so great that for centuries it was assumed that little could be done to make shipping safer. During the nineteenth century, this almost fatalistic attitude began to change. The invention of the steam engine meant that ships were less at the mercy of wind and tide. At the same time, maritime commerce was increasing and vast numbers of people were moving from continent to continent. Accidents involving the loss of hundreds of lives led to demands for action and several international treaties and agreements, which were developed as a result.

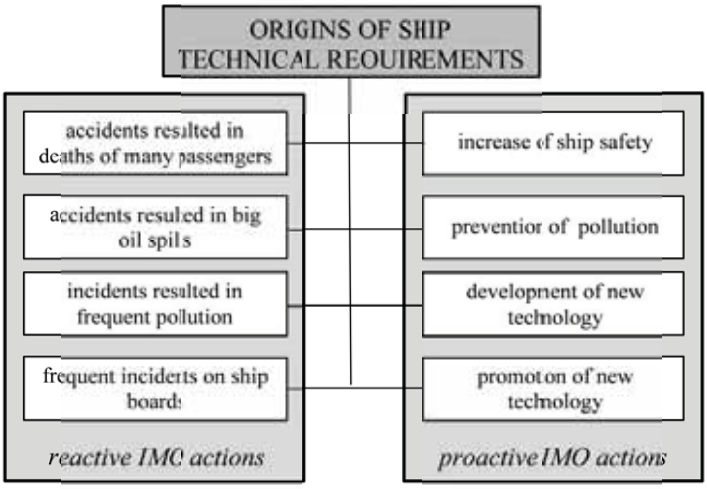

Fig. 1. Origins of ship technical requirements and types of IMO actions

Several countries proposed that a permanent international body should be established to promote maritime safety more effectively, but it was not until the establishment of the United Nations itself that these hopes were realized. In 1948 a conference convened by the United Nations in Geneva to consider the establishment of organization to deal with international shipping. The conference ended on 6 March 1959 with the successful adoption of a convention establishing the International Maritime Organization (IMO as the specialized agency of the United Nations. Its primary purpose is to develop and maintain a comprehensive regulatory framework for shipping and its responsibility today includes: safety, environmental concerns, legal matters, technical cooperation, maritime security and, the efficiency of shipping. In order to achieve its objectives, the IMO has promoted the adoption more than 40 conventions and protocols and adopted well over 700 codes and recommendations concerning maritime safety, the prevention of pollution and related matters. These IMO documents include many provisions concerning various technical aspects of the mentioned matters. Many of them include the ship safety requirements. In order to apply them to ships, they first should be generated, prepared and recorded. This paper deals exactly with the origins of ship safety requirements.
The ship safety requirements are generated on the IMO forum and they have various origins. Generally, they could be divided into several different groups (Fig. 1). Depending on the

mentioned sources, the IMO actions can get the reactive or proactive character. Reactive actions are used in response to a particular situation being observed, whereas proactive actions involve acting in advance of a future situation, rather than just reacting. It means taking control and making things happen rather than just adjusting to a situation or waiting for something to happen.

2. Reactive IMO actions

2.1. Accidents resulted in of numerous passenger's deaths

Milestones in developing ship technical requirements have been disasters of passenger vessels:

- Herald of Free Enterprise
- Estonia.

The *Herald of Free Enterprise* was a roll-on roll-off (RORO) car and passenger ferry. The ferry capsized on the night of 6 March 1987, moments after leaving the Belgian port of Zeebrugge, killing 193 passengers and crew. On the day the ferry capsized, the she was working the route between Dover and Zeebrugge. This was not her normal route and the linkspan at Zeebrugge had not been designed specifically for such a class of vessels. The linkspan used comprised a single deck and so could not be used to load lower deck and upper deck simultaneously (Fig. 2a). The ramp could also not be raised high enough to meet the level of upper deck due to the high spring tides being encountered at that time (Fig. 2b). This was commonly known and was overcome by trimming the ship bow heavy by filling forward. In such situation, the linkspan could meet the level of upper deck. Before dropping moorings, it was normal practice for the Assistant Boatswain to close the bow doors. However, the Assistant Boatswain had taken a short break after cleaning the car deck upon arrival at Zeebrugge. He had returned to his cabin and was still asleep when the harbour-stations call sounded and the ship dropped its moorings. The First Officer normally stayed on deck to make sure the doors were closed, but he had returned to the wheelhouse to stay on schedule. The Captain could only assume that the doors had been closed since he could not see them from the wheelhouse due to their construction and had no indicator lights in the wheelhouse. The ship left Zeebrugge and when the ferry reached 18.9 knots 90 seconds after leaving the harbour, water began to enter the car deck in large quantities. The resulting free surface effect destroyed her stability. In a matter of seconds, the ship began to list 30 degrees to port. The ship briefly righted herself before listing to port once more, this time capsizing. The water quickly reached the ship electrical systems, destroying both main and emergency power and leaving the ship in darkness.

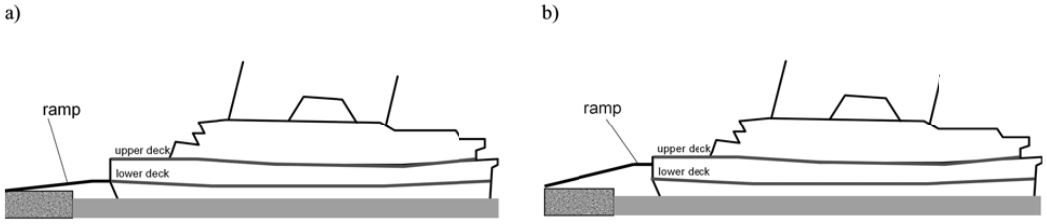

Fig. 2. The linkspan for a single deck used to load lower and upper decks: a) the linkspan uses to load the lower deck; b) the linkspan does not reach the upper deck

As the response of this accident, the new IMO regulations were introduced that prohibit an open (undivided) deck of this length on a passenger RORO vessel. Moreover, several improvements to the design of this type of vessel have been made, these include:

- indicators that display the state of the bow doors on the bridge,

– watertight ramps being fitted to the bow sections of the front of the ship,
– 'freeing flaps' to allow water to escape from a vehicle deck in the event of flooding.

The most important consequences of the *Herald of Free Enterprise* capsizing were introducing International Safety Management (ISM) Code. Because of the potential beneficial impact of the Code in advancing safety and pollution prevention the IMO Assembly recognized that the Code should be mandatory. The Assembly determined that the best way to achieve this was by adding the ISM Code to International Convention for the Safety of Life at Sea (SOLAS 1974) . In 1994, SOLAS was amended to add Chapter IX entitled 'Management for the Safe Operation of Ships'. The Code became mandatory for passenger ships, high-speed craft, oil tankers, and other cargo ships and to mobile offshore drilling units of 500 gross tonnage.

The stated purpose of the ISM Code is to establish minimum standards for safety management and operation of ships and for pollution prevention. The objectives of the Code are to:

– ensure safety at sea,
– prevent human injury and,
– avoid damage to the environment and to property.

The Code does not create specific operating rules and regulations, but provides a broad framework for vessel owners and operators to ensure compliance with existing regulations and codes, to improve safety practices and to establish safeguards against all identifiable risks.

The *Estonia* was a car and passenger ferry built in 1980. The ship sunk in the Baltic Sea on 28 September 1994, claimed 852 lives and was one of the deadliest maritime disasters of the late twenty century. According to the final disaster report, the weather was rough, with a wind of force 7–8 on the Beaufort scale and a significant wave height of 3 to 4 metres compared with the highest measured significant wave height in the Baltic Sea of 7.7 metres. The official report says that while the exact speed at the time of the accident is not known, the *Estonia* had very regular voyage times, averaging 16–17 knots, perhaps implying she did not slow down for adverse conditions. In the night, the bow visor (Fig. 3) (allows the bow to articulate up and down, providing access to the cargo ramp and storage deck near the water line) separated and the ship took on a heavy starboard list. Soon the vessel lurched some 30 to 40 degrees to starboard, making it practically impossible to move safely inside the ship. The official report blamed the accident on the failure of locks on the bow visor that broke under the strain of the waves. When the visor broke off the ship, it damaged the ramp that covered the opening to the car deck behind the visor [2]. This allowed water into the car deck, which destabilized the ship and began a catastrophic chain of events.

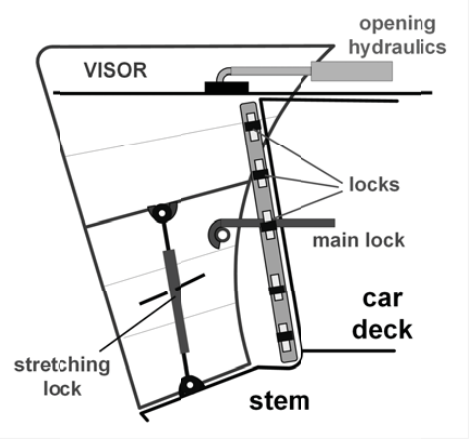

Fig. 3. The bow visor providing access to the cargo ramp and storage deck near the water line

As consequence of this disaster, the new SOLAS regulations regarding RORO passenger ships were introduced. The most important changes relate to:

- the ship stability (to ensure damaged ships have sufficient buoyancy to remain afloat),
- fitting with public address systems,
- full information on the details of passengers on board,
- the provision of a helicopter pick-up or landing area.

Moreover, the *Estonia* accident showed that lifeboats and life rafts alone could not effectively save lives. Therefore the new regulation was also introduced. It states that all RORO passenger ships shall be equipped with a fast rescue boat.

2.2. Accidents resulted in big oil spills

Typical examples of accidents resulted in the big oil spills were ships: Torrey Canyon, Amoco Cadiz, Exxon Valdez, Erika and, Prestige.

The *Torrey Canyon* was a super tanker capable of carrying a cargo of 120 000 tons of crude oil, which was shipwrecked causing an environmental disaster. At that time, the tanker was the largest vessel ever to be wrecked. On 18 March 1967, owing to a navigational error, the *Torrey Canyon* struck Pollard Rock on Seven Stones reef between the Cornish mainland and the Scilly Isles. An inquiry found that the ship master was guilty because he took a shortcut to save time in getting to Milford Haven. The disaster led to many changes in international regulations, for example the Civil Liability Convention (CLC) of 1969, which imposed strict liability on ship owners without the need to prove negligence, and the 1973 International Convention for the Prevention of Pollution from Ships.

The *Amoco Cadiz* was a very large crude carrier (VLCC) that ran aground on Portsall Rocks, 3.1 Nm from the coast of Brittany, France, on 16 March 1978, and ultimately split in three and sank, all together resulting in the largest oil spill of its kind in history to that date. A heavy wave hit the rudder of a ship causing to a lack of responding to the helm. In turn, this was due to the shearing of thread studs in the steering gear, causing a loss of hydraulic fluid. The major cause of this tragedy was the loss of steering because the steering system was a single system. The disaster led to many changes in international regulations, for example redundant steering systems.

On 24 March 1989, the oil tanker *Exxon Valdez* ran aground on the Bligh Reef causing a breach of the super tanker hull. The National Transportation Safety Board has presented findings [3]:

- failure of the third mate to properly manoeuvre the vessel, possibly due to fatigue and excessive workload,
- failure of the master to provide a proper navigation watch, possibly due to impairment from alcohol,
- the failure of Exxon Shipping Company to supervise the master and provide a rested and sufficient crew for the *Exxon Valdez*,
- failure of the U.S. Coast Guard to provide an effective vessel traffic system,
- the lack of effective pilot and escort services.

The *Exxon Valdez* disaster led to many changes of IMO legislation in history:

- mandates, among other things, double hulls-bottoms for tankers or an alternative,
- worldwide implications on tanker design, operation and economics.

The *Erika* was a 24 year old, single hulled, badly maintained ship. On the 12 December 1999, this ship ran into trouble in a heavy storm 40 Nm off the coast of Bretagne. The ship broke in half and sank to the bottom of the sea. Of the 30 000 tons of heavy furnace oil it carried, 14 000 tons spilled into the sea. Classification Society for classed the *Erika* reported that the tanker was in good condition, and that it routinely requires certificates of good condition for vessels more than 20 years old. It was the faulty inspection procedures by Classification Society. The *Erika* disaster led to many changes in IMO regulations, for example:

– single hull phase out,
– tighter inspections by class and port state control,
– establishment of European Maritime Safety Agency (EMSA),
– better information and monitoring,
– liability and compensation regime.

During stormy weather on 13 November 2002 the 26 years the old tanker *Prestige* suffered a 50 meters gash in the right side of the hull. She sunk to the depth of 3600 meters with a large quantity of oil still on board - spilled oil in excess of 5 000 tonnes. The leakage so far has affected more than 1000 km of coast in different degrees, from the North Portugal to the South West France. Prestige suffered a fracture in the side shell. The fracture of hull has enlarged due to the external wave forces, more cracks formed. Structural failure caused ballast tank flooding and heavy listing.

The *Prestige* disaster led to many changes in IMO regulations, for example:

– accelerate single hull phase-out,
– ban on heavy fuel oil transport by single hulls,
– ban on single hulls inside 200 mile zone.

2.3. Incidents resulted in frequent pollutions

Incidents resulted in the frequent marine pollution led to demands for reactive actions of IMO. Typical examples of origins such marine pollution can be:

– ship recycling,
– ballast water exchanges.

It is obvious that in the developing countries recycled materials have value whereas in the developed countries recycled materials do not have much value. Moreover, in the developed countries the cost of dismantling a ship is high (even when the process is mechanized) whereas in the developing countries the cost of dismantling a ship is relatively low. Consequently, the natural home of ship recycling is in developing countries. Ship breaking, scrapping, demolition in these countries are dangerous for health and safety of workers, and contaminate environment. The implementation of measures for health and safety and for the prevention of pollution is not considered essential in the developing countries.

Fig. 4. Concept of the Hong Kong Convention regarding ship recycling

As a result of reactive IMO actions, the Hong Kong International Convention for the Safe and Environmentally Sound Recycling of Ships was adopted in 2009. The Convention is aimed at

ensuring that ships, when being recycled after reaching the end of their operational lives; do not pose any unnecessary risks to human health, safety and to the environment (Fig. 4). The Hong Kong Convention intends to address all the issues around ship recycling, including the fact that ships sold for scrapping may contain environmentally hazardous substances such as asbestos, heavy metals, hydrocarbons, ozone-depleting substances and others. It also addresses concerns raised about the working and environmental conditions at many of the world ship recycling locations.

Shipping moves over 80% of the world commodities. Ballast water is essential for safe ship operation, balance and stability. Serious environmental problems occur when ballast contains marine life. The problem is compounded as most marine species have microscopic life cycle stages. Non-native species are considered the second greatest threat to biodiversity after habitat destruction. Many non-native species are capable of causing significant ecological, economic or human health impacts.

The ballast exchange at the deep ocean is the most practical approach to minimizing the introduction of aquatic species from ballast. Therefore, the International Convention for the Control and Management of Ships Ballast Water and Sediments was adopted at IMO in 2004. The Convention will require all ships to implement a Ballast Water and Sediments Management Plan. All ships will have to carry a Ballast Water Record Book and will be required to carry out ballast water management procedures to a given standard. Moreover, it includes general recommendations for current new buildings:

- minimize use of ballast water,
- design for efficient flushing,
- minimize uptake of sediments,
- facilitate removal of sediments,
- prepare for delivery of ballast water to shore facilities,
- prepare space for later installation of ballast water treatments systems, etc.

2.4. Frequent Incidents on Ship Boards

The shipping industry is experiencing an alarming number of accidents, for example:

- fatal accidents during drills life boats,
- fires triggered by oil fuel, lubricating oil and other flammable oil system.

In recent years, there have been a number of accidents during routine lifeboat drills, despite updated training and new designs of hooks, boats and davits. Part of the problem is the number of designs of hooks and lifeboats in service, estimated at more than 70, and it is essential that the crew are familiar with and capable of operating the equipment fitted on their ship. The shipping community recognizes that there is a problem, and new regulations have been enacted in an attempt to address this.

The IMO has recently initiated a number of amendments to SOLAS regulations in response to casualties involving lifeboats. Some of the more relevant changes include:

- lifeboats can be lowered without crew but must be launched with operating crew on board,
- (weekly drills) lifeboats (except free-fall) can be moved from their stowed position without crew on board,
- (monthly drills) lifeboats (except free-fall) can be turned out from their stowed position, weather permitting, without any crew on board.

The IMO sub-committee on Ship Design and Equipment are, at its meetings, reviewing:

- standard on-load release hooks and systems,
- changes to seat sizes in lifeboats,
- guidance for qualification and certification of personnel carrying out servicing and

maintenance of lifeboats, launching appliances and on load release gear,
- worldwide servicing facilities for lifeboats.

The IMO recognized that oil fuel, lubricating oil and other flammable oil system failures are a major source of shipboard fires. And also, there are many potential ignition sources in a machinery space, the most common being hot surfaces, e.g., exhaust pipes and steam pipes.
As a response of such situations, the IMO introduced regulation to convention SOLAS 1974 which states that all external high pressure fuel delivery lines between the high pressure fuel pumps and fuel injectors shall be protected with a jacketed piping system capable of containing fuel from a high pressure line failure. The jacketed piping system is composed to a jacketed pipe, means for collection of leakage and alarm device (Fig. 6). Each of them is designed by engine manufacturer or a factory which is certified by ISO or classification society.

3. Proactive IMO actions

3.1. Increase of ship safety

The large passenger vessel trade has increased dramatically in recent years and projections are for even greater increases in the future. This increase in business has been accompanied by an increase in vessel size and attendant public exposure. For example, the *Oasis of the Seas* has 16 passenger decks and can carry 5 400 passengers and a crew of 2 800. Operation of such large passenger ships generate many problems for ship-owners and caller harbours, regarding to:

- fire safety measures - such as escape routes and fire protections systems for the large atrium typical of cruise ships,
- life-saving appliances and arrangements,
- responsibility for Search and Rescue (SAR) at sea in the small country region,
- a tremendous amount of waste produced during voyages.

One is solution of fire safety measures is the concept of the ship as 'its own best lifeboat', what means that in the event of a casualty, persons can stay safely on board as the ship proceeds to port.
A comprehensive package of amendments to the IMO regulations affecting new passenger ships entered into force on July 2010. The amendments include, *inter alia*:

- alternative designs and arrangements,
- safe areas and the essential systems to be maintained while a ship proceeds to port after a casualty, which will require redundancy of propulsion and other essential systems,
- on-board safety centres, from where safety systems can be controlled, operated and monitored,
- fixed fire detection and alarm systems,
- fire prevention,
- time for orderly evacuation and abandonment.

3.2. Prevention of pollution

Ship emissions one of the last major ship pollutants to be regulated. The work started at IMO in the late 1980's. Annex VI to MARPOL convention was adopted in 1997 and was revised in 2010. Its essential provisions concern:

- prohibits Ozone Depleting Substances (ODS) in line with the Montreal Protocol,
- regulates exhaust gas: oxides of nitrogen (NOx) and sulphur oxides (SOx).

Annex VI prohibits deliberate emissions of ODS, which include halons and chlorofluorocarbons (CFCs). New installations containing ODS are prohibited on all ships. But new installations containing hydro-chlorofluorocarbons (HCFCs) are permitted until 1 January 2020.

NOx emission limits are set for diesel engines depending on the engine maximum operating speed (n, rpm). Tier I and Tier II limits are global, while the Tier III standards apply only in NOx Emission Control Areas.
Tier II standards are expected to be met by combustion process optimization. The parameters examined by engine manufacturers include fuel injection timing, pressure, and rate (rate shaping), fuel nozzle flow area, exhaust valve timing, and cylinder compression volume.
Tier III standards are expected to require dedicated NOx emission control technologies such as various forms of water induction into the combustion process (with fuel, scavenging air, or in-cylinder), exhaust gas recirculation, or selective catalytic reduction.
Annex VI regulations include caps on sulphur content of fuel oil as a measure to control SOx emissions and, indirectly, particulate matter (PM) emissions (there are no explicit PM emission limits). Special fuel quality provisions exist for SOx Emission Control Areas (SOx ECA or SECA).

3.3. Development of new technology

The IMO tries to keep up with the changes of technology. Examples could be the IMO provisions regarding development of Wing-in-Ground effect crafts (Fig. 7).

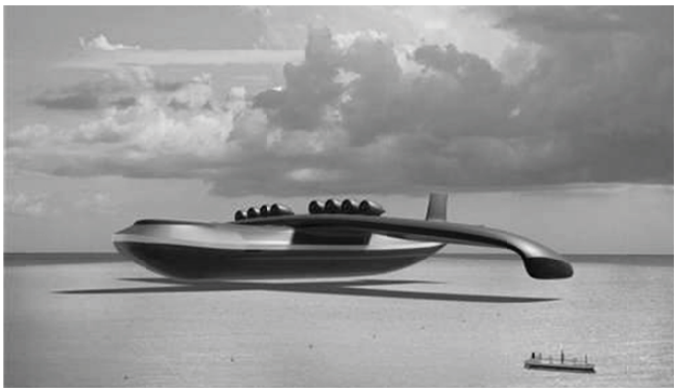

Fig. 5. Wing-in-Ground effect craft [5]

The WIG is a vessel with wings that cruises just above the water surface, it is floating on a cushion of relatively high-pressure air between its wing and the water surface. It is also known as a WIGE (Wing-in-Ground Effect), or a Wingship. It is the ultimate low-drag marine craft with a very high-speed, sea-based platform. Some WIG vehicles have the ability to fly without ground effect as well, but inefficiently as compared to aircraft.
The IMO has studied the application of rules based on the International Code of Safety for High-Speed Craft (HSC code) which was developed for fast ships such as hydrofoils, hovercraft, catamarans, etc. Accordingly, their arrangement, engineering characteristics, design, construction and operation have a high degree of commonality with those of aircraft. However, WIG craft operate with other waterborne crafts and must utilize the same collision avoidance rules as conventional shipping. Amendments to the International Regulations for Preventing Collisions at Sea take into account the operational peculiarities of WIG craft.

3.4. Promotion of new technology

The IMO promotes development of new technology increasing maritime safety, the prevention of pollution and related matters. For instance, to promote the prevention of oil pollution from machinery spaces of ships, it is very important to minimize the amount of oily

bilge water generated in machinery spaces. The IMO recognized the concept of an Integrated Bilge Water Treatment System (IBTS).
The IBTS concept was promoted by Japan and recognized by the IMO through its document MEPC.1/Circ 511 [5] as an excellent concept to minimize the amount of oily bilge water generated in machinery spaces and with an integrated means to process the oily bilge water and oil residue (sludge). In principle, the IBTS is a concept of an installation containing a bilge primary tank and proper control of the flow of drain streams, aiming to segregate as much as possible oily streams from the drain streams of clean water, and avoid their admixture. Unfortunately, ships which use oily water separator systems based on the IBTS concept have reported negative experiences with port state control officers who are not convinced that ships can generate significantly low oily water volumes. To avoid this, Japan and the International Association of Classification Societies (IACS) have suggested that ships equipped with installations based on the IBTS concept.

4. Preparation and enforcement of ship technical requirements

From the start, IMO has been primarily a technical organization, with shipping safety and pollution prevention being its greatest priorities. Its governing body is Assembly, which meets once every two years. Between its sessions, Council acts as the IMO governing body. Most of IMO work is carried out in a number of its committees and sub-committees. The Maritime Safety Committee (MSC) is the most senior of these. It has a number of sub-committees which titles indicate the subjects they deal with. The Marine Environment Protection Committee (MEPC) is responsible for co-ordinating IMO activities in the prevention and control of pollution of the marine environment from ships.
As it was mentioned, ship technical requirements should be generated, prepared and recorded. In order to do this, the IMO uses several types of documents. They can be divided into four different groups (Fig. 6):

- documents related with preparation international agreements,
- documents related with decisions of IMO bodies,
- documents related with preparation decisions of IMO bodies,
- documents related with realizing of decisions taken.

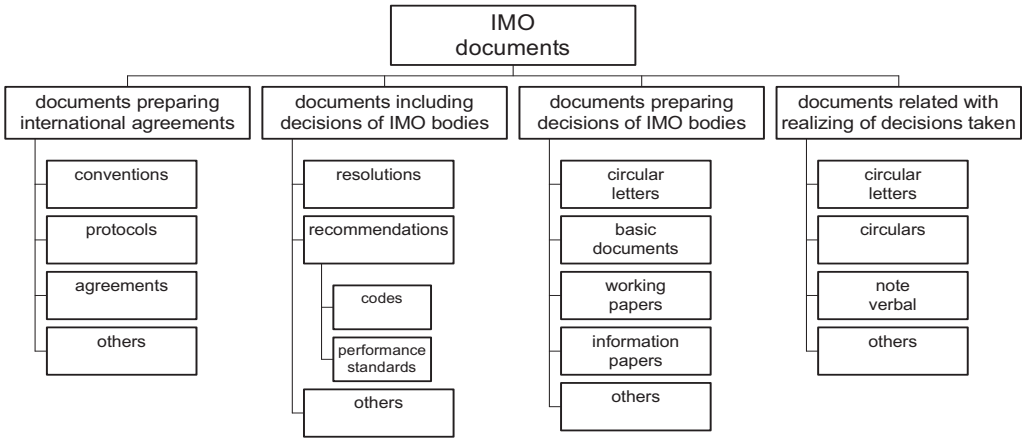

Fig. 6. Types of the IMO documents

All IMO bodies can make any decisions but only decisions taken by the Assembly, the Council, Maritime Safety Committee, and Marine Environment Protection Committee have legal meaning.

The IMO document management structure has been presented in Figure 7.

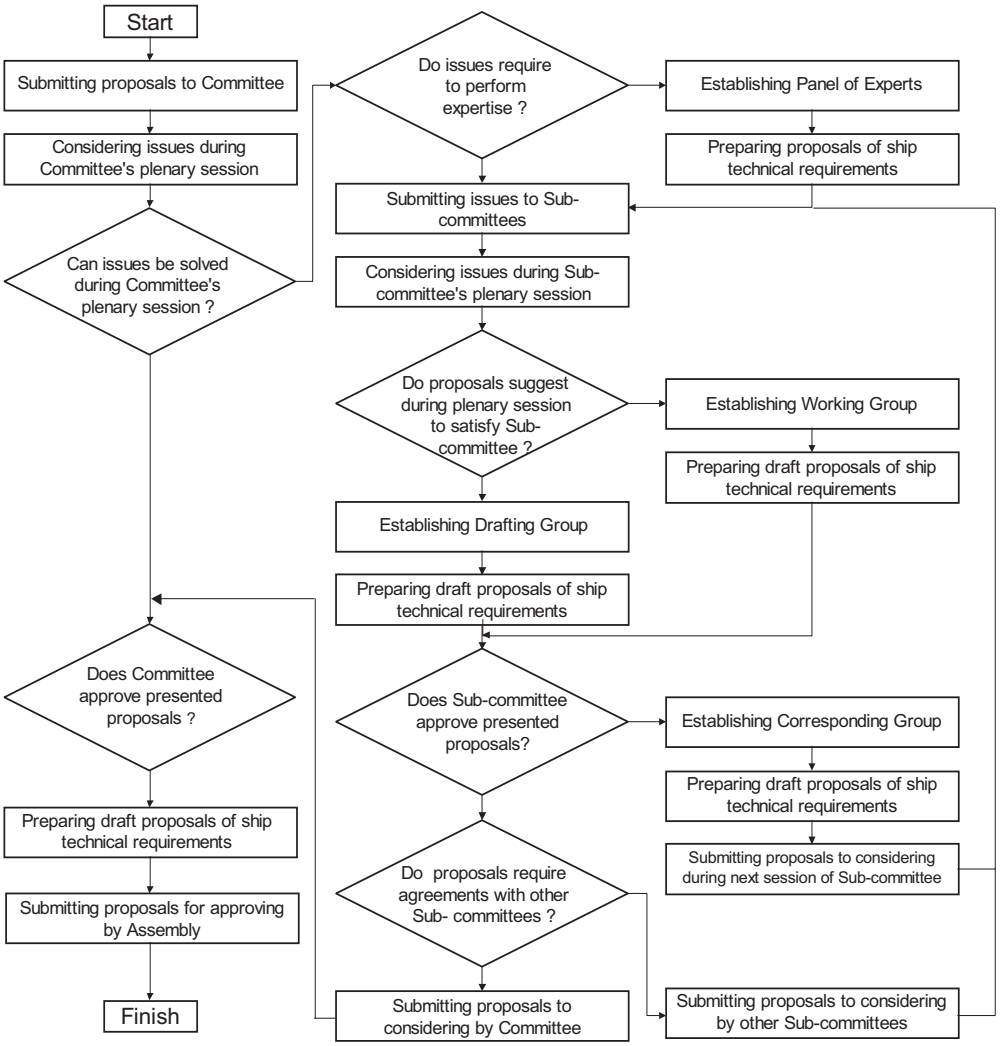

Fig. 7. Structure of the IMO document circulation

As a rule, the majority of IMO activities regarding to generating, preparing and recording of ship technical requirements have the proactive character. It means that the IMO policy based on the following assumptions:

- early stage identification of main factors that affect ship safety,
- development of regulatory action to prevent undesirable events,
- formulation of policy before event,
- formulation of policy after careful analysis of its implications.

The most important ship technical requirements have been reflected in the following IMO documents:

- the International Convention for the Safety of Life at Sea (SOLAS),
- the International Convention for the Prevention of Pollution From Ships (MARPOL).

The SOLAS Convention requires flag States to ensure that their ships comply with minimum safety standards in construction, equipment and operation. It includes articles setting out general obligations, etc, followed by an annex divided into twelve chapters.

The MARPOL Convention is designed to minimize pollution of the seas, including dumping, oil and exhaust pollution. It contains 6 annexes, concerned with preventing different forms of marine pollution from ships. Its stated object is: to preserve the marine environment through the complete elimination of pollution by oil and other harmful substances and the minimization of accidental discharge of such substances.
The majority of the IMO members have turned these international requirements into national laws. Flag states enforce IMO technical requirements through inspections of ships conducted by a network of international surveyors. Much of this work is delegated to bodies called classification societies.
However, flag state enforcement is supplemented by what is known as Port State Control, whereby officials in any country which a ship may visit can inspect foreign flag ships to ensure that they comply with international requirements. Port State Control officers have the power to detain foreign ships in port if they do not conform to international standards. As a consequence, most IMO regulations are enforced on a more or less global basis.

5. Conclusion

It is difficult to state precisely how effective the ship technical requirements have been in increasing shipping safety. Due to economic factors, the average age of the world ships has risen steadily. The fleets of the traditional maritime countries have declined, while many of the flags that are growing most rapidly have relatively poor records. Statistics show that old ships have more accidents than young ones.
The IMO, over the years of its existence, has continually evolved to meet changing conditions and requirements. Some of the IMO efforts have very significant results. For example, oil pollution of the sea is less of a threat now than it was 20 years ago.
As a result, nobody can be satisfied and the IMO is concentrating not only on better implementation of ship technical requirements but also on improving such factors as management and training.

References

[1] Vasudevan Aji. Tonnage Measurement of Ships: Historical Evolution, Current Issues and Proposals for the Way Forward. World Maritime University. Malmö, Sweden. http://www.wmu.sof.or.jp/fd2011_vasudevan.pdf
[2] Final Report- Research Study on the Sinking Sequence of MV Estonia. SSPA Consortium. 2008 http://www.sspa.se/files/estonia/Final-Report-Research-Study-on-the-Sinking-Sequence-of-MV-Estonia.pdf
[3] Skinner S. K., Reilly W. K. A Report to the President. The National Response Team. May 1989
http://docs.lib.noaa.gov/noaa_documents/NOAA_related_docs/oil_spills/ExxonValdez_NRT_1198_report_to_president.pdf
[4] Flightglobal - serious about aviation
http://www.flightglobal.com/airspace/media/concepts/wing-in-ground-effect-craft-10404.aspx
[5] Revised Guidelines for Systems for Handling Oily Wastes in Machinery Spaces of Ships Incorporating Guidance Notes for an Integrated Bilge Water Treatment System (IBTS). MEPC.1/Circ.511. 18 April 2006. International Maritime Organization. London.

Journal of Polish CIMAC
Gdansk University of Technology
The Faculty of Ocean Engineering and Ship Technology

THE PROGNOSIS OF MACHINES CONDITION STATE

Henryk Tylicki

University of Technology and Life Science
ul. S. Kaliskiego 7, 85-789 Bydgoszcz, Poland
tel.: +48 52 3408208, fax.: +48 52 308283
e-mail:tylicki@utp.edu.p

Abstract

In this paper we introduce problem of estimating state prognosis algorithms which are the basis for determining conclusion rules for estimating the next machine operation term.

Keywords: *machine state prognosis, procedure algorithmization, conclusion rules*

1. Introduction

Using in the exploitation process methods of machine state prognosis as a basis for automatization of state recognition process, it requires the diagnostic parameters sets optimization and prognosis methods. The solution of these problems depends on many factors connected with the level of machine complexity, application of multi-symptom observations, and exploitation process quality. The prognosis of vehicles' states is a process which ought to enable the anticipation of machine's state in the future, basis on an incomplete history of diagnostic tests research results. It allows to estimate the time of a faultless machine usage or the value of work done by it in the future.
In the process of state prognosis, very important problem is to choice [1]:

a) a set of diagnostic parameters depending on the machine's work time, quality of time step and the size of an optimal diagnostic parameters set;
b) prognosis method depending on the prognosis horizon, the minimal number of elements of time row indispensable for running the prediction and the machine's operation time.

The question of testing the above problems in the process of machine state prognosis, as well as the legal acts concerning the users' safety and environmental protection, are an impulse for searching new diagnostic methods and determining new measures and tools describing their contemporary states in their exploitation process, which are further presented as appropriate procedures, algorithms and conclusion rules.

2. Optimization procedure of diagnostic parameters sets

Diagnostic parameters set is derived from the set of output parameters. Basis on researches results, aiming at confirming some of the proposals included in works concerning the reduction of diagnostic information in prognosis process, it is considered that the determination of diagnostic parameters set in the process of machine state prognosis ought to include:

a) the ability to reflect the machine state changes in exploitation time;
b) the quantity of information on the machine's state;
c) relevant changeability of diagnostic parameters values in the machine's exploitation time.

The above postulates can be presented as methods. They are [1,2]:

1. Correlation method of diagnostic parameters values with the machine's state. It consists in examining the correlations of diagnostic parameters values with the state of the machine $r_j=r$(W, y_j) (or the time of machine's exploitation ($r_j = r((\Theta, y_j))$:

$$r_j = \frac{\sum_{k=1}^{K}(\Theta_k - \overline{\Theta})(y_{j,k} - \overline{y_j})}{\sqrt{\sum_{k=1}^{K}(\Theta_k - \overline{\Theta})^2 \sum_{k=1}^{K}(y_{j,k} - \overline{y_j})^2}} \tag{1}$$

$$\overline{\Theta} = \frac{1}{K}\sum_{k=1}^{K}\Theta_k \ , \quad \overline{y_j} = \frac{1}{K}\sum_{k=1}^{K} y_{j,k} \ , \tag{2}$$

where $r_j = r(W, y_j)$, j = 1,..., m – coefficient of correlations between variables the W (state of the machine) and y_j; $r_{jn} = r(y_j, y_n)$; j, n = 1,..., m; j≠n – coefficient of correlations between the variables y_j and y_n.

In case of lack of data from the set W, they are replaced, assuming that the determination of state recognition procedures is realized within the range of normal wear, with the time of machine's exploitation. Then, $r_j = r(\Theta_k, y_j)$; j=1,..., m; k=1,...,K (r_j – coefficient of correlation between the variables $\Theta_k \in (\Theta_1, \Theta_b)$ (Θ_k – machine's exploitation time) and y_j).

2. Method of informational size of diagnostic parameter. The object of this method consists in the choice of the parameter which provides the largest quantity of information on the machine's state. A diagnostic parameter is the more important for the state change estimation, the more it is correlated with it and the less it is correlated with other diagnostic parameters. This relation is presented in the form of the size indicator of the diagnostic parameter h_j, which is a modification of the indicator relating to the set of variables explaining the econometric model [12]:

$$h_j = \frac{r_j^2}{1 + \sum_{j,n=1, j\neq n}^{m} \left| r_{j,n} \right|} \tag{3}$$

$$r_{j,n} = \frac{\sum_{k=1}^{K}(y_{j,k} - \overline{y_j})(y_{n,k} - \overline{y_n})}{\sqrt{\sum_{k=1}^{K}(y_{j,k} - \overline{y_j})^2 \sum_{k=1}^{K}(y_{n,k} - \overline{y_n})^2}} \tag{4}$$

$$\overline{y_j} = \frac{1}{K}\sum_{k=1}^{K} y_{j,k} \ ; \quad \overline{y_n} = \frac{1}{K}\sum_{k=1}^{K} y_{n,k} \tag{5}$$

In case of lack of data from the set W, they are replaced, assuming that the determination of state recognition procedures is realized within the range of normal wear, with the time of machine's exploitation.

An advantage of the presented methods is a fact that both allow to choose single-element as well as multi-element sets of diagnostic parameters from the set of output parameters. A single-element set refers case, when the machine is decomposed into units, and it is necessary to choose one diagnostic parameter. A multi-element set is acquired when in presented procedures less strict limitation is used, which consists in classifying into the diagnostic parameters set these parameters

whose indicator values are higher (lower) than, accepted respectively for the method, high (low) positive numbers.

The estimation methodology algorithm of the optimal machines diagnostic parameters set consists stages [2,3]:

1. Data acquisition:
   a) the set of diagnostic parameters values in the function of machine's exploitation time $\{y_j(\Theta_k)\}$, acquired in the time of passive-active experiment realization, where $\Theta_k \in (\Theta_1, \Theta_b)$;
   b) the set of diagnostic parameters values: $\{y_j(\Theta_1)\}$ – nominal values, $\{y_{jg}\}$– boundary values, j=1,…, m;
   c) the set of machine's states $\{\Theta_k: \{s_i\}$, k=1, …, K; i=1,…, I} determined in the time of passive-active experiment realization, where $\Theta_k \in (\Theta_1, \Theta_b)$;;

2. The optimization of diagnostic parameters set values (only in case of large size of Y, e.g. m>10). Diagnostic parameters set is estimated with use of:
   a) correlation method of machine's state diagnostic parameters (exploitation time), $r_j = r(W, y_j)$, $(r_j = r((\Theta, y_j))$
   b) method of machine's state diagnostic parameters information quantity h_j.

In order to choose a diagnostic parameters set, weight values are used:
   a) standardized calculation weights w_{1j}:

$$w_{1j} = \frac{1}{d_j}, \; d_j = \sqrt{(1 - r_j^*)^2 + (1 - h_j^*)^2} \tag{6}$$

$$r_j^* = \frac{r_j}{\max r_j}, \; h_j^* = \frac{h_j}{\max h_j} \; ; \tag{7}$$

   b) as the criterion of diagnostic parameter (diagnostic parameters) selection, the maximization of the values of weights w_{1j} and the diagnostic parameters selection according to the above criterion were accepted.
   c) in order to consider the user's preferences, it ought to be possible for him/her to insert the weights w_{2j} (standardized values) from the range (0,1) and choose parameters according to the above criterion.

3. The procedure of machine state prognosis

The machine's state prognosis process can by realized with different methods at the same time that determine the aim and form of the prognosis [4,5,6,7,8]. Applying the criteria concerning the requirements are connected with:
   a) the form of prognosis (forecasted symptom value, machine operation date or another for machine state prognosis);
   b) the influence of machine's exploitation changes and maintenance actions conditions over the machine's exploitation characteristics, which should be considered while choosing the prognosis method;
   c) possible to use prognosis methods (e.g. extrapolation trend methods and adaptation methods) [4,9]

several solutions are possible.

One of them is usage the diagnostic parameter value change in function of machine exploitation. It uses the assumption that the phenomenon of the machine's technical state worsening is represented by the time row $y_\Theta = \langle y_1, y_2, ..., y_b \rangle$, i.e. the set of discrete observations $\{y_\Theta = \zeta(\Theta); \Theta = \Theta_1, \Theta_2, ..., \Theta_b\}$ of a certain non-stationary stochastic process $\zeta(\Theta)$. As the acceptable period of the machine's usage, accepted is the time of it's work in which the boundaries of mistake range for separate prognoses determined on the subset $\Omega^y \subset \Omega$ of available realizations

of the observed parameters $\{y_j(\Theta)\}$and their prognoses $\{y_{j,p}\}$ according to the accepted predictor $P(y_\Theta,\tau)$ do not exceed the boundary values $\{y_{j,gr}\}$ [11].

The date of the next operation Θ_{b1} of the machine is therefore determined by the prognosis time horizon τ^* [2,11,12]:

a) for which there will be no excess of the diagnostic parameter boundary value y_{gr} by the boundary of the prognosis mistake range appointed by the radius r_σ;
b) for which there will be no excess of the diagnostic parameter boundary value y_{gr} by the forecasted value of the diagnostic parameter;
c) for which there will be no excess of the diagnostic parameter boundary value y_{gr} by the estimated value of the diagnostic parameter;
d) for which there will be no excess of the diagnostic parameter boundary value y^*_{gr} by the value of the diagnostic parameter at the time Θ_b.

In the levelling method of prognosis mistake value for the value Θ_{b1} are acceptable values of the time determined by the horizon value τ^*, appointed as the intersection point of the line of diagnostic parameter boundary value y_{gr} with the bottom (with the assumption that $y(\Theta_b) > y_{gr}$) or top (with the assumption that $y(\Theta_b) < y_{gr}$) boundary of the prognosis mistake range appointed by the radius r_σ for the trust level $1-\gamma=0,95$ or $1-\gamma=0,99$, which corresponds to the probability of the value $p=0,05$ or $p=0,01$ that in the range appointed by the horizon τ^* the diagnostic parameter will reach the boundary value y_{gr}.

Then, the following interpretations of the obtained terms are possible:

a) not exceeding by the controlled diagnostic parameter the boundary appointed by the radius $r_\sigma^{0.01}$ is interpreted as the alarm signal for thorough and more accurate diagnostic observation of the vehicle's unit or system;
b) exceeding by the controlled diagnostic parameter the boundary appointed by the radius $r_\sigma^{0.01}$ is interpreted as the lack of alarm signal for thorough and more accurate diagnostic observation of the vehicle's unit or system (alert threshold);
c) the moment of exceeding by the controlled diagnostic parameter the boundary appointed by the radius $r_\sigma^{0.05}$ is interpreted as the time Θ_{b1} – the operation date of the vehicle's unit or system (alert threshold).

In such situation, the time range (Θ_1, Θ_b) will be the estimation period of the prognosis mistake expected value e_p and the boundary radius of the prognosis mistake range r_σ, whilst the time period after Θ_b will be the period of the active prognosis, i.e. estimation of:

a) the prognosis value of diagnostic parameter after prognosis horizon time τ, $y_{jp}(\Theta_b+\tau)$;
b) the estimation of the value of boundary radius of the prognosis mistake range $r_\sigma(\Theta_b+\tau)$;
c) the estimation of the next diagnosis and operation time of the machine Θ_{b1}.

In the levelling method of diagnostic parameter boundary value the date of the next operation of device Θ_{b1} is determined by the horizon value τ^*, estimated as the intersection point of the diagnostic parameter trend line $y(\Theta)$ with:

a) the bottom (with the assumption that $y(\Theta_b)>y_{gr}$) border of the boundary value y_{gr}^*:

$$y_{gr}^* = \frac{1}{10}\left| y(\Theta_1) - y_{gr}\right| + y_{gr} \tag{8}$$

b) or the top (with the assumption that $y(\Theta_b) < y_{gr}$) order of the boundary value y_{gr}^*:

$$y_{gr}^* = y_{gr} - \frac{1}{10}\left| y(\Theta_1) - y_{gr}\right| \tag{9}$$

The values $S_p(\Theta_b+\tau)$ and Θ_{b1} are estimated with one of the prognosis methods, whilst the date of diagnosis and operation according to the relation:

$$\Theta_{b1} = \Theta_b + \frac{\tau\ (y^*_{gr} - y(\Theta_b))}{y(\Theta_b + t) - y(\Theta_b)} \tag{10}$$

In the method of determination of the diagnostic parameter value change, with the assumption of:

a) exponential decomposition of the diagnostic parameter at the time Θ_b;
b) probability of the machine's reliable work P_r: $1 < P_r < 0.8$
c) dynamics of the parameter S growth in the time (with $S(\Theta) < S_{gr}$):

$$S(\Theta) = \frac{S(\Theta_b)}{S_{gr} - S(\Theta_b)} \tag{11}$$

The value Θ_{b1} is estimated as:

$$\Theta_{b1} = \frac{(1 - P_r)(S_{gr} - S(\Theta_b))}{S(\Theta_b)}\Theta_b \tag{12}$$

In the date estimation method Θ_{b1} the effort to simplify the procedures of date estimation Θ_{b1} led to creating the date estimation method Θ_{b1}, in which there is no need to estimate the prognosis value of the parameter y_p. In this method, like in the levelling method of the boundary value, a certain level of the boundary value y^*_{gr} is determined, different from the boundary value y_{gr}, e.g. according to the relation (8,9) and compared to it the diagnostic parameter value. Then, as the date of the next device operation Θ_{b1} it is suggested to accept the value of working time (course) of the machine, determined by the horizon value τ^*, estimated as the intersection point of the diagnostic parameter value $y(\Theta_b)$ with the value y^*_{gr}:

$$\Theta_{b1} = \Theta_b \tag{13}$$

The estimation of the date Θ_{b1} on the basis of the presented methods is determined by many problems, most important of which are:

a) the determination of the optimal diagnostic parameter set describing the change of the machine state in function of its "lifetime";
b) the determination of weight function for a multi-element optimal set of diagnostic parameters;
c) the determination of "the best" method for date estimation Θ_{b1}.

The solution of the above problems, as it show in [2,11,13] requires the use of appropriate multi-criteria optimization methods and prognosis methods enabling the estimation of the prognosis value of the diagnostic parameter $y_{j,p}$ and the necessity to know the boundary value of the diagnostic parameter y_{gr}.

Analyzing, basis on researches results, presented methods of diagnosis and operation term estimation, the most suitable methods are:

a) method of levelling the prognosis mistake;
b) method of levelling the diagnostic parameter boundary value.

The algorithm of machine state prognosis includes the following stages [2,14]:

1. The prognosis of the diagnostic parameter value y_j^*:
   a) with the Brown-Mayer adaptation method type 1 (B-M1) with the coefficient $\alpha = (0.5 - 0.8)$ and for the prognosis horizon $\tau = (1 - 3)\Delta\Theta$ determined for the time range (Θ_1,Θ_b),
   b) with the Holt adaptation method with the coefficient $\alpha_1 = (0.6 - 0.8)$ and $\alpha_2 = (0.4 - 0.8)$ for the prognosis horizon $\tau = (1 - 3)\Delta\Theta$ determined for the time range (Θ_1,Θ_b),
   c) with the use of analytical methods (linear, exponential for the prognosis horizon $\tau = (1 - 3)\Delta\Theta$ determined for the time range (Θ_1,Θ_b),
2. The estimation of the next operation and diagnosis date for the machine Θ_d:

a) Θ_{d1} with the prognosis mistake levelling method for the radius of the prognosis mistake r_p (for the importance level β=0,05) according to the relation:

$$\text{for } y_j(\Theta_b) > y_{jg}: \qquad \Theta_{jd1} = \Theta_{jb} + \frac{\tau\left\lfloor y_j(\Theta_b) - y_{jg} - r_\sigma \right\rfloor}{y_j(\Theta_b) - y_{j,p}(\Theta_b + \tau)} \tag{13}$$

$$\text{for } y_j(\Theta_b) < y_{jg}: \qquad \Theta_{jd1} = \Theta_{jb} + \frac{\tau\left\lfloor y_{jg} - y_j(\Theta_b) - r_\sigma \right\rfloor}{y_{j,p}(\Theta_b + \tau) - y_j(\Theta_b)}\ , \tag{14}$$

where r_σ - the radius of the prognosis mistake range (calculated a'posteriori appropriately for each method of the prognosis value determination $y_{j,p}(\Theta_b+\tau)$);

b) Θ_{d2} with the levelling method of the diagnostic parameter boundary value ($y_{jg1}= y_{jg}$; $y_{jg1}= y_{jg} +\gamma(y_{jn} - y_{jg})$ for $y_{jn} > y_{jg}$ and $y_{jg1}= y_{jg}$; $y_{jg1}= y_{jg} - \gamma\ (y_{jg} - y_{jn})$ for $y_{jg} > y_{jn}$), e.g. for γ =0,1:

$$\text{for } y_j(\Theta_b) > y_{jg}: \qquad \Theta_{jd2} = \Theta_{jb} + \frac{\tau\left\lfloor y_j(\Theta_b) - y_{jg1} \right\rfloor}{y_j(\Theta_b) - y_{j,p}(\Theta_b + \tau)} \tag{15}$$

$$\text{for } y_j(\Theta_b) < y_{jg}: \qquad \Theta_{jd2} = \Theta_{jb} + \frac{\tau\left\lfloor y_{jg1} - y_j(\Theta_b) \right\rfloor}{y_{j,p}(\Theta_b + \tau) - y_j(\Theta_b)}\ ; \tag{16}$$

c) the determination of the next operation and diagnosis date of the machine $\Theta_d^* = \min(\Theta_{d1}, \Theta_{d2})$.

4. Examining procedures of machine state prognosis

Examining procedures includes:

a) examining the set of diagnostic parameters in the aspect of estimating an optimal set of diagnostic parameters for prognosing diagnostic parameters values according to the algorithm (point 2);
b) estimating prognosis methods of diagnostic parameters values and methods of estimating the next examination term of a machine according to the algorithm (point 3);
a) examining the prognosis value of diagnostic parameters with the prognosis mistake, and the manner of estimating the next examination and operation term of a machine depending on the following parameters:
   - prognosis value of diagnostic parameters values,
   - the size of the diagnostic parameters set,
   - prognosis horizon.

In order to obtain measurement data for procedure researches, the set of diagnostic parameters Y_1 was used from stationary researches of the combustion engine UTD-20 [1,11,14] in the form of time rows whose elements are the values of diagnostic parameters: P_{sil} – engine power [kW], p_{spr} – compression pressure [MPa], p_{wtr} – fuel injection pressure [MPa], p_{ol} – engine oil pressure [MPa].

Examining procedure of estimating an optimal diagnostic parameters set for the prognosis of diagnostic parameters values consisted in:

1. Estimating an optimal set of diagnostic parameters according to the algorithm (point 2). For the set of output parameters Y_1, the set of diagnostic parameters with appropriate weight values was obtained.

Result analysis for the engine UTD-20 showed that:

a) the highest weight values w_{j1} are possessed by the diagnostic parameters p_{wtr} and p_{ol}, and the lowest weight values w_{j1} by the diagnostic parameter P_{sil};
b) the accepted optimization criteria unambiguously identify sets of parameter values with largest quantity of information on technical state changeable in time of exploitation of the

engine UTD-20, which confirms the propriety of formulating optimization procedures of diagnostic parameters set.

2. Examining the optimal set of diagnostic parameters in the aspect of the influence of time row size (research results are gathered in the appendix B) through estimating weight values w_{j1} for the set Y_1 and the set Y_2 in elation to the length of time row. For this purpose, time rows for set sizes: k=10, k=20, k=40, k=50 were considered;

Result analysis in it field indicated that:

a) there are value changes of the weight w_{j1} in the function of time rows lengths;
b) for the combustion engine UTD-20 the order of parameters p_{wtr}, p_{ol}, p_{spr}, P_{sil} is not sustained, which indicates that the accepted criteria for parameter sets of real objects unambiguously identify sets of parameter values changeable in time of machine and having the highest quantity of information on the machines' technical state.

Summing up the performed researches for the optimization procedure of the diagnostic parameters set, it is concluded that:

a) examining diagnostic parameters sets in the aspect of the influence of time row size for the set Y_1 showed a considerable influence of time row length on estimating weight values w_{j1} for the group Engine UTD-20.
b) in examining the methodology of machine state recognition, it is suggested to accept diagnostic parameters of the highest weight values, e.g. for the combustion engine UTD-20: $w_{j1} \geq (0{,}02 - 0{,}05)$, in order to obtain a set of at least 3 elements.

Examining the procedures of machine state prognosis in the aspect of determining a prognosis method according to the prognosis mistake function, examining the influence of prognosis horizon value on the prognosis mistake, and examining the influence of diagnostic parameters set size on the prognosis mistake, were realized on the basis of:

1. Determining the set of prognosis methods of diagnostic parameters values, and estimation method of the next examination and operation date of the machine according to the algorithm (point 3). For the set of diagnostic parameters $Y_2=\{p_{wtr}, p_{ol}\}$ (of the highest weight values), the visualization of their prognoses value was obtained (linear model, exponential model, Brown-Mayer model, Holt's model), and two methods of determining the dates of next machine examination (Θ_{d1},Θ_{d2}) for three values of the prognosis horizon ($\tau=\Delta\Theta$, $\tau=2\Delta\Theta$, $\tau=3\Delta\Theta$).

The analysis of research results for the combustion engine UTD-20 showed that:

a) different best (according to the minimum value of prognosis mistake) prognosis methods of diagnostic parameters values are accepted:
   - for p_{wtr} – Holt method ($\alpha=0{,}1$; $\beta=0{,}1$), prognosis mistake = 3,02%;
   - for p_{ol} – Holt method ($\alpha=0{,}1$; $\beta=0{,}1$), prognosis mistake = 3,39%;

b) different values of the next machine examination are obtained in relation to the prognosis horizon and the size of the diagnostic parameters set:
   - for p_{wtr} – Holt method ($\alpha=0{,}1$; $\beta=0{,}1$), examination dates: $\Theta_d(\tau=\Delta\Theta)=8775{,}62$; $\Theta_d(\tau=2\Delta\Theta)=86993{,}23$; $\Theta_d(\tau=3\Delta\Theta)=8610{,}85$;
   - for p_{wtr} – Holt method ($\alpha=0{,}1$; $\beta=0{,}1$) and p_{ol} – Holt method ($\alpha=0{,}1$; $\beta=0{,}1$) weighed examination dates $\Theta_{dw}(\tau=\Delta\Theta)=8740{,}03$, $\Theta_{dw}(\tau=2\Delta\Theta)=8622{,}07$; $\Theta_{dw}(\tau=3\Delta\Theta)=8504{,}11$.

Summing up the performed researches for the state prognosis method, it is stated that:

a) considering low values of the curvilinear correlation coefficient (< 0,8) and high values of prognosis mistakes, and negative values of the next operation dates of the examined objects in analytical models (power model, exponential model and exponential model) for potential applications, it is necessary to use the Brown–Mayer model and Holt model;
b) the accepted optimization criteria and the presented algorithm unambiguously identify the prognosis method and the method of estimating the next examination date, which confirms

the propriety of the formulated procedure, and will be the basis for examining the methodology of machine state recognition in the field of state prognosis for other objects.

The analysis of research results of machine state prognosis methodology allows to formulate dedicated conclusion rules of type "IF – THEN" or "IF – THEN – ELSE" in the area of:

a) diagnostic parameters optimization;
b) state prognosis.

In case of the combustion engine UTD-20, the generated rules have form:

a) for diagnostic parameters set Y^o:
   - if $w_{1j} \geq 0{,}05$ then $y_j \in Y^o$,
   - or if $w_{1j} = w_{1jmax}$ then $y_j \in Y^o$;
b) for state prognosis:
   - if $w_{1j} = w_{1jmax}$ and if $w_{1j} \geq 0{,}9$ then $y_j \in Y^o$ and the set Y^o is a single-element set, $Y^o = Y^{o1}$,
   - if $w_{1j} = w_{1jmax}$ and if $w_{1j} < 0{,}9$ then $y_j \in Y^o$ and the set Y^o is not a single-element set, $Y^o = Y^{oo}$,
   - if the prognosis mistake of Holt method (with appropriate values of the parameters α, β) for the set Y^{o1} < prognosis mistake of the Brown–Mayer method (with an appropriate value of the parameter α) for the set Y^{o1}, then the method of value prognosis of the set Y^{o1} is the Holt method (with appropriate values of the parameters α, β), otherwise the prognosis method of the value Y^{o1} is the Brown–Mayer method (with an appropriate value of the parameter α),
   - if the value of the next examination date of the engine UTD-20 Θ_{d1} (Y^{o1}) ≤ value of the next examination date of the engine Θ_{d2} (Y^{o1}), then the method to estimate the next examination date of the engine is the method of levelling the prognosis mistake value, otherwise it is the prognosis method of diagnostic parameter boundary value,
   - if the prognosis mistakes for methods: Holt (with appropriate values of the parameters α, β) or Brown–Mayer (with an appropriate value of the parameter α) for diagnostic parameters of the set Y^{oo} take minimum values, then prognosis methods of values of appropriate diagnostic parameters of the set Y^{oo} are the above methods,
   - if the value of the next examination date of the engine UTD-20 Θ_{d1} (Y^{oo}) ≤ value of the next examination date of the engine Θ_{d2} (Y^{oo}) then the method to estimate the next examination date of the engine (for the considered diagnostic parameter) is the method of levelling the prognosis mistake value, otherwise it is the prognosis method of diagnostic parameter boundary value,
   - if the value of the next examination date of the engine UTD-20 Θ_d is determined for Y^{oo}, then this values is the weighed value of the value Θ_{dw}.

The presented conclusion rules in range of machine state prognosis, after performing appropriate verification researches, could be the basis for dedicated software of a machine state recognition system in an on–line mode (for an on-board system) and off–line (for a stationary system).

5. Conclusion

The carried out presentation of machine state prognosis procedures allows to formulate the following conclusions:

1. Presented procedures allow to determine optimal, as far as the accepted criterion is concerned:
   a) diagnostic parameters set;
   b) diagnostic parameters values prognosis and machine operation date estimation.

2. In order to determine the set of diagnostic parameters and state prognosis, the above presented procedures can be the basis for estimating conclusion rules in the range of:
   a) determining an optimal set of diagnostic parameters;
   b) estimating the values of diagnostic parameters in the future, and estimating the date of the next machine operation.

References

[1] Tylicki, H., Conception of the optimization of devices technical condition forecasting process, Machine Dynamics Problems, Vol. 9 (1994), Warszawa 1995.
[2] Tylicki, H., Optimization of the prognosis method of mechanical vehicles technical state (in Polish), ATR, Bydgoszcz 1998.
[3] Tylicki, H, Żółtowski, B., The Forecasting Technical Condition of Machines, The 16th International Conference on CAD/CAM, Robotics and Factories of the Future, Cars & Fof 2000, Trynidad & Tobago, Port of Spain - St. Augustine 2000.
[4] Batko, W., Synthesis methods of prediction diagnoses in technical diagnostics (in Polish), Mechanika, v. 4, AGH University of Science and Technology, Kraków 1984.
[5] Bowerman, B.L., O`Connel, R.T., Forecasting and Time Series, Doxbury Press, USA, 1979.
[6] Box, G., Jenkins, G., Time series analysis, forecasting and control, London 1970.
[7] Brown, R. G., Statistical Forecasting for Invertory Control, Mc Graw-Hill, New York 1959.
[8] Cempel, C., Evolutionary symptom models in machine diagnostics (in Polish), Proceedings of 1th International Congress of Technical Diagnostics, Gdańsk 1996.
[9] Theil, H., Applied economic forecasting, North-Holland, Amsterdam 1971.
[10] D. J. Inman, D. J., Farrar, C. J., Lopes, V., Valder, S., Damage prognosis for aerospace, civil and mechanical systems, John Wiley & Sons, Ltd. New York 2005.
[11] Tylicki, H., Żółtowski, B., Determination methods of the next diagnosis term of transport vehicle, Archives of Transport, Vol.12, Warsaw 2001.
[12] Zeliaś, Z., Prognosis theory (in Polish), PWE, Warszawa 1984.
[13] Żółtowski, B., Diagnostic system for the metro train, ICME, Science Press, Chengdu, China, 2006, pp.337-344.
[14] Tylicki, H., Report on the researches of optimization methodology of machine state recognition, Unpublished materials (in Polish), UTP, Bydgoszcz 2007.

Journal of Polish CIMAC
Gdansk University of Technology
The Faculty of Ocean Engineering and Ship Technology

DETERMINATION OF CYLINDER LINER FREE VIBRATION FREQUENCIES IN DIESEL MARINE ENGINES

Aleksander Valishin, Andrzej Adamkiewicz

Maritime University of Szczecin, Faculty of Mechanical Engineering,
Diagnostics and Machine Repairs Department, str. Podgórna 51/53,
70-205 Szczecin, Poland
tel.: +48 91 4318555, fax: +48 91 4318541
e-mail: a.valishin@am.szczecin.pl, a.adamkiewicz@am.szczecin.pl

Abstract

This article presents a method to determine free vibration frequencies of cylinder liners in marine gas engines based on the power method. The cylinders were treated as thin-walled tubes getting distorted because of a long term variable load. The assumptions for the model have been made, mathematical procedure has been shown as well as a description of cylinder free vibration types. The final description of free vibrations was related to the way in which the cylinder was mounted searching for a minimum free vibration frequency.

Key words: *marine engine, cylinder liner, vibrations, frequency of resonance vibrations*

1. Introduction

Determination of free vibrations of cylinder liners is a significant task at the designing stage and an important one at Diesel engine operation. Cylinder vibrations induced as a result of interaction of the impulse force accompanying piston strokes when the crankshaft is passing the Top Dead Center (TDC), are the main cause of cavity formation in the cylinder block cooling areas [4, 5]. It is valid for medium and high speed engines whose cylinders get damaged as a result of cavitation.

2. Simplifying assumptions for the model

The ratio of the thickness of a cylinder of an engine with self-ignition to its radius fulfills the inequality $\delta/R < 0{,}1$, which was the basis for accepting a cylinder liner as a thinned-wall one that is getting distorted under variable load [1]. To determine the frequency of free vibrations, the following assumptions have been taken [6]:

- cylinder material does not have mechanical hysteresis,
- the sum of kinetic and potential energy is constant and energy dissipation does not occur,
- during cylinder vibrations only a continuous process of transition from one form of energy into another takes place,
- cylinder vibrations are generated as a result of interactions of the impulse piston force when the crankshaft is passing the Top Dead Center (TDC),

– action of forces generating cylinder vibrations are asymmetrical as the contact of the piston with the cylinder wall takes place in the plane of the crankshaft movements.

Parameters of liner distortion are influenced by the type of vibration generating forces and the properties of the liner which are determined by the possible types of vibrations and frequency values accompanying them. As a consequence, the searched for vibration type will also be asymmetrical. In such a case, radial displacements are accompanied by those on the circumference tangent to the contour of the cross-section as well as diagonal distortions along the axis of the cylinder. A calculation diagram of the cylinder as well as a thin-walled liner with the discussed asymmetrical load is shown in Figure 1 [6].

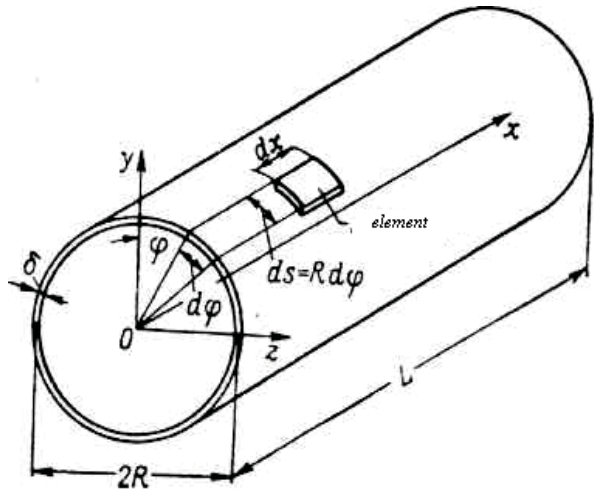

Fig. 1. A calculation diagram of a cylinder as a thin-walled liner

Determination of thin-walled cylinder liner vibration types and their corresponding frequencies was carried out using the power method suggested in paper [1]. A static equilibrium of the system was assumed there, treating mass inertia forces as a load for the external construction.

3. Mathematical description of vibrations

With such assumptions, a single element of the surface gets displaced in radial direction *w,* direction *v* and axial direction *u* . Then, in the central area of the cross-section of the cylinder, relative deformations of surface elements will take place:

along the x axis

$$\varepsilon_x = \frac{\partial u}{\partial x} \tag{1}$$

in the circumferential direction

$$\varepsilon_\varphi = \frac{w}{R} + \frac{1}{R}\frac{\partial v}{\partial \varphi} \tag{2}$$

and displacement deformations of the central area of the cross-section

$$\gamma = \frac{\partial u}{R\partial \varphi} + \frac{\partial v}{\partial x} \tag{3}$$

In relation to the cross-section of the central area of the cross-section, the following hypotheses were applied: on the rigidness of the liner in the circumferential direction and on the lack of displacements which point to $\varepsilon_\varphi = 0$ and $\gamma = 0$ deformations. Such an assumption allows to find a relationship between displacements in *w*, *v* and *u* directions which finally makes it possible to substitute all unknown forces and deformations with one, which significantly simplifies the task.

As a result of surface deformation, a simultaneous change of central area curvature will take place :
in the direction of generatrix

$$\kappa_x = -\frac{\partial^2 w}{\partial x^2} \tag{4}$$

and in the circumferential direction

$$\kappa_\varphi = -\frac{1}{R^2}\left(\frac{\partial^2 w}{\partial \varphi^2} - \frac{\partial v}{\partial \varphi}\right) \tag{5}$$

Radial displacements can be presented as a product of three functions dependent on *x, φ* coordinates and on time, t:

$$w(x,\varphi,t) = \psi(x)\cos n\varphi \sin \omega t \tag{6}$$

where:

ω – frequency of liner free vibrations,

n = 2, 3, 4,... – natural numbers characterizing the number of half-periods in the cross-section.

To determine the unknown types of vibrations *ψ(x)* and their frequencies, the condition of the minimum potential energy was applied. Considering relations (2) and (3), circumferential and axial distortions have been presented in the form of following relationships:

$$v(x,\varphi,t) = -\frac{1}{n}\psi(x)\sin n\varphi \sin \omega t \tag{7}$$

$$u(x,\varphi,t) = -\frac{R}{n^2}\frac{d\psi(x)}{dx}\cos n\varphi \sin \omega t \tag{8}$$

The total potential energy of the system may be obtained from the following expression :

$$U = \int_0^L \Gamma dx \tag{9}$$

where: Γ – the total potential energy of the liner per length (L) unit of the cylinder

$$\Gamma = \oint\left[\frac{1}{2}m_\varphi \kappa_\varphi + \frac{1}{2}\sigma_x \delta\varepsilon_x + \frac{1}{2}\rho\delta_\Sigma\left(\frac{\partial^2 w}{\partial t^2}w + \frac{\partial^2 v}{\partial t^2}v + \frac{\partial^2 u}{\partial t^2}u\right)\right]Rd\varphi =$$
$$= \left(\frac{D_{uu}(n^2-1)^2}{2R^4}\psi^2 + \frac{E\delta R^2}{2n^4}\left(\frac{d^2\psi}{dx^2}\right)^2 - \frac{\omega^2\rho\delta_\Sigma}{2}\left(\psi^2\left(1+\frac{1}{n^2}\right) + \frac{R^2}{n^4}\left(\frac{d\psi}{dx}\right)^2\right)\right)\pi R \sin^2 \omega t. \tag{9a}$$

In (9a) the following symbols denote:

$D_{ш} = \frac{E\delta_{ш}^3}{12\left(1-\mu^2\right)}$ – cylinder rigidness, characterizing cylinder wall resistance to bending,

E – modulus of elasticity of the material (Young's modulus),

R – radius of the cylinder,

P – density of the cylinder material,

μ – Poisson's coefficient,

$m_{\varphi} = D_{ш}\left(\kappa_{\varphi} + \mu\kappa_x\right)$ – bending momentum in the circumferential direction,

$\sigma_x = \frac{E}{1-\mu^2}\frac{\partial u}{\partial x}$ – axial tension.

It has been assumed that external load is due to mass inertia forces whose projections on unitary area of the cross-section were defined in the following way

$$P_x = -\rho\delta_{\Sigma}\frac{\partial^2 u}{\partial t^2}; \qquad P_y = -\rho\delta_{\Sigma}\frac{\partial^2 w}{\partial t^2}; \qquad P_{\varphi} = -\rho\delta_{\Sigma}\frac{\partial^2 v}{\partial t^2}$$

Then expression $\frac{1}{2}\rho\delta_{\Sigma}\left(\frac{\partial^2 w}{\partial t^2}w + \frac{\partial^2 v}{\partial t^2}v + \frac{\partial^2 u}{\partial t^2}u\right)$ determines the potential of external forces, used with a reverse sign.

As in expression (9a) defining Γ the potential of external forces with a reverse sign is used, then from formula (9) the following condition emerges:

$$U = \int_0^L \Gamma dx = 0 \tag{10}$$

meaning that at radial displacement, the equity of work performed by internal and external forces is noted when the liner is in the equilibrium state.

The choice of thickness δ, δ_{Σ}, $\delta_{ш}$ used for calculations depends on the cylinder shape. For cylinders whose external part of the wall is made in the form of spiral grooves as $\delta_{ш}$ wall thickness in the region of protrusions should be taken and for δ wall thickness in the groove region should be assumed. Then, the total thickness of the reinforced liner may be defined as the sum of the following form:

$$\delta_{\Sigma} = \delta + \frac{f_{ш}}{a} \tag{11}$$

where:

a – spiral step; $f_{ш}$ – the area of the cross-section of the protrusion.

For cylinders with smooth walls and collars $\delta_{ш}$ is equal to the corresponding wall thickness defined according to the generally used relationship:

$$\delta_{ш} = d = d_1\left[\frac{\left(\eta^2-1\right)}{\frac{1+\mu}{1-\mu}\eta^2+1}\right]^{\frac{1}{3}} \tag{12}$$

where:

d_1 – collar thickness; $\eta = \frac{a_2}{a_1}$;

a_1 – external radius of the cylinder; a_2 – cylinder radius in the collar region.

δ refers to the wall thickness at the end of the cylinder (generally denoted as d in the applied methodology – formula 12) and the total thickness of the liner is determined taking into consideration all non-uniformities of the whole thickness of cylinder walls

$$\delta_\Sigma = \frac{1}{L}\sum_i f_{wi} \tag{13}$$

where: f_{wi} – is the cross-section area of particular parts with defined wall thickness (supportive belt, dredging, scarf etc).

4. Problem solving method

Relying on the condition of the minimum potential energy of the system, radial displacements $\psi(x)$, which were used to determine all deformations, internal forces and external loads can be determined using Euler equation for the variation problem:

$$\frac{\partial \Gamma}{\partial \psi(x)} - \frac{d}{dx}\frac{\partial \Gamma}{\partial \psi'(x)} + \frac{d^2}{dx^2}\frac{\partial \Gamma}{\partial \psi''(x)} = 0 \tag{14}$$

As

$$\frac{\partial \Gamma}{\partial \psi(x)} = \left(D_w \frac{\left(n^2-1\right)^2}{R^4} - \omega^2 \rho \delta_\Sigma \left(1 + \frac{1}{n^2}\right)\right)\psi(x)\pi R \sin^2 \omega t \tag{15}$$

$$\frac{d}{dx}\frac{\partial \Gamma}{\partial \psi'(x)} = -\omega^2 \rho \delta_\Sigma \frac{R^2}{n^4}\frac{d^2\psi}{dx^2}\pi R \sin^2 \omega t \tag{16}$$

$$\frac{d^2}{dx^2}\left(\frac{\partial \Gamma}{\partial \psi''(x)}\right) = E\delta \frac{R^2}{n^4}\frac{d^4\psi}{dx^4}\pi R \sin^2 \omega t \tag{17}$$

Then from relations (14) – (17) a uniform differential equation of the fourth order was obtained:

$$\frac{d^4\psi}{dx^4} + \frac{\rho\delta_\Sigma}{E\delta}\omega^2 \frac{d^2\psi}{dx^2} - \left(\omega^2 \frac{\rho\delta_\Sigma\left(n^2+1\right)n^2}{E\delta R^2} - D_w \frac{\left(n^2-1\right)n^4}{E\delta R^6}\right)\psi(x) = 0 \tag{18}$$

whose solution is function (19):

$$\psi(x) = C_1 ch\ k_1 x + C_2 \cos ik_2 x + C_3 sh\ k_1 x + C_4 \sin ik_2 x \tag{19}$$

describing the type of vibrations along the x axis, where :

C_1, C_2, C_3, C_4 – integral constants dependent on the limiting conditions,

k_1 , k_2 – roots of the fourth order characteristic equation,

$$k^4 + ak^2 + b = 0 \tag{19a}$$

where: $a = \frac{\rho\delta_\Sigma}{E\delta}\omega^2$; $b = D_{uu}\frac{(n^2-1)^2 n^4}{E\delta R^6} - \omega^2\frac{\rho\delta_\Sigma n^2(n^2+1)}{E\delta R^2}$;

$$k_1^2 = \frac{-a+\sqrt{a^2-4b}}{2}; \qquad k_2^2 = \frac{-a-\sqrt{a^2-4b}}{2} \tag{19b}$$

If for the actual construction of the cylinder, the following conditions are fulfilled:

$b < 0$; $|a| << |b|$ and $k_1^2 \approx -k_2^2 \approx \sqrt{|b|}$

Then, it can be assumed that

$$k_1 \approx ik_2 = k\,.$$

Substituting relation (19), which describes *ψ(x)*, free frequency of the cylinder has been obtained in the following form:

$$\omega_m^2 = \frac{(k_m R)^4 + \frac{D_{uu}}{R^2 E\delta}(n^2-1)^2 n^4}{\frac{\rho\delta_\Sigma}{E\delta}R^2\left((k_m R)^2 + (n^2+1)n^2\right)} \tag{20}$$

5. Summary

In contrast to the generally used methods of calculations applied for determination of free vibration of cylinders [1, 6, 7], relation (20) is a general one, valid for all limiting ways of cylinder mountings and its application has no restrictions regarding different mounting of the cylinder in the block, not only at the edges but also with intermediate support.

Taking into account limiting conditions, referring to the way in which the cylinder is mounted in the block, leads to a series of exact values k_m. Limiting conditions for the ψ (x) function constitute a system of equations versus C_1, C_2, C_3, C_4 constants, whose solution uncommonly exists when the system determinant equals zero.

In the simple cases of symmetrical mounting at the edges of the cylinder, trigonometric equations, whose known roots are expressed with the π number, can be obtained. Taking into consideration the actual mounting of the cylinder in the block, set up both at the edges as well as between them, leads to more complicated limiting conditions.

Then, it is indispensable to determine the k_m value from the condition that the determinant is equal to zero for limiting conditions, and the expression for calculating free vibrations of the cylinder is given in the from:

$$\omega_m^2 = \frac{(k_m R)^4 + \frac{D_{uu}}{R^2 E\delta}(n^2-1)^2 n^4}{\frac{\rho\delta_\Sigma}{E\delta}R^2\left((k_m R)^2 + (n^2+1)n^2\right)},\ m= 1,2,3..., \tag{21}$$

where: m – the number of half- periods along the x axis. The first type of vibrations m=1 is the one without knots with the minimum frequency where: ω_m. Each vibration type in the axial direction is characterized by m half-terms along the x axis and has one value in the circumferential direction, n_m, at which the frequency of vibrations will be minimal [2, 3].

References

[1] Kan.S.: Stroitelna mechanika oboloczek. Maszynostroenie.Moskva 1966.
[2] Krylow E.: Sowerszenstwowanie techniczeskoj ekspluatacji sudowych dizelej. Trasport, Moskva, 1983.
[3] Cempel C.: Drgania mechaniczne – wprowadzenie. Politechnika Poznańska, Poznań, 1982.
[4] Jmmisch H., Loebell R.: Erfahrungenmit Nűral- Perimatic-Regel Kolben in Diselmotoren fur Vehffzing von Kavitationsschoden an Zylinderlaufbuchsen, MTZ, 1983, 34, №2, p. 45-48.
[5] Wheeler W.H.: Identation of metals by cavitation. Trans. ASME, Series D, 82, №1, 1960, p. 184-194
[6] Valishin A.,Poroshina S.: Metodika rasczeta wibracyonnych charakteristik cilindrowych wtułok DWS: Nauka i technologia tom 1. Moskva, RAN 2006.
[7] Żółtowski B.: Badania dynamiki maszyn. Akademia Techniczno-Rolnicza w Bydgoszczy, Bydgoszcz 2002. ISBN 83-916198-3-4

Journal of Polish CIMAC
Gdansk University of Technology
The Faculty of Ocean Engineering and Ship Technology

ANALYSIS OF PISTON-CRANK SYSTEM BALANCING IN V-VR ENGINES

Sławomir Wierzbicki

University of Warmia and Mazury in Olsztyn
ul. Słoneczna 46A, 10-710 Olsztyn, Poland
tel. +48 89 5245222, fax. +48 89 5245150
e-mail: slawekw@uwm.edu.pl

Abstract

The advances made in materials science and modern material production and processing technologies support the design and serial production of structural solutions which could not have been applied in the past on account of their complexity or high cost.

The piston-crank system of a combustion engine remained practically unchanged over decades, and the only structural modifications involved the use of new materials for improved fatigue strength or attempts to limit the mass of system components to minimize inertial forces. Since the invention of the piston engine, in-line engines have been the predominant type of engine configuration on the market. Larger engines are built sporadically, and most of them have a "V" arrangement of cylinders and pistons for easier mounting. Selected vehicles, in particular sports cars, are equipped with boxer-type piston-crank systems. Recent years have witnessed the advance of new engine configurations with VR or V-VR piston-crank systems which are often referred to as W engines due to a unique arrangement of the connecting rod. The V-VR crankshaft-piston configuration supports the design of engines characterized by high displacement and reduced size for easier assembly in the vehicle's engine compartment. Such solutions are often deployed in upper class cars.

There is a general scarcity of information about V-VR piston-crank systems in literature, therefore, this study presents an overview of the above configuration and analyzes inertial forces impacting the discussed system.

Keywords*: piston-crank system, V-VR (W) engine, inertial force, engine balancing*

1. Introduction

The piston-crank system is one of the main structural units of a combustion engine. Crankshaft-piston configurations have to meet numerous requirements, the most important being:

- smooth engine operation,
- small size and weight relative to engine power,
- ease of assembly in a vehicle,
- low level of vibrations transmitted to the power transmission system and engine block,
- dynamic engine operation within a wide range of speeds and loads [1, 4, 5].

Cylinder arrangement is one of the characteristic features of a piston-crank system. Since the invention of the piston engine, in-line engines have been the predominant type of engine configuration characterized by simple structure of the crankshaft, the engine block and the cylinder head. Owing to the simplicity of the applied solutions, in-line engines are relatively inexpensive to build. However, in in-line engines with a higher number of cylinders, the piston-crank system and

the entire engine are characterized by relatively low rigidity. The above poses assembly problems, in particular in selected types of passenger cars.

A different configuration of the piston-crank system is found in a V engine. The cylinders are aligned in two separate banks that are positioned towards one another at a certain angle. This configuration produces engines with reduced length and high rigidity. The discussed solution is ideal for vehicles with high performance requirements and a small engine compartment. A V engine incorporates two separate cylinder heads, an expanded engine block and cooling system, therefore, its main disadvantage are high production costs.

Boxer-type crankshaft-piston configurations are often encountered in sports cars. They are characterized by small overall height, which makes them the ideal solution for vehicles with a small engine compartment. Similarly to V engines, boxer configurations are quite expensive, and they are relatively rarely used.

2. Kinematic analysis of a piston-crank system

A piston-crank system in a combustion engine may rotate around its axis (simple setup) (Fig. 1) or off the central axis (eccentric setup) with a relatively small axial offset. According to the dependences described in literature [1, 4, 5], piston movement as a function of crankshaft rotation in a simple system can be expressed as:

$$x = r\left(1 - \cos\alpha + \frac{1}{2}\cdot\lambda\cdot\sin^2\alpha\right), \tag{1}$$

where:

α – crank angle,
$\lambda = r/l$,
r – crank radius,
l – length of connecting rod.

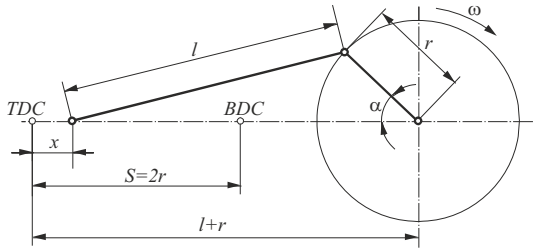

Fig. 1. Diagram of a simple piston-crank system

Instantaneous piston velocity is:

$$v = r\cdot\omega\cdot\left(\sin\alpha + \frac{\lambda}{2}\cdot\sin 2\alpha\right). \tag{2}$$

Instantaneous piston acceleration can be expressed as:

$$a = r\cdot\omega^2\cdot\left(\cos\alpha + \lambda\cdot\cos 2\alpha\right). \tag{3}$$

In kinematic analyses of eccentric piston-crank systems, the above equations take on a more complex form, but since the values of eccentricity which are practically applied in engines have an insignificant effect on piston location, velocity or acceleration, the formulas for simple crankshaft-piston arrangements can be used instead [1, 4].

Eccentric crankshaft-piston setups are less popular, and they are used mostly in light engines to minimize lateral pressure on cylinder bearing surface and facilitate piston movement past a dead center position. In eccentric arrangements, maximum acceleration does not take place at extreme

positions of the piston. Piston accelerations for a simple system and an eccentric setup with eccentricity of $e = 0.3 \cdot r$ are presented in Fig. 2. The diagram clearly indicates that eccentricity has a minor influence on acceleration. In practice, even smaller eccentricity values are applied below $e = 0.2 \cdot r$ [1, 5].

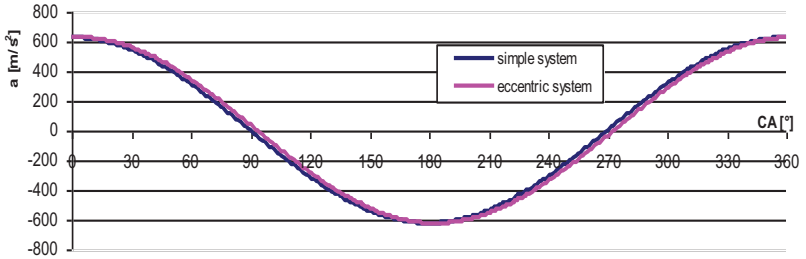

Fig. 2. Effect of crankshaft eccentricity on piston acceleration at e=0.3r

3. Piston-crank system in a V-VR engine

Recent years have witnessed the advance of new engine configurations with a V-VR piston-crank system which are often referred to as W engines due to a unique arrangement of the connecting rod. The architecture of a V-VR engine differs from that of a W engine which is equipped with three cylinder banks [1, 5]. A V-VR engine is characterized by a unique arrangement of the piston-crank system where cylinders are located in four banks. The discussed configuration is largely based on the original VR setup which has the features of an in-line engine and a V engine and combines the advantages of both solutions [6]. The main advantage of in-line engines is the relative structural simplicity of the engine block, timing gear and cooling system as well as the option of using only one cylinder head, which significantly lowers production costs. A V engine is characterized by reduced length and greater rigidity. A VR configuration is basically a V engine with a relatively small offset angle between cylinder banks, which reaches 10.5° to 15° in most applications. This solution produces a highly compact and rigid structure, a much shorter engine with only one cylinder head. A V engine with 6 cylinders is significantly shorter and less prone to vibrations than an in-line engine with 6 cylinders [6].

A VR engine evolved into a V-VR engine which combines two VR engines in a V-type arrangement. The piston-crank system of a V-VR engine is presented in Fig. 3, and the kinematic diagram of the discussed cylinder setup is shown in Fig. 4. The contemporary V-VR engines have 8, 12 or 16 cylinders. This solution produces a short, compact and rigid engine with low weight and relatively high capacity.

The engine block (Fig. 5) and the cylinders are manufactured of aluminum alloys, and this structure ensures high engine rigidity. The crankshaft is mounted to the engine block with a single compact cover which significantly increases engine rigidity.

In the analyzed arrangement, the crankshaft has non-standard architecture (Fig. 6a). The cylinders are arranged in four asymmetric banks for steady operation, the crankshaft has a spatial structure and the shared crankpins are mutually offset (Fig. 6b). Their offset is determined by the number of cylinders in the engine, and it is necessary to ensure uniform distribution of ignition force. A common crankpin is used for connecting rods of cylinders separated by an angle of 72°. In the discussed configuration, the ignition distance is 90°, and the crankpin serving the right-hand cylinder is offset by an angle of 18° in a direction opposite to crankshaft rotation. The above solution guarantees uniform ignition distances. In 12 cylinder engines, crankpins are separated by an angle of 12° but in an opposite direction to that noted in 8 cylinder engines, therefore in cylinders offset by 72°, the ignition distance is 60°. To guarantee adequate compression and shared use of the cylinder head in adjacent cylinder banks, pistons have beveled ends (Fig. 6c) – a single

flat head can be used when one piston rotates relative to the other. The firing order in an 8 cylinder engine is 1-5-2-6-4-8-3-7.

Fig. 3. 3D model of a piston-crank system in a V-VR8 engine

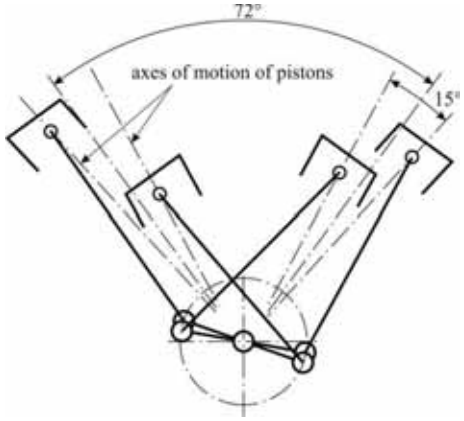

Fig. 4. Kinematic diagram of a piston-crank system in a V-VR engine

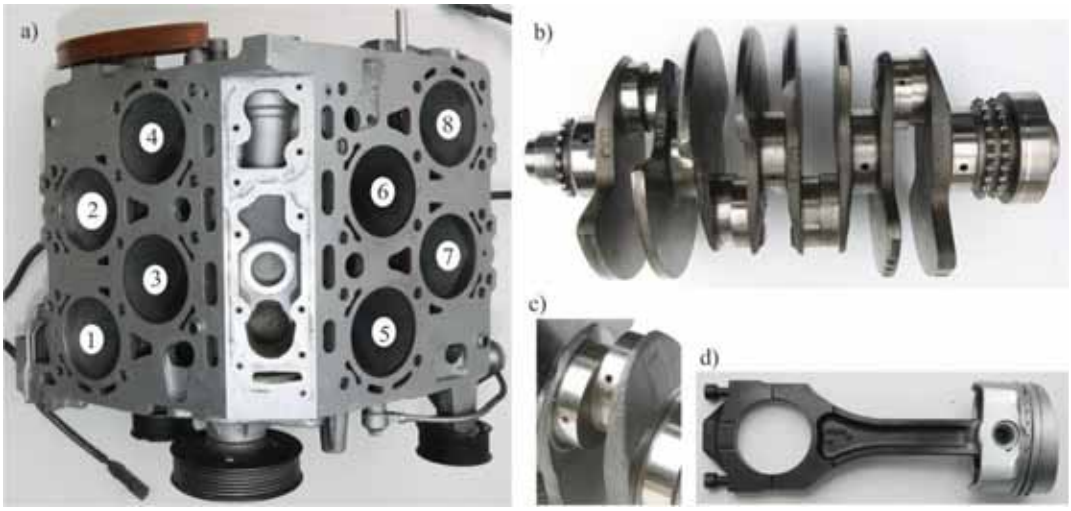

Fig. 5. Components of a piston-crank system in a V-VR engine: a) block with cylinder order, b) crankshaft of a W8 engine, c) crankpin, d) piston with connecting rod

4. Analysis of inertial forces in a piston-crank system of a V-VR engine

In a combustion engine, pistons move with variable acceleration, as per formula (3). For this reason, in multiple-cylinder engines, the inertial forces of reciprocating masses create a spatial force system and moments of inertia. Subject to the number of cylinders and their position, those forces can be mutually reduced or they can create an unbalanced system where a significant load is imposed on the piston-crank system and transferred to the vehicle frame.

In line with the principles of mechanics, the inertial forces of reciprocating masses in an engine are determined by the mass of those components and their instantaneous acceleration. Inertial forces can be minimized by reducing the mass of each component and distributing cylinders in a way that supports the self-balancing of inertial forces in the engine.

Most analyses of inertial forces in piston-crank systems in combustion engines focus on first-order and second-order inertial forces and their moments. Higher-order forces are omitted due to their insignificant value [1, 4, 5].

In a V-VR engine, cylinders are positioned in four banks, and in order to determine inertial forces in the analyzed crankshaft-piston arrangement, the formula for piston acceleration (3) has to be generalized by accounting for the displacement between the cylinder and the main axis γ and the displacement between individual cranks and the first cylinder crank ρ (Fig. 7). In this case, the acceleration of a single piston in its axis of motion is calculated using the following formula:

$$a = r \cdot \omega^2 \cdot \left[\cos(\alpha + \rho - \gamma) + \lambda \cdot \cos 2(\alpha + \rho - \gamma)\right], \tag{4}$$

where:

γ – displacement between the cylinder and the main axis.,

ρ – angular displacement between a crank relative to the assumed position of the first cylinder crank.

The piston acceleration formula can be written as the sum of first-order *a'* and second-order *a"* accelerations which equal:

$$a' = r \cdot \omega^2 \cdot \left(\cos(\alpha + \rho - \gamma)\right), \tag{5}$$

$$a'' = r \cdot \omega^2 \cdot \lambda \cdot \cos\left(2(\alpha + \rho - \gamma)\right), \tag{6}$$

Piston acceleration and reciprocating mass *m* can be then used to determine the inertial forces acting on the axis of one of the cylinders:

$$F' = m \cdot r \cdot \omega^2 \cdot \left(\cos(\alpha + \rho - \gamma)\right), \tag{7}$$

$$F'' = m \cdot r \cdot \omega^2 \cdot \lambda \cdot \cos\left(2(\alpha + \rho - \gamma)\right). \tag{8}$$

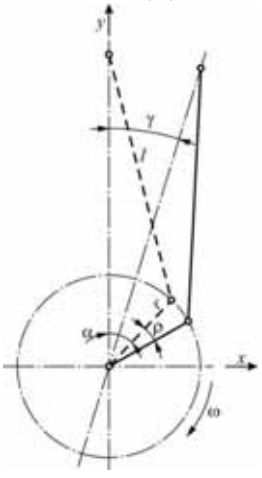

Fig. 6. Diagram of the analyzed piston-crank system

In the analyzed engine, vectors of inertial forces of reciprocating masses are not found in a single plane, therefore, the projections of individual forces onto two perpendicular axes should be analyzed for greater convenience. The inertia components of every piston $F[i]$ will have the following projection on the coordinate axes (Fig. 6):

$$F'_x[i] = \sin\gamma[i] \cdot m \cdot \left(r \cdot \omega^2 \cdot \cos\left(\alpha + \rho[i] - \gamma[i]\right)\right), \tag{9}$$

$$F'_y[i] = \cos\gamma[i] \cdot m \cdot \left(r \cdot \omega^2 \cdot \sin\left(\alpha + \rho[i] - \gamma[i]\right)\right), \tag{10}$$

$$F''_x[i] = \sin\gamma[i] \cdot m \cdot \left(r \cdot \omega^2 \cdot \lambda \cdot \cos\left(2\left(\alpha + \rho[i] - \gamma[i]\right)\right)\right), \tag{11}$$

$$F''_y[i] = \cos\gamma[i] \cdot m \cdot \left(r \cdot \omega^2 \cdot \lambda \cdot \sin\left(2\left(\alpha + \rho[i] - \gamma[i]\right)\right)\right), \tag{12}$$

where:

$a[i]$, $\gamma[i]$, $\rho[i]$ – acceleration, cylinder displacement and angular displacement of the crank of the i-th cylinder relative to the crank of the first cylinder, respectively.

A procedure was developed in the Matlab application for determining the moment of inertia in any crankshaft-piston configuration. The following parameters of the piston-crank system were used:

r = 45 mm,
l = 168.5 mm.

The vector of angular displacement between individual cranks and the first cylinder crank in an 8 cylinder engine was:

$\rho[i]$ = [0, 180, 195, 15, 342, 162, 177, 357].

The vector of displacement between cylinders and the y-axis was:

$\gamma[i]$ = [316.5, 316.5, 331.5, 331.5, 28.5, 28.5, 43.5, 43.5].

The projections of first-order inertial forces on two perpendicular axes for each cylinder in an 8 cylinder engine are presented in Fig. 7. This diagram clearly indicates that the forces of inertia are mutually balanced. In the analyzed engine, the ignition distance is 90°CA, and similarly to a V engine where the banks form a 90° angle, those forces are mutually balanced [1, 5]. The projections of second-order inertial forces on each axis are shown in Fig. 8. Second-order forces of inertia are mutually balanced only in one plane, whereas in the second plane, they are summed, causing the system to be out of balance. In practice, inertial forces are balanced with the use of additional balance shafts which rotate at twice the speed of the crankshaft [1, 5, 6]. The forces of inertia, presented in Figs. 8 and 9, are expressed in relative units, and the actual values of those forces are proportional to the square of the instantaneous velocity of the crankshaft.

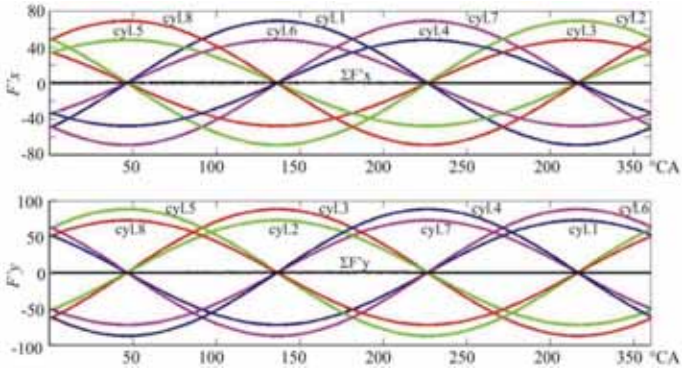

Fig. 7. First-order inertial forces of cylinders in a V-VR8 engine

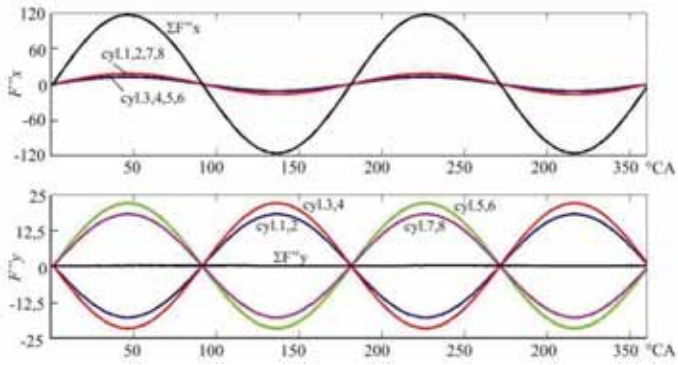

Fig. 8. Second-order inertial forces of cylinders in a V-VR8 engine

The moments of inertia relative to the longitudinal center axis of the crankshaft are summed to determine the resultant moment of inertia in the analyzed engine. The resultant moments of inertia relative to the x-axis and the y-axis are:

$$M_x = \sum_{i=1}^{8} \left(F_y[i] \cdot k[i] \right), \tag{13}$$

$$M_y = \sum_{i=1}^{8} \left(F_x[i] \cdot k[i] \right). \tag{14}$$

First-order and second-order moments of inertia in each bank of an 8 cylinder engine are shown in Fig. 9 and Fig. 10 (similarly to the forces of inertia, also the values of the moments of inertia are given in relative units). They were calculated using the following vector of distance between the cylinders and the longitudinal center axis of the crankshaft $k[i]$:

$k[i]$ = [-0.104, 0.026, -0.039, 0.091, -0.091, 0.039, -0.026, 0.104] [m].

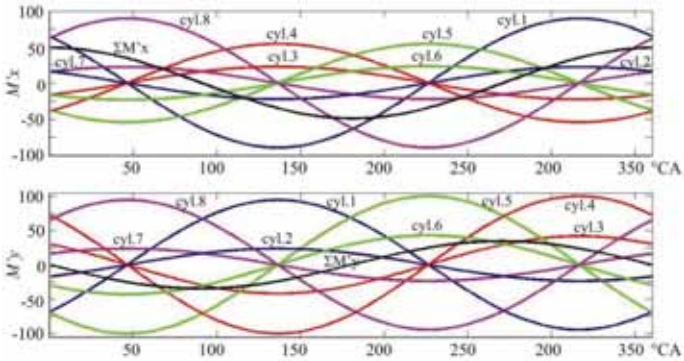

Fig. 9. First-order moments of inertia in a V-VR8 engine

An analysis of moments of inertia in the discussed engine indicates that the first-order moment is relatively small and it changes with the crankshaft rotation angle, therefore, it can be reduced by applying additional counterweights to the crankshaft [1, 2, 3, 5]. Second-order moments of inertia are even smaller, and they do not exert significant loads on the system.

In a 12 cylinder engine with a V-VR piston-crank system, first-order and second-order inertial forces are balanced out. Each of the four banks contains three cylinders whose crankpins are

separated by an angle of 120°, and similarly to a 3-cylinder in-line engine, the resulting inertial forces are balanced [1, 5]. The moments of inertia remain unbalanced, but their sum is relatively small and it does not exert a significant load on the engine.

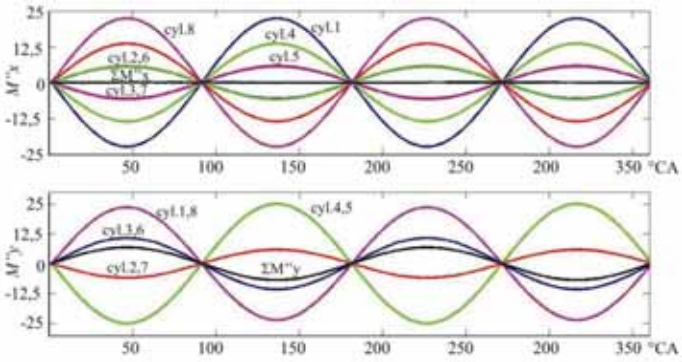

Fig. 10. Second-order moments of inertia in a V-VR8 engine

5. Conclusions

In an 8 cylinder engine with a V-VR piston-crank system, first-order inertial forces are balanced, and additional balance shafts are applied to equalize second-order forces. Balance shafts are increasingly often used in 4 cylinder engines to ensure smooth engine operation. First-order and second-order moments of inertia are not completely balanced in a V-VR8 engine where cylinders are not symmetrically distributed relative to the longitudinal center axis of the crankshaft. In part, the moments of inertia are mutually balanced, the resulting moments are very small, and they do not exert a significant load on the system.

Owing to its specific architecture, a 12 cylinder engine is characterized by mutually balanced first-order and second-order inertial forces, and similarly to an 8 cylinder engine, its moments of inertia remain unbalanced.

The crankshaft-piston configuration of a V-VR engine contributes to smooth engine operation without exerting inertial load on the engine or the engine suspension system. The discussed cylinder arrangement produces compact engines with reduced length and high capacity which can be easily assembled in vehicles. The compact architecture of the crankshaft guarantees low inertia of the entire system, and it contributes to high engine performance.

References

[1] Jędrzejowski, J.: *Mechanika układów korbowych silników samochodowych*. WKiŁ, Warszawa 1986.

[2] Mosakowski, R.: *Analiza wyrównoważenia silników rzędowych dwusuwowych czterocylindrowych*. Archiwum Motoryzacji, nr. 4/2006, pp. 343-358, 2006.

[3] Mosakowski, R.: *Analysis of balancing of six-cylinder in-line two-stroke internal combustion engines*. Combustion Engines – Silniki Spalinowe, nr 4/2009 (139), pp. 22-33, PNTSS, 2009.

[4] Niewiarowski, K.: *Tłokowe silniki spalinowe*. WKiŁ, Warszawa, 1983.

[5] Wajand, J. A., Wajand, J. T.: *Tłokowe silniki spalinowe średnio- i szybkoobrotowe*. WNT Warszawa, 1993.

[6] VW, Audi – materiały reklamowe i prasowe.

Journal of Polish CIMAC
Gdansk University of Technology
The Faculty of Ocean Engineering and Ship Technology

STRATEGIES IN DEDICATED DIAGNOSTIC SYSTEMS

Joanna Wilczarska

University of Technology and Life Sciences in Bydgoszcz
Faculty of Mechanical Engineering
ul. Prof. Kaliskiego 7 85-789 Bydgoszcz, Poland
tel.: +48 52 340 8283 fax: +48 52 340 82 86
e mail: asiulazol@ut.edu.pl

Abstract

So far the research on machine reliability has been done with the use of statistical methods on the basis of observed events. Now it is being replaced by computer simulation technology and programmed reliability tests. Requirements concerning the quality, marketing and logistics are radically changing the machine assessment criteria resulting in further, constantly growing, interest in the methods and means of technical diagnostics as well as computer technology involving the use of diagnostic procedures. Implemented procedures of the machine state identification are a basis of the Dedicated Diagnostic Systems. These systems enable determination of dedicated results of the procedures application effect in the field of the machine state assessment, its genesis and prognosis. It applies to any machine (with a given dynamics of its state degradation, with different diagnostic and process parameters, different environments and dynamics of value changes during operation) . Automation of the machine state assessment process requires elaboration of strategies for the dedicated diagnostic systems. In this study, special attention has been given to the strategy according to the machine technical state which involves making decisions according to a current assessment of the machine technical state. Another important strategy is based on economic efficiency as it is an indicator of the machine operation cost-effectiveness and provides basis for deciding on the machine withdrawal from use.

Keywords: *strategy of operation and maintenance, diagnostic system, diagnostic parameter, technical condition of machines*

1. Introduction

The methodology of the machine state identification process involves the following stages of assessment activities, in the below presented forms [3]:

a) diagnosis – process involving determination of the machine state in time Θ_b;
b) prognosis – process of involving prediction of the machine future states, allowing to, eg. schedule the next term of the machine servicing Θ_d ;
c) genesis - process involving tracing back the machine history, eg. in order to estimate the machine state in the past;

which provides the possibility of:

a) identification of the machine technical state in current time on the basis of results of diagnostic tests. This enables control of the state and localization of failure in case of the machine being out of service.
b) predicting the machine state in the future on the basis of incomplete history of diagnostic tests results. It allows to estimate the time of the machine reliable operation or the value of work to be performed by it in the future.

c) Defining the machine state in the past on the basis of incomplete history of diagnostic results which allows to estimate the machine state in the past.

Dedicated Diagnostic System consists of implemented procedures of the machine state identification, which enable [2]:

a) determination of an optimal set of diagnostic parameters and, on their basis, control of the machine state and localization of a failure, prognosis and genesis of the machine state,
b) establishing a test for an assessment of the machine state through:
   - determination of a relation matrix: value of diagnostic parameter – technical state (or time of the machine operation and maintenance),
   - establishing a control test for the machine state and localization of a failure;
c) prognosis of the machine state through:
   - determination of a method for the diagnostic parameter value prognosis according to the prognosis error function;
   - establishing a method for determination of the next servicing time;
   - determination of a method for the diagnostic parameter value genesis according to the function of error genesis,
   - estimation of the cause of machine damage found during testing.

Problems solved by procedures of the Dedicated Diagnostic Systems include:

- selection of the best diagnostic parameters describing the machine current state and analysis of their value changes during the machine operation.
- determination of a diagnostic test
- determination of the diagnostic parameter prognosis value $y_{jp}(\Theta_b + \tau_1)$ for prognosis horizon τ_1, by means of 'the best' prognosis method and scheduling the next servicing time Θ_0;
- determination of the diagnostic parameter genesis value $y_{jg}(\Theta_b + \tau_2)$ for genesis horizon τ_2 by means of 'the best' genesis method and determination of the machine cause of damage found during performance of the diagnostic test.

Once the procedures are triggered it is necessary to have the knowledge of data obtained from the machine experimental or static tests. These are:

a) set of the machine diagnostic parameters values $\{y_{jg}(\Theta_i)\}$ with the set of boundary values $\{y_{jg}\}$ and nominal values $\{y_{jn}\}$;
b) set of the machine diagnostic parameters values $\{y_n(\Theta_i)\}$;
c) and a set of the environment parameters values $\{y_k(\Theta_i)\}$;
d) set of the machine states $\{s_m(\Theta_i)\}$ recorded during operation .

Due to different diagnostic parameters which are to be determined for particular machines (automotive vehicle, working machine, assembly line, and others) the implemented DSD procedures determine, automatically and/or with the system operator's interference, appropriate (dedicated for each machine) methods in particular operating groups of DSD, that is, the machine state assessment, its genesis and prognosis. Thus, they provide a particular machine, with adequate, dedicated results of the procedures operation effects, such as:

a) set of diagnostic parameters dedicated for a machine
b) dedykowany dla maszyny zbiór parametrów diagnostycznych;
c) dedicated control test for the machine state and failure localization;
d) dedicated to the machine time of servicing
e) dedicated to the machine result of the failure cause estimation.

The DSD system should guarantee that the diagnostician will interfere with its operating only in case of:.

- change of the state diagnosis subject;
- change of the state diagnosis prognosis and genesis algorithm;
- removal of failures automatically detected within the system hardware and software.

The basic requirements to be met by DSD system are:

a) reliability;
b) high performance speed;
c) unification;
d) cost efficiency (low production and operation costs).

Moreover, the machine DSD system should provide:

a) simple, possibly optimal, algorithm of functioning;
b) universality, that is, possibilities of identification of states of different types of machines;
c) possibility of the state identification of high and low complexity machines ;
d) automatic generation of diagnosis;
uniqueness and clarity of the presented diagnoses;
e) user friendliness.

2. Strategies of operation and maintenance in dedicated diagnostic systems

Automation of the system of the machine state evolution requires elaboration of strategies to be used in dedicated diagnostic systems. An operation strategy involves determination of methods for the machine use and maintenance and establishing relations between them in terms of the accepted criteria,

There can be distinguished following strategies[3]:

- according to economic efficiency,
- according to performer work,
- according to technical state,
- authorized strategy for machine operation and maintenance.

Strategy according to reliability

Operation and maintenance of machines according to this strategy involves making decisions on the basis of regular control of reliability level of different devices (various indexes of reliability), used until occurrence of a failure. Strategy according to reliability, also referred to as strategy according to failures, involves using the object until occurrence of a failure. There is no need to prove that this strategy can be used only when the consequences of failures do not violate rules of safety and do not increase costs of the machine operation and maintenance.

Strategy based on the input of work

Machines operating according to this strategy are limited by the amount of performed work which can be defined by the number of working hours, the amount of used fuel, the number of traveled kilometers, the number of work cycles etc. General rule of this strategy is to prevent failures (wear, aging) through servicing procedures within the defined limits of performed work, before a boundary wear level is reached. From the point of view of making use of the machine real potential this strategy is rather inefficient as the basis of acceptance of the permitted amount of work are extreme working conditions. The most unfavorable ones are accepted, such as: the weakest links (elements, parts) of the machine, extreme loads which may not always and not to the same extent be revealed during operation.

Authorized strategy of machine operation and maintenance

Qualitative changes forced by the market economy are of great importance in all fields of economy including the use of fixed assets. Needs and conditionings of the market economy justify the necessity of implementation of an authorized strategy of machines manufacture and operation. In the proposal of this strategy the so far existing achievements of the latest, state related operation and maintenance strategy, are not lost but creatively modified.

Special attention has been given to the strategy according to economic efficiency and the technical state. In the strategy according to economic efficiency the machine cost effectiveness is of key importance for the decision on the machine withdrawal from use. Results of economic efficiency can often lead to withdrawal from use of machines that are still serviceable though not efficient enough from the point of view of the user.

Proper application of this strategy needs a lot of statistical information from the field of financial management of the operation department, knowledge of decision models, measuring methods of values and economic efficiency indicators and optimization account.

Strategy based on the machine technical state involves making decisions on the basis of current assessment of technical state of the machines, their systems or elements and (fig.2.1).

It enables elimination of the most common defects connected with operation of machines according to other strategies.

The success of this strategy is connected with availability of simple and efficient diagnostic methods, preferably incorporated in the constructed machines which in turn are controlled by the system of the state monitoring.

Each automatic diagnostic system should be designed with regard to the costs caused by mistakes of alpha and beta type, and its decision strategies should be optimized in terms of global cost minimization expressed by the weighted sum of those costs. Error of alpha type, that is ‚false alarm', occurs when the system will not notice the object real deficiency due to insufficiently precise diagnostic procedure or wrong data. In radiolocation systems (which the names of errors come from) costs of a false alarm are measurable and equal to the price of an unnecessarily launched missile or dispatch of an squadron of airplanes. The costs of errors of beta type in these systems can be catastrophic, for instance because of bombing a high security object.

Generally, it can be said that for objects less complicated than vehicles, the errors of alpha and beta type involve costs of machines down time and unnecessary overhauls, whereas, errors of beta type can generate costs equal to the price of an object damaged during the failure or its replacement. Obviously, it is not possible to eliminate both types of errors at the same time, and reduction of frequency (probability) of one type of error occurrence usually involves a more frequent occurrence of the second type of error. Therefore, each technical solution needs to take into account the difference between costs of the two kinds of errors and be a compromise between technological capabilities, costs of operation and maintenance and the legislation requirements. Strategy of identification and signaling of failures in deck systems must account for the fact that symptoms of failures of the vehicle elements and subsystems can occur not only due to their wear or damage but also because of extreme and unnatural conditions of operation caused by the style of driving, quality of the road, low quality of fuel or its contamination, weather conditions, engine freezing or moistness, etc. Symptoms of failures recorded in such situations disappear along with disappearance of external causes. Because of this the diagnostic system should have a built-in mechanism of inactivation of failure situations caused by symptoms of this kind [3].

In order to be successful in implementing technical solutions of dedicated systems, manufacturers must focus on[1]:

- reduction to minimum, the probability of detection of errors of the type alpha and beta in control tests,
  activation of the module of failure signal as rarely as possible,
- self-turning off of a given module when the failure symptoms disappear,

- providing all the persons interested in repair and diagnosing an object with the most complete diagnostic information enabling easy identification of failures.

The operation principle of a decision strategy for vehicles (fig.2.2), which will further be called strategy of symptom confirmation SPS, can be specified in the following way. A system state is considered to be fit for use when in its controller memory there have been recorded no codes of errors. It can be obtained after a longer time of the object operation without occurrence of errors – after erasing diagnostic information recorded in the system by means of a proper reading apparatus or after resetting it.

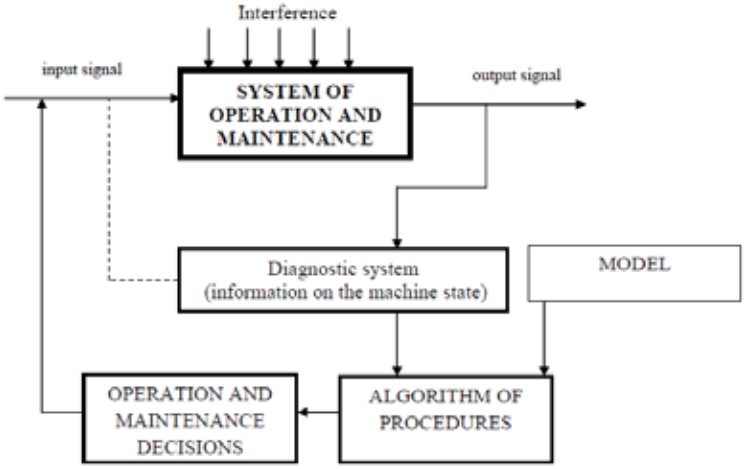

Fig.2 Diagnostic control of the system of machine operation and maintenance [3]

Once the first symptom of failure is discovered the system enters the state of first degree alert. Then a set of momentary parameters defining the object operation state, measured when the negative result occurs, the so called frozen frame', must be registered, also codes of errors whose symptoms have been discovered can be remembered as well. These codes, which will further be referred to as code of waiting errors (KO), have the same form as codes of recorded errors (KZ). KO codes, in literature named 'pending DTC', need to be distinguishable in the system from appropriate codes KZ.

The system goes from the state of first degree alert to the state of fitness for use if during 80 full cycles there have not been observed conditions similar to the ones recorded during occurrence of the first symptom. The system goes to second degree alert to fitness for use state after performing 40 cycles if there have occurred no failures.

Apart from the above described decision rule SPS, there has been used a strategy of statistical treatment of tests results which the most effective in eliminating errors of alpha type. Strategy which from now on be referred to as SOS, makes use of digital averaging with Exponentially Weighted Moving Average EWMA. Averaging of this type is a known method of elimination of big measurement deviations maintaining unchanged the mean value of measurement values series.

Digital algorithm of this averaging is used by the following equation[1]:

$$\overline{P_n} = P_n \cdot F + (1 - F)\overline{P}_{n-1} \tag{2.1}$$

where :

$\overline{P}_n$ -current mean value computed after n cycles

P_n -value of diagnostic parameter measured in the n-th cycle.

$\overline{P}_{n-1}$ - mean 'previous' value computed afer n-1 cycles.

F – a constant of filter.

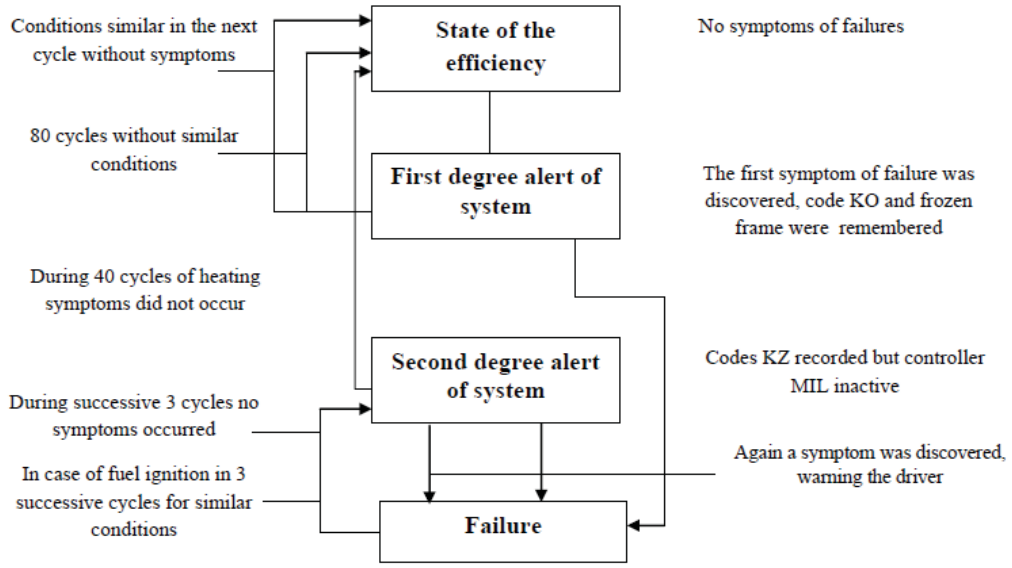

Fig.2.2.State of alert for dedicated diagnostic system [1]

As it is known, a digital filter with such properties is characterized by ex-potential response to a sequential change of the input value. Time constant (falling or rising) is defined by equation:

$$T = [1/F - 1] \times T_{\max} \tag{2.2}$$

where T_m is time of calculation of a diagnostic parameter usually equal to one cycle duration time length.

Whereas, the SOS procedure is used for identification of damage to elements which undergo gradual degradation rather than rapid failures and whose damage does not threaten other elements. This applies especially to failures of a catalytic reactor. The basic diagnostic parameter of such elements is their properly defined efficiency, expressed by analogue quantity.

3. Summary

Application of optimal methods for the machine technical state assessment in the process of operation and maintenance is the basis of the state identification process automation. This automation requires elaboration of a strategy for application of dedicated diagnostic systems. These systems enable : determination the optimal set of diagnostic parameters and according to them, control of the machine state and detection of a failure, prognosis and genesis of the machine state and determination of the machine state assessment test.

In this work there have been described rules of operation and maintenance strategies, with special emphasis on decision strategy, according to which once the first symptom of failure is detected the system enters the state of alert and strategy of statistical tests results treatment, which is fairly widespread.

References:

1. Merkisz J.: *Pokładowe systemy diagnostyczne pojazdów samochodowych*. WKiŁ, Warszawa 2002.
2. Niziński S., Wierzbicki S.: *Zintegrowany system diagnostyczny sterowania pojazdów*. Kongres Diagnostyki, Politechnika Poznańska, 2004.
3. Żółtowski B.: *Podstawy diagnostyki maszyn*. Wyd.ATR, Bydgoszcz 1996.

Journal of Polish CIMAC
Gdansk University of Technology
The Faculty of Ocean Engineering and Ship Technology

THE IMPORTANCE OF MEASURING MASS INTENSITY OF FLOW AIR THROUGH THE COMPRESSOR IN DIAGNOSTICS THE TURBOCHARGER SYSTEM MARINE ENGINE

Kazimierz Witkowski

Gdynia Maritime University, Mechanical Faculty
Morska Street 83, 81-225 Gdynia
Phone: (081) 69 01 332,
e-mail: wika@am.gdynia.pl

Abstract

The paper presents an analysis of the possibility of diagnosing the elements of turbocharger system marine diesel engine. Meaning of diagnostics of this system has also been discussed pointing out the most important consequences resulting from deterioration of supercharger system activity. Work evaluation of supercharger system is usually carried out on the basis of the following parameters: temperature and pressure of supercharging air in the scavenging air receiver (t_d, p_d), pressure drop in air filter and air cooler (Δp_f, Δp_{ch}), temperature exhaust gases before and after the turbine ($t_{wyl\,1}$, $t_{wyl\,2}$), temperature of overboard water before and after the air cooler ($t_{chl\,1}$ i $t_{chl\,2}$), turbocharger rotational speed (n_{TS}), pressure drop on the exhaust gas boiler (Δp_{ku}) – counterpressure of exhaust.

In exploitation practice of turbocharger system diagnostic, mass intensity of flow air through the turbocharger is not used and unfortunately measurement of this size is not realized. But in compressor diagnostics however, it is the basic exit parameter and the enter one for the rest of the elements.

Based on research results demonstrated the possibility to use to calculation the mass intensity of flow air through the compressor, measurement pressure drop on the confusor of the compressor. This calculation should be widely used in exploitation practice. This method is easy enough and sufficiently precise, in order to be used in the diagnostics the marine diesel engines.

Keywords: *marine diesel engines, operation, turbocharger system, diagnosis , air compressor diagnosis*

1. Introduction

Marine diesel engines, both main propulsion and auxiliary turbo-charged. Charging system, in addition to the injection system has a significant impact on the quality of the working process, the economics and reliability of operation.

Application turbochargers to turbocharging allows the use of energy contained in exhaust gases. Between the engine and turbocharger exists only gas-dynamics connection: stream of exhaust gases from the turbine and a stream of air from the compressor. The balance of power down through the turbine and the compressor needs shows the amount of energy used to compress air in the turbocharging system.

The structure of the mechanical-flow turbocharger and its quality is shaped at the design stage [14, 15]. This structure describes a set of values of design features, including:

- connection of a turbocharger with the engine (the foundation),
- the air collecting pipe,

- the compressor,
- the exhaust collecting pipe,
- the turbine,
- the turbocharger shaft,
- the turbocharger shaft bearings.

The deterioration of the technical condition of charging system is equivalent to the deterioration of the course working processes engine, but not necessarily directly and immediately affect the performance and parameters engine.

Due to the significant influence of the turbocharging system on the running engine, the relationship between business process flow and work of this agreement, shall be in operation in real time to diagnose his condition, including a turbocharger and air cooler. There is a close relationship and interaction (feedback) between the air charging unit (compressor, condenser), the worker process, the turbine driving the compressor and the compressor.

Complexity of the construction of the modern turbocharger and responsibility for the quality of the tasks causes the need to ensure rapid and reliable information on their current condition to the operator.

Due to the different diagnostic methods [1, 2, 3, 4, 5, 6, 7], using processes generated by the machine, parameters, and other volumes that contain diagnostic information.

The evaluation charging system work is usually carried out on the basis of the following parameters:

- temperature and pressure charge air in the scavenging air receiver (t_d, p_d),
- pressure drop across the filter and air cooler (Δp_f, Δp_{ch}),
- exhaust gas temperature before and after the turbine ($t_{wyl\,1}$, $t_{wyl\,2}$),
- sea water temperature before and after the cooler ($t_{chł\,1}$ i $t_{chł\,2}$),
- turbocharger rotational speed (n_{TS}),
- pressure drop on the exhaust gas boiler (Δp_{ku}).

In operational practice, the diagnosis of the loading system shall not use the mass flow of air through the compressor and, it is not implemented the measurement of this size. In diagnosing the compressor but it is the primary output parameter, and for other elements of the input.

2. Assessment of technical condition of the air filter

Ongoing impurity of the air filter reduces the cross section caused by the deposition of sediment on the filter cartridge. Increases resistance to flow and filtration efficiency decreases. After reaching the limit of adhesion strength of the agglomerates to the filter fibers, ends with the stable operation range of the filter. Increases aerodynamic forces and agglomerates are detached from the fibers. Increase the flow resistance in the filter is manifested to distort the flow of the intake air stream and deterioration of the compressor working.

Drops pressure at the inlet to the compressor by the pressure drop over the filter Δp_f. At the same time maintaining an unchanging compressor compression ratio π_S, air pressure decreases as the compressor p_k, a reduction in mass intensity of flow air $\dot{m}_s$ and a decrease in excess air number λ [11]. As a consequence, will among other things to supercharging pressure p_d, exhaust gas temperature T_g increases and the turbocharger rotational speed n_{TS}, and decrease the maximum combustion pressure p_{max}. This may also lead to an increase in specific fuel consumption g_e. As with the foregoing, the consequence of the impurity compressor air filter (Z_f) is:

$$Z_f \Rightarrow (\Delta p_f\uparrow;\ p_k\downarrow;\ p_d\downarrow;\ \dot{m}_s\downarrow) \Rightarrow (g_e\uparrow;\ T_g\uparrow;\ n_{TS}\uparrow;\ \lambda\downarrow;\ p_{max}\downarrow)$$

3. Assessment of technical condition of the air compressor

In the flow channels of the air compressor are deposited contaminants, despite the security air filter. It is primarily a viscous oily (sticky) mass, weakly bound to the surface elements. The compressors that consume air from the engine room cross-section of the diffuser after about 2000 hours may be from 10 to 20% reduced [16]. Deposits on the walls of the flow channels and the erosion effects of sea spray cause an increase in friction losses and change the angles of leading and trailing blades and aerodynamic flow. Deposits on the walls of the flow channels and the erosion effects of sea spray cause an increase in friction losses and change the angle of attack and angle of discharge rotor blades, and deterioration in the aerodynamic flow. As a result, there is reduction in the efficiency of the compressor η_S and the amount of air supplied to the engine. This affects the process of working in a quantity of gas flowing into the turbine, and hence a decrease in the rotational speed of the turbocharger. Decrease the amount of air supplied to the engine can cause deterioration of cylinder scavenging, increase heat loads of the components combustion chamber and increase exhaust gas temperature [12]. As the above shows, the consequence of the impurity compressor (Z_s) is:

$$Z_S \Rightarrow (\eta_S\downarrow; \pi_S\downarrow; p_k\downarrow; p_d\downarrow; \dot{m}_s\downarrow) \Rightarrow (g_e\uparrow; T_g\uparrow; \lambda\downarrow; p_{max}\downarrow)$$

4. Assessment of technical condition of the turbine

In the turbocharging systems of marine diesel engines, the compressor is usually driven by an axial turbine (rarely used radial turbine). During operation turbine comes to contamination. There may also be mechanical damage the blades caused by the solid materials such as, fragments of the damaged engine components and hard pieces of coke, which did not stop the turbine protection grill. Producers of marine diesel engines provide the possibility the progressive contamination the turbine. So equip turbine the special systems: water washing system, water with the addition of surfactants washing system [1] or dry-cleaning system using granulate. These activities should be performed periodically, according to the manufacturer, which allows the turbine to restore good condition (clean to keep the turbine). Deposits on the surfaces of the flow (impurity the turbine Z_T) causes a change in their profile, reducing the cross section, the increase in gas flow resistance, which has the following effect on the work of turbocharger system (increasing the values: turbine expansion ratio π_T, pressure drop on the exhaust gas boiler Δp_{ku}, specific fuel consumption g_e, exhaust gas temperature T_g; decrease the values: efficiency of the turbine η_T, mass intensity of flow air $\dot{m}_s$, excess air number λ):

$$Z_T \Rightarrow (\pi_T\uparrow; \eta_T\downarrow; \Delta p_{ku}\uparrow; \dot{m}_s\downarrow) \Rightarrow (g_e\uparrow; T_g\uparrow; \lambda\downarrow)$$

5. Possibility and importance of measuring delivery of a compressor in the diagnosis of turbocharger system the marine engine

The air intensity of flow through the compressor

As follows from previous considerations, as well as many other studies [8, 9, 13], the flow of air through the charging system should play a role in the diagnosis of the basic. It results from the fact that in the balance of this system one of the most important conditions is the balance of mass flow continuity, it is:

$$\dot{m}_S = \dot{m}_C \quad \text{and} \quad \beta \cdot \dot{m}_C = \dot{m}_T, \tag{1}$$

where:

$\dot{m}_S$ - mass intensity of flow air through the compressor [kg/s],

$\dot{m}_C$ - mass intensity of flow air through the cylinders [kg/s],

$\dot{m}_T$ - mass intensity of flow gases through the turbine [kg/s],

β - coefficient related to the increase in gas mass relative to the air mass, due to the dose delivered to the cylinders of fuel [-].

Methods of determining the air intensity of flow through the compressor

In the laboratory or in the engine test bench most often used to determine the air intensity of flow through the compressor ($\dot{m}_S$) leminiscate. Directly measured quantity is the pressure drop across the leminiscate. Then, based on appropriate mathematical relations are calculated $\dot{m}_S$. Although this method is very accurate, but in operational practice not used. Another method is to measure the air drop pressure on inlet the compressor - on the the confusor of the compressor (Δp_{konf}) [13] and use the formula (2):

$$\dot{m}_S = k \cdot \sqrt{\Delta p_{konf}} \quad , \tag{2}$$

were:

$\dot{m}_S$ – mass intensity of flow air through the compressor [kg/s],

k – constant, characteristic of the charging system [-],

Δp_{konf} – pressure drop on the confusor of the compressor [mmH_2O].

Due to the simplicity of the method indicated it should be generally applied. The author is not a known case of the practical utilization of this method. Therefore, decided to see if it is effective and sufficiently accurate. Therefore were performed laboratory tests on the marine engine, in order to determine the constant *k* turbocharging system and verify that the *k* does not change when you change the engine operating conditions.

Laboratory tests

The research was conducted on a four-stroke marine engine SULZER 3AL25/30, supercharged turbocharger VTR160N. Their goal was to test the effectiveness of the methods of determining the mass intensity of flow air through the compressor, based on the measurement of pressure drop on its confusor (Δp_{konf}). Using the possibility of imposing a $\dot{m}_S$ using leminiscate and measuring Δp_{konf}, determination of the factor *k* appearing in equation (2). Measurements were made repeatedly - for different engine loads and air temperatures at the inlet to the engine. Research was carried out in the range of loads from 200 to 280 kW, and charge air temperatures 45, 50, 55, 60 and 65 ^{0}C. V For each of the states were determined mass intensity of flow air through the compressor using an leminiscate, and measured the pressure drop across the confuzor compressor. This allowed to calculate each value of factor *k*. The results are summarized in Tab.1. Regardless of the load engine and charge air temperature, the coefficient k, in each case calculated on the basis of defined $\dot{m}_S$ and measured Δp_{konf}, has a constant value approximately equal to 0.18. The average value of *k* for the whole measurement cycle, i.e., with 75 measurements (25 states, in each of three parallel measurements) is 0.179.

Tab. 1. The results of measurements

t_k [°C]	N_e [kW]	Δp_{konf} [mmH_2O]	$\dot{m}_s$ [kg/h]	k [-]
45	200	9	0,5452	0,1868
	220	10	0,5853	
	240	10	0,6169	
	260	12	0,6519	
	280	14	0,6885	
50	200	9	0,5445	0,1804
	220	10	0,5776	
	240	12	0,6152	
	260	12	0,6404	
	280	15	0,6809	
55	200	10	0,5446	0,1752
	220	11	0,5534	
	240	12	0,6179	
	260	13	0,6092	
	280	15	0,6769	
60	200	9	0,5404	0,1761
	220	11	0,5718	
	240	12	0,6092	
	260	13	0,6408	
	280	15	0,6769	
65	200	8	0,5376	0,1805
	220	10	0,5676	
	240	11	0,6052	
	260	13	0,6399	
	280	15	0,6708	
The average value of *k*:				**0,179**

6. Conclusions

Among the many volumes of great significance in the diagnosis of the turbocharger system, a very important parameter is the - mass intensity of flow air through the compressor.

The diagnosis is the primary compressor output parameter, and for other elements of the input.

Determination of this parameter in the operational practice should be universal, and a method based on drop air pressure compressor on confusor is so simple, yet accurate enough to seriously take it into consideration in the application of operational marine engines.

Establishment of a fixed k, specific charging system, should do the engine manufacturer, after completion of procedures for the selection of turbochargers and enter the value of *k* to the documentation of the turbocharger.

References

[1] Charchalis A., *Diagnozowanie okrętowych silników turbinowych*, AMW, Gdynia 1991.

[2] Charchalis A., *Diagnozowanie zanieczyszczeń kanału przepływowego turbinowych silników spalinowych na podstawie wielkości opisujących rozruch,* Zagadnienia Eksploatacji Maszyn, PAN nr1-2, 1993.

[3] Charchalis A., *Komputerowy system pomiarowy dla oceny charakterystyk napędowych oraz stanu technicznego siłowni kombinowanych,* Wydawnictwo politechniki Szczecińskiej, Szczecin 1995.

[4] Charchalis A., *System diagnozowania okrętowych układów napędowych z turbinowymi silnikami spalinowymi*, Problemy eksploatacji, 4/97 (27).
[5] Charchalis A., Korczewski Z., *Metody diagnozowania okrętowych turbinowych silników spalinowych*, Przegląd mechaniczny. Z. 3-4, 1997.
[6] Cholewa W., Drobniak S., Elsner W., Kiciński J., *Zintegrowany system nadzoru diagnostycznego turbozespołu*, ZN WSI, Opole, 1996.
[7] Dąbrowski Z., *Wykorzystanie efektu rezonansu nieliniowego jako symptomu w diagnozowaniu silników turbinowych,* III Sympozjum Naukowo-Techniczne „Silniki spalinowe w zastosowaniach wojskowych", Jurata, 1997.
[8] Włodarski J.K., *Okrętowe silniki spalinowe. Podstawy teoretyczne*, Wydawnictwo WSM, Gdynia 1996.
[9] Włodarski J.K., *Stany eksploatacyjne okrętowych silników spalinowych,* Fundacja Rozwoju WSM, Gdynia 2001.
[10] Witkowski K., Piotrowski I., *Eksploatacja okrętowych silników spalinowych,* Fundacja Rozwoju WSM, Gdynia 2001.
[11] Witkowski K., *Wpływ zanieczyszczenia filtra powietrza na parametry procesu roboczego,* Budownictwo Okrętowe 5/1989.
[12] Witkowski K., *Wpływ niesprawności sprężarki i chłodnicy powietrza na parametry procesu roboczego silnika spalinowego,* Budownictwo Okrętowe 9/1989.
[13] Woznickij I.W., inni., *Raboczije procesy sudowych dizjelej,* Transport, Moskwa 1979.
[14] Żółtowski B., *Identyfikacja diagnostyczna obiektów technicznych*, Zagadnienia Eksploatacji maszyn Z.1(105) PAN, 1996.
[15] Żółtowski B., Ćwik. Z., *Methoden der technischen Identifikation der Objekte,* IV Kolloquim Technische Diagnostik, Technische Universitat Dresden, 1966 (s.98-116).
[16] *Turbocharger compressors – the phenomenon of surfing,* Turbo Magazine, 1995. ABB Turbo Systems Ltd., Switzerland.

Journal of Polish CIMAC
Gdansk University of Technology
The Faculty of Ocean Engineering and Ship Technology

AN ANALYSIS OF THE ASSESSMENT OF THE TECHNICAL CONDITION OF A MARINE DIESEL-ELECTRIC SET BASED ON THE EXHAUST GAS PRESSURE AND OTHER ENERGY PARAMETERS MEASUREMENTS

Marcin Zacharewicz

Polish Naval Academy
Ul. Śmidowicza 69, 81-103 Gdynia, Poland
Tel.:+48 58 626 23 82
e-mail: M.Zacharewicz@amw.gdynia.pl

Abstract:

In the paper an analysis of the assessment of the technical condition of a marine diesel-electric set with limited monitoring susceptibility, on the basis of the diesel engine and generator energy parameters measurements, is presented. The proposed method is based on the assumption, that there is a relationship between technical state of engine and generator, and measurable parameters of the generating set. The structure of the power station has been analyzed to select parameters for measurements. The chosen parameters are as follows: exhaust gas pressure in the outlet manifold, phase-to-phase generated voltage, and acceleration of some parts of the diesel engine and synchronous generator. The research program, characteristics of the equipment, and representative results for various technical conditions of the engine are presented.

Keywords: *generating set, marine auxiliary diesel engine, synchronous generator, diagnostic*

1. Introduction

One of the most important research problems taken up on the Mechanic-Electric Faculty of the Polish Naval Academy, is to develop some alternative methods of the assessment of the technical condition of selected parts of marine diesel engines [1, 2, 3, 5, 6, 12].The concern in alternative diagnostic methods results from the fact that in the Polish Navy there is a great number of marine diesel engines, both auxiliary and main propulsion, not equipped with indicator valves. For example, engines ZVIEZDA M401, M503 and M520 type, DETROIT DIESEL DDA149TI type, and licensed by LEYLAND diesels SW400 type. Since that is not possible to operate them with applying to them classical diagnostic methods, they are exploited according to so-called overhaul life strategy. The main goal of developing alternative methods of assessment of the technical condition of marine diesel engines, is to implement in the Navy strategies according to technical state of such engines. During the research it was assumed that due to the lack of possibility to measure the pressure inside engine's cylinders, one should seek

other measurable parameters of interest carrying diagnostic information. After an analyze, the following diagnostic parameters were determined: exhaust gas pressure in the manifold, phase-to-phase voltage of the synchronous generator, and acceleration of the certain diesel and generator elements. Exhaust gas pressure measurements performed at two cross-sections of the outlet channel, allowed to determine the speed of the peak amplitude of the pressure wave propagation and the enthalpy flux there. Usefulness of such an attitude was proved during tests in order to evaluation of the technical condition of three supercharged marine diesel engines: ZVIEZDA M401 type, DIETROIT DIESEL DDA149TI type and SULZER 6AL20/24 type [5, 6, 12]. Another parameter providing an important diagnostic information is phase-to-phase voltage of the synchronous generator [2]. It is because of the fact that for the synchronous generator the phase-to-phase voltage strictly depends on the angular speed of the engine's crankshaft. The accelerations of selected engine and generator elements were chosen as well as an important diagnostic parameter.

2. Test stand description

A marine generating set type ZE400/52 was the object of the research. It is equipped with a diesel engine type SW 400 and a three phase synchronous generators GCP-94c/1, installed in the laboratory of Mechanic-Electric Faculty of the Polish Naval Academy (Fig. 1). Such generating sets are installed on small Polish warships as well. The tested engine SW400 type is a four-stroke, six cylinders, in-line, undercharged auxiliary diesel engine. Its main technical data are shown in Table 1. Each set can generate electric power as a single set or in parallel, synchronously on a common net. Exhaust gases from running engines are directed to one manifold as it is shown in Fig.2. Rated constant rotational speed of the engine crankshaft 1500 rpm is connected with the frequency f = 50 Hz of the generated electric power. Diesel engine load with the brake torque can be changed by means of effective resistance of air resistors which makes electric load of generators. They enable loading each generator in the range of 0 ÷ 25 kW.

Fig. 1. General view of marine generating set ZE400/52 mounted on the test bed

Table 1. Technical characteristic of SW400 diesel engine [13]

Rated output	54,06 kW	Injection type	Direct
Rated crankshaft speed	1500 rpm	Injection order	1-5-3-6-2-4
Number of cylinders	6	Injection pressure	16,18 – 16,67 MPa
Piston stroke	120,65 mm	Specific fuel consumption	190 g/kWh
Cylinder bore	107,19 mm	Intake valve opening commencement	10^0 before the TDC

Schematic diagram of the exhaust gas system in the laboratory is shown in Fig. 2.

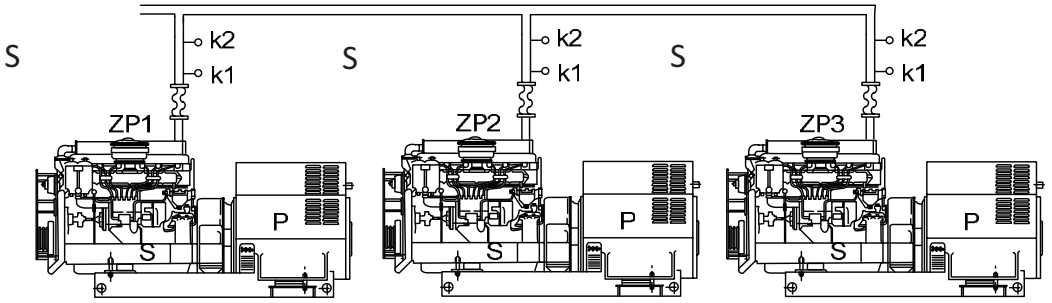

Fig.2. Schematic diagram of the exhaust gas system in the laboratory: S – diesel engine, P – generator, ZP – generating set, k_1, k_2 – control cross-section [2, 3, 13].

3. Measuring equipment

Multifunction data acquisition module Advantech type USB-4711A (Fig. 3) was used for measurements. The module characteristics: 16 analog input channels, input range ±10V, ±5V, ±2.5V, ±1.25V, ±0.625V, resolution 12bits, and max. sampling rate 150 kS/s. It has a USB 2.0 interface, too. Measured quantity converter PWM-2010 (Fig. 3) was designed and constructed for the needs of conducted tests. It enables adjustment signals from sensors to USB module features. Besides it makes generated voltage up to 400V measurements safe due to voltaic separation from the module and computer. PWM-2010 is compatible with pressure sensors OPTRAND type C11294-Q, and accelerometer KD35 type or Brüel & Kjaer 4384 type [1].

Fig.3. Measuring equipment: 1-computer, 2-multifunction data acquisition module Advantech USB-4711A, 3-converter PWM-2010.

The measuring instrument PWM-2010 provides simultaneous, inertia-less and accurate measurement of certain physical quantities and adjusts the level of signals from transducers and phase-to-phase voltage of the synchronous generator to values acceptable for data acquisition module.

The way of instantaneous value of the exhaust gas pressure measurement in the selected sections of the outlet channel is shown in Fig. 2. Transducers OPTRAND type C11294-Q were used in measurements because of their resistance to exhaust gas high temperatures. Due to the so-called temperature drift, those transducers eliminate the constant component of the pressure and allow to measure the pressure pulsation in the range of 0÷0.7 MPa, with the sampling frequency to 30kHz. The range of the transducer output signal value is 0.5÷5 V and resolution of the multifunction data acquisition module 12 bits what enables recording with an accuracy of 171 Pa.

Instantaneous value of the generator phase-to-phase voltage (~400V) was another measured parameter. Due to safety of the personnel and to prevent the slotted line from damage phototransistors were used for galvanic separation such relatively high generator voltage from the measuring instrument.

The measuring circuit contains phase-to-phase converter. Its function is to match the generator voltage to voltage accepted by the data acquisition module. This converter is composed of adjustable voltage dividers and enables to achieve ±5V at the output so as to adapt currents in the system to provide the optocoupler linear characteristic.

A constant voltage component was added in order to ensure proper working conditions of the optocoupler. Due to an analog voltage signal at the output of the optocoupler in the range of 0.5÷5V and the resolution of the module 12 bits voltage measurement with the precision of 1.22V is possible. However, it should be taken into consideration that both characteristic of the voltage divider and the optocoupler are dependent on the temperature. To minimize the temperature effect on the measurement results, all the instruments were switched on for 5 minutes until their temperature become steady during measurements.

Vibrations of selected elements of the generating set construction structure were measured, too. The measuring vibrations line was calibrated by means of standard oscillator. In addition, while the measuring line was calibrated, acceleration test was conducted by means of another instrument but in the same measuring points.

The fuel injectors vibration accelerations measurement accuracy was not significant due to the fact that the signal has been used for synchronous averaging (qualitative analysis rather than quantitative).

Low-pass filters with a frequency range twice as much as the sampling frequency to avoid the aliasing effect were built in all the measuring lines.

It was assumed that the measurement of all energetic parameters is simultaneous. Time base was considered constant due to quartz resonator class used, and timing accuracy error which does not exceed 2% of the sampling frequency 150kS/s. Besides, PWM-2010 as an analog measuring device without inductive and capacitive elements, introduces very little signal distortion in the time domain.

4. Research methodology

In order to work out the methodology of research it was assumed that all the tests would be carried out for steady operating conditions. That is why a static plan was applied. At the beginning all values of input parameters were assumed. Those parameters were selected on the

basis of the logical analysis of the construction structure of the generating set and its working conditions. In conducted tests, the determined plan was applied where input parameters were: engine load with brake torque T (directly proportional to generator load) and implemented to the system certain unserviceable states. For practical reasons a selective plan was adopted so it was possible to confine a number of input parameters [10]. A complete plan would be very complicated because engine loads with the brake torque may change continuously in its operating range. Therefore it was decided to adopt the second degree polyselective plan [10]. It was assigned engine load with the brake torque adequate to diesel engine running idle and when electric power delivered by the generator was 20kW. To know the way of changing the measured parameters as a function of engine break torque, additionally measurements at the generator load 10kW were made. The second input parameter in the investigation plan was technical condition of the generating set. There were assumed two different cases – "good" and "poor" condition of technical suitability of the set [4, 9]. As "good" was recognized the normal condition of the set. "Poor" condition was achieved by cutting off fuel to one of diesel injectors by means of a three-way pass valve as it is shown in Fig.4. Experimental plan is shown in Table 2.

Table 2. Experimental plan

Number of input parameters value arrangement	Generator power [kW]	Technical condition of the generating set [-]
1	0	good
2	20	good
3	0	poor
4	20	poor

Fig.4. Engine SW400 type fuel system with three-way pass valve to cut off fuel supply to the chosen injector

After an analysis of the construction structure, the following energetic parameters of the generating set were chosen for the measurements:

- phase-to-phase generator voltages (after the automatic voltage regulator) [7, 8],
- exhaust gas pressure pulsations in two cross-sections of exhaust manifold,
- fuel injectors vibration accelerations,
- accelerations of the selected elements of the generator driven by the diesel engine [11].

Places where measurements were carried out are shown in Figs. 2 and 5.

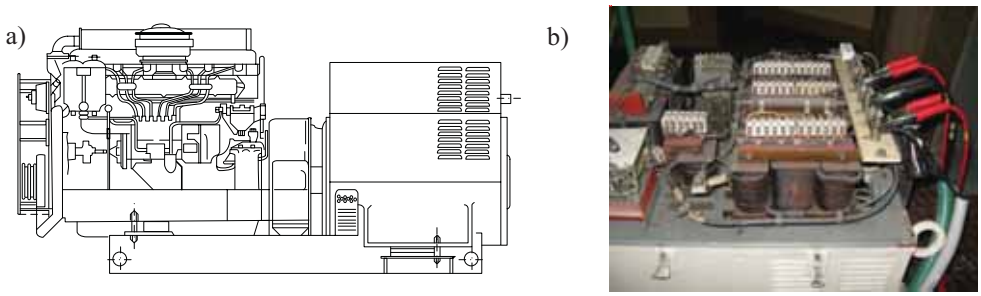

Fig.5. a) arrows point out where accelerometers were placed, b) arrows point out where phase-to-phase voltage was measured

The measurements of variable pressure in control cross-sections of the exhaust manifold enable to measure the enthalpy flux of the exhaust gas from engine cylinders, speed of the peak amplitude of the exhaust gas pressure wave propagation, and spectral analysis of the registered signal [5, 6, 12]. Analysis of pressure waveforms as a function of time, especially in terms of determining the enthalpy flux of exhaust gas, is troublesome. Much more convenient is to analyze these signals as a function of the engine crank angle. To do this one needs to find any periodically repeated signal (synchronizing) of period T equal to the duration of the engine cycle of operation. Parameters that satisfy above requirements are accelerations measured at the engine injectors. They allow to convert all measured parameters from the time domain into the engine crank angle domain (synchronous averaging). Moreover, vibration accelerations measured at the injectors allow to precise determine average crankshaft speed during the engine cycle of operation. Similarly, based on the synchronous signal, phase-to-phase voltages as a function of crank angle domain were determined. Both the pressure waveforms as a function of time, and phase-to-phase voltages, were analyzed using Fast Fourier Transformation (FFT). The last group of parameters that were measured and recorded, are accelerations of the clutch connecting the engine and generator, generator stator, and generator thrust bearing. The measurement results were analyzed using FFT.

5. Experimental results

The measurements have been carried out according to the presented plan. Rated crankshaft speed 1500 rpm was kept constant so that electric voltage frequency to be constant. Diesel engine load with the brake torque was changed from idle running, 10kW to 20kW. It was assumed that the generating set was in good technical condition and, after cutting off fuel to one of injectors, in poor technical condition. Representative results of experiment when the engine was in good and poor technical conditions are shown in the following figures.

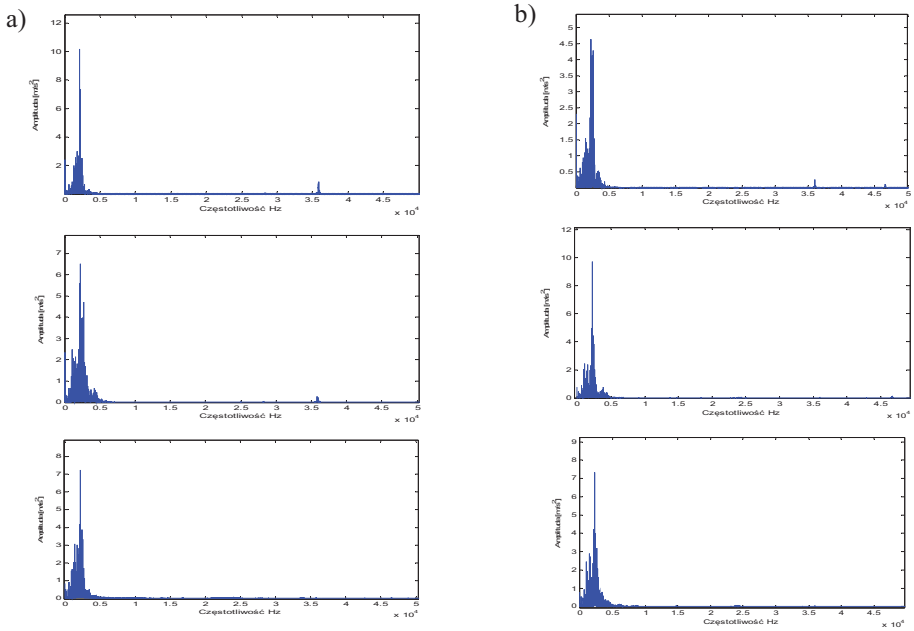

Fig. 6. Amplitude spectrum of vibrations from the generator stator: a) good technical state, b)poor technical state, 1 – idle running, 2 – load 10kW, 3 – load 20kW [3].

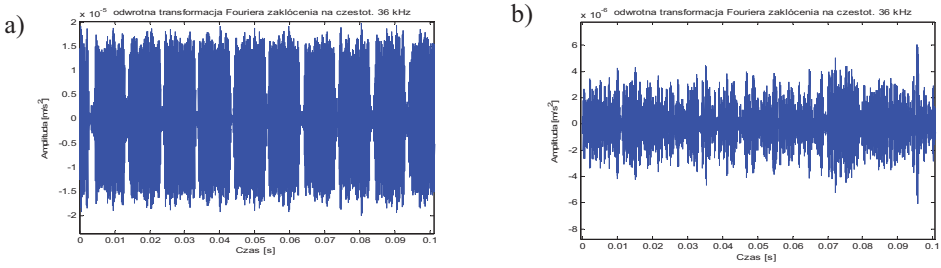

Fig. 7. Time waveforms of vibrations from the generator bearing for frequency between 35 and 37 kHz for 10kW load: a) good technical state, b) poor technical state [3].

The comparison of the pressure waveform in control cross-section k_2 as a function of the crankshaft angle for two technical states of the engine, "good" and "poor", is shown in Fig.8.

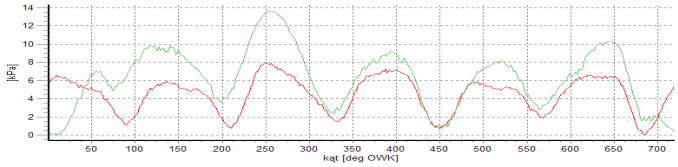

Fig. 8. Exhaust gas pressure in control cross-section k_2 as a function of crankshaft angle (load 10kW): 1 – good technical condition, 2 – poor technical condition [2].

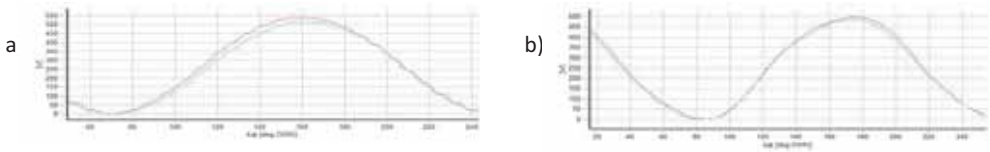

Fig. 9. Phase-to-phase voltage as a function of crank angle: a) idle running, b) load 20kW; 1- good condition of technical suitability, 2-fuel to one cylinder cut off [2].

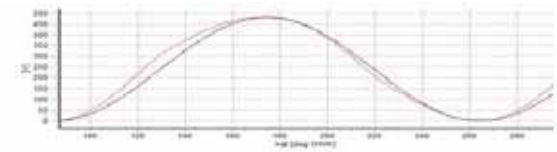

Fig.10. Phase-to-phase voltage as a function of crank angle when engine is idle running and fuel to cyl. no. 2 is cut off. 1-measured value, 2-theoretical value [2].

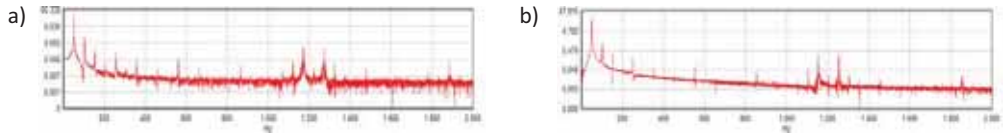

Fig. 11. Amplitude spectrum of phase-to-phase voltage (load 20kW): a) good condition of technical suitability, b) fuel to one cylinder cut off.

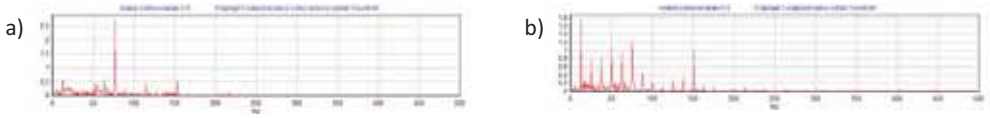

Fig.12. Amplitude spectrum of exhaust gas pressure pulsation in the control cross-section k_1 in the outlet channel (load 20kW): a) good condition of technical suitability, b) fuel to one cylinder cut off.

Time waveforms of measured parameters as a function of crank angle for different values of engine load for good technical state are shown in the following figures:

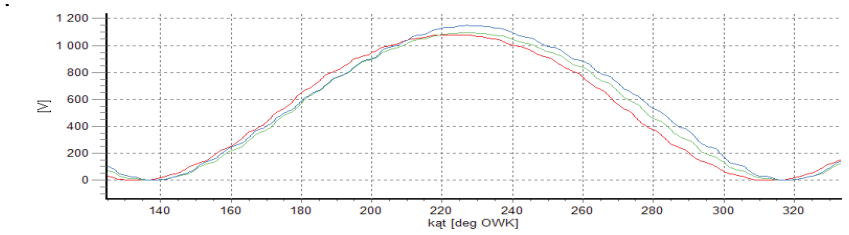

Fig.13 Phase-to-phase voltage as a function of crank angle (a part of the cycle); 1-idle running, 2-load 10kW, 3-load 20kW

Based on qualitative and quantitative analysis of the data presented in Figs .6 and 7 it can be stated that introduced technical unfitness of the engine causes changes in vibrations power spectrum. The increase in the frequency range from 35 to 37 kHz is characteristic for such a failure. It can be seen in Fig.7 where inverse Fourier transform of vibrations is shown.

Analysis of the data presented in Fig.8 allows to conclude that when fuel to one of the engine cylinders is off, it causes visible pressure deformation in the exhaust gas manifold. The usefulness of this parameter for the assessment of the technical condition of the engine is described in literature [1, 3, 12]. The recorded gas pressure waveform as a function of time (Fig.8) was analyzed in frequency domain after Fourier transform (Fig. 11).

Based on a comparative analysis of the spectrum of exhaust gas pressure when the engine is in "good" and "poor" technical condition it can be stated that due to unfitness, the value of the harmonic corresponding to the number of engine cylinders (150Hz) significantly increased. Has also increased the value of the harmonics that are multiples of the fundamental harmonic 8.33Hz.

Analysis of the recorded voltage waveforms as a function of time, after the transition to the angle of the crankshaft rotation, allows to conclude that both the engine load (Fig. 13) and its technical condition affects the shape of the course (Figs.9 and 10). Waveform distortion, their slope, result from changes in the instantaneous angular velocity of the crankshaft during engine cycle of operation. The increase in engine load causes deformations of the course for entire engine cycle of operation, i.e. 720^0 crankshaft revolution. On the other hand, the state of unfitness when one of cylinders does not work causes furthermore the course distortion for a particular crankshaft angle corresponding to the phase of cycle the cylinder that is faulty.

This observation allows to evaluate the technical condition of the generating set. Knowing the injection order it is possible to identify the faulty cylinder section.

6. Conclusions

The results presented in this paper provide an introduction to development of a non-invasive method of assessing the technical condition of a marine generating set when diesel engine is not equipped with indicator valves. Analysis of the experimental data presented in the form of diagrams led to conclusion that changes of certain energetic parameters are the function both the technical condition and the load (electric power) of the generating set. This observation motivates for further research to find out diagnostic relations between the technical condition of the generating set and variations of its energetic parameters. As a consequence, it should allow to point out a set of diagnostic parameters which can identify explicitly technical condition of the generating set.

References

[1] Cwalina A. , Zacharewicz M., *Conception and practical application of a measuring device for energetic parameters measurement of a mechatronic object.* Mechatronic Systems, Mechanics and Materials, pp. 185-193, Solid State Phenomena, Zurich – Durnten 2011.

[2] Cwalina A. , Zacharewicz M., *Preliminary investigations of a generating set of the ship's power station in the aspect of diagnosing selected parts of its constructional structure.* Combustion Engines No. 3/2011.

[3] Cwalina A. , Zacharewicz M., *The conception of diagnosis the technical condition of marine diesel engine driving a synchronous generator*. Combustion Engines No. 3/2011
[4] Kluj S.: *Diagnostyka urządzeń okrętowych*. WSM, Gdynia 2000.
[5] Korczewski Z, Zacharewicz M., *Metoda diagnozowania silników okrętów wojennych o ograniczonej możliwości pomiaru ciśnień wewnątrz cylindrowych na podstawie wyników badania procesów gazodynamicznych w układzie turbodoładowania*. Opracowanie w ramach projektu badawczego MNiSW No: 0T00B02129, Gdynia 2008.
[6] Korczewski Z., Zacharewicz M., *Evaluation of working spaces' technical condition of marine diesel engine on the basis of operation research*. Journal of Polish CIMAC, vol. 4 No. 1 pp. 85-94, 2010.
[7] Kurowski W., *Podstawy diagnostyki systemów technicznych. Metodologia i metodyka*. Warszawa-Płock 2008 .
[8] Mindykowski J, Tarasiuk T, Szweda M., Evans I.C., *Electric power quality measurements on All-electric ship with AC active front end propulsion drives*. Technical report No. 68 Polskiego Rejestru Statków, Gdańsk 2007.
[9] Moczulski W.A., *Diagnostyka techniczna*. Metody pozyskiwania wiedzy, Gliwice 2002.
[10] Polański, Z., *Planowanie doświadczeń w technice.* PWN, Warszawa 1984.
[11] Randall R.B., *Frequency Analysis. Application of B&K Equipment.* 1977.
[12] Zacharewicz M.: *Metoda diagnozowania przestrzeni roboczych silnika okrętowego na podstawie parametrów procesów gazodynamicznych w kanale zasilającym turbosprężarkę*. Rozprawa doktorska, Gdynia 2009.
[13] Dokumentacja Techniczna Zespołu Prądotwórczego typu ZE400/52.

Journal of Polish CIMAC
Gdansk University of Technology
The Faculty of Ocean Engineering and Ship Technology

NEW ELEMENTS IN THE TESTS PROGRAMMES OF MACHINE VIBRATIONS

Bogdan ŻÓŁTOWSKI Henryk TYLICKI
Faculty of Mechanical Engineering
University of Technology and Life Sciences in Bydgoszcz
bogzol@utp.edu.pl, tylicki@utp.edu.pl

Abstract

This paper discusses selected issues of technical diagnostics and mechanics system status monitoring. The issues presented new elements in the test of quality vibrations machines in exploitation. Investigation of machinery destruction processes accompanying every machine just after its manufacturing until its liquidation. This gives a basis for rational maintenance of machines in newly created diagnostic maintenance systems. State evaluation depending on a good model and appropriate symptoms leads to entity-related technologies and the bionics of the existence of technical systems. The descriptors of diagnostic maintenance system enable to create modern maintenance strategies in enterprise systems, keeping modern machinery in motion.

Keywords*: signal processing, diagnostics, programmes test, vibrations, statistics optimization*

1. Introduction

The development of virtual technologies gives rise to many new solutions in the field of modelling, simulation, diagnostic information gathering and processing. Some of these possibilities were hinted at in this article, namely signal processing, statistical optimization of results and diagnostic inference.

The role and significance of technological diagnostics in every phase of machine life are extremely important. They were presented in numerous works against a background of tasks performed by a product in specific maintenance strategies [2,3,4,5,6,7,8,9,10,11,12]. The assessment of machines' technical state with the use of physical processes generated by them requires the gathering of crucial information on the state and proper association of functional parameters of an assessed item, along with a set of measures and evaluation of output processes.

In machinery diagnostics, tests of the evolution of technical state of a particular item occurring in a lifecycle and time $0 \le \theta \le \theta_b$ determined by the next planned or extorted item renovation in θ_b constitute a basis for many scientific initiatives. A diagnostic observation of the advancement of item's wear and tear is conducted through measuring various symptoms of technical state and comparing their values (strength, amplitude) with pre-determined allowed values – for a particular symptom and in a particular application.

The actual breakthrough in the valuation of contents and extraction of diagnostic information from the observation matrix occurred thanks to centring and regulating symptoms to their starting value, that is for a model item state with no wear and tear ($\theta = 0$).

A multi-dimensional symptomatic representation of item's technical state in programmed tests, already available, as well as the possibility to extract this information online gives new perspectives in item diagnosing. This in particular relates to new or modernized constructions and new start-ups of innovative items with no operating experience.

This paper presents the issues of redundancy reduction, the assessment of single measures of a diagnostic signal and multi-dimensional diagnostic information processing in program tests.

2. Initial data processing

In practical applications, the initial preparation of data obtained from measurements is a key stage in the classification of data influencing the effectiveness of state distinction, speed, easiness of construction and learning the cause and effect model, as well as its further generalization.
A registered time signal of an investigated process in an Excel spreadsheet is a basis for further processing, i.e. in the field of time, frequency and amplitudes, resulting in many measures enabling the decomposition of an output signal into the signals of specific failure in development. The decision-making process consists of a sequence of operations from the moment of obtaining the information on machinery state, its gathering and processing, until making a decision and forwarding it for implementation.

At the beginning, however, three types of initial data processing can be distinguished: data transformations, filling in the missing values and dimensionality reduction.

Data transformations

The analysis of experimental data is connected with the occurrence of different types of measuring scales, which can be symbolic or numeric. In the systems of diagnostic information processing usually all the features describing the analyzed items have to be numeric.

In the case of classification models making use of distances as similarity measures it is very common for specific features to characterize any physical state on the basis of various physical values, and as a result they influence distance differently. A few transformations unifying the influence of specific features in relation to distance values can be applied here. The most popular ones include normalization and standardization.

Normalization

Normalization is conducted according to the following formula:

$$X_N = \frac{x_i - x_{i\min}}{x_{i\max} - x_{i\min}} \qquad (1)$$

where: x_{imax} is a maximal value in the set for i-feature, and x_{imin} a minimal value for i-feature.

As a result of normalization, we obtain vectors with feature values in the range [0,1].

This transformation does not take into account the distribution of values of a specific symptom; consequently, in the case of the occurrence of a few symptoms with considerably different values, most values are pressed in a very narrow range as a result of normalization.

Standardization

Making use of the distribution of values in specific symptoms leads to a transformation known as standardization, as per the following relations (2).

$$X_S = \frac{x_i - \bar{x}_i}{\sigma_i(x)}; \quad \bar{x} = \frac{1}{n}\sum_j^n x_j^i$$

$$\sigma_i(x) = \frac{1}{n-1}\sum_j^n (x_i^j - \bar{x}_i)^2 \qquad (2)$$

As a result of this transformation symptoms with an average value of x=0 are obtained, while a standard deviation equals σ=1, thanks to which all the symptoms have identical input in information value.

Precision constant – takes into account the range of changeability and an average value of measured parameters, as well as ensures non-dimensionality, as per the following relation:

$$p_i = \frac{\bar{x}_i}{w_i} \qquad (3)$$

Symptom sensitivity w_i contained together with an average value in one number ensures non-dimensionality and changeability range:

$$w_i = \frac{x_{i\max} - x_{i\min}}{\bar{x}_i} \qquad (4)$$

Giving the possibility of further mutual consideration of data of comparable weight obtained in measuring is an important and necessary step.

3. Ideal point method - *OPTIMUM*

Measured diagnostic signals reflect in various ways the observation space, and indirectly also failure development in a machine - fig.1. With the use of optimization techniques, it is possible to characterize measured symptoms' sensitivity to state changes on the basis of measured distance. Distinguishing failure is possible after projecting symptoms onto respective axes: *x, y, z.*

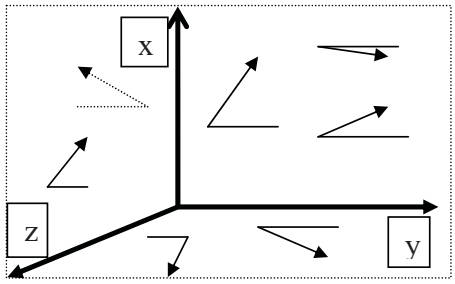

Fig.1. Multi-dimensional observation space

The algorithm below enables to statistically assess individually elaborated diagnostic signals, resulting in a ranking list of their sensitivity and usefulness. The next steps of such proceedings are as follows:

1. The creation of an observation matrix of measured symptoms: s_1, s_2, s_3,…,s_m;
2. The results of measuring symptoms for various states are subject to statistical evaluation with the help of different criteria, i.e.

- the changeability of symptoms:

$$f_1 = \frac{s_j}{\vec{y}} \qquad (5)$$

where: S_j – standard deviation, $\bar{y}$ - average value.

- the assessment of symptom sensitivity to state changes:

$$w_i = \frac{x_{i\max} - x_{i\min}}{\bar{x}_i} \qquad (6)$$

- the correlation with technical state, mileage (determining the coefficient of symptom-state correlation):

$$f_2 = r\,(y,w); \qquad r_{xy} = \frac{1}{n-1} \frac{\sum_{i=1}^{n} (x_i - x_{ir})(y_i - y_{ir})}{\sigma_x \; \sigma_y} \qquad (7)$$

In order to make the considerations easier and the results possible to present on a plane, two selected quality indicators are sufficient.

3. Performing the maximization and normalization of assumed indicators of signal quality further, the statistical descriptions of their sensitivity are obtained (f_1^*, f_2^*), which further enables to determine the coordinates of the ideal point. Then, the determination of distances of specific signal measures from the ideal point is possible, as per the following relation (7):

$$L = \sqrt{(1 - f_1^*)^2 + (1 - f_2^*)^2} \qquad (8)$$

4. General sensitivity coefficients (weights) for each tested signal are determined on the basis of the following relation:

$$w_i = \frac{1}{\frac{1}{L_i} \cdot \sum_{i=1}^{n} L_i}, \qquad \text{where: } \sum w_i = 1 \qquad (9)$$

The presented algorithm can be easily realized in Excel, giving a qualitative arrangement of measured symptoms. Fig.2 presents a final result of the effect of the described procedure on sample measuring data. Distance points of specific measures form the ideal point (1,1) prove the sensitivity of the assessed signal measures, with the nearest points (1,1) being the best symptoms.

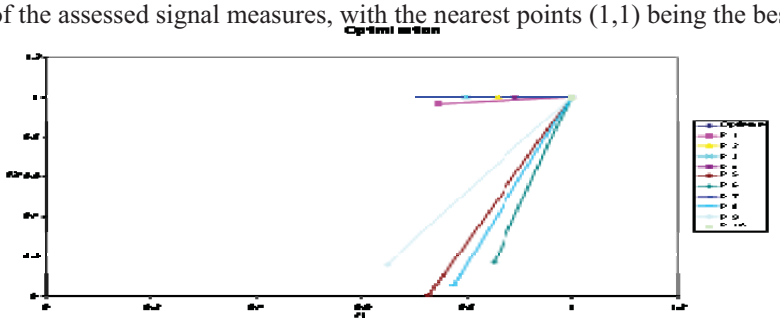

Fig.2. The result of ideal point method - OPTIMUM

With highlighted, statistically good symptoms, cause and effect models can be built on them at the stage of state inference. The quality of the model depends, however, on the number of measures taken into account, which indirectly can be evaluated with the determinance coefficient R^2 in the simplest regressive models.

4. Multi-dimensional observation of the system - SVD

SVD (Singular Value Decomposition) is a numeric procedure for the multi-dimensional monitoring of item's state changes. It detects failure in development and selects maximally informative state symptoms in a given situation.

Let us take a complex mechanical item operating in time into consideration; $0 < \theta < \theta_b$, where evolutionarily a few independent **failures** are progressing, $F_t(\theta)$, t=1,2,..u. Their development can be understood through observing the phenomenon field, making a linear vector of technical state symbols; $[\mathbf{s_m}] = [\mathbf{s_1,...,s_r}]$, of various physical nature. In order to monitor the changes in item's technical state, several dozens of equally distant readings of vector value in time are made; θ_n, n=1,...p, $\theta_p \leq \theta_b$. In this way, the following lines of the symptomatic observation matrix (SOM) are obtained. We already know [Cempel01], [Cempel02] that the maximum of diagnostic information can be obtained from the matrix if all the readings are initially centred (distracted) and normalized to the initial value $\mathbf{S_m\ (0)} = \mathbf{S_{0m}}$ of a given symptom. In this way we obtain a non-dimensional symptomatic matrix of observation:

$$O_{pr} = [S_{nm}], \qquad S_{nm} = \frac{\mathbf{S}_{nm}}{\mathbf{S}_{0m}} - 1 \tag{10}$$

where: bold lettering symbolizes original dimensional values of symptoms.

Hence, for describing a system's lifecycle there is a non-dimensional observation matrix O_{pr} with **r –** columns resulting from the number of observed symptoms and **p** – lines resulting form the total number of subsequent observations. A procedure of decomposition in respect of singular values can be applied for this non-dimensional observation matrix:

$$O_{pr} = U_{pp} * \Sigma_{pr} * V_{rr}^{T}, \tag{11}$$

where: (T- transposition) U_{pp} is a p - dimensional orthogonal matrix of left-sided singular vectors, and V_{rr} is an r – dimensional orthogonal matrix of right-sided singular vectors, and in the centre – a diagonal matrix of singular values Σ_{pr} of the following properties:

$$\Sigma_{pr} = diag\ (\sigma_1, \ldots, \sigma_l), \ \ where: \ \sigma_1 > \sigma_2 > \ldots > \sigma_u > 0 \tag{12}$$

and: $\sigma_{u+1} = \ldots \sigma_l = 0, \quad l = max\ (p, r), \quad u = min\ (p, r).$

This means that of r – measured symptoms only $u \leq r$ independent information on failure in development can be obtained. Such a distribution of SVD observation matrix can be conducted after finishing each observation; n= 1, ..., p, and in this way monitor the evolution of failure F_t (θ_n) in an item.

One failure F_t can be described by new values; SD_t and σ_t. The first one is a generalized symptom of failure **t**, which can be called a discriminant of this failure and obtained as a right-sided product of an observation matrix and vector $\mathbf{v_t}$ [4]:

$$SD_t = O_{pr} * \boldsymbol{v_t} = \sigma_t \cdot \boldsymbol{u_t} \tag{13}$$

Since vectors v_t and u_t are normalized to entity, the length of vector SD_t equals its energetic norm, as follows:

$$Norm\ (SD_t) \equiv ||SD_t|| = \sigma_t \tag{14}$$

Thus, for an assigned lifetime θ, utility advancement of failure F_t can be reflected by a singular value $\sigma_t(\theta)$, whereas its momentary evolution by the discriminant SD_t (θ). The equivalence of new measures obtained form SVD to the descriptions of failure spaces id postulated in the whole lifecycle θ of an item:

$$SD_t(\theta) \sim F_t(\theta), \ with\ the\ norm\ |F_t(\theta)| \sim |SD_t(\theta| = \sigma_t(\theta) \tag{15}$$

$SD_t(\theta)$ could also be called a failure profile, whereas $\sigma_t(\theta)$ its advancement. Fig.2 visualizes the idea of SVD.

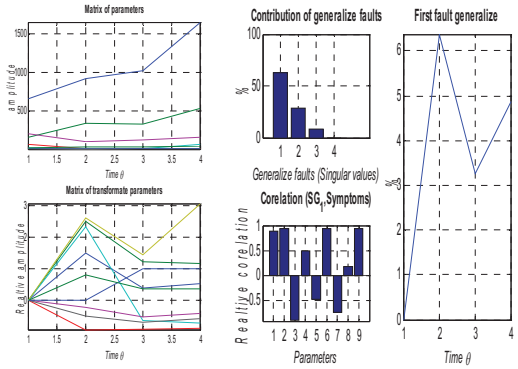

Fig.2 The contents of diagnostic information with independent failures in the symptomatic matrix of observation and the detected discriminants SD_i and measure of advancement σ_i

The aim of SVD also includes the selection of maximally informative symptoms measured in a given instance of diagnostic observation.

From the matrix of observation $O_{pr} = [S_{nm}]$, we can define two square covariance matrices **r** and **p** dimensional, as shown below ($*^T$ – matrix, vector transponing):

$$W_1 = (O_{pr})^T * O_{pr}, \text{ and; } W_2 = O_{pr} * (O_{pr})^T \qquad (16)$$

The solution of this issue of such matrices (EVD) shows that singular vectors in demand obtained from SVD observation matrix, as well as squares of singular values can be obtained:

$$W_1 * v_\nu = \sigma^2_\nu * v_\nu, \ \nu = 1,...r; \text{ and; } W_2 * u_i = \sigma^2_i * u_i, \ i = 1,...p. \qquad (17)$$

Hence, solving two own issues (Eigen Value Decomposition - EVD) of both matrices of covariance defined on the observation matrix, we obtain the exact result as from the procedure SVD; the only difference is the squares of singular values instead of their original values. It is commonly known that squaring favours the biggest values, which can thus cause a different evaluation of information input significance by different symptoms, but the rejection of the ones with the lowest values is obvious.

A good example illustrating the application of these considerations is a diagnostic observation of a twelve-cylinder traction Diesel engine, where in one chosen point measurements of a dozen vibration symptoms in the whole lifecycle were made every $\Delta\theta$ = 10 thousand km. In total, the amplitudes of 3 accelerations, 3 speeds, 3 displacements and 3 Rice frequencies were measured.

The upper-left corner image shows 12 measured symptoms forming an abundance of information, which, however, after being processed by SVD, is easily decoded into two main failure types due to the fact that σ_1 and σ_2 constituting approximately 50% and 20% of the total amount of diagnostic information in an observation matrix (upper right corner) measured as a quotient of the value of a given σ_i to the sum of all singular values. On top of that, the first failure SD_1 (lower left corner) rises almost monotonically, whereas the second one is unstable and starts to rise only after the twentieth measurement (200 thousand km), which is shown in the course of failure intensity σ_2 in the lower right corner of Fig.3.

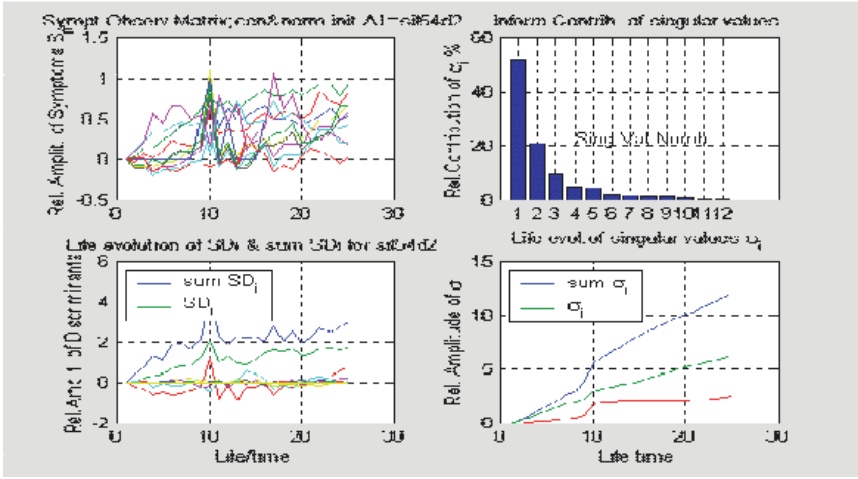

Fig.3 SVD applied in engine tests

Hence, the SVD procedure in the latest program implementations is of base character and contains only approximately 70 lines. Naturally, the algorithm can be further expanded, automatically searching for superfluous measuring symptoms for a given diagnostic issue. It was presented in Fig.3 in a simplified form – in the image in the upper right corner, where the participation of specific symptoms in discriminant SD_1 is clearly visible.

5. CONCLUSIONS

The issues related to diagnosing complex technological items are constantly developed, and the procedures of obtaining and processing diagnostic information constantly improved. This paper deals with reduction redundancy for single state symbols and a multi-dimensional state test.

A new, simple and effective method of the assessment of sensitivity of single state measures was proposed – the *OPTIMUM* method, as well as the core of the *SVD* method. The latter is applied and still improved for the needs of multi-dimensional diagnostics.

The GSVD procedures are already implemented in the majority of advanced calculation systems, i.e. in *MATLAB*®. Thus, a diagnostic interpretation, calculation details concerning additional knowledge accumulated in matrices describing an item and measuring environment are worth considering. Such additional data do not always have to be digital; in many cases linguistic or fuzzy variables are sufficient.

LITERATURE

[1] Bishop R.D., Gladwell G.M., Michaelson S.: The matric analysis of tremblings. PWN, Warsaw, 1972.
[2] Cempel C.: Multidimensional condition monitoring of mechanical systems in operation. Węgierska Górka, 2002 s.109-118.
[3] Cempel C.: The cancellation of the class of data in the diagnostics of machine engines. ZEM, Exercise book 4 (44), 1980.
[4] Cempel C., Tabaszewski M., Krakowiak M.: Metods of the multidimensional information diagnostic extraction. The diagnostics of machine engines, 2003, s.109-118.
[5] Giergiel J., Uhl T.: Identification of arrangements of mechanical. PWN, Warsaw, 1990.
[6] Żółtowski B.: Diagnostic identification of technical objects. PAN, ZEM. Z.1 (105). 1996.

[7] Tylicki H., Żółtowski B.: Terra-technology of the exploitation of vehicles. ATR, Bydgoszcz 2004 s.260.
[8] Żółtowski B., Niziński S.: Modelling the processes of exploitation machines. ISBN – 83-916198-3-4, Bydgoszcz-Sulejówek, 2002 pp.250.
[9] Żółtowski B.: Investigation of dynamics machines. UTP, Bydgoszcz, 2002 pp.335.
[10] Żółtowski B., Cempel C.: Engineering of diagnostics machines. ITE Radom, 2004 s.1109.
[11] Żółtowski B., Niziński S.: The computer system of the exploitation of vehicles. PWSZ, Pila 2004 pp.234.
[12] Żółtowski B., Tylicki H.: The chosen problems of the machines exploitation. PWSZ, Pila 2004 pp.294.